

# **Stomatal acclimation to dynamic light: implications for photosynthesis and water use efficiency**

**Jack S. A. Matthews**

A thesis submitted for the degree of Doctor of Philosophy



School of Biological Sciences

University of Essex

September 2018

## Abstract

Although stomata typically occupy only a small portion of the leaf surface (0.3-5%), stomata control approximately 95% of all gas exchange between the leaf interior and external environment. Therefore, stomatal behaviour has major consequences for photosynthetic CO<sub>2</sub> fixation and water loss from leaf to canopy levels, influencing carbon and hydrological cycles at global scales. Plant acclimation to growth light environment has been studied extensively; however, the majority of these studies have focused on constant light intensity and photo-acclimation, with few studies exploring the impact of dynamic growth light on stomatal acclimation and behaviour.

Initially, in this thesis natural variation in the response of stomatal conductance ( $g_s$ ) to light was assessed in the model tree species *Populus nigra*. Dynamic growth light regimes (varying in intensity and pattern) were subsequently used, to explore how stomatal acclimation to growth light impacts stomatal behaviour, photosynthesis ( $A$ ) and water use efficiency ( $W_i$ ). The rate, magnitude and diurnal behaviour of the response of  $g_s$  to light varied significantly between genotypes and growth light treatments, which promoted differences in  $A$  and therefore  $W_i$  over the course of the day.

The findings in this study illustrate the impact of growing plants in dynamic light regimes, similar to those experienced by plants in the natural environment, on the physiology and performance of model species *Populus nigra* and *Arabidopsis thaliana*. Furthermore, it emphasizes that growing plants under laboratory conditions and square-wave illumination does not accurately represent plant acclimation and development under a natural environment. Highlighting the need to potentially rethink how we grow plants as a community if we are to infer results from the lab to the field. Finally, this study highlights the importance of considering plant acclimation to growth light, and the impact this has on the functional response of stomata, when attempting to model the response of  $g_s$  across leaf to ecosystem and global scales.

## Acknowledgements

Firstly, I would like to thank my supervisor Professor Tracy Lawson. I am supremely confident that without your continued advice, supervision and encouragement I would not have succeeded. Your unconditional support and effort in pushing me forward is something I greatly appreciate, and has shaped the scientist I am today, and for that I will forever be in your debt.

Furthermore, I would like to thank members of the Plant physiology lab at Essex, for their inspiration, teamwork and procrastinating discussions which helped to keep me focused and remind me of the love I have for research. Special thanks must be given to Phil Davey and Silvere Violet-Chabrand, for whom this PhD would have been immensely more difficult, your technical advice and expertise kept me afloat and I will forever be grateful for your patience. Of course, I would like to thank all the other members of the Plant productivity group for their support and invaluable encouragement throughout my time at the University of Essex.

I sincerely thank my family for their encouragement, and mental support. I would especially like to thank my mum and dad for always having a board game ready whenever I needed an escape, without your support this PhD would have never gotten off the ground.

Finally, to my wife Sunne. You are truly the most amazing wife and mother, and I thank you for your love and patience, and for giving me two beautiful sons. You are truly my driving force.

For Rupert and Arlen.

I am grateful to the Natural Environment Research Council (NERC) and Forest Research for the generous financial support throughout this PhD.

# List of Contents

Abstract	i
Acknowledgements	ii
List of Contents	iii
List of Figures	viii
List of Tables	xiii
Publications	xiv
Abbreviations	xv
<b>Chapter 1 – Introduction</b>	<b>1</b>
1.1. Background	2
1.2. Stomatal and photosynthetic acclimation to growth light	4
1.3. Influence of stomatal anatomy on the response to light	5
1.4. Temporal response of stomatal conductance ( $g_s$ ): Impact on photosynthesis and water use efficiency	7
1.4.1. Impact of fluctuations in light on stomatal response	7
1.4.2. Determining the temporal response of stomatal conductance ( $g_s$ )	9
1.5. Stomatal behaviour and co-ordination of $A$ and $g_s$ over the diurnal period	10
1.5.1. Mechanisms of coordination between $g_s$ and $A$	11
1.5.2. Diurnal stomatal behaviour	12
1.6. Aims and Objectives	14
<b>Chapter 2 – Materials and Methods</b>	<b>15</b>
2.1. Plant material and growth conditions	16
2.1.1. Fluctuating growth light regime	16
2.1.2. Simulating daily light fluctuations for sinusoidal growth light regime.	17
2.2. Leaf gas exchange	18
2.2.1. $A/Q$ (net photosynthetic rate/ $PPFD$ ) response curves	18
2.2.2. $A/C_i$ (net photosynthetic rate/intercellular $CO_2$ concentration) response curves	18
2.2.3. Temporal response of $A$ and $g_s$	19
2.2.4. Diurnal measurements	19
2.2.5. Measurements and modelling of diurnal stomatal conductance under constant light	19
2.3. Modelling gas exchange parameters	21

2.3.1. Determination of mass integrated net CO <sub>2</sub> assimilation	21
2.3.2. Estimating photosynthetic capacities	22
2.3.3. Assessing stomatal limitation from $A/C_i$ response curves	22
2.3.4. Modelling net CO <sub>2</sub> assimilation rates	22
2.3.5. Determining the rapidity of stomatal conductance response	23
2.3.6. Determining the rapidity of net CO <sub>2</sub> assimilation response	23
2.3.7. Including diurnal stomatal behaviour in the Ball-Berry model for predicting $g_s$	24
2.4. Leaf and stomatal characteristics	24
2.4.1. Stomatal anatomical measurements	24
2.4.2. Leaf anatomical measurements	25
2.4.3. Leaf optical properties	25
2.4.4. Analysis of photosynthetic pigments	26
2.4.5. Leaf cross-section analysis	26
2.4.6. Protein Extraction and Western Blotting	26
2.5. Light use efficiency	27
2.5.1. Daily light use efficiency	27
2.6. Statistical analysis	28
<b>Chapter 3 – Natural variation in stomatal response to light in <i>Populus nigra</i>: implications for photosynthesis and water use efficiency</b>	<b>29</b>
3.1. Introduction	30
3.2. Materials and Methods	32
3.2.1. Plant material and growth conditions	32
3.2.2. Leaf gas exchange	34
3.2.3. Modelling gas exchange parameters	35
3.2.4. Leaf and stomatal characteristics	36
3.3. Results	38
3.3.1. Photosynthetic response to photosynthetic photon flux density ( <i>PPFD</i> )	38
3.3.2. Leaf size and absorbance properties	38
3.3.3. Intra-specific variation in photosynthetic capacity	41
3.3.4. Limitation of CO <sub>2</sub> uptake ( <i>A</i> ) imposed by stomata conductance	43
3.3.5. Diurnal responses of $g_s$ , <i>A</i> , and $W_i$ to a fluctuating pattern of light	44
3.3.6. Limitation of diurnal photosynthesis imposed by stomata	47
3.3.7. Response of $g_s$ and <i>A</i> to a step change in <i>PPFD</i>	50
3.3.8. Speed of $g_s$ response to a step change in <i>PPFD</i>	51

3.3.9. Stomatal anatomy	53
3.3.10. Impact of stomatal density and speed of response on intrinsic water use efficiency	53
3.4. Discussion	56
3.5. Main conclusions	60
<b>Chapter 4 – Acclimation to growth light intensity impacts stomatal response, photosynthesis and water use efficiency in <i>Populus nigra</i></b>	61
Transition Statement	62
4.1. Introduction	63
4.2. Materials and Methods	65
4.2.1. Plant material and growth conditions	65
4.2.2. Leaf gas exchange	67
4.2.3. Modelling gas exchange parameters	67
4.2.4. Leaf and stomatal characteristics	68
4.3. Results	70
4.3.1. Photosynthetic response to photosynthetic photon flux density ( <i>PPFD</i> )	70
4.3.2. Leaf size and absorbance properties	70
4.3.3. Variation in photosynthetic capacity between growth light treatments	73
4.3.4. Limitation of CO <sub>2</sub> uptake ( <i>A</i> ) imposed by stomata conductance	75
4.3.5. Diurnal responses of <i>g<sub>s</sub></i> , <i>A</i> , and <i>W<sub>i</sub></i> to a fluctuating pattern of light	76
4.3.6. Limitation of diurnal photosynthesis imposed by stomata	78
4.3.7. Response of <i>g<sub>s</sub></i> and <i>A</i> to step changes at different <i>PPFDs</i>	80
4.3.8. Speed of <i>g<sub>s</sub></i> response to step changes at different <i>PPFDs</i>	82
4.3.9. Response of <i>g<sub>s</sub></i> and <i>A</i> to a step change in <i>PPFD</i> as a function of time of day	84
4.3.10. Speed of <i>g<sub>s</sub></i> response to a step change in <i>PPFD</i> as a function of time of day	86
4.3.11. Stomatal anatomy	88
4.3.12. Impact of stomatal density and speed of response on intrinsic water use efficiency	90
4.4. Discussion	93
4.5. Main conclusions	98
<b>Chapter 5 – Importance of fluctuations in light on plant photosynthetic acclimation in <i>Arabidopsis</i></b>	100
Transition Statement	101
5.1. Introduction	102
5.2. Material and methods	104

5.2.1. Plant material and growth conditions	104
5.2.2. Growth Analysis	104
5.2.3. Leaf gas exchange	106
5.2.4. Modelling gas exchange parameters	107
5.2.5. Light use efficiency	107
5.2.6. Statistical analysis	107
5.3. Results	108
5.3.1. Photo-acclimation of plants grown under different light regimes	108
5.3.2. Leaf properties in plants acclimated to different light regimes	110
5.3.3. Impact of growth light on photosynthetic capacity	113
5.3.4. Diurnal leaf level responses of gas exchange and chlorophyll fluorescence	117
5.3.4.1. Measurements under diurnal high light fluctuating conditions ( $DF_{high}$ )	117
5.3.4.2. Measurements under diurnal low light fluctuating conditions ( $DF_{low}$ )	119
5.3.5. Comparison of measured diurnal photosynthesis with predicted from $A/Q$ analysis	121
5.3.6. Influence of growth light regimes on plant development	123
5.4. Discussion	126
5.5. Main conclusions	130
<b>Chapter 6 – Acclimation to fluctuating light impacts the rapidity of response and diurnal rhythm of stomatal conductance in <i>Arabidopsis</i></b>	<b>131</b>
Transition Statement	132
6.1. Introduction	133
6.2. Material and Methods	135
6.2.1. Plant material and growth conditions	135
6.2.2. Leaf gas exchange	137
6.2.3. Modelling gas exchange parameters	138
6.2.4. Including diurnal stomatal behaviour in the Ball-Berry model for predicting $g_s$	138
6.2.5. Stomatal anatomical measurements	138
6.3. Results	139
6.3.1. Diurnal responses of $g_s$ , $A$ , and $W_i$ to a square wave pattern of light	139
6.3.2. Response of $g_s$ and $A$ to a step change in PPFD as a function of time of day	143
6.3.3. Speed of $g_s$ response to a step change in PPFD	147
6.3.4. Stomatal anatomy	150
6.3.5. Impact of diurnal stomatal behaviour on predictive models of $g_s$ in a dynamic environment	152

6.4. Discussion	154
6.5. Main conclusions	157
<b>Chapter 7 – General discussion</b>	159
<b>Chapter 8 – References</b>	167

## List of Figures

### Chapter 2

<b>Figure 2.1</b>	Light regimes used for plant growth and leaf level diurnal measurements of gas exchange.	16
<b>Figure 2.2</b>	First five days of the simulated sinusoidal high light regime ( $SN_{High}$ ).	17
<b>Figure 2.3</b>	Parameters derived from the Gaussian function describing the bell shaped variation of $g_s$	21

### Chapter 3

<b>Figure 3.1</b>	Representative examples of leaf genotypes used in this study.	33
<b>Figure 3.2</b>	Preparation of <i>Populus nigra</i> cuttings.	33
<b>Figure 3.3</b>	Representation of the numbering of <i>Populus nigra</i> leaves for selection for gas exchange and anatomical analysis.	34
<b>Figure 3.4</b>	Photosynthesis as a function of light intensity ( $PPFD$ ) for the four small-leaved and six large-leaved genotypes.	39
<b>Figure 3.5</b>	Leaf and Optical properties of the ten poplar genotypes.	40
<b>Figure 3.6</b>	Photosynthesis as a function of intercellular $CO_2$ concentration ( $C_i$ ) for the four small-leaved and six large-leaved genotypes.	42
<b>Figure 3.7</b>	Estimation of the limitation placed on net $CO_2$ assimilation by stomata and leaf boundary layer, calculated from the $A/C_i$ response curves ( $ACI_{Limit}$ ).	44
<b>Figure 3.8</b>	Diurnal measurements of gas exchange.	45
<b>Figure 3.9</b>	Total daily net $CO_2$ assimilation, stomatal conductance, and intrinsic water use efficiency for the five selected genotypes.	46
<b>Figure 3.10</b>	Diurnal measurements of observed and predicted net $CO_2$ assimilation modelled from the $A/Q$ response curves.	48
<b>Figure 3.11</b>	Correlation between the estimations of the limitation placed on net $CO_2$ assimilation by stomata.	48
<b>Figure 3.12</b>	Temporal response of stomatal conductance, net $CO_2$ assimilation, and intrinsic water use efficiency, to a step increase in light intensity.	49

<b>Figure 3.13</b>	Temporal response of stomatal conductance to a step decrease in light intensity.	50
<b>Figure 3.14</b>	Time constant for stomatal opening ( $\tau_i$ ), Final values of stomatal conductance after an increased step change in light ( $G_i$ ); time constant for stomatal closure ( $\tau_d$ ), Final values of stomatal conductance after a decreased step change in light ( $G_d$ ); difference in $g_s$ following the step increase ( $\Delta G_i$ ) or decrease ( $\Delta G_d$ ) in light; light saturated rate of carbon assimilation ( $\tau_{ai}$ ) to a step change in light; and saturation of net CO <sub>2</sub> assimilation ( $A_i$ ).	52
<b>Figure 3.15</b>	Stomatal anatomical characteristics for the four small-leaved and six large-leaved genotypes.	54
<b>Figure 3.16</b>	Correlations between abaxial stomatal density ( $SD_{Ab}$ ), time constant for stomatal opening ( $\tau_i$ ), and daily intrinsic water use efficiency during the diurnal ( $W_i$ ).	55
 <b>Chapter 4</b>		
<b>Figure 4.1</b>	Structures built to create growth light conditions: at ambient; ca. 60% of ambient; and ca. 20% of ambient.	66
<b>Figure 4.2</b>	Photosynthesis as a function of light intensity ( $PPFD$ ) for the three Poplar light treatments: Ambient; P60; and P20.	71
<b>Figure 4.3</b>	Leaf and Optical properties of the three Poplar light treatments.	72
<b>Figure 4.4</b>	Photosynthesis as a function of intercellular CO <sub>2</sub> concentration ( $C_i$ ) for the three Poplar light treatments; Ambient; P60; and P20.	74
<b>Figure 4.5</b>	Estimation of the limitation placed on net CO <sub>2</sub> assimilation by stomata and leaf boundary layer, calculated from the $A/C_i$ response curves ( $ACI_{Limit}$ ).	75
<b>Figure 4.6</b>	Diurnal measurements of gas exchange.	77
<b>Figure 4.7</b>	Total daily net CO <sub>2</sub> assimilation, stomatal conductance, and intrinsic water use efficiency for the three Poplar light treatments.	78
<b>Figure 4.8</b>	Diurnal measurements of observed and predicted net CO <sub>2</sub> assimilation modelled from the $A/Q$ response curves for the three Poplar light treatments.	79
<b>Figure 4.9</b>	Correlation between the estimations of the limitation placed on net CO <sub>2</sub> assimilation by stomata.	79
<b>Figure 4.10</b>	Temporal response of stomatal conductance ( $g_s$ ), net CO <sub>2</sub> assimilation ( $A$ ), and intrinsic water use efficiency ( $W_i$ ), to step increases in light intensity (50-250; 100-1000; and 500 to 1500 $\mu\text{mol m}^{-2} \text{s}^{-1} PPFD$ ).	81
<b>Figure 4.11</b>	Temporal response of stomatal conductance ( $g_s$ ) to step decreases in light intensity (250-50; 1000-100; 1500 to 500 $\mu\text{mol m}^{-2} \text{s}^{-1} PPFD$ ).	82

<b>Figure 4.12</b>	Time constant for stomatal opening ( $\tau_i$ ), Final values of stomatal conductance after an increased step change in light ( $G_i$ ); time constant for stomatal closure ( $\tau_d$ ), Final values of stomatal conductance after a decreased step change in light ( $G_d$ ); light saturated rate of carbon assimilation ( $\tau_{oi}$ ) to a step change in light; and saturation of net CO <sub>2</sub> assimilation ( $A_i$ ), at three different light steps (50-250; 100-1000; and 500-1500 $\mu\text{mol m}^{-2} \text{s}^{-1}$ PPF <sub>D</sub> ).	83
<b>Figure 4.13</b>	Temporal response of stomatal conductance ( $g_s$ ), net CO <sub>2</sub> assimilation ( $A$ ), and intrinsic water use efficiency ( $W_i$ ), to a step increase in light intensity (100-1000 $\mu\text{mol m}^{-2} \text{s}^{-1}$ PPF <sub>D</sub> ), at different times of day (Morning, Midday, Evening).	85
<b>Figure 4.14</b>	Temporal response of stomatal conductance ( $g_s$ ) to a step decrease in light at different times of the day: Morning; Midday; and Evening.	86
<b>Figure 4.15</b>	Time constant for stomatal opening ( $\tau_i$ ), Final values of stomatal conductance after an increased step change in light ( $G_i$ ); time constant for stomatal closure ( $\tau_d$ ), Final values of stomatal conductance after a decreased step change in light ( $G_d$ ); light saturated rate of carbon assimilation ( $\tau_{oi}$ ) to a step change in light; and saturation of net CO <sub>2</sub> assimilation ( $A_i$ ), at different times of day (Morning, Midday, Evening).	88
<b>Figure 4.16</b>	Stomatal anatomical characteristics.	89
<b>Figure 4.17</b>	Correlation between abaxial stomatal density ( $SD_{Ab}$ ) and daily intrinsic water use efficiency during the diurnal ( $W_i$ ).	90
<b>Figure 4.18</b>	Correlations between abaxial stomatal density ( $SD_{Ab}$ ), time constant for stomatal opening ( $\tau_i$ ), and daily intrinsic water use efficiency during the diurnal ( $W_i$ ), at three different light steps: 50-250; 100-1000; and 500-1500 PPF <sub>D</sub> .	91
<b>Figure 4.19</b>	Correlations between abaxial stomatal density ( $SD_{Ab}$ ), time constant for stomatal opening ( $\tau_i$ ), and daily intrinsic water use efficiency during the diurnal ( $W_i$ ), at different times of the day: Morning; Midday; and Evening.	92
 <b>Chapter 5</b>		
<b>Figure 5.1</b>	Diurnal light regimes used for plant growth and leaf level measurements of gas exchange.	105
<b>Figure 5.2</b>	Photosynthesis as a function of light intensity (PPFD) of plants grown under the four light regimes SQH; FLH; SQL; and FLL.	109
<b>Figure 5.3</b>	Optical properties including absorbance; transmittance and reflectance of leaves grown under the four different light regimes.	111
<b>Figure 5.4</b>	Leaf anatomical properties including total thickness; palisade layer thickness and Spongy layer thickness.	111
<b>Figure 5.5</b>	Cross section of leaves grown under the four light treatments.	111

<b>Figure 5.6</b>	Photosynthesis as a function of intercellular CO <sub>2</sub> concentration ( $C_i$ ) of plants grown under the four light treatments <i>SQH</i> ; <i>FLH</i> ; <i>SQL</i> and <i>FLL</i> .	114
<b>Figure 5.7</b>	Percentage of change in protein concentration relative to <i>FLL</i> treatment determined from 4 replicate immunoblot analysis of leaves grown under the four light treatments.	116
<b>Figure 5.8</b>	Diurnal measurements of gas exchange of net CO <sub>2</sub> assimilation on an area basis ( $A$ ); net CO <sub>2</sub> assimilation on a leaf mass basis ( $A_{mass}$ ); stomatal conductance ( $g_s$ ); internal CO <sub>2</sub> concentration ( $C_i$ ); and chlorophyll fluorescence parameters $F_q'/F_m'$ ; $F_q'/F_v'$ ; $F_v'/F_m'$ and $NPQ$ estimated under fluctuating high light ( $DF_{high}$ ).	118
<b>Figure 5.9</b>	Diurnal measurements of gas exchange of $A$ , $A_{mass}$ , $g_s$ , $C_i$ , and chlorophyll fluorescence parameters $F_q'/F_m'$ ; $F_q'/F_v'$ ; $F_v'/F_m'$ and $NPQ$ estimated under fluctuating low light ( $DF_{low}$ ).	120
<b>Figure 5.10</b>	Diurnal measurements of observed and predicted net CO <sub>2</sub> assimilation modelled from the $A/Q$ light response curves.	122
<b>Figure 5.11</b>	Growth analysis of plants grown under the four light regimes.	123
<b>Figure 5.12</b>	Total daily absorbed light, net carbon gain and carbon loss by dark respiration, modelled <i>Daily</i> light use efficiency ( $LUE$ ), and overall long-term light use efficiency of plants grown under the four light treatments.	125
 <b>Chapter 6</b>		
<b>Figure 6.1</b>	Diurnal light regimes used for plant growth conditions and leaf level gas exchange measurements.	136
<b>Figure 6.2</b>	First five days of the simulated sinusoidal high light regime ( $SN_{High}$ ), highlighting the random fluctuations in light intensity unique to each day.	137
<b>Figure 6.3</b>	Diurnal measurements of gas exchange; net CO <sub>2</sub> assimilation ( $A$ ); stomatal conductance ( $g_s$ ); Intrinsic water use efficiency ( $W_i$ ), measured under square wave regimes of light.	140
<b>Figure 6.4</b>	Gaussian signal of stomatal conductance ( $g_s$ ) during diurnal measurements of square wave light. Shown is a diagrammatic example highlighting the parameters extracted from the data.	141
<b>Figure 6.5</b>	Parameters extracted from the gaussian signal of stomatal conductance ( $g_s$ ) during diurnal measurements of square wave light	142
<b>Figure 6.6</b>	Temporal response of stomatal conductance ( $g_s$ ), net CO <sub>2</sub> assimilation ( $A$ ), and intrinsic water use efficiency ( $W_i$ ), to a step increase in light intensity, at different times of the day. Plants grown under the three high light treatments.	144

<b>Figure 6.7</b>	Temporal response of stomatal conductance ( $g_s$ ), net CO <sub>2</sub> assimilation ( $A$ ), and intrinsic water use efficiency ( $W_i$ ), to a step increase in light intensity, at different times of the day. Plants grown under the three low light treatments.	145
<b>Figure 6.8</b>	Temporal response of stomatal conductance ( $g_s$ ), to a step decreased in light intensity, at different times of the day.	146
<b>Figure 6.9</b>	Time constants for stomatal opening ( $\tau_i$ ), stomatal closure ( $\tau_d$ ), and light saturated rate of carbon assimilation ( $\tau_{ai}$ ) to a step change in light intensity. Final values of stomatal conductance after an increased step change in light intensity ( $G_i$ ); after a decreased step change in light intensity ( $G_d$ ); and saturation of net CO <sub>2</sub> assimilation at 1000 $\mu\text{mol m}^{-2} \text{s}^{-1}$ ( $A_i$ ), at different times of the day. Plants grown under the three high light treatments.	147
<b>Figure 6.10</b>	Time constants for stomatal opening ( $\tau_i$ ), stomatal closure ( $\tau_d$ ), and light saturated rate of carbon assimilation ( $\tau_{ai}$ ) to a step change in light intensity. Final values of stomatal conductance after an increased step change in light intensity ( $G_i$ ); after a decreased step change in light intensity ( $G_d$ ); and saturation of net CO <sub>2</sub> assimilation at 1000 $\mu\text{mol m}^{-2} \text{s}^{-1}$ ( $A_i$ ), at different times of the day. Plants grown under the three low light treatments.	148
<b>Figure 6.11</b>	Stomatal anatomical characteristics.	151
<b>Figure 6.12</b>	Correlation between stomatal conductance characteristics; maximum stomatal conductance ( $g_{s\text{max}}$ ) and nocturnal stomatal conductance ( $g_{s\text{night}}$ ) of plants grown under the six light treatments.	152
<b>Figure 6.13</b>	An example of adjustment made on an existing independent data set measured under a dynamic light environment, for the Ball-Berry model with and without the Gaussian element.	153

## List of Tables

### Chapter 3

<b>Table 3.1</b>	Summary of <i>Populus nigra</i> genotypes and environmental conditions at origin of genotypes.	32
<b>Table 3.2</b>	Photosynthetic parameters ( $V_{\text{cmax}}$ and $J_{\text{max}}$ ) estimated from the response of <i>A</i> to $C_i$ of the ten poplar genotypes.	43

### Chapter 4

<b>Table 4.1</b>	Photosynthetic photon flux density ( <i>PPFD</i> ) measurements taken at ambient conditions and under the two shade covers.	65
<b>Table 4.2</b>	Photosynthetic parameters ( $V_{\text{cmax}}$ and $J_{\text{max}}$ ) estimated from the response of <i>A</i> to $C_i$ of the three Poplar light treatments.	75

### Chapter 5

<b>Table 5.1</b>	Parameter values estimated from the response of <i>A</i> to light intensity, from plants grown under the four light regimes: <i>SQH</i> ; <i>FLH</i> ; <i>SQL</i> ; <i>FLL</i> .	110
<b>Table 5.2</b>	Cell size (width, length) and shape (length/width) from leaf tissues of plants grown under the four light treatments.	112
<b>Table 5.3</b>	Chlorophyll a/b ratio (Chl a/b) and total carotenoid:total chlorophyll ratio (Car/Chl) of plants grown under the four light treatments.	113
<b>Table 5.4</b>	Photosynthetic parameters estimated from the response of <i>A</i> to $C_i$ of plants grown under the four light regimes.	115
<b>Table 5.5</b>	Parameters describing the increase in area of the rosette as a function of time.	124

## Publications

All publications listed below were produced using data and/or ideas associated with this thesis. With the thesis author named as first, joint first or second author in each case.

**Matthews, J.S., Violet-Chabrand, S.R. and Lawson, T (2018)** Acclimation to fluctuating light impacts the rapidity of response and diurnal rhythm of stomatal conductance. *Plant Physiology* **176**(3): 1939-1951.

**Matthews, J.S., Violet-Chabrand, S.R. and Lawson, T (2017)** Diurnal variation in gas exchange: the balance between carbon fixation and water loss. *Plant Physiology* **174**(2): 614-623.

**Violet-Chabrand, S., Matthews, J.S., Simkin, A.J., Raines, C.A. and Lawson, T (2017)** Importance of Fluctuations in Light on Plant Photosynthetic Acclimation. *Plant Physiology* **173**(4): 2163-2179.

**Violet-Chabrand, S.R., Matthews, J.S., McAusland, L., Blatt, M.R., Griffiths, H. and Lawson, T (2017)** Temporal dynamics of stomatal behavior: modeling and implications for photosynthesis and water use. *Plant physiology* **174**(2): 603-613.

**Violet-Chabrand, S.R., Matthews, J.S., Brendel, O., Blatt, M.R., Wang, Y., Hills, A., Griffiths, H., Rogers, S. and Lawson, T (2016)** Modelling water use efficiency in a dynamic environment: An example using *Arabidopsis thaliana*. *Plant Science* **251**: 65-74

## Abbreviations

<b><i>A</i></b>	Net CO <sub>2</sub> assimilation rate per unit leaf area
<b><i>AC<sub>i</sub>Limit</i></b>	Limitation of <i>A</i> imposed by stomatal conductance
<b><i>A<sub>i</sub></i></b>	Light saturated carbon assimilation rate at 1000 μmol m <sup>-2</sup> s <sup>-1</sup>
<b><i>A<sub>mass</sub></i></b>	Net CO <sub>2</sub> assimilation rate per unit leaf dry mass
<b><i>A<sub>mass-sat</sub></i></b>	Light saturated rate of CO <sub>2</sub> assimilation on a mass basis
<b><i>A<sub>max</sub></i></b>	Light and CO <sub>2</sub> saturated rate of CO <sub>2</sub> assimilation
<b><i>A<sub>mass-max</sub></i></b>	Light and CO <sub>2</sub> saturated rate of CO <sub>2</sub> assimilation on a mass basis
<b><i>A<sub>sat</sub></i></b>	Light saturated rate of CO <sub>2</sub> assimilation
<b><i>A/C<sub>i</sub></i></b>	Net CO <sub>2</sub> assimilation rate ( <i>A</i> ) as a function of [CO <sub>2</sub> ]
<b><i>A/Q</i></b>	Net CO <sub>2</sub> assimilation rate ( <i>A</i> ) as a function of light intensity ( <i>Q</i> )
<b><i>C<sub>i</sub></i></b>	Intercellular CO <sub>2</sub> concentration
<b><i>C<sub>ic</sub></i></b>	<i>C<sub>i</sub></i> at which limitation of <i>A</i> switches between Rubisco- and RuBP regeneration
<b><i>Daily LUE</i></b>	Daily light use efficiency
<b><i>DF<sub>high</sub></i></b>	Measurements under diurnal high light fluctuating conditions
<b><i>DF<sub>low</sub></i></b>	Measurements under diurnal low light fluctuating conditions
<b><i>Diur<sub>Limit</sub></i></b>	Limitation of <i>A</i> imposed by stomata over the diurnal period
<b><i>FL</i></b>	Plants grown under fluctuating light
<b><i>FLH</i></b>	Plants grown under fluctuating high light
<b><i>FLL</i></b>	Plants grown under fluctuating low light
<b><i>FL<sub>High</sub></i></b>	Measurements under diurnal fluctuating high light conditions
<b><i>FL<sub>Low</sub></i></b>	Measurements under diurnal fluctuating low light conditions
<b><i>F<sub>q</sub>'/F<sub>m</sub>'</i></b>	Operating efficiency of photosystem II
<b><i>F<sub>q</sub>'/F<sub>v</sub>'</i></b>	Photosystem II efficiency factor
<b><i>F<sub>v</sub>'/F<sub>m</sub>'</i></b>	Maximum efficiency of photosystem II
<b><i>g<sub>m</sub></i></b>	Mesophyll conductance
<b><i>g<sub>smax</sub></i></b>	Anatomical maximum stomatal conductance
<b><i>g<sub>snight</sub></i></b>	Nocturnal conductance/ <i>g<sub>s</sub></i> when <i>PPFD</i> is at 0 at beginning of diurnal
<b><i>g<sub>s</sub></i></b>	Stomatal conductance to water vapour
<b><i>G<sub>d</sub></i></b>	Final values of <i>g<sub>s</sub></i> at 100 <i>PPFD</i> for stomatal closure
<b><i>G<sub>i</sub></i></b>	Final values of <i>g<sub>s</sub></i> at 1000 <i>PPFD</i> for stomatal opening
<b><i>G<sub>sin</sub></i></b>	Maximum <i>g<sub>s</sub></i> reached in the Gaussian element during the diurnal measurement
<b><i>J<sub>max</sub></i></b>	Maximum electron transport demand for RuBP regeneration

<b>LMA</b>	Leaf mass area
<b>LUE</b>	Light use efficiency
<b>NPQ</b>	Non-photochemical quenching
<b>PPFD</b>	Photosynthetic photon flux density
<b>PSI</b>	Photosystem I
<b>PSII</b>	Photosystem II
<b>R<sub>day</sub></b>	Day respiration
<b>R<sub>diurnal</sub></b>	Dark respiration measured at the beginning of the diurnal period
<b>R<sub>model</sub></b>	Dark respiration derived from A/Q curve analysis
<b>R<sub>sin</sub></b>	Relative percentage of Gaussian driven $g_s$
<b>SD<sub>Ab</sub></b>	Abaxial stomatal density
<b>SD<sub>Ad</sub></b>	Adaxial stomatal density
<b>SLA</b>	Specific leaf area
<b>SN</b>	Plants grown under sinusoidal light
<b>SNH</b>	Plants grown under sinusoidal high light
<b>SNL</b>	Plants grown under sinusoidal low light
<b>SN<sub>High</sub></b>	Measurements under diurnal sinusoidal high light conditions
<b>SN<sub>Low</sub></b>	Measurements under diurnal sinusoidal low light conditions
<b>SQ</b>	Plants grown under square-wave light
<b>SQH</b>	Plants grown under square-wave high light
<b>SQL</b>	Plants grown under square-wave low light
<b>SQ<sub>High</sub></b>	Measurements under diurnal square wave high light conditions
<b>SQ<sub>Low</sub></b>	Measurements under diurnal square wave low light conditions
<b>Tm<sub>sin</sub></b>	Time at the peak of the Gaussian element during the diurnal measurement
<b>Ts<sub>sin</sub></b>	Width of the peak of the Gaussian element during the diurnal measurement
<b>V<sub>cmax</sub></b>	Maximum rate of carboxylation by Rubisco
<b>VPD</b>	Vapour pressure deficit
<b>W<sub>i</sub></b>	Intrinsic water use efficiency
<b>Γ</b>	Light-compensation point
<b>τ<sub>ai</sub></b>	Time constant for light saturated rate of carbon assimilation at 1000 μmol m <sup>-2</sup> s <sup>-1</sup>
<b>τ<sub>d</sub></b>	Time constant for stomatal closure
<b>τ<sub>i</sub></b>	Time constant for stomatal opening
<b>[CO<sub>2</sub>]</b>	Atmospheric CO <sub>2</sub> concentration

# CHAPTER 1



## Introduction

## 1.1. Background

Plants fix carbon dioxide (CO<sub>2</sub>) from the atmosphere through photosynthesis, the dominant driver of terrestrial primary production. This is accompanied by the loss of water vapour through stomata; small pores on the leaf surface that regulate the diffusion of CO<sub>2</sub> and water vapour between the leaf and atmosphere. As the surface of most leaves are virtually impermeable to CO<sub>2</sub> and water, nearly all CO<sub>2</sub> fixed and water lost by plants passes through stomatal pores (Cowan and Troughton, 1971; Caird et al, 2007; Jones, 2013), and although typically occupying only a small proportion of the leaf surface (between 0.3 and 5%), stomata control the majority of all gas exchange between the external environment and leaf interior (Morison, 2003). Globally, an estimated 32 x 10<sup>18</sup> g of water vapour and 440 x 10<sup>15</sup> g of CO<sub>2</sub> are thought to pass through stomatal pores each year (Hetherington and Woodward, 2003), with estimations that 60% of all precipitation that falls on terrestrial ecosystems is taken up by plants and transpired through stomata (Morison, 2003; Katul et al, 2012). Furthermore, stomata account for 95% of all gaseous flux of CO<sub>2</sub> and water vapour in terrestrial vegetation, with an estimated 98% of the uptake of water by roots being transpired through stomatal pores (Morison, 2003). Therefore, stomatal behaviour has major consequences for photosynthetic CO<sub>2</sub> fixation and water loss from leaf to canopy levels, influencing carbon and hydrological cycles at global scales (Hetherington and Woodward, 2003; Keenan et al, 2012).

It has been shown, that changes in climatic conditions has had major implications for stomatal behaviour and ecosystem level water use efficiency (WUE; ratio of CO<sub>2</sub> fixation to water loss via transpiration) in northern hemisphere temperate forests (Keenan et al, 2013). Where increased levels of atmospheric CO<sub>2</sub> have driven reductions in stomatal conductance at the ecosystem level, with no observable cost to carbon uptake (Keenan et al, 2013, 2014); impacting the economics of carbon and water movement (Keenan et al, 2013). Furthermore, with recent research highlighting differences in the dynamic response of stomatal between and within species (Vico et al, 2011; Drake et al, 2013; McAusland et al, 2016), there is a need to re-assess the role of stomata in regulating the flux of carbon and water through terrestrial ecosystems in response to climate change, potentially improving the prediction of the impact of stomatal conductance dynamics in vegetation-climate models.

The capacity of stomata to allow CO<sub>2</sub> into or lose water vapour out of the leaf is known as stomatal conductance ( $g_s$ ), measured as mole of flux per unit of area ( $\text{mol m}^{-2} \text{s}^{-1}$ ). Stomatal behaviour regulates  $g_s$  and net photosynthetic rate ( $A$ ) through the diffusion of CO<sub>2</sub> into the leaf, depending on the needs of the plant, with the ratio between these two factors characterized as intrinsic water use efficiency ( $W_i =$

$A/g_s$ ). It has been shown that although potentially saving water, low  $g_s$  can restrict  $\text{CO}_2$  uptake into the leaf thereby reducing  $A$  (Farquhar and Sharkey, 1982; Barradas et al, 1994) and conversely negatively affect biomass accumulation (Fischer et al, 1998), whereas high  $g_s$  enables higher rates of  $A$  but at a greater cost of water loss via transpiration (Naumburg and Ellsworth, 2000; Lawson et al, 2010; Lawson and Blatt, 2014). Many studies have reported a strong correlation between  $A$  and  $g_s$  (see Wong et al, 1979) and it has been theorized that synchronicity exists to optimize the trade-off between photosynthesis and water loss (Buckley 2017). In order to maintain this optimal balance at the leaf level, stomata continually adjust aperture to balance the requirement for  $\text{CO}_2$  entry for photosynthesis against the need to maintain leaf hydration by reducing the transpiration of water vapour. This opening and closing is driven by a number of external environmental (e.g light) and internal signaling cues (Lawson and Blatt, 2014), and significant variation in response to these signals is known to exist between species (McAusland et al, 2016). In general, stomata open with increasing or high light, low atmospheric  $\text{CO}_2$  ( $[\text{CO}_2]$ ), and low vapour pressure deficit (VPD), while the reverse drives closure; low light, high  $[\text{CO}_2]$ , and high VPD (Raschke, 1975; Outlaw, 2003). However, a plant rarely experiences these environmental stimuli in isolation; therefore, stomata must respond continuously to multiple signals (Lawson and Morison, 2004; Lawson et al, 2010; Aasamaa and Söber, 2011), with some signals having a greater impact on stomatal response than others.

Light is the greatest environmental driver of photosynthesis, and stomata respond to changes in light intensity more than any other environmental signal (Shimazaki et al, 2007). Many studies have investigated steady-state stomatal responses to light, yet as these responses were measured under constant light conditions, the situation, which they represent, is rarely found in the natural environment (Jones, 2013). Measurements of  $g_s$  collected under field conditions correlate poorly with laboratory measurements under steady-state conditions as they are highly variable (Poorter et al, 2016), usually due to slow responses of  $g_s$  (see, McAusland et al, 2016) meaning that when measured, stomatal conductance has often not yet reached a new steady state value (Whitehead and Teskey, 1995; Kaiser and Kappen, 2000; Lawson et al, 2010). Whilst the majority of stomatal research has focused on steady state responses of stomatal conductance to environmental and internal signals, less time has been given to how the dynamic response of  $g_s$  impacts photosynthesis and therefore water use efficiency, and how this may change depending on the growth conditions of the plant. Therefore, a greater appreciation of stomatal functionality under different growth light acclimation states is required to improve the prediction of  $g_s$  behaviour in terrestrial vegetation-climate models.

## 1.2. Stomatal and photosynthetic acclimation to growth light

During growth, plants experience a range of different environmental conditions that impact the development of stomata and photosynthetic machinery. As mentioned above, light drives photosynthesis and influences stomatal behaviour, and therefore impacts acclimation (Ticha, 1982). Plants experience light in a range of intensities and spectral properties, largely due to changes in cloud and canopy cover, and self-shading from overlapping leaves, which represents major consequences for carbon gain (Percy, 1990; Chazdon and Percy, 1991) and water use (Hetherington and Woodward, 2003; Drake et al, 2013; McAusland et al, 2016). Stomata acclimate to the growth light environment by adjusting anatomy, morphology and function to directly maintain or even improve performance, fitness and survival (Ticha, 1982; Sage, 1994; Franks and Farquhar, 2001; Lake et al, 2001; Hetherington and Woodward, 2003).

Plant acclimation is often defined as 'physiological and morphological changes, which improve performance and survival of an individual plant by enhancing growth, resource use, reproductive output, stress tolerance, and/or lifespan during environmental change' (Sage, 1994). Acclimation to changes in light environment can be categorized as either dynamic or developmental. Developmental acclimation refers to changes in morphology (leaf thickness and area), anatomy (stomatal density), and photosynthetic biochemistry (e.g. Rubisco content), which are permanent and irreversible (Weston et al, 2000; Murchie, 2005). On the other hand, dynamic acclimation is usually a biological response to a change in environment or during stress that is largely reversible, and often occurs on shorter time scales (Walters and Horton, 1994; Mullineaux, 2006). Previously, studies investigating developmental acclimation have focused on the effect of light intensity, with less emphasis given to the effect of dynamic light during growth. The importance of light intensity on the anatomical acclimation of stomata in 'sun' and 'shade' (high and low light) leaves is well established. However, it is not clear if developmental acclimation of stomata (both anatomically and functionally) to dynamic light regimes exists, and if so how it may influence temporal stomatal responses and the synchronicity of  $A$  and  $g_s$  over the diurnal and seasonal period.

The speed and magnitude of the temporal response of  $g_s$  is known to vary between species (Vico et al, 2011; Drake et al, 2013; McAusland et al, 2016), but little is known about the heterogeneity in these dynamic responses associated with the acclimation of stomata to different light regimes. It has been hypothesized that variations in stomatal response may occur due to the spatial heterogeneity in gas exchange over individual leaves (Lawson and Weyers, 1999) and within canopies (Weyers and Lawson,

1997), and the differences in anatomical stomatal features associated with growth under different light intensities (sun/shade conditions), but this has yet to be characterized under a dynamic light regime.

Many studies have investigated the dynamics of stomatal response and photosynthesis to changes in light intensity, and the influence sun/shade flecks have on carbon gain (Knapp and Smith, 1987; Kirschbaum et al, 1988; Tinoco-Ojanguren and Pearcy, 1992, 1993; Lawson et al, 2010; Wong et al, 2012; McAusland et al 2016). However, to date the majority of these have only considered the influence of sun and shade flecks on carbon gain and stomatal response in species that have acclimated to shaded conditions, such as understory forest dwelling species (Chazdon, 1988; Chazdon and Pearcy, 1991). Furthermore, studies that have investigated acclimation to these conditions have generally focused on the photosynthetic acclimation (Terashima et al, 2006) rather than the stomatal acclimation, and these often ignore the dynamics of stomatal response and the potential limitation these may impose on carbon gain and water loss. Studies that have investigated stomatal acclimation to light (Givnish, 1988) primarily focused on the change in anatomical features (stomatal density, index, size), often associated with plants developmentally acclimated to sun and shade conditions (often performed under square wave light intensities), rather than the change in the functional response of stomata following acclimation to a 'natural' pattern of light like those experienced in the field.

### **1.3. Influence of stomatal anatomy on the response to light**

Stomatal anatomical features such as stomatal density, size and pore area are known to determine steady-state values of stomatal conductance ( $g_s$ ) (Franks and Farquhar, 2001), and are the key determinants for calculating the theoretical maximum of stomatal conductance ( $g_{smax}$ ) of a plant (Dow et al, 2014). Stomatal size and density vary greatly between plant species, and often change in response to the growth environment (Willmer and Fricker, 1996; Hetherington and Woodward, 2003; Franks and Beerling, 2009), with stomatal density regularly negatively correlated with stomatal size (Hetherington and Woodward, 2003; Franks and Beerling, 2009). Recently a great deal of consideration has been given to the impact of stomatal anatomical features on stomatal function and gas exchange, particularly to the diversity in stomatal morphology with reference to performance and plasticity in stomatal response (Franks and Farquhar, 2007).

Recent studies have implied that stomatal kinetics in response to fluctuations in the environment are affected by anatomical attributes including size and density (Drake et al 2013; Raven, 2014), the presence or absence of subsidiary cells (Franks and Farquhar, 2001) as well as guard cell shape

(McAusland et al, 2016), and that manipulation of these features could have positive effects for the efficiency of carbon assimilation and water use (Lawson et al, 2012; Doheny-Adams et al, 2012; Tanaka et al, 2013; Franks et al, 2015). Drake et al, (2013) investigated the correlation between stomatal density and size, with the speed of stomatal responses and found that the maximum rate of stomatal opening was driven by the surface-to-volume ratio of stomata, attributed to changes in stomatal density and size. Although the work of Drake et al (2013) and subsequent review from Raven (2014) made substantial progress in linking stomatal size to function, including the speed of  $g_s$  response to light, the size of stomata is not the only determinant of the speed of response. It has been shown that stomatal density (Franks et al, 2015; McAusland et al, 2016) and even stomatal clustering (Papanatsiou et al, 2016) can greatly affect  $g_s$  kinetics independent of the stomatal dimensions. The results of Drake et al, (2013) could have been skewed also by the experimental condition as step changes to high light from a state of darkness will not only incur biochemical limitations on stomatal movement and assimilation, but represent a state that is rarely seen in the natural environment except prior to dawn. Further recent work from Kaiser et al, (2016) using similar experimental conditions to those of Drake et al (2013), demonstrated that the limitation imposed on carbon assimilation ( $A$ ) by the slow response of  $g_s$  to a step change in light, was marginal and mostly biochemical. However, these authors may have potentially overestimated the biochemical limitation and underestimated the diffusional limitation on  $A$  due to the slow response of  $g_s$  and  $A$  from a state of darkness. Producing a step change from low to high light is more representative of the shifting light conditions regularly experienced by plants in nature during a diurnal period, caused by passing clouds and overlapping leaves (McAusland et al, 2016). In a recent study, McAusland et al (2016) compared the speed of stomatal responses to a step change in light, in a range of species, including model species and crops that differed in stomatal morphology. These authors reported that slow stomatal opening in response to increasing light intensity limited carbon assimilation by ca. 10%, which could equate to substantial losses in carbon gain over the course of the day, potentially negatively impacting productivity and yield. Whereas, slow stomatal closure when PPFD decreased resulted in a significant decrease in intrinsic water use efficiency, as overshoots in  $g_s$  by up to 80% were observed with only a negligible 5% gain in  $A$ . Closer coupling of  $A$  and  $g_s$  therefore has the potential to enhance carbon gain and  $W_i$ , and in turn improve performance, productivity and yield (Lawson et al, 2010; Lawson and Blatt, 2014; McAusland et al, 2016; Li et al, 2016; Qu et al, 2016).

#### **1.4. Temporal response of stomatal conductance ( $g_s$ ): Impact on photosynthesis and water use efficiency**

Most studies concerning stomatal behaviour on intact leaves have utilized stomatal conductance ( $g_s$ ) as

a substitute for pore area, to investigate stomatal movements to changes in environmental conditions. This has proved to be a useful tool for understanding stomatal dynamics, however, it should be noted that the relationship between  $g_s$  and pore area is not linear, as the influence of pore area on  $g_s$  decreases rapidly with the magnitude of stomatal opening (Kaiser and Kappen, 2001). Nevertheless, it was shown by Kaiser and Kappen (1997, 2000, 2001) that  $g_s$  and pore area measurements, would generally lead to the same assumption regarding investigations into the limitations on photosynthesis ( $A$ ) and water use efficiency. It is well known that a low  $g_s$  or slow stomatal opening can restrict the uptake of  $\text{CO}_2$  and therefore  $A$  (Farquhar and Sharkey, 1982; Barradas et al, 1994; Barradas and Jones, 1996; McAusland et al 2016), whilst high  $g_s$  facilitates higher rates of  $A$ , but inevitably at the 'cost' of greater water loss through transpiration ( $E$ ) (Barradas et al, 1994; Naumburg and Ellsworth, 2000; Lebaudy et al, 2008; Lawson et al, 2010; Lawson and Blatt, 2014; McAusland et al, 2013; 2016). It is commonly assumed that in response to fluctuating environmental parameters such as light, plants try to synchronize stomatal opening with the mesophyll demand for  $\text{CO}_2$ , and stomatal closure with the need to minimize water loss (Cowan and Farquhar, 1977; Farquhar et al, 1980; Mott, 2009; Drake et al 2013; Lawson et al 2012; Jones 2013). However, slow kinetics of the response of  $g_s$  (e.g. McAusland et al, 2016) will mean that stomatal aperture often lags behind the steady state target (Kaiser and Kappen, 2000), which substantially impacts photosynthesis and water use.

#### **1.4.1. Impact of fluctuations in light on stomatal response**

The dynamic response of stomata and photosynthesis to fluctuations in light has been studied extensively (Knapp and Smith, 1987; Kirschbaum et al, 1988; Tinoco-Ojanguren and Pearcy, 1993; Barradas et al, 1994; Lawson et al, 2010; Wong et al, 2012; McAusland et al 2016). However, the majority of these have focused on the impact of sun and shade flecks on photosynthesis in forest species that have evolved in a deep shade, understory environment (Chazdon, 1988; Chazdon and Pearcy, 1991; Tinoco-Ojanguren and Pearcy, 1993; Pearcy, 1994), or on plants that are acclimated to exposed conditions (Knapp and Smith 1987, 1988). In nature the response of  $A$  and  $g_s$  is largely dominated by fluctuations in photosynthetic photon flux density ( $PPFD$ ), which can vary on a scale of seconds, minutes, days, and even seasons (Assmann and Wang, 2001), and is predominantly driven by sun angle, cloud and canopy cover, and self-shading from overlapping leaves (Pearcy, 1990; Chazdon and Pearcy, 1991; Way and Pearcy, 2012), as a consequence leaves are subjected to varying spectral qualities and light intensities. It should also be noted that such rapid changes in  $PPFD$  will result in modifications to leaf temperature, with greater levels of  $g_s$  offering improved evaporative cooling through increased transpiration, and possibly enhanced protection against heat damage (Schymanski et

al, 2013). Therefore, the speed of stomatal response to environmental fluctuations should be considered crucial when assessing carbon uptake and water use efficiency in the field (Raschke, 1975; Kirschbaum and Pearcy, 1988; Lawson and Morison, 2004; Lawson et al, 2010).

As mentioned above many studies have focused on species that have developmentally acclimated to shade conditions, such as forest understory species, and have reported that sun flecks may contribute between 10 to 60% of the total daily carbon gain (Way and Pearcy, 2012), depending on forest type and plant age. Limitations on  $A$  imposed by stomata have been estimated at up to 30%, which is said to have significant implications for carbon sequestration and yield across many species types (Fischer et al 1998; Lawson and Blatt, 2014). Indeed Kirschbaum et al (1988), found that if initial  $g_s$  values before a step change in light intensity were high,  $A$  could be up to six times higher one minute after an increase in  $PPFD$  than if the initial  $g_s$  was low, with values of up to 82% reported for the limitation on  $A$  imposed by stomatal conductance, which illustrates the importance of  $g_s$  responses in natural dynamic conditions such as those found in the field. Continued increases in  $g_s$  after  $A$  has reached light saturation, have also been reported which led to a decrease in intrinsic water use efficiency ( $W_i$ ) with higher water loss for no extra  $CO_2$  gain (Kirschbaum et al, 1988; Tinoco-Ojanguren and Pearcy, 1993; Lawson et al, 2010).

It is well known that differences in the magnitude of change in  $g_s$  and the speed of stomatal opening and closing in response to sun and shade flecks, exist between and within species and even within individual plants (Assmann and Grantz, 1990; Ooba and Takahashi, 2003; Franks and Farquhar, 2007; Vico et al, 2011; Drake et al, 2013; McAusland et al, 2016). The response of  $g_s$  is also dependent upon leaf age (Urban et al, 2008), whole plant water status (Lawson and Blatt, 2014), and the duration and magnitude of the change in  $PPFD$  (Weyers and Lawson, 1997; Lawson et al, 1998; Lawson et al, 2012; Lawson and Blatt, 2014). Evidence also suggests that changes in the environment during growth and stomatal development, such as the history of stress (Pearcy and Way, 2012; Porcar-Castell and Palmroth, 2012; Wong et al, 2012; Zhang et al, 2012; Gerardin et al, 2018), influence the speed and dynamic response of stomata in mature leaves (Arve et al, 2017). The speeds of opening and closing in response to changing  $PPFD$  in many species are not correlated (Ooba and Takahashi 2003; McAusland et al, 2016); however, Vico et al (2011) compared 60 published gas exchange data sets on stomatal responses to  $PPFD$ , to determine the impact of delays in changes in  $g_s$  on photosynthesis. The authors discovered that a parallel relationship in the rates of stomatal opening and closing generally exists across all plant types, concluding that rates of stomatal opening were essentially correlated with the rate of closure.

It is often assumed that if there is no delay in stomatal opening or closing, optimal leaf gas exchange could be achievable (Cowan and Farquhar, 1977; Lawson and Blatt, 2014; Buckley, 2017), although it

must be taken into account that delays in stomatal movement may be specific to each plant type or species, and may be indicators of the current needs of the plant (Ooba and Takahashi, 2003; Manzoni et al, 2011; Vico et al, 2011; Drake et al, 2013). The response of  $g_s$  is thought to reflect this; where under well-watered conditions, stomata will remain open, particularly in lower canopy levels where other conditions (e.g. vapour pressure deficit; VPD) are more favorable, in order to readily exploit light energy from sunflecks. Maintaining high magnitudes of  $g_s$  through increased stomatal opening, would potentially maximize CO<sub>2</sub> diffusion into the leaf and therefore carbon assimilation (Pearcy, 2007; Way and Pearcy 2012; Lawson et al, 2012), even at the cost of further water loss (Allen and Pearcy, 2000). However, under drought or water-limited conditions stomata will often close, and remain so, to prioritize water conservation over carbon gain (Knapp and Smith, 1988; Ooba and Takahasi, 2003; Lawson et al, 2010, 2012; Lawson and Blatt, 2014).

#### **1.4.2. Determining the temporal response of stomatal conductance ( $g_s$ )**

Dynamic stomatal behaviour plays a crucial role in regulating the flux of carbon and water through the soil-plant-atmosphere continuum, and is an important element in scaling leaf level measurements of water use and photosynthesis to the canopy level (Weyers et al, 1997). The importance of integrating stomatal resistance and behavior into scaling models has long been recognized (Monteith et al, 1965; Weyers et al, 1997; Bernacchi et al, 2007; Lawson et al, 2010; Bonan et al, 2014; Barman et al, 2014; De Kauwe et al, 2015), and determining stomatal responses to environmental conditions through modeling efforts, is generally considered to be the most effective tool for simulating stomatal behaviour (Damour et al, 2010). Many current models calculate  $g_s$  in steady state, and are useful in predicting the impact of  $g_s$  on water and carbon fluxes at ecosystem and regional scales. However, heterogeneity in the spatial and temporal stomatal responses are often overlooked (Weyers et al, 1997; Lawson and Weyers, 1999), limiting the confidence with which these current models can predict larger scale responses or the impact of predicted climate change (Buckley et al, 2003; Dewar et al, 2009; Baldocchi, 2014). The addition of dynamic stomatal responses to existing models has the potential to reveal the extent to which  $g_s$  has been inaccurately predicted by steady-state models (Lawson and Blatt, 2014; Vialet-Chabrand et al, 2016; Poorter et al, 2016). This is an important factor, as stomata are continuously responding to changes in environmental conditions, and therefore  $g_s$  is rarely in steady-state. This reinforces the need for improved mechanistic models that incorporate the dynamic response of  $g_s$  (Damour et al, 2010; Vialet-Chabrand et al, 2013, 2016). In future modelling efforts that are attempting to scale from the leaf to canopy level, greater consideration should be given to the integration of temporal stomatal dynamics in response to fluctuations in environmental signals (Vico et al, 2011; Vialet-Chabrand et al, 2013, 2016). This would be to predict the impact of large-scale heterogeneity in

stomatal behaviour on water and CO<sub>2</sub> fluxes through the canopy, ecosystem and global scales. Furthermore, as stomata are exposed to constant fluctuations in the environment over the diurnal period, it is often the speed of stomatal response to a change in condition that is key in determining CO<sub>2</sub> uptake and transpiration over the course of the day (Mencuccini et al, 2000; Tallman, 2004), rather than the steady state values often reported that are often the basis of many existing models.

### **1.5. Stomatal behaviour and co-ordination of $A$ and $g_s$ over the diurnal period**

In the field, environmental conditions are rarely stable and influence  $A$  and  $g_s$  responses continuously through the day, leading to complex kinetic patterns over the diurnal period. Stomatal conductance ( $g_s$ ) appears to be closely linked with mesophyll demands for CO<sub>2</sub>, and a strong correlation between photosynthetic rate ( $A$ ) and  $g_s$  is often observed (Wong et al, 1979; Farquhar and Sharkey, 1982; Mansfield et al, 1990; Buckley and Mott, 2013), and although conserved, it is not always constant (Lawson and Morison, 2004; Bonan et al, 2014). The close correlation between photosynthesis ( $A$ ) and stomatal conductance ( $g_s$ ) is thought to help maximize  $A$  and minimize transpiration over a diurnal period depending on the current needs of the plant. This is thought to be the result of co-ordination in response to environmental factors, such as light intensity, with  $g_s$  often limiting  $A$  irrespective of whether  $A$  is the main optimization target. For example, it has been shown that maintaining leaf water status under drought conditions is often more important than carbon fixation and, as such, the plant will prioritize this signal and respond accordingly (Lawson and Morison, 2004; Lawson et al, 2010; Aasamaa and Söber, 2011).

Cowan and Farquhar (1977) deduced that the coordination between  $A$  and  $g_s$  can be seen as a plant response to control  $g_s$  in a way that will maximize  $A$  and minimize transpiration over a typical diurnal light pattern (Buckley, 2017). However, observations of  $g_s$  in response to variations in light intensity revealed that, stomatal responses do not often mimic these simulations. Instead,  $g_s$  responses are an order of magnitude slower than  $A$  and can continue to increase even when  $A$  reaches a new steady state level, resulting in a limitation of  $A$  during the initial part of the response followed by an unnecessary increase in transpiration driven by the overshoot in  $g_s$  (Vico et al, 2011; Lawson et al, 2012; Vialet-Chabrand et al, 2013; Drake et al, 2013; Lawson and Blatt, 2014; McAusland et al, 2016). This will often result in more water loss than is necessary for the gain in CO<sub>2</sub> (Lawson and Blatt, 2014). In order to understand how plants balance carbon gain and water loss, gas exchange needs to be considered at the plant or canopy scale, and for that reason, it is important to recognize the spatial and temporal aspects of the stomatal response over a diurnal period.

A number of current models (Damour et al, 2010) predict the diurnal time course of  $g_s$  and  $A$  based on equations developed by Ball et al. (1987) and Farquhar et al. (1980), respectively. These models predict  $g_s$  and  $A$  in steady state and do not include any temporal (speed) or long term (diurnal) effect as well as how the relationship between  $A$  and  $g_s$  may vary across the leaf surface. The model of Ball et al. (1987) used the apparent coordination of  $A$  and  $g_s$  as a basis to predict  $g_s$  but does not consider the slow temporal response of stomata, which can often lead to imprecise predictions of the diurnal time course of  $g_s$  (Violet-Chabrand et al, 2013). In general, the diversity of coordination between  $A$  and  $g_s$  observed in steady state across species, suggests that there is no strong selective pressure for this trait in the field, which highlights the need for improvements in understanding the patterns of  $g_s$  over the diurnal period in predictive models.

### **1.5.1. Mechanisms of coordination between $g_s$ and $A$**

For many years internal  $\text{CO}_2$  concentration ( $C_i$ ) was considered to link stomatal responses to photosynthetic demands for  $\text{CO}_2$  (Ball and Berry, 1982; Mott, 1988). For example, when photosynthetic rate ( $A$ ) increases when a plant is subjected to an increase in light,  $C_i$  is reduced as carbon is fixed and stomata respond to the increased demand for  $\text{CO}_2$  by increasing aperture, and conversely when the demand for  $\text{CO}_2$  decreases with higher  $C_i$  it results in stomatal closure. However, recent research has suggested that  $C_i$  is not the only driver of the coordination between  $A$  and  $g_s$ . Von Caemmerer et al (2004) suggested that guard cells might not sense  $C_i$  but instead sense external atmospheric  $\text{CO}_2$  concentrations ( $[\text{CO}_2]$ ), whilst other reports have suggested that stomatal responses to  $C_i$  are too small to account for the observed change in  $g_s$  in response to light (Raschke, 1975; Farquhar and Raschke, 1978; Sharkey and Raschke, 1981; Farquhar and Sharkey, 1982). More recent studies on transgenic plants showed increases in  $g_s$  in response to photosynthetic photon flux density ( $PPFD$ ) even in plants with reduced  $A$  and higher  $C_i$  values (von Caemmerer et al, 2004; Baroli et al, 2008; Lawson et al, 2008), which agrees with reports that  $g_s$  responds to various environmental (and internal) stimuli even when  $C_i$  is held constant (Messinger et al, 2006; Lawson et al, 2008; Wang and Song, 2008). This has led to the suggestion that an unknown signal produced by the mesophyll is sensed by the guard cells triggering a stomatal response. Early research suggested an aqueous signal (Lee and Bowling, 1992; 1995), including photosynthetic metabolites such as ATP, NADPH and ribulose 1, 5-bisphosphate (RuBP) (Wong et al, 1979; Farquhar and Wong, 1984; Lee and Bowling, 1992; Zeiger and Zhu, 1998; Tominaga et al, 2001; Buckley et al, 2003), as well as malate and sugar (Hedrich and Marten, 1993; Hedrich et al, 1994; Lee et al 2008), whilst more recent research has suggested a gaseous signal (Mott et al, 2008; Sibbersen and Mott, 2010; Mott and Peak, 2013). Furthermore, a number of alternative suggestions have been put

forward including guard cell photosynthesis itself (Lawson et al, 2003; Lawson and Morison, 2004; Lawson, 2009). Most of these experiments mentioned above were performed on herbaceous angiosperms and evidence suggests that these stomatal responses may differ between species and plant type (Chater et al, 2011; Ruszala et al, 2011; McAdam and Brodribb, 2012). This includes differences in the way stomata perceive signals such as: CO<sub>2</sub>, Abscisic acid (ABA; Brodribb, 2017), leaf to air vapour pressure deficit (VPD; Martins et al, 2016; McAdam and Brodribb, 2015) and the intensity and quality of light (Doi et al, 2015). Differences in the stomatal response to these signals will influence the diffusion of CO<sub>2</sub> to mesophyll tissues and therefore impact the coordination between  $A$  and  $g_s$ . These mechanisms mainly refer to short-term responses (seconds to minutes) and are not necessarily sufficient to explain the diurnal influence on  $A$  and  $g_s$ . Sucrose metabolism has been proposed to play a role in the longer-term co-ordination (over the diurnal period) of  $A$  and  $g_s$  (Lawson et al, 2014), where excess sucrose during periods of high photosynthesis is carried towards the stomata by the apoplast, stimulating stomatal closure either through some signalling mechanism or by acting as an osmoticum (Lu et al, 1997; Outlaw and William, 2003; Kang et al, 2007; Kelly et al, 2013). Such a process could only occur over longer timescales as high rates of photosynthesis are not associated with low  $g_s$ , however decreases in  $g_s$  are often seen towards the end of the diurnal period despite environmental conditions being similar to morning conditions (Lawson et al, 2014).

In nature, environmental conditions that are rarely stable influence  $A$  and  $g_s$  responses continuously through the day, leading to complex kinetic patterns in the co-ordination of  $A$  and  $g_s$ . Therefore, increasing the speed of stomatal response and/or improving the coordination between mesophyll and stomatal responses, represents an unexploited potential avenue to improve  $A$  and plant water use efficiency (Lawson et al, 2010).

### **1.5.2. Diurnal stomatal behaviour**

Stomatal movements of most plants are due to the transport and accumulation of osmotically active solutes. Therefore, as a large body of evidence supports the role of ion transport in both stomatal opening and closing (Willmer and Fricker, 1996; Blatt, 2000; Chen et al, 2012; Hills et al, 2012), it must be taken into consideration when attempting to model dynamic and diurnal stomatal behaviour. The main inorganic transporters and anions that make up the bulk of solutes driving the flux of water and guard cell turgor, are K<sup>+</sup>, Cl<sup>-</sup>, malate<sup>2-</sup> and Suc (Willmer and Fricker, 1996; Roelfsema and Hedrich, 2005; McAinsh and Pittman, 2009), which must be transported across the plasma membrane as mature guard cells lack plasmodesmata. Because of this the dynamic responses of stomata are ultimately linked

to characteristics of the guard cells, such as the capacity for solute transport and the speed with which transport responds to an environmental stimulus (Lawson and Blatt, 2014).

Current models describing diurnal variations in gas exchange use predicted steady state values of  $g_s$ , which presume instantaneous variations in  $g_s$  at each light level (Damour et al, 2010). These models describe the response of  $g_s$  to light intensity but fail to accurately predict variations in  $g_s$ , as they neglect the temporal aspect of stomatal response (Violet-Chabrand et al, 2013). Over the diurnal period, a number of species display a decrease in  $g_s$  and  $A$  that is not driven by decreases in light intensity or the temporal response of  $g_s$  (Mott and Parkhurst, 1991; Allen and Percy, 2000; Mencuccini et al, 2000; Moriana et al, 2002; Dodd et al, 2006; de Dios et al, 2012), although the exact mechanism for this requires further investigation. As mentioned earlier, sugar accumulation at high photosynthetic rates are believed to provide a long-term photosynthetic feedback on  $g_s$  (Lu et al, 1995, 1997; Outlaw and William, 2003; Kang et al, 2007; Kelly et al, 2013), which also needs to be taken into account when considering the incorporation of temporal responses into models of stomatal behaviour. Models have been proposed that work on the assumption that the pool of sugars in the mesophyll, resulting from the difference between the rate of sugar production by photosynthesis and their rate of export, increasingly inhibit  $A$  over the diurnal period (Noe and Giersch, 2004). These models agree with recent research that has focused on the role of sugars in the regulation of guard cell aperture and the co-ordination between stomatal behaviour and mesophyll photosynthesis over the diurnal period (Lugassi et al, 2015; Santelia and Lawson, 2016; Daloso et al, 2016).

Toward the end of the day, the often-slow response of  $g_s$  to changes in the environment can result in the maintenance of high  $g_s$ , which leads to substantial water losses that are not accompanied by any carbon uptake (Blom-Zandstra et al, 1995; Lawson and Blatt, 2014). Improving the rapidity of the response of  $g_s$  may fundamentally reduce the limitation of  $A$  and prevent the slow decrease in  $A$  and  $g_s$  through the day, potentially helping to maintain photosynthetic carbon assimilation for longer, whilst positively influencing plant productivity and biomass. It should also be kept in mind that the water status of the plant will affect temporal responses of  $g_s$  (Lawson and Blatt, 2014), which will often be species specific as the transduction of the light signal triggering stomatal opening could be modified or reduced to maintain leaf turgor (Aasamaa and Sober, 2011; Inoue and Kinoshita, 2017). As a consequence, the water status of the plant is an important determinant of the steady state value of  $g_s$  and could result in a strong limitation on  $A$  throughout the diurnal period (Tuzet et al, 2003; Yan et al, 2016). However, as most studies have been carried out under 'ideal' well-watered conditions or using steady state approaches (Wolf et al, 2016; Sperry et al, 2016), there are very few data sets describing the influence of leaf water status or drought on the temporal response of  $g_s$  (Lawson and Blatt, 2014),

and even less on the modelling of this stomatal behaviour. Water availability and its transport from roots to the stomata could also be a limiting factor for the rapidity of  $g_s$  response, with factors such as hydraulic conductance, leaf vein density and stomatal distribution potentially playing an important role in spatial and temporal stomatal responses.

To help evaluate the impact of dynamic stomatal responses to perturbations in environmental conditions over the diurnal period, more substantial data would need to be collected for and by the community to develop and validate future predictive and descriptive models.

## 1.6. Aims and Objectives

Plant acclimation to growth light has been studied extensively, however, the majority of studies have focused on light intensity and photo-acclimation, concentrating on how intensity under constant light impacts stomatal anatomy and photosynthetic capacity. Few have truly explored the impact of dynamic growth light on the acclimation of stomatal behaviour and response.

The aim of this study is to understand how acclimation to dynamic light will impact stomatal behaviour and diurnal response, to realize the influence this has on photosynthesis and water use efficiency. Having a greater understanding of the acclimation of stomatal behaviour to light will improve the prediction of stomatal conductance in vegetation-climate models, which will facilitate greater understanding of ecosystem response and fitness to changing climatic conditions. To investigate how the acclimation of stomatal behaviour to light impacts carbon gain and water use efficiency, the aims were addressed by the following objectives:

- Evaluate intra-specific variation in the kinetics of  $g_s$  response, carbon assimilation and water use efficiency to light in the model tree species *Populus nigra*. (Chapter 3)
- Assess the impact of growth light intensity on the acclimation of stomatal behaviour, carbon assimilation and water use efficiency in *Populus nigra*. (Chapter 4)
- Determine to what extent growth under dynamic fluctuating light impacts photosynthetic acclimation in the model species *Arabidopsis*. (Chapter 5)
- Does growth under fluctuating light influence the acclimation of stomatal behaviour and anatomy in *Arabidopsis*? (Chapter 6)
- To what extent does acclimation to growth light impact the prediction of stomatal conductance ( $g_s$ ) over the diurnal period? (Chapter 6)

# CHAPTER 2

---

## Materials and Methods

*This section outlines methods generic to all experimental chapters. Modifications made to protocols outlined here and protocols specific to a chapter can be found in the methods section of each experimental chapter.*

## 2.1. Plant material and growth conditions

For information regarding growth and selection of plant material, growth environment and experimental set up, please refer to individual chapters.

### 2.1.1. Fluctuating growth light regime

The fluctuating light regime used for growth of *Arabidopsis* and for diurnal measurements was recreated and adjusted over a 12h period, from natural variations in light intensity recorded during a relatively clear day in July 2014 at the University of Essex (Fig. 2.1). The average light intensity integrated over the entire light regime was  $460 \mu\text{mol m}^{-2} \text{s}^{-1}$  photosynthetic photon flux density (*PPFD*). This light regime was considered as the fluctuating high light treatment, with the same regime but with half the average light intensity ( $230 \mu\text{mol m}^{-2} \text{s}^{-1}$ ) set as the fluctuating low light treatment. Using these average light intensities, square wave high and low light regimes were created and set over the same 12h period (Fig. 2.1).

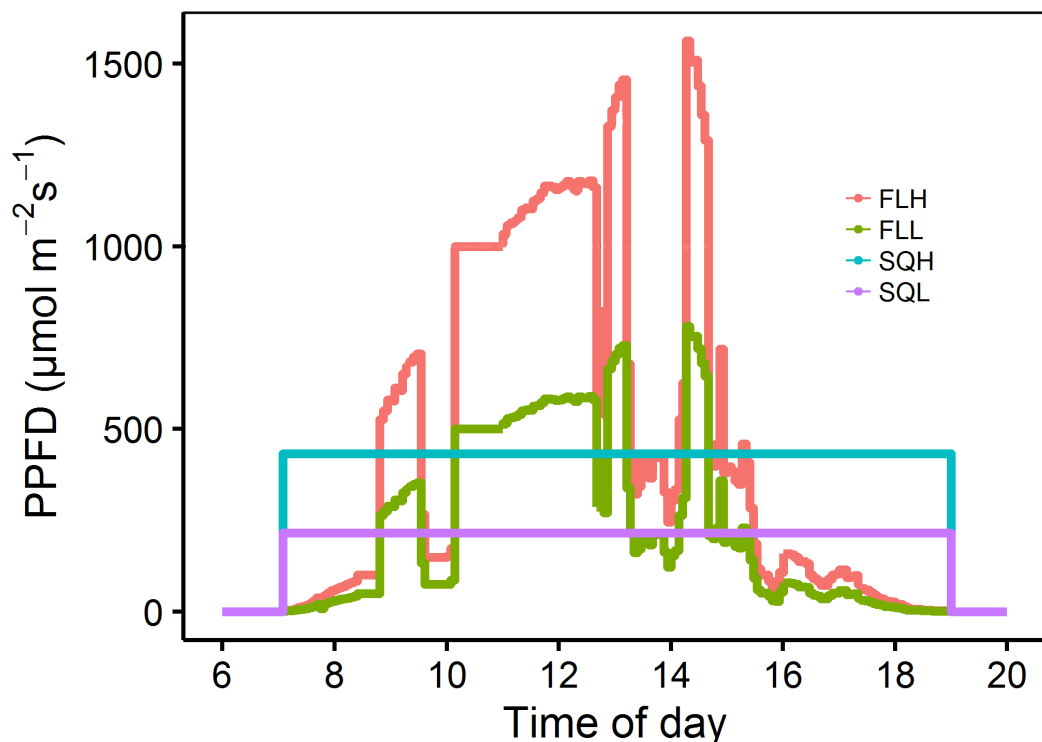


**Figure 2.1.** Light regimes used for plant growth and leaf level diurnal measurements of gas exchange. Areas under the curve represent the same average amount of light intensity over the 12-h light regime depending on the light intensity:  $460 \mu\text{mol m}^{-2} \text{s}^{-1}$  = square wave high light (*SQH*) and fluctuating high light (*FLH*),  $230 \mu\text{mol m}^{-2} \text{s}^{-1}$  = square wave low light (*SQL*) and fluctuating low light (*FLL*).

### 2.1.2. Simulating daily light fluctuations for sinusoidal growth light regime.

The sinusoidal light regime was simulated using a specific algorithm (devised by Silvere Vialet-Chabrand) including a sinusoidal variation with random alterations in light to maintain the average daily amount of light intensity (*PPFD*) constant during the growth. The sinusoidal variation as a function of time (*t*) was obtained by:

$$PPFD = ae^{-\frac{(t-b)^2}{2c^2}} - ae^{-\frac{(t_1-b)^2}{2c^2}}$$

where *a* is the maximum *PPFD* reached during the peak, *b* is the time at which the peak is reached and *c* a parameter related to the width of the peak. The value of *a* was arbitrarily set to 1000 for convenience as the whole curve is rescaled at the final step of the algorithm.

A random number of increases and decreases in light intensity at different times throughout the diurnal period were added, and ranged between 0 and 80% of the original light level. This guaranteed a light intensity that mimics the daily variation of diffuse light through changes in cloud cover, canopy cover, and self-shading.

The curve was scaled to obtain an average light intensity of 460  $\mu\text{mol m}^{-2} \text{s}^{-1}$  for the sinusoidal high light treatment (*SN<sub>High</sub>*) and 230  $\mu\text{mol m}^{-2} \text{s}^{-1}$  for the sinusoidal low light treatment (*SN<sub>Low</sub>*) as used in the fluctuating and square wave light intensities. The same process was repeated for the number of days required for the complete life cycle of *Arabidopsis* and was then programmed into the Heliospectra LED light source (Heliospectra AB, Göteborg, Sweden). The five first days simulated are shown in Fig. 2.2, highlighting that each day had a unique pattern of light intensity, mimicking a natural light environment.

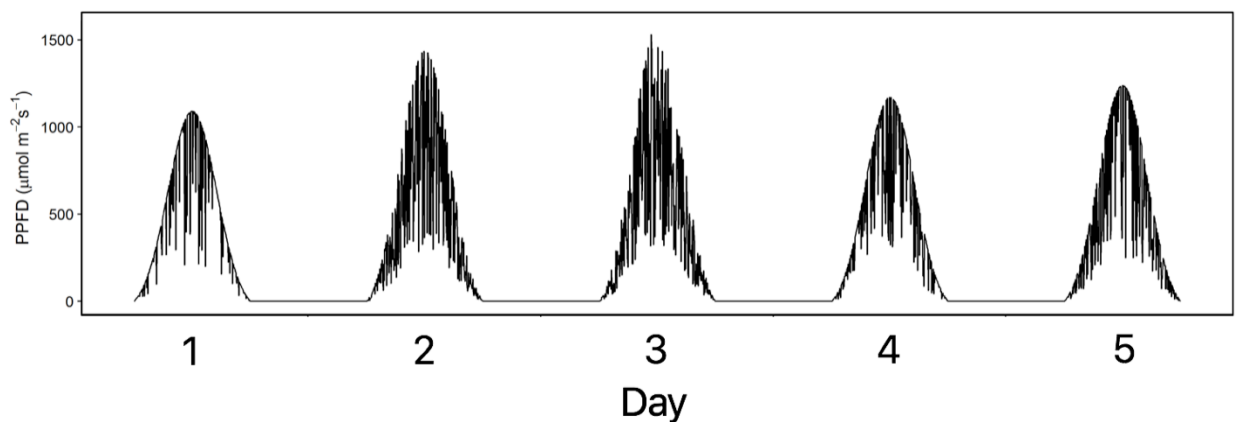


**Figure 2.2.** First five days of the simulated sinusoidal high light regime (*SN<sub>High</sub>*), highlighting the random fluctuations in light intensity unique to each day.

## 2.2. Leaf gas exchange

All gas exchange ( $A$  and  $g_s$ ) parameters were recorded using a Li-Cor 6400XT portable gas exchange system, with light delivered via a Li-Cor 6400-40 fluorometer head unit (Li-Cor, Lincoln, Nebraska, USA), with blue and red LEDs. For all gas exchange measurements, a constant flow rate was set at  $300 \mu\text{mol s}^{-1}$ , with cuvette conditions maintained at a  $\text{CO}_2$  concentration of  $400 \mu\text{mol mol}^{-1}$ , a leaf temperature of  $25^\circ\text{C}$  (unless otherwise stated). To maintain a leaf to air water vapour pressure deficit of  $1 (\pm 0.2) \text{ kPa}$ , the system was connected to a Li-Cor 610 portable dew point generator. All measurements were taken using the youngest, fully expanded leaf and were made between 10am and 3pm (except for diurnal measurements) to guarantee a high level of stomatal opening and photosynthetic activation, and to reduce diurnal effects. Intrinsic water use efficiency was calculated as  $W_i = A/g_s$ .

### 2.2.1. $A/Q$ (net photosynthetic rate/ $PPFD$ ) response curves

The response of net  $\text{CO}_2$  assimilation rate ( $A$ ) to photosynthetic photon flux density ( $PPFD$ ) ( $A/Q$  response curves) was measured under cuvette conditions as mentioned above. Leaves were initially stabilised at irradiance above saturation at  $1800 \mu\text{mol m}^{-2} \text{ s}^{-1}$  and a measurement was recorded, at which point  $PPFD$  was decreased in 13 steps ( $1500, 1300, 1100, 900, 700, 550, 400, 300, 200, 150, 100, 50, 0 \mu\text{mol m}^{-2} \text{ s}^{-1}$ ) with a new recording being taken at each new light level once  $A$  had reached a new steady-state (approx. 1-3 min), and before stomatal conductance ( $g_s$ ) decreased to the new light levels to reduce the possibility of stomatal limitation of  $A$ .

### 2.2.2. $A/C_i$ (net photosynthetic rate/intercellular $\text{CO}_2$ concentration) response curves

The response of net  $\text{CO}_2$  assimilation rate ( $A$ ) to intercellular  $\text{CO}_2$  concentration ( $C_i$ ) ( $A/C_i$  response curves) was measured at a saturating light intensity of  $1500 \mu\text{mol m}^{-2} \text{ s}^{-1}$ . Leaves were initially stabilized for a minimum of 10-15 minutes at ambient  $\text{CO}_2$  concentration of  $400 \mu\text{mol mol}^{-1}$ , upon reaching a stable signal a measurement was taken before ambient  $\text{CO}_2$  was decreased to  $250, 150, 100, 50 \mu\text{mol mol}^{-1}$  before returning to the initial value of  $400$ , and increased to  $550, 700, 900, 1100, 1300, 1500, 1750 \mu\text{mol mol}^{-1}$ . Recordings were taken at each new  $\text{CO}_2$  level when  $A$  had reached a new steady state (approx. 1-3 min), and before stomatal conductance ( $g_s$ ) changed to the new  $\text{CO}_2$  levels to reduce the possibility of stomatal limitation of  $A$ .

### 2.2.3. Temporal response of $A$ and $g_s$

For the step change in light, leaves were placed in the Li-Cor cuvette and equilibrated at a PPFD of  $100 \mu\text{mol m}^{-2} \text{s}^{-1}$  until both  $A$  and  $g_s$  were at steady state. Steady state in this case was defined as less than a 2% change of the given parameter over a 5-minute period (this would take *ca.* 10-30 min). Once at steady state, PPFD was increased to  $1000 \mu\text{mol m}^{-2} \text{s}^{-1}$  for 1.5h before returning to  $100 \mu\text{mol m}^{-2} \text{s}^{-1}$  for a further 1h.  $A$  and  $g_s$  were recorded every 20 seconds.

For measurements at different light levels the protocol remained the same (as above), however the starting PPFD was changed to either 50 or  $500 \mu\text{mol m}^{-2} \text{s}^{-1}$ , and the target to either 250 or  $1500 \mu\text{mol m}^{-2} \text{s}^{-1}$  respectively.

For measurements at the different times of day (Morning, Midday, Evening), plants were removed from the growth chamber at 8am, 1pm, and 6pm, and the increase in PPFD from  $100$  to  $1000 \mu\text{mol m}^{-2} \text{s}^{-1}$  was initiated at approximately 9am, 2pm, and 7pm respectively. To prevent previous step changes in light (e.g. Morning) having an effect on the response to step changes later in the day (e.g. midday), individual leaves that were subjected to a step change in light were not subjected to another measurement until the following day.

### 2.2.4. Diurnal measurements

Leaves were initially placed in the cuvette (Li-Cor 6400-40 fluorometer head) in darkness, with  $A$  and  $g_s$  allowed to stabilize under the controlled cuvette conditions (as shown above) for a minimum of 15-30 minutes. After readings of  $A$  and  $g_s$  were stable for at least 5 minutes, the 12h light program was started, with measurements of  $A$ ,  $g_s$  and chlorophyll fluorescence parameters recorded every 2 minutes.

### 2.2.5. Measurements and modelling of diurnal stomatal conductance under constant light

To investigate the acclimation of diurnal stomatal response in plants grown under the six light treatments, all plants were subjected to a square wave light regime corresponding to their growth light intensity ( $SQ_{High}$ : high light treatments;  $SQ_{Low}$ : low light treatments; Fig. 2.1), with net  $\text{CO}_2$  assimilation ( $A$ ) and stomatal conductance ( $g_s$ ) measured continuously over the diurnal period.

On the day of measurement, plants were removed from the growth chamber prior to the initiation of the diurnal regime of light. Leaves were placed in the Li-Cor cuvette (for conditions see 2.2.) in darkness

and both  $A$  and  $g_s$  were allowed to stabilize for a minimum of 15-30 minutes. After  $A$  and  $g_s$  were at steady state for at least 5 minutes (<2% change over this time period), the automatic 12 h light programs ( $SQ_{High}$  and  $SQ_{Low}$ ) were started, with  $A$  and  $g_s$  recorded every 2 minutes.

As with the fluctuating light regimes laid out in section 2.1.1, the  $SQ_{High}$  regime had an average PPFD of  $460 \mu\text{mol m}^{-2} \text{s}^{-1}$  and the  $SQ_{Low}$  regime an average of  $230 \mu\text{mol m}^{-2} \text{s}^{-1}$  PPFD.

The temporal response of  $g_s$  to external and internal cues was modelled using an exponential equation:

$$\frac{dg_s}{dt} = \frac{(G - g_s)}{\tau}$$

where  $G$  represents the steady state target of  $g_s$  and  $\tau$  the time constant to reach 63% of  $G$ . Due to the asymmetry of response during a step increase or decrease in light intensity, a different value of  $\tau$  was used in each condition ( $\tau_i$  and  $\tau_d$ ).

The steady state target ( $G$ ) was calculated as the sum of three processes: the decrease of  $g_s$  through the diurnal period ( $D$ ), the bell shape variation of  $g_s$  through the diurnal period ( $S$ ), the response of  $g_s$  to light intensity variation ( $G_1, G_2, G_3$ ). Before and after the lighted period, the response of  $g_s$  to light was set to  $G_1$  and  $G_3$  respectively, two values representing the steady state  $g_s$  at the beginning and end of the dark period. During the lighted period, it was set to  $G_2$  assuming that the internal cues were activated by light.

The decrease of  $g_s$  ( $D$ ) as a function of time ( $t$ ) was modelled using an exponential function constrained over the lighted portion of the diurnal period (between  $t_{on}$  and  $t_{off}$ ):

$$D = \begin{cases} G_{sl} \left( 1 - e^{-\frac{t-t_{on}}{\tau_{sl}}} \right), & \text{if } t > t_{on} \text{ and } t < t_{off} \\ 0, & \text{if } t < t_{on} \text{ and } t > t_{off} \end{cases}$$

where  $G_{sl}$  is the steady state target of the decrease in  $g_s$  and  $\tau_{sl}$  the time constant to reach 63% of  $G_{sl}$ .

The bell shape variation of  $g_s$  ( $S$ ) as a function of time ( $t$ ) was modelled using a Gaussian function:

$$S = G_{sin} e^{-\frac{(t-Tm_{sin})^2}{(2Ts_{sin}^2)}}$$

where  $G_{sin}$  is the maximum  $g_s$  reached during the peak,  $Tm_{sin}$  the time at the centre of the peak and  $Ts_{sin}$  a parameter related to the width of the peak (see Fig. 2.3).

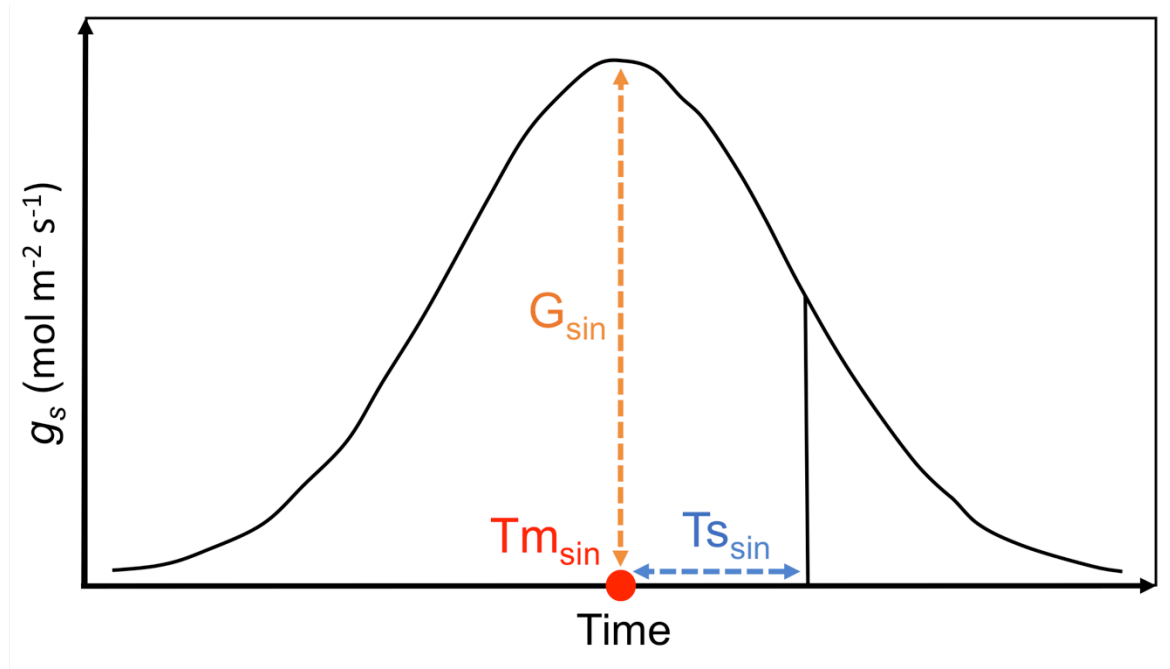


**Figure 2.3.** Parameters derived from the Gaussian function describing the bell shaped variation of  $g_s$ .  $G_{sin}$ ; the maximum  $g_s$  reached during the peak,  $Tm_{sin}$ ; the time at the centre of the peak and  $Ts_{sin}$ ; parameter related to the width of the peak.

This model was implemented using the stan language and adjusted on the observation using R and the RStan package (<http://mc-stan.org/users/interfaces/rstan>), with assistance from Silvere Vialet-Chabrand.

## 2.3. Modelling gas exchange parameters

### 2.3.1. Determination of mass integrated net CO<sub>2</sub> assimilation

Net CO<sub>2</sub> assimilation ( $A$ ) was converted to a mass integrated measurement using leaf mass area ( $LMA$ ) measured on the youngest fully expanded leaf:

$$A_{mass} (\mu\text{mol } g^{-1} s^{-1}) = \frac{A (\mu\text{mol } m^{-2} s^{-1})}{LMA (g m^{-2})}$$

### 2.3.2. Estimating photosynthetic capacities

The maximum velocity of Rubisco for carboxylation ( $V_{cmax}$ ), the maximum rate of electron transport for RuBP regeneration ( $J_{max}$ ), respiration rate during the day ( $R_{day}$ ), and mesophyll conductance ( $g_m$ ) were estimated using the curve fitting method described by Sharkey *et al.* (2007). Maximum rates of CO<sub>2</sub> assimilation ( $A_{max}$ ) were determined from recorded values at 1500  $\mu\text{mol mol}^{-1}$  CO<sub>2</sub> concentration.

### 2.3.3. Assessing stomatal limitation from $A/C_i$ response curves

The hypothetical  $A$  that could be obtained if the mesophyll had free access to CO<sub>2</sub> in the ambient air was calculated to quantify the limitation that the combined stomatal and boundary layer conductance ( $g_L$ ) impose on leaf CO<sub>2</sub> uptake. This leads to the assumption that the ambient CO<sub>2</sub> concentration equals the intercellular CO<sub>2</sub> concentration ( $C_a=C_i$ ). This was calculated from the  $A/C_i$  response curves using the graphical method outlined by Farquhar and Sharkey (1982); the limitation ( $l$ ) imposed by  $g_L$  is given by:

$$l = (A'' - A')/A''$$

Where  $A'$  is the photosynthetic rate ( $A$ ) at ambient CO<sub>2</sub> conditions; and  $A''$  the hypothetical  $A$  that would be obtained if there was free access to ambient CO<sub>2</sub> concentrations.

### 2.3.4. Modelling net CO<sub>2</sub> assimilation rates

Net CO<sub>2</sub> assimilation ( $A$ ) as a function of light intensity ( $PPFD$ ) was modelled using an adapted non-rectangular hyperbola to simulate the maximum diurnal variations of  $A$  in absence of stomatal limitation under different light intensity conditions:

$$A = \frac{\alpha_i PPFD + (A_{sat} + R_{day}) - \sqrt{(\alpha_i PPFD + (A_{sat} + R_{day}))^2 - 4\theta\alpha_L PPFD(A_{sat} + R_{day})}}{2\theta} - R_{day}$$

with  $\alpha_i$  the quantum yield of photosynthesis,  $A_{sat}$  the maximum net CO<sub>2</sub> assimilation at saturating light,  $R_{day}$  the day respiration and  $\theta$  the curvature parameter. This equation was used to simulate the maximum diurnal variations of  $A$  in absence of stomatal limitation under different light intensity conditions.

### 2.3.5. Determining the rapidity of stomatal conductance response

The rapidity of the stomatal response following a step change in light intensity was assessed as a function of time ( $t$ ) using a custom exponential equation (Violet-Chabrand et al, 2013) including a slow linear increase of the steady state target ( $G$ ):

$$g_s = (G + S_l t) + (g_0 - (G + S_l t))e^{-t/\tau}$$

where  $S_l$  is the slope of the slow linear increase of  $G$  observed during the response,  $g_0$  the initial value of  $g_s$ , and  $\tau$  the time constant to reach 63% of  $G$  (when  $\tau = t$ ,  $\frac{g_s - g_0}{((G + S_l t) - g_0)} = 1 - e^{-1} \sim 0.63$ ).

Due to the asymmetry of response during a step increase or decrease in light intensity, a different value of  $\tau$  was used in each condition ( $\tau_i$  and  $\tau_d$ ). Even if  $g_s$  did not reach a plateau within the given timeframe, the model was able to predict the final asymptotic response and therefore the time constant ( $\tau_i$  and  $\tau_d$ ). This equation was adjusted on response curves of each treatment at different times of the day using a nonlinear mixed effect model. Parameter  $G$ ,  $g_0$  and  $S_l$  were assumed to vary at individual level (random effects) and  $\tau$  was assumed to vary only at treatment level (fixed effect). R and the nlme package were used to perform the analysis. Confidence interval at 95% were reported at treatment level.

### 2.3.6. Determining the rapidity of net CO<sub>2</sub> assimilation response

The rapidity of the photosynthesis response following a step change in light intensity was assessed as a function of time ( $t$ ):

$$A_t = (A_s + S_l t) + (A_0 - (A_s + S_l t))e^{-t/\tau}$$

where  $A_t$  is the net CO<sub>2</sub> assimilation ( $A$ ) at time  $t$ ,  $A_s$  is the plateau of  $A$  reached in steady state,  $S_l$  is the slope of the slow linear increase of  $A$ ,  $A_0$  the initial value of  $A$ , and  $\tau$  the time constant to reach 63% of  $A_s$ . This equation was adjusted on response curves using the same method described above for  $g_s$ .

### 2.3.7. Including diurnal stomatal behaviour in the Ball-Berry model for predicting $g_s$

An addition was made to the original Ball-Berry model (Ball et al, 1987) to take into consideration the time of the day ( $t$ ) effect on  $g_s$ :

$$g_s = g_0 + \left( g_1 \frac{AH_s}{C_s} \right) + \left( g_2 e^{-\frac{(t-T_m)^2}{2T_s^2}} \right)$$

where  $g_0$  is the minimal conductance or intercept,  $g_1$  the slope of the relationship between  $g_s$  and the Ball index ( $AH_s/C_s$ ),  $g_2$  the amplitude of the Gaussian function,  $T_m$  the time to reach the peak of the Gaussian,  $T_s$  a parameter related to the width of the peak, and  $A$  the net CO<sub>2</sub> assimilation. The conditions imposed at the surface of the leaf are represented by  $H_s$  the relative humidity, and  $C_s$  the CO<sub>2</sub> concentration in the chamber.

Using R and the nls function, two versions (with and without the third above) were adjusted on an independent dataset described previously in Chapter 5. The fluctuating light regime and different light intensities applied on plants grown in different conditions give a large range of variation to test the performance of the Ball-Berry model against our modified version.

The difference between observation (*Obs.*) and predictions (*Mod.*) of both models were assessed using the root mean square error (*rmse*):

$$rmse = \sqrt{\frac{\sum (Obs. - Mod.)^2}{n}}$$

where  $n$  represented the number of recorded data.

## 2.4. Leaf and stomatal characteristics

### 2.4.1. Stomatal anatomical measurements

Stomatal impressions of the abaxial and adaxial surface of the leaves were taken from the same area measured during gas exchange. Following the methods of Weyers and Johansen (1985), negative impressions of the leaf surface were made using Xantopren dental polymer (Heraeus Kulzer Ltd, Hanau, Germany). Once dry the Xantopren polymer was removed from the leaf, and clear nail varnish was

spread over the polymer to produce a positive impression, upon drying the nail varnish was then peeled from the surface of the polymer and placed on a microscope slide for analysis. Stomatal density, stomatal pore length and pore width were measured via light microscopy (Olympus BX60, Southend-on-sea, Essex, UK) using an eyepiece graticule. Maximum stomatal conductance ( $g_{s\ max}$ ) to water vapour as defined by stomatal anatomy when subjected to  $1000\ \mu\text{mol m}^{-2}\ \text{s}^{-1}$  PPFD for 1 hour (functional  $g_{s\ max}$ ) was estimated for each treatment using a version of the equation by Dow et al (2014):

$$g_{s\ max} = \frac{\text{Stomatal Density} \times \text{Pore Area} \times \text{Formula mass of air} \times \text{Effective Diffusion Coefficient}}{\text{Pore Depth} \times \text{"end correction"}}$$

Where the effective diffusion coefficient of water vapour and the formula mass of air were taken as  $24.9 \times 10^{-6}\ \text{m}^2\ \text{s}^{-1}$  and  $40.9\ \text{mol}^{-3}$  respectively (Jones, 2013). Pore depth was calculated as  $0.5 \times$  pore width, assuming guard cell was circular. An 'End correction' was used in the equation to consider the semi-circular diffusion pathway that forms either end of the stomatal pore, calculated as  $2\pi$  (pore length/2)/4. Pore area was defined as an ellipse with the major axis equal to the pore length and minor equal to the pore width. Nocturnal conductance (referred to here as  $g_{s\ \text{night}}$ ) was defined by the value of  $g_s$  at the beginning of each diurnal measurement when PPFD was at zero.

#### **2.4.2. Leaf anatomical measurements**

Total leaf area ( $\text{cm}^2$ ), dry weight (g), and specific leaf area (SLA,  $\text{cm}^2/\text{g}$ ), were measured using the youngest, fully expanded leaves. Total leaf area was calculated using IMAGE J software (National Institute of Health, Bethesda, Maryland, USA).

#### **2.4.3. Leaf optical properties**

Leaf absorbance was measured using a Skye Instruments light meter (Skye instruments, Llandrindod Wells, Powys, UK) and an Ulbricht integrating sphere (built at University of Essex). Ten measurements of transmittance and reflectance were made per treatment, using the youngest fully expanded leaf. The transmittance and reflectance for each leaf was used to calculate absorbance, with the mean absorbance for each treatment determined from ten combined measurements.

#### **2.4.4. Analysis of photosynthetic pigments**

For pigment analysis, leaf discs (1.0 cm<sup>2</sup>) were taken from attached leaves 5 hours into the light treatment without dark adaptation and frozen in liquid nitrogen, and stored at -80°C until extraction. Pigments were extracted as described by Matsubara et al, (2005), and were separated by Ultra-performance liquid chromatography as described by Zapata et al, (2000) with chlorophyll *a*, chlorophyll *b*, and total carotenoid content identified via their absorption spectra and retention times.

#### **2.4.5. Leaf cross-section analysis**

The most recent fully expanded leaves were collected from plants after 28 days of growth. 1 mm wide strips were cut from the centre of the leaf, extending from the mid-vein to the edge of the leaf. Samples were preserved in 5% glutaraldehyde, and refrigerated for min. 24h. The samples were then subjected to ethanol series (20, 40, 80, 100%) for duration of 15 min at each concentration. The samples were placed in 100% ethanol for 24 h before being placed in LR white acrylic resin (Sigma-Aldrich, Gillingham, UK), and refrigerated for a further 24h. After which the cleared leaf material was embedded in gelatin capsules filled with LR white resin and placed in an oven at 60°C for a further 24h to harden. For light microscopy, 0.5 µm sections were cut from the samples using a Reichert-Jung Ultracut microtome (Ametek GmbH, Munich, Germany), stained with Toluidine blue and viewed under a microscope following the method described by Lopez-Juez et al, (1998).

#### **2.4.6. Protein Extraction and Western Blotting**

Four leaf discs (1.0 cm diameter) were collected from 4 plants per treatment at 12 pm and immediately plunged into liquid nitrogen, and stored at -80°C. With assistance from Andy Simkin, protein was extracted in extraction buffer (50 mM 4-(2-Hydroxyethyl) piperazine-1-ethanesulfonic acid (HEPES) pH 8.2, 5 mM MgCl<sub>2</sub>, 1 mM Ethylenediaminetetraacetic Acid Tetrasodium Salt (EDTA), 10% Glycerol, 0.1% Triton X-100, 2 mM Benzamidine, 2 mM Aminocaproic acid, 0.5 mM Phenylmethanesulfonyl fluoride (PMSF) and 10 mM DTT) and the insoluble material was removed by centrifugation at 14000 g for 10 min (4°C) and protein quantification determined (Harrison et al, 1998). Samples were loaded on a leaf area basis, separated using 12% (w/v) SDS-PAGE, transferred to polyvinylidene difluoride membrane, and probed using antibodies raised against the Rubisco small subunit (Foyer et al. 1993). In addition to the aforementioned antibody, samples were probed using antibodies raised against transketolase

(Henkes et al, 2001), the cytochrome *b<sub>6</sub>f* complex proteins *cyt f* (PetA: (AS08306), *cyt b<sub>6</sub>* (PetB: (AS03034), Rieske FeS (PetC: AS08330), the photosystem I Lhca1 (AS01005) and PsaA (AS06172) proteins, and the Photosystem II PsbD/D2 (AS06146) protein, all purchased from Agrisera (via Newmarket Scientific UK). FBPA antibodies were raised against a peptide from a conserved region of the protein [C]-ASIGLENTEANRQAYR-amide (Cambridge Research Biochemicals, Cleveland, UK). Proteins were detected using horseradish peroxidase conjugated to the secondary antibody and ECL chemiluminescence detection reagent (Amersham, Buckinghamshire, UK). Protein content was determined as a percentage of protein levels in plants grown in *FLL* and quantified using a Fusion FX Vilber Lourmat imager (Peqlab, Lutterworth, UK).

## 2.5. Light use efficiency

Light use efficiency (*LUE*) was calculated as the ratio between leaf dry mass (g) and absorbed light intensity (MJ). The absorbed light was calculated by taking into consideration the increase in area of the Arabidopsis rosette through time. The rosette area for each day of growth ( $R_A$ ) was predicted by using a sigmoidal model adjusted on the observed data:

$$R_A = a / (1 + e^{-b * (Day - c)})$$

Where  $a$  represents the curves maximum value;  $b$  the steepness/slope of the curve; and  $c$  the day at the sigmoid midpoint.

### 2.5.1. Daily light use efficiency

Daily light use efficiency was calculated as the ratio between the predicted daily-integrated photosynthesis ( $A$ ) and the daily-absorbed light intensity (Mega Joules, MJ), which represents an instantaneous estimate of the light use efficiency. The daily-integrated photosynthesis was predicted using the response of  $A$  to light intensity. For each light intensity during the day, the corresponding photosynthesis was calculated and integrated over the time. The integrated photosynthesis in  $\mu\text{mol m}^{-2} \text{s}^{-1}$  was converted into g by using the molecular mass of C (12 g/mol). Light intensity in  $\mu\text{mol m}^{-2} \text{s}^{-1}$  was converted into J (Joules) by using a conversion factor (0.16) described in the manual of the Licor 6400 (Red-Blue light source; Li-Cor, Lincoln, Nebraska, USA).

## **2.6. Statistical analysis**

Statistics were conducted using R software ([www.r-project.org](http://www.r-project.org); version 3.2.4). A one-way ANOVA was used to test for single factor differences where more than one group existed. When significant differences were observed, a Tukey post-hoc test was used to compare the different treatments. These analyses were used for all chapters, although specific changes and additions are highlighted in each chapter method section.

# CHAPTER 3

---

**Natural variation in stomatal response to light in *Populus nigra*: implications for photosynthesis and water use efficiency**

### 3.1. Introduction

Stomata control the uptake of CO<sub>2</sub> and exchange of water vapour between the plant and atmosphere, by regulating stomatal conductance ( $g_s$ ) and net photosynthetic rate ( $A$ ), with the ratio between these two characterized as intrinsic water use efficiency ( $W_i = A/g_s$ ). Stomata adapt to changing environmental conditions by altering anatomical features and functional response, with changes in the behaviour of stomatal opening and closure essential for maximizing photosynthesis and water use depending on the current needs of the plant (Casson and Hetherington, 2010).

The control of stomatal density and functional stomatal response is often a long-term developmental acclimation to the plants native environmental conditions (Casson and Hetherington, 2010). However, depending on the current needs of the plant, stomatal density and responses can also dynamically acclimate between leaves of the same plant. For example, where stomatal traits change from leaf to leaf as shown under changing atmospheric CO<sub>2</sub> conditions (Lake et al, 2001), and even through time on the same leaf when subject to a change in light (Alter et al, 2012). Much is known about how plants alter stomatal anatomy via acclimation to growth light (Gay and Hurd, 1975), however little is known how the functional response of stomata acclimates to growth light, and the implications for carbon gain and water use efficiency (Lawson and Blatt, 2014). In the natural environment, the response of stomatal conductance ( $g_s$ ) is influenced by fluctuations in light, driven by cloud cover, sun angle, and often most importantly shading via neighboring plants, canopy structure, and self-shading via overlapping leaves (Allen and Pearcy, 2000; Chazdon and Pearcy, 1991; Way and Pearcy, 2012). As a consequence, leaves experience a range of light intensities, that vary on a scale of seconds, minutes, days and over the course of the growth season (Assmann and Wang, 2001), which fundamentally has major implications for photosynthetic carbon gain and water use efficiency (Lawson and Blatt, 2014).

The majority of studies investigating the acclimation or adaptation of plants to dynamic light, have concentrated on the effect sunflecks (rapid changes in incident PPFD over the course of seconds and even minutes) have on carbon gain in plants developmentally acclimated to shaded conditions (Knapp and Smith, 1987; 1988), often in understory forest dwelling species (Chazdon and Pearcy, 1991; Tinoco-Ojanguren and Pearcy, 1993; Pearcy, 1994; Leakey et al, 2005). It is often the speed of stomatal response and behaviour over the diurnal period that is critical when assessing carbon uptake and water use efficiency in a dynamic light environment (Kirschbaum and Pearcy, 1988; Lawson and Morison, 2004; Lawson et al, 2010; McAusland et al, 2016). Over the diurnal period fluctuations in light will drive the dynamics of stomatal behaviour (Lawson and Blatt, 2014), with differences in the sensitivity of

stomata, the magnitude of  $g_s$ , and the speed of stomatal opening and closing, known to exist between species (Ooba and Takahashi, 2003; Vico et al, 2011; McAusland et al, 2016), and between individuals of the same species grown under different habitat conditions (Drake et al, 2013).

The rate of  $g_s$  response to changing environmental conditions has often been correlated with stomatal anatomical traits including stomatal density and size (Franks and Farquhar, 2007; Drake et al, 2013). However, less attention has been given to how stomatal behaviour and the rate of  $g_s$  response to light influences  $W_i$  at a given time point and over the entire diurnal period. Furthermore, it is important to consider natural variation within species through developmental acclimation of stomatal anatomy and function to a particular light environment. This is important because it will give us a basis for which to understand the plasticity in stomatal response to a light environment in a given species.

*Populus nigra* is a species of poplar tree commonly known as Black poplar, whose range expands from the United Kingdom to North Africa and Central Asia, although is predominantly found along riparian habitats in Western and Central Europe (Muller et al, 2002; Dickmann and Kuzovkina, 2014). Due to its abundance alongside river systems and riparian woodlands it is known to have considerable sensitivity to drought (Vanden Broeck, 2003), which could potentially induce intraspecific adaptations of stomatal behaviour between genotypes when subject to vastly different light environments. The population used here consisted of poplar genotypes originally collected from 5 different sites across Europe with contrasting latitudes of origin, and therefore differing annual amounts of light radiation, precipitation, and temperature.

The aim of this chapter is to identify whether the stomatal response to light, both anatomically and behaviorally, varied within a natural population of *Populus nigra* genotypes. It is also to assess the influence this may have on carbon gain ( $A$ ) and consequently intrinsic water use efficiency ( $W_i$ ), the identification of which may lead to greater understanding of adaptation of the response of  $g_s$  in a model species from different native environments.

## 3.2. Materials and Methods

This section outlines methods specific to this chapter and modifications made to protocols outlined in Chapter 2 – “Materials and Methods”.

### 3.2.1. Plant material and growth conditions

Cuttings from ten genotypes of *Populus nigra* were collected from a field site at the University of Southampton, and were selected for their country of origin and were grouped according to leaf phenotype (Table. 3.1 and Figure 3.1): Small-leaved (France, Spain), and Large-leaved genotypes (Italy, Germany, Netherlands).

**Table 3.1:** Summary of *Populus nigra* genotypes and environmental conditions at origin of genotypes.

Geno-type	Country of origin	Mean annual irradiance (kWh/m <sup>2</sup> )	Min/Max Monthly temp (°C)	Mean annual precip. (mm)	Min/Max Monthly precip. (mm)	Leaf type	Graphic colour
<b>Fr2</b>	France	1300-1700	0/28.7	639	21/90	Small	
<b>Fr4</b>	France	1300-1700	0/28.7	639	21/90	Small	
<b>Sp1</b>	Spain	1500-1700	1.8/29.7	365-439	17/55	Small	
<b>Sp2</b>	Spain	1500-1700	1.8/29.7	365-439	17/55	Small	
<b>It1</b>	Italy	1300-1500	-1/29	966-982	55/122	Large	
<b>It3</b>	Italy	1300-1500	-1/29	966-982	55/122	Large	
<b>Ge2</b>	Germany	900-1200	-2/24.5	605	37/67	Large	
<b>Ge4</b>	Germany	900-1200	-2/24.5	605	37/67	Large	
<b>NI1</b>	Netherlands	800-1000	-1.3/21.8	731-1021	43/100	Large	
<b>NI3</b>	Netherlands	800-1000	-1.3/21.8	731-1021	43/100	Large	

Cuttings with replicates for each genotype were planted in 1L pots in Westland John Innes no.2 soil (Westland Horticulture, Dungannon, Northern Ireland) with rooting compound, and moved to the greenhouse (University of Essex). After three weeks of initial growth under shade (Fig. 3.2A) to

encourage root growth, the shading mesh was removed and the plants were transferred into 4L pots and left to grow in the greenhouse for a further week (Fig. 3.2B). At this point plants were transferred to the roof garden where they were left to grow for a further four weeks in six plots, with the plants spaced at random to reduce environmental error effects (Fig. 3.2C + D).



**Figure 3.1.** Representative examples of leaf genotypes used in this study. Italy, Germany, and Netherlands genotypes are characterized as ‘Big leaf’, whilst Spain and France genotypes as ‘Small leaf’.

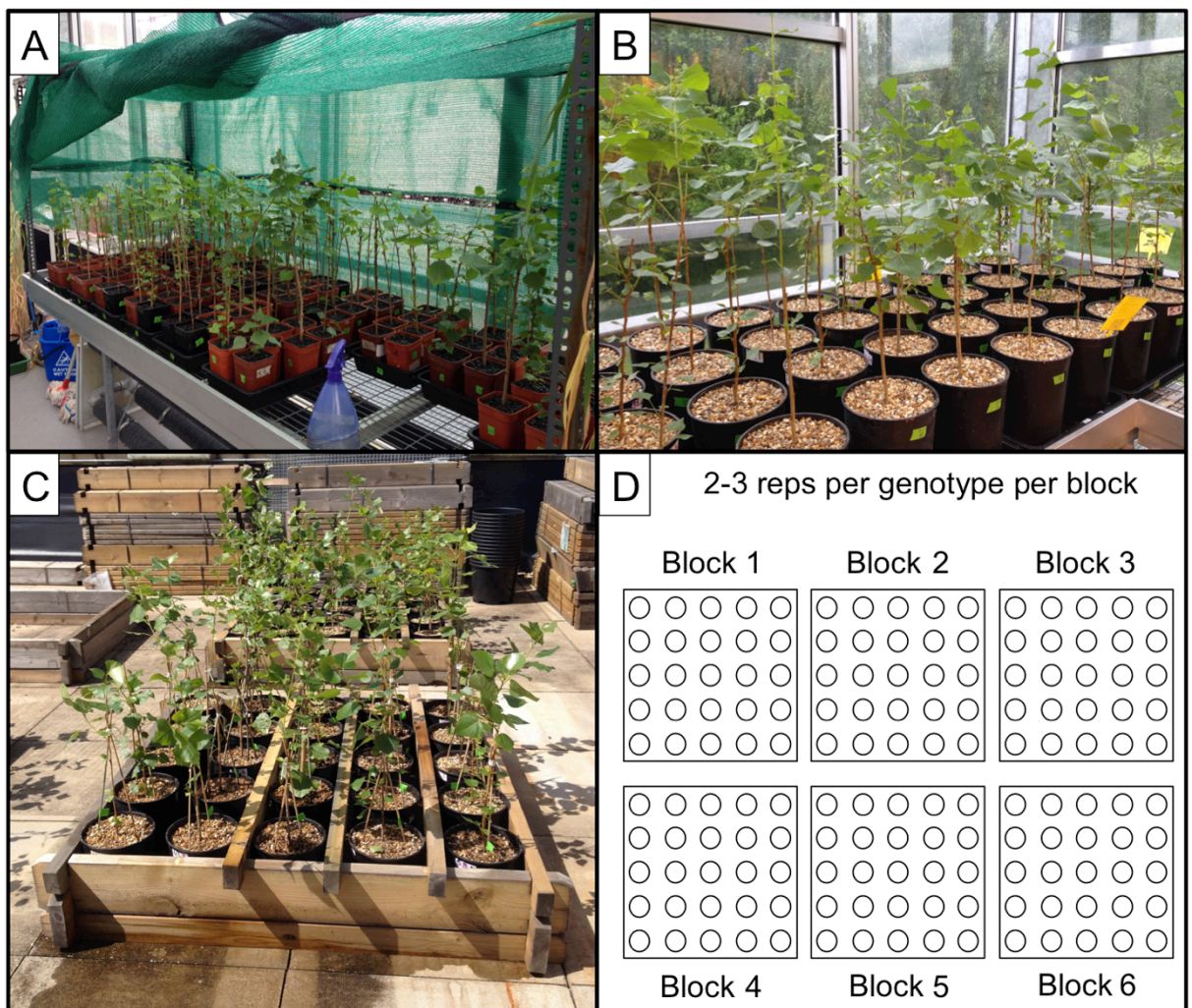


**Figure 3.2.** Preparation of *Populus nigra* cuttings: under initial shade (A); and after removal from shade in the greenhouse (B); plants in plots on the roof garden (C); and layout of randomized plots (D).

### 3.2.2. Leaf gas exchange

All gas exchange parameters, including net carbon assimilation ( $A$ ) and stomatal conductance ( $g_s$ ) were recorded and cuvette conditions maintained as laid out in Method 2.2, using a Li-Cor 6400XT portable gas exchange system (Li-Cor, Lincoln, Nebraska, USA). All measurements were taken using the youngest, fully expanded leaf, between leaves 5-8 as shown in Figure 3.3.

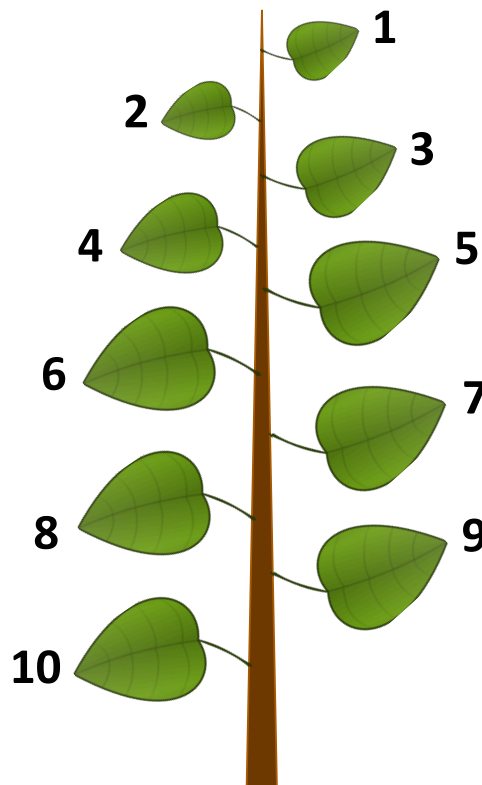


**Figure 3.3.** Representation of the numbering of *Populus nigra* leaves for selection for gas exchange and anatomical analysis. Leaves are counted from the top to ensure similar age range during selection.

#### 3.2.2.1. $A/Q$ (net photosynthetic rate/ $PPFD$ ) response curves

The response of net  $CO_2$  assimilation rate ( $A$ ) to photosynthetic photon flux density ( $PPFD$ ) was measured and recorded under cuvette conditions as described in method 2.2.1, although the following changes were made to the protocol:

- Leaves were initially stabilized (5-10 minutes) at irradiance above saturation at  $2100 \mu\text{mol m}^{-2} \text{s}^{-1}$   $PPFD$  and a measurement was recorded.
- $PPFD$  was then decreased in 15 steps (1900, 1700, 1500, 1300, 1100, 900, 700, 550, 400, 300, 200, 150, 100, 50,  $0 \mu\text{mol m}^{-2} \text{s}^{-1}$ ) with a new recording being taken at each new light level.

### **3.2.2.2. $A/C_i$ (net photosynthetic rate/intercellular CO<sub>2</sub> concentration) response curves**

The response of net CO<sub>2</sub> assimilation rate ( $A$ ) to intercellular CO<sub>2</sub> concentration ( $C_i$ ) was measured and recorded under cuvette conditions as described in method 2.2.2, with the following changes to the protocol:

- Leaves were initially stabilized for a minimum of 10-15 minutes at a saturating light intensity of 2100  $\mu\text{mol m}^{-2} \text{s}^{-1}$  and ambient CO<sub>2</sub> concentration of 400  $\mu\text{mol mol}^{-1}$ , upon reaching steady state a measurement was recorded.
- Ambient CO<sub>2</sub> was then decreased to 300, 200, 125, 50  $\mu\text{mol mol}^{-1}$  before returning to the initial value of 400, and increased to 550, 700, 900, 1100, 1300, 1500, 1800 and 2100  $\mu\text{mol mol}^{-1}$ . Recordings were taken at each new CO<sub>2</sub> level.

### **3.2.2.3. Temporal response of photosynthesis ( $A$ ) and stomatal conductance ( $g_s$ )**

The response of net CO<sub>2</sub> assimilation rate ( $A$ ) and stomatal conductance ( $g_s$ ) to a step change in photosynthetic photon flux density ( $PPFD$ ), was carried out as described in method 2.2.3, with the following changes to the protocol:

- leaves were equilibrated to a  $PPFD$  of 500  $\mu\text{mol m}^{-2} \text{s}^{-1}$  until both  $A$  and  $g_s$  were at steady state.
- $PPFD$  was then increased to 1500  $\mu\text{mol m}^{-2} \text{s}^{-1}$  for 1.5h with  $A$  and  $g_s$  recorded every 30 seconds, before returning to 500  $\mu\text{mol m}^{-2} \text{s}^{-1}$  for a further 1h.

### **3.2.2.4. Diurnal measurements**

Diurnal gas exchange measurements of  $A$  and  $g_s$  were carried out as described in method 2.2.4.

## **3.2.3. Modelling gas exchange parameters**

### **3.2.3.1. Determination of mass integrated net CO<sub>2</sub> assimilation**

Net CO<sub>2</sub> assimilation ( $A$ ) was converted to a mass integrated measurement using leaf mass area ( $LMA$ ) – see method 2.3.1.

### **3.2.3.2. Estimating photosynthetic capacities**

Photosynthetic capacities ( $V_{C_{max}}$  and  $J_{max}$ ) were estimated from the  $A/C_i$  response curves using method 2.3.2.

### **3.2.3.3. Assessing stomatal limitation from $A/C_i$ response curves**

The hypothetical  $A$  that would be obtained if the mesophyll had free access to the  $CO_2$  in the ambient air was calculated to quantify the limitation that the combined stomatal and boundary layer conductance impose on leaf  $CO_2$  uptake using the method described in section 2.3.3.

### **3.2.3.4. Modelling net $CO_2$ assimilation rates**

Net  $CO_2$  assimilation ( $A$ ) as a function of light intensity ( $PPFD$ ) was modelled to simulate the maximum diurnal variations of  $A$  in absence of stomatal limitation under different light intensity conditions. For methods see 2.3.4.

### **3.2.3.5. Determining the rapidity of stomatal conductance response**

The rapidity of the stomatal response following a step change in light intensity was assessed using method 2.3.5.

### **3.2.3.6. Determining the rapidity of net $CO_2$ assimilation response**

The rapidity of the photosynthesis response following a step change in light intensity was assessed using method 2.3.6.

## **3.2.4. Leaf and stomatal characteristics**

### **3.2.4.1. Stomatal anatomical measurements**

Stomatal density, pore area, index, ratio, and theoretical maximum of stomatal conductance ( $g_{smax}$ ) were assessed by taking impressions of the surface of the leaf, following method 2.4.1.

#### **3.2.4.2. Leaf anatomical measurements**

Total leaf area (cm<sup>2</sup>), dry weight (g), and specific leaf area (SLA, cm<sup>2</sup>/g), were measured on all poplar genotypes using method 2.4.2, and were taken using the youngest, fully expanded leaf, between leaves 5-8 as shown in Figure 3.3.

#### **3.2.4.3. Leaf optical properties**

Measurements of transmittance and reflectance for each leaf was used to calculate absorbance, transmittance, and reflectance, and were measured on the youngest, fully expanded leaf, between leaves 5-8 as shown in Figure 3.3. See method 2.4.3.

### 3.3. Results

#### 3.3.1. Photosynthetic response to photosynthetic photon flux density (PPFD)

The response of net CO<sub>2</sub> assimilation rate ( $A$ ) as a function of photosynthetic photon flux density (PPFD) ( $Q$ ) ( $A/Q$  curves, Fig. 3.4) was measured on all ten genotypes to investigate differences in photosynthetic potential. Similar values of  $A$  at PPFDs below 400  $\mu\text{mol m}^{-2} \text{s}^{-1}$  were observed between all genotypes (Fig. 3.4A + C), whereas at PPFD above this level there were noticeable differences in  $A$  between genotypes with the small leaf genotypes (Fr, Sp) displaying higher values of  $A$  than two of the large leaf genotypes (Ge, NI). Photosynthesis is generally measured per unit leaf area; however, area does not consider changes in leaf thickness that can differ between and within species. To take into consideration photosynthesis per unit leaf volume,  $A$  was integrated by mass of dry leaf ( $A_{mass}$ ) calculated from measurements of leaf mass area (LMA).  $A_{mass}$  was found to be higher in the large leaved genotypes compared to small leaved at PPFD above ca. 300  $\mu\text{mol m}^{-2} \text{s}^{-1}$  (Fig. 3.4B + D). Measurements of  $A$  at saturating light ( $A_{sat}$ ) were significantly higher in small leaved genotypes ( $P < 0.05$ ), with both the Spanish genotypes exhibiting significantly higher values than three of the large leaf genotypes (Ge2, NI1, NI3) (Fig. 3.4E). Interestingly both the Italian genotypes displayed values of  $A_{sat}$  more comparable to the small leaved genotypes than the other large leaved. No significant difference was observed between genotypes for  $A_{mass-sat}$ , although there was a trend toward the large leaved genotypes displaying higher values, indeed when they are grouped in this manner the difference becomes significant (Fig. 3.4F).

#### 3.3.2. Leaf size and absorbance properties

Leaf area measured on fully expanded mature leaves was as expected significantly higher ( $P < 0.05$ ) in large leaved genotypes compared to small leaved genotypes with values ranging from ca. 19  $\text{cm}^2$  (Sp2) to ca. 61  $\text{cm}^2$  (It1) (Fig. 3.5A). Italian genotypes had larger leaves than all other genotypes. Similar differences were found for leaf dry weight, with small leaved genotypes significantly ( $P < 0.05$ ) lower than large leaved genotypes, with values ranging from 0.18g (Sp2) to 0.48g (It1) (Fig. 3.5B). Italian genotypes again had the highest dry weight than all other genotypes. As expected, the large leaved genotypes had significantly ( $P < 0.05$ ) higher specific leaf area (SLA) than the small leaved genotypes when grouped by size (Fig. 3.5C), with Sp1 being significantly lower than all six large leaved genotypes and Fr4, Sp2 significantly lower than both German genotypes (Ge2, Ge4). No significant differences were observed between genotypes for leaf absorbance (Fig. 3.5D), reflectance or transmittance (Fig. 3.5E + F). However, there was a trend toward small leaved genotypes exhibiting lower levels of reflectance

compared to large leaved genotypes, with two of the small leaved (Fr4, Sp1) showing significantly lower levels than one large leaved genotype (NI1).

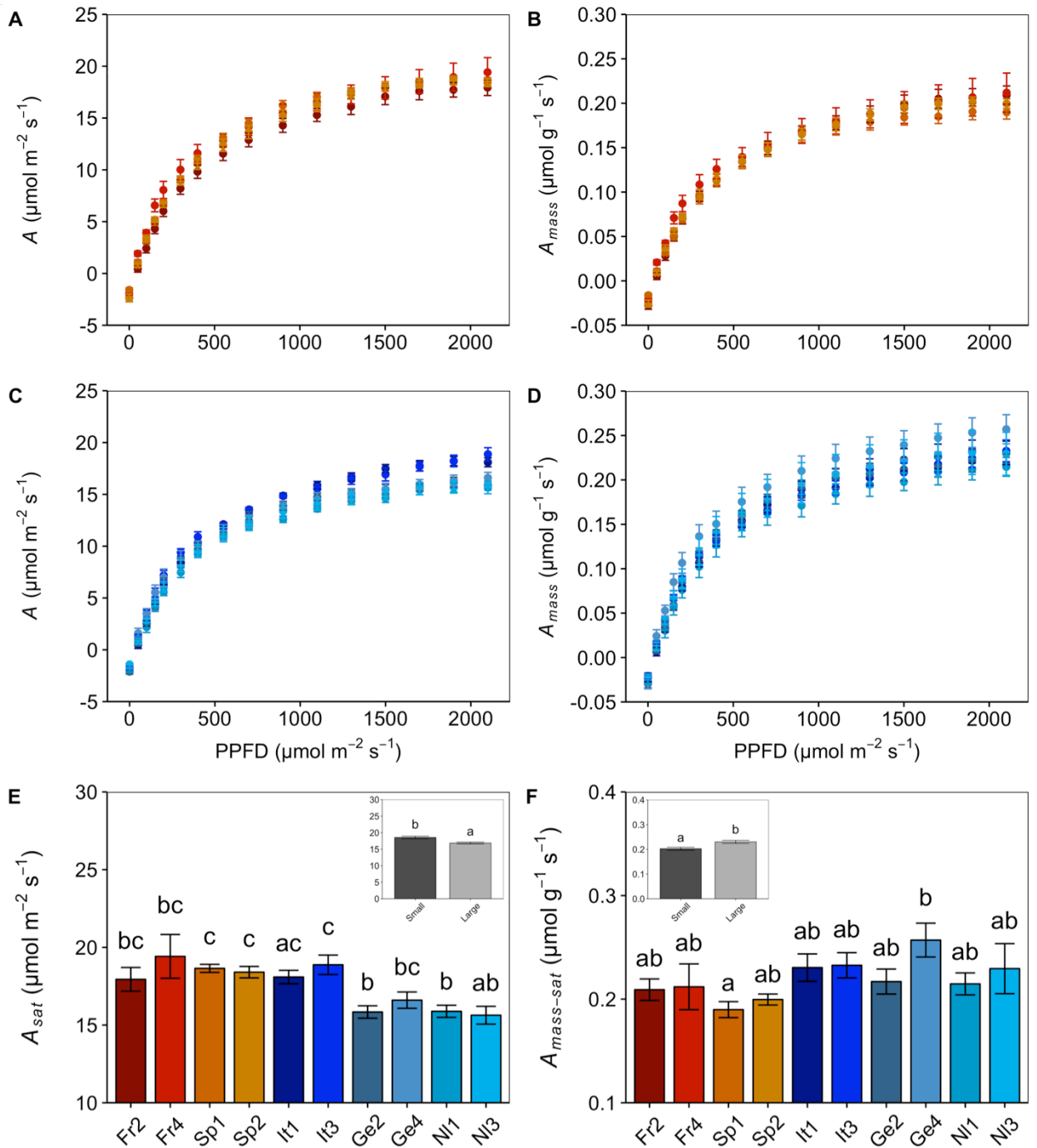


**Figure 3.4.** Photosynthesis as a function of light intensity (PPFD) for the four small-leaved genotypes (red and orange), and the six large-leaved genotypes (Blue and turquoise). Net CO<sub>2</sub> assimilation on an area basis (A; A + C); relative to leaf mass (A<sub>mass</sub>; B + D); light saturated rate of photosynthesis (A<sub>sat</sub>) on an area (E) and mass (F) basis. Inset graphs (E + F) highlight differences between grouped small and large leaf genotypes for A<sub>sat</sub> and A<sub>mass-sat</sub>. Error bars represent mean ± SE. n = 4-6. Letters represent the results of Tukey's *post-hoc* comparisons of group means, between genotypes and than leaf size.

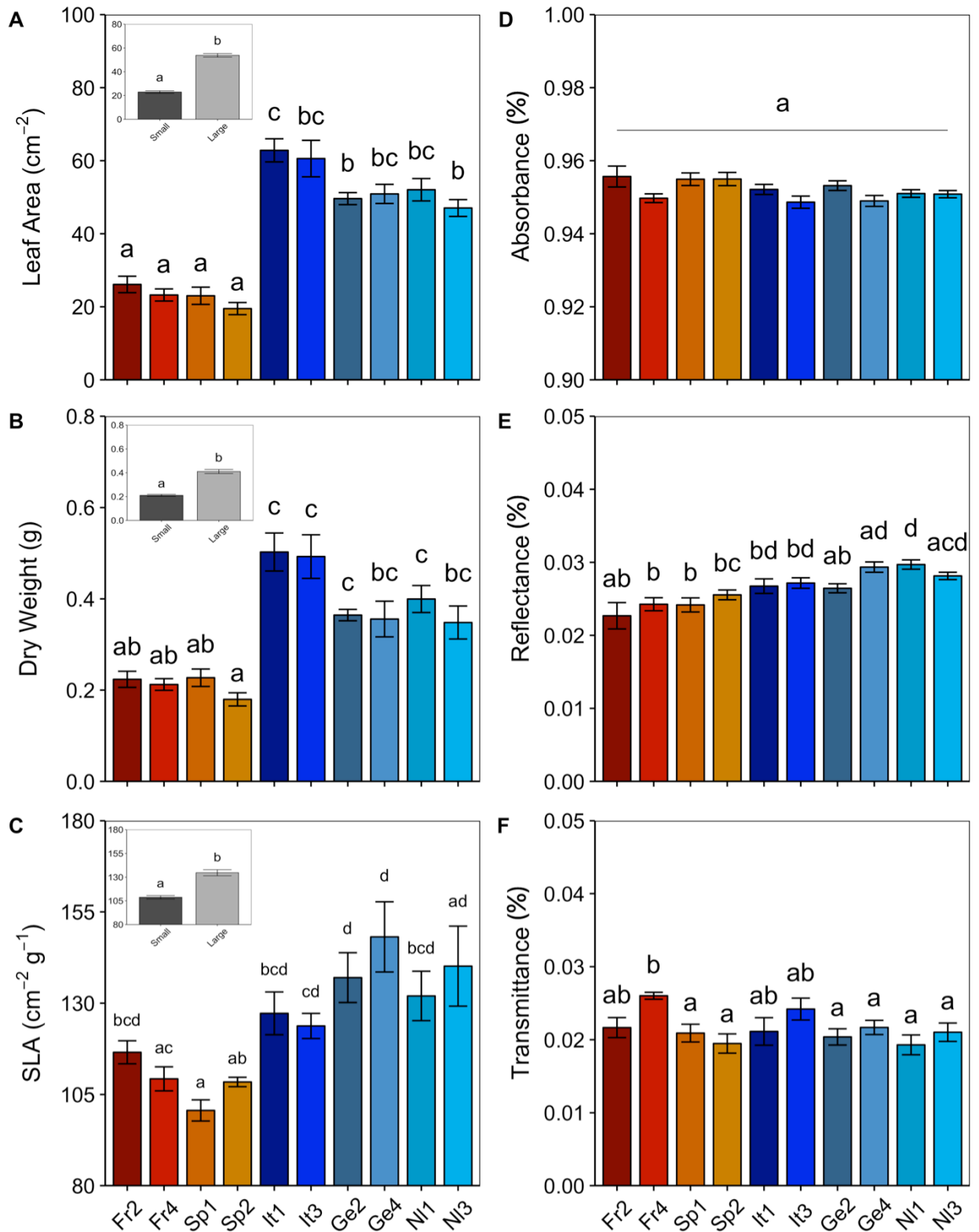


**Figure 3.5.** Leaf and Optical properties of the ten poplar genotypes, including; Leaf area (A); Dry weight (B); Specific leaf area (SLA, C); Absorbance (D); reflectance (E); and transmittance (F). Inset graphs (A-C) highlight difference between grouped small and large leaved genotypes for LA, DW, and SLA. Error bars represent mean  $\pm$  SE. n = 6-10. Letters represent the results of *Tukey's post-hoc* comparisons of group means, between genotypes and than leaf size.

### 3.3.3. Intra-specific variation in photosynthetic capacity

Assimilation rate measured as a function of intercellular CO<sub>2</sub> ( $C_i$ ) on an area basis, was generally higher in plants characterised as small leaved genotypes (Fig. 3.6A + C), with the two Spanish genotypes (Sp1 and Sp2) consistently displaying higher values of  $A$  than all other genotypes. In contrast, the light and CO<sub>2</sub> saturated rate of  $A$  integrated by mass ( $A_{mass}$ ) was higher in large leaved genotypes, with German (Ge2, Ge4) genotypes higher than all other genotypes (Fig. 3.6B + D). Values of the light and CO<sub>2</sub> saturated rate of photosynthesis ( $A_{max}$ ), were significantly higher in small leaved genotypes compared to large leaved genotypes when grouped by size (Fig. 3.6E). However, individually  $A_{max}$  was only significantly different ( $P < 0.05$ ) between two small leaved genotypes (Fr4 and Sp2) and one large leaved (NL3). Values of  $A_{max}$  as a function of mass ( $A_{mass-max}$ ), were also significantly higher ( $P < 0.05$ ) in large leaved genotypes when grouped by leaf size, but no significant differences were observed by individual genotype (Fig. 3.6F). Despite this, a large range in  $A_{mass-max}$  values was observed, with values ranging from 0.33 (Sp1) to 0.48  $\mu\text{mol g}^{-1} \text{s}^{-1}$  (Ge4). No differences in the maximum rate of carboxylation by Rubisco ( $V_{cmax}$ ) and the maximum electron transport rate ( $J_{max}$ ) for RuBP regeneration (Table. 3.2) were found between genotypes. However, there was a trend toward small leaved genotypes and the Italian genotypes having higher levels of  $V_{cmax}$  and  $J_{max}$  compared to the Ge and NL large leaved genotypes, with Fr2 exhibiting the highest value for  $V_{cmax}$  (102.7) and NI1 the lowest (62.4), and Sp2 the highest value for  $J_{max}$  (156.9) with NI1 the lowest (125).

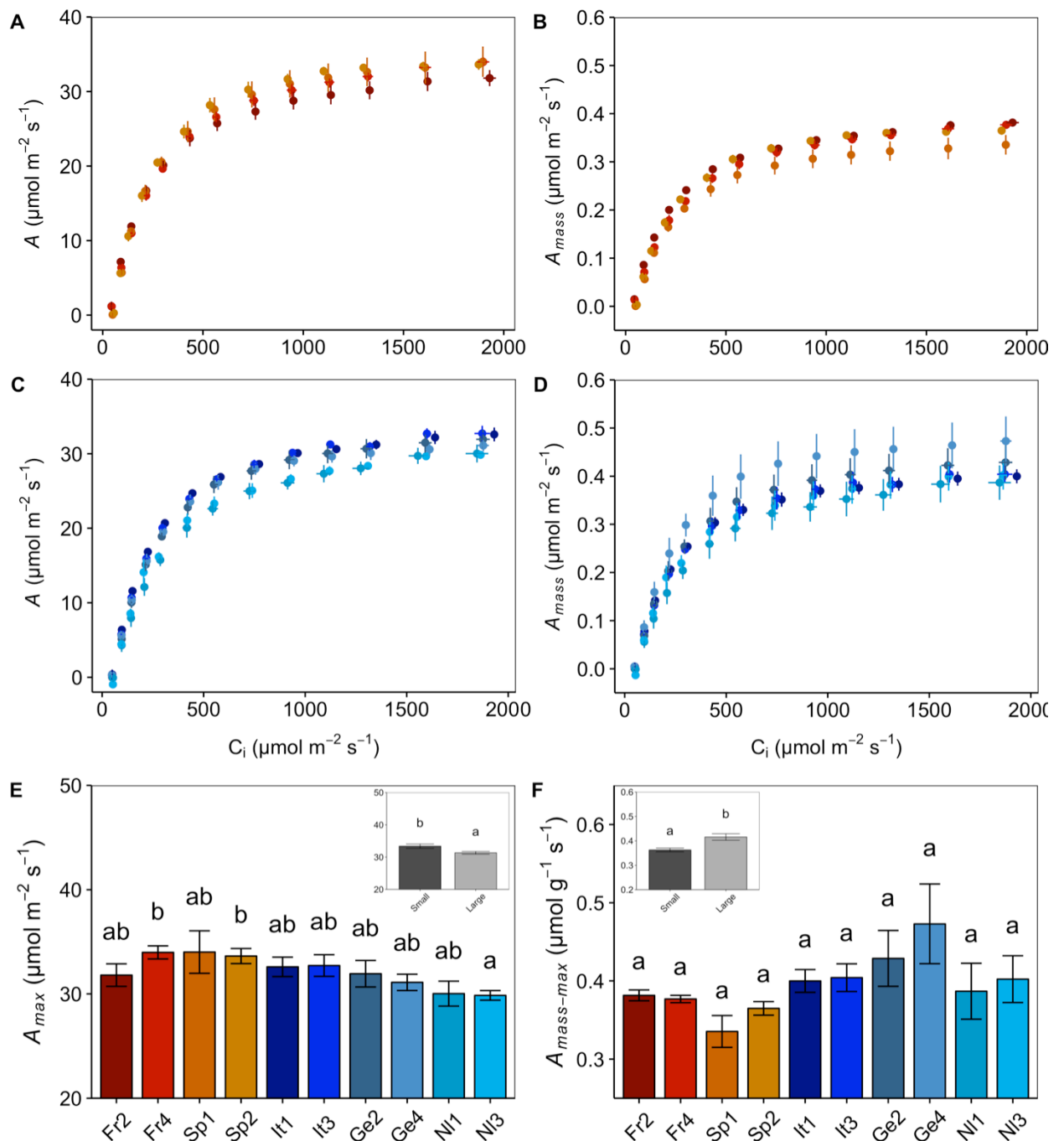


**Figure 3.6.** Photosynthesis as a function of intercellular CO<sub>2</sub> concentration (C<sub>i</sub>) for the four small-leaved genotypes (red and orange), and the six large-leaved genotypes (Blue and turquoise). Net CO<sub>2</sub> assimilation on an area basis (A; A + C); relative to leaf mass (A<sub>mass</sub>; B + D); light and CO<sub>2</sub> saturated rate of photosynthesis (A<sub>max</sub>) on an area (E) and mass (F) basis. Inset graphs (E + F) highlight differences between grouped small and large leaf genotypes for A<sub>max</sub> and A<sub>mass-max</sub>. Error bars represent mean ± SE. n = 4-6. Letters represent the results of Tukey's post-hoc comparisons of group means, between genotypes and than leaf size.

**Table 3.2.** Photosynthetic parameters ( $V_{\text{cmax}}$  and  $J_{\text{max}}$ ) estimated from the response of  $A$  to  $C_i$  of the ten poplar genotypes. Mean  $\pm$  SE. Letters represent the results of Tukey's post-hoc comparisons of group means.

Genotype	$V_{\text{cmax}}$ ( $\mu\text{mol m}^{-2} \text{s}^{-1}$ )	$J_{\text{max}}$ ( $\mu\text{mol m}^{-2} \text{s}^{-1}$ )
Fr2	102.7 $\pm$ 10.7 <sup>ab</sup>	139.3 $\pm$ 8.6 <sup>ab</sup>
Fr4	71.6 $\pm$ 6.7 <sup>ab</sup>	141.6 $\pm$ 6.2 <sup>ab</sup>
Sp1	86.9 $\pm$ 7.4 <sup>ab</sup>	149.6 $\pm$ 9.1 <sup>ab</sup>
Sp2	99.4 $\pm$ 9.4 <sup>ab</sup>	156.9 $\pm$ 4.8 <sup>a</sup>
It1	87.5 $\pm$ 6.4 <sup>ab</sup>	146.9 $\pm$ 8.5 <sup>ab</sup>
It3	90.9 $\pm$ 15.4 <sup>ab</sup>	149.1 $\pm$ 4.1 <sup>ab</sup>
Ge2	85.5 $\pm$ 5.7 <sup>ab</sup>	145.8 $\pm$ 6.5 <sup>ab</sup>
Ge4	77.7 $\pm$ 6.2 <sup>ab</sup>	138.6 $\pm$ 1.9 <sup>ab</sup>
NI1	62.4 $\pm$ 2.8 <sup>ab</sup>	125 $\pm$ 3.8 <sup>b</sup>
NI3	78.1 $\pm$ 10.3 <sup>ab</sup>	135.1 $\pm$ 3.2 <sup>ab</sup>

### 3.3.4. Limitation of CO<sub>2</sub> uptake (A) imposed by stomata conductance

$A/C_i$  curves were used to estimate the limitation imposed on  $A$  by stomata (and the leaf boundary layer), assuming the hypothetical  $A$  that could be achieved if the mesophyll had free access to CO<sub>2</sub> in ambient air (therefore;  $C_i=C_a$ ) (Farquhar and Sharkey, 1982). Large differences in the limitation of  $A$  by stomata from  $A/C_i$  analyses ( $ACi_{\text{Limit}}$ ) were observed between genotypes (Fig. 3.7), with a small leaved genotype exhibiting the lowest limitation of  $A$  (Fr2; 15.5%) and a large leaf genotype the highest (NI1; 29.5%) with differences between these two genotypes recognized as significant ( $P<0.05$ ). Despite no other significant differences between other genotypes occurring, there was a distinct trend toward small leaved genotypes demonstrating the lowest levels of  $ACi_{\text{Limit}}$ , with the Italian genotypes revealing values of limitation more akin to the small leaved rather than the other large leaved genotypes. It is noteworthy, that the limitation imposed by stomata was substantial in all genotypes and highlighted that even under 'ideal' conditions the limitation of CO<sub>2</sub> flux to the site of carboxylation was potentially biologically significant.

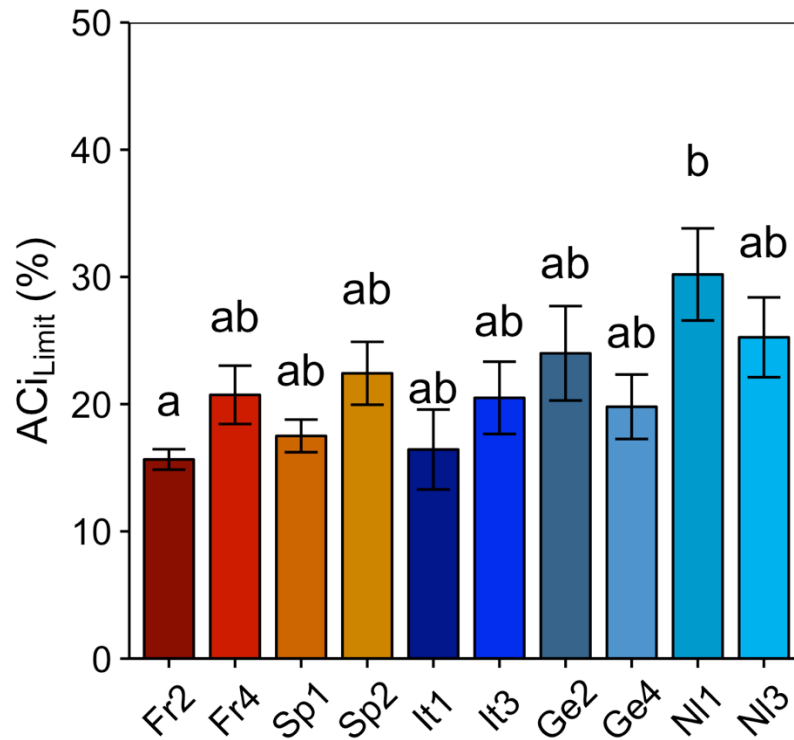


**Figure 3.7.** Estimation of the limitation ( $ACi_{Limit}$ ) placed on net  $CO_2$  assimilation by stomata and leaf boundary layer, calculated from the  $A/C_i$  response curves (Fig. 3.6), represented as the percentage (%) loss in  $A$  enforced by this limitation ( $ACi_{Limit}$ ). Error bars represent mean  $\pm$  SE.  $n = 4-6$ . Letters represent the results of *Tukey's post-hoc* comparisons of group means.

### 3.3.5. Diurnal responses of $g_s$ , $A$ , and $W_i$ to a fluctuating pattern of light

To investigate stomatal and photosynthetic response over the diurnal period, and the implications for diurnal intrinsic water use efficiency, plants from five genotypes (one from each region) were subjected to a diurnal fluctuating light regime (see FLH; Figure 2.1), with stomatal conductance ( $g_s$ ; Fig. 3.8A), net  $CO_2$  assimilation ( $A$ ; Fig. 3.8B), intercellular  $CO_2$  concentration ( $C_i$ ; Fig. 3.8C), and intrinsic water use efficiency ( $W_i$ ; Fig. 3.8D) measured continuously over the diurnal period. In general, the pattern of  $g_s$  response over the diurnal period was similar between genotypes. However, the Italian genotype (IT) was higher in the magnitude of  $g_s$  response than all other genotypes, reaching a peak during the diurnal of ca.  $0.4 \text{ mol m}^{-2} \text{ s}^{-1}$ , whereas the next closest genotype (Fr) only reached  $0.27 \text{ mol m}^{-2} \text{ s}^{-1}$  (Fig. 3.8A). Net photosynthesis ( $A$ ) displayed a similar response over the diurnal period in all genotypes (Fig. 3.8B). However, the large leaved genotypes Ge and NL exhibited lower peaks at high light periods (ca. 6-9 hours into the light) compared with the small leaved (Fr, Sp) and Italian genotype (IT). With the IT genotype reaching the highest value (ca.  $17.2 \mu\text{mol m}^{-2} \text{ s}^{-1}$ ) and NL the lowest value of  $A$  (ca.  $12.6 \mu\text{mol m}^{-2} \text{ s}^{-1}$ ) during the diurnal. A similar response was observed in the response of intercellular  $CO_2$

concentration ( $C_i$ ), as with an increase in  $A$  there was a corresponding increase in  $C_i$  (Fig. 3.8C). When integrated over the diurnal period, the Italian genotype (IT) consistently displayed the highest values of  $C_i$  throughout the measurement, with two of the three lowest values exhibited by two of the large leaved genotypes; Ge and NL.  $W_i$  (measured here as  $A/g_s$ ) was consistently found to be lowest in the IT and NL genotypes (Fig. 3.8D), and highest in two small leaved genotypes (Fr, Sp). In the IT genotype this lower  $W_i$  was driven by the large increase in  $g_s$  during the whole diurnal period, whilst the NL genotype exhibited lower levels of  $W_i$  because of the lower levels of  $A$  compared to the other genotypes over the entire diurnal.

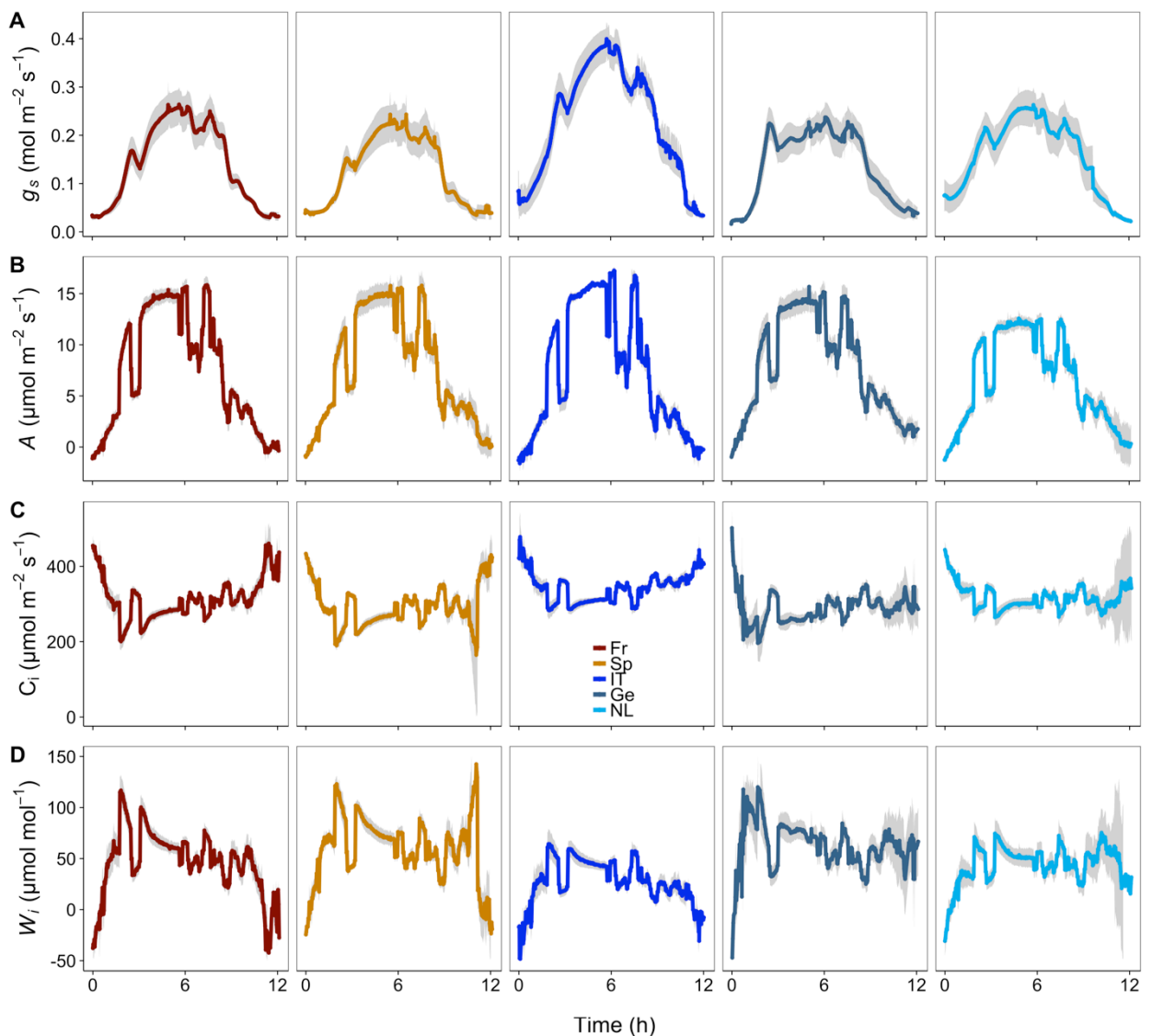


**Figure 3.8.** Diurnal measurements of gas exchange of stomatal conductance ( $g_s$ , A); net CO<sub>2</sub> assimilation (A; B); internal CO<sub>2</sub> concentration ( $C_i$ , C); and intrinsic water use efficiency ( $W_i$ , D) for the five selected genotypes (one from each region). Error ribbons represent mean  $\pm$  SE.  $n = 4-6$ .

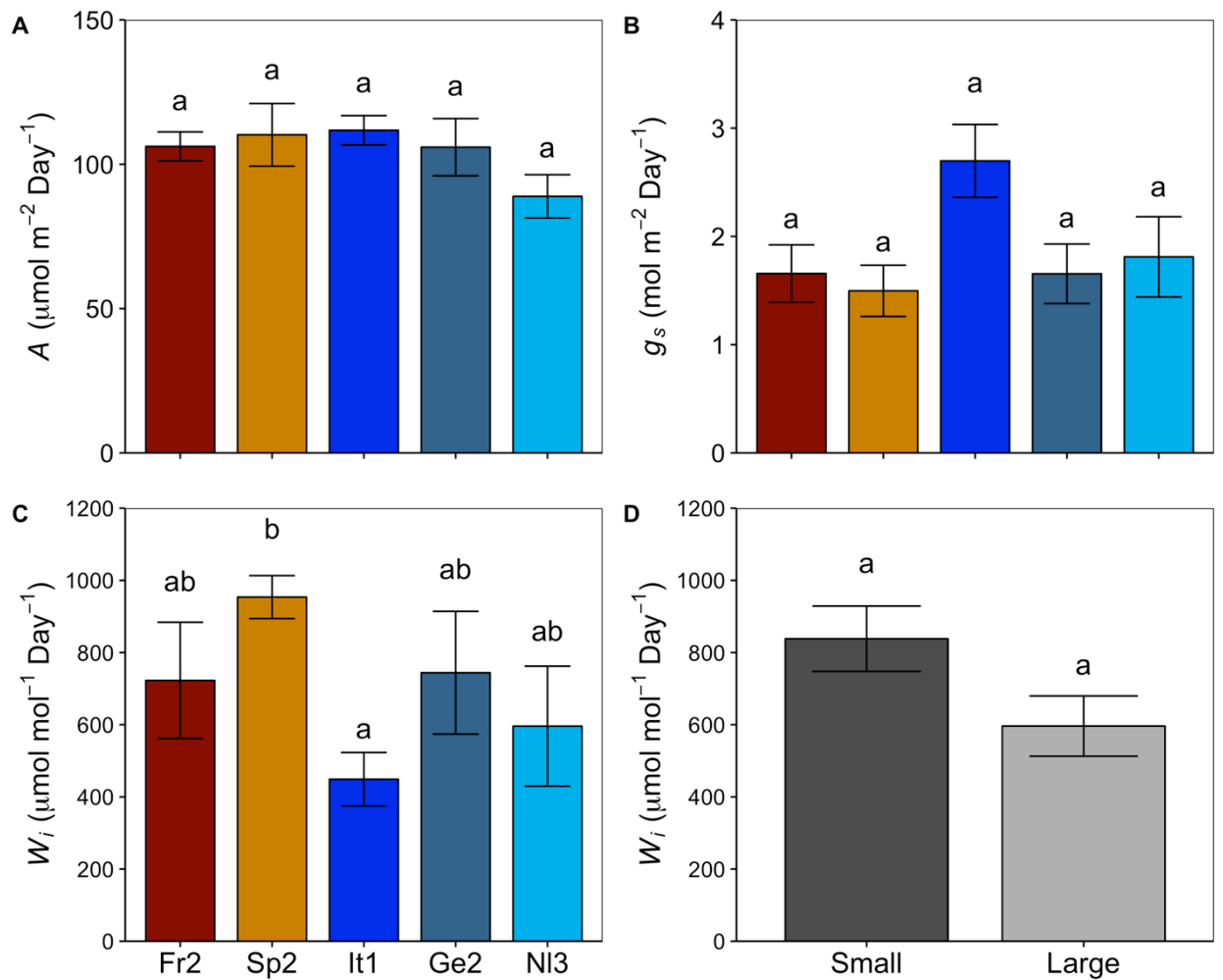


**Figure 3.9.** Total daily net CO<sub>2</sub> assimilation ( $A$ ; A); stomatal conductance ( $g_s$ , B); intrinsic water use efficiency ( $W_i$ , C) for the five selected genotypes (one from each region); and intrinsic water use efficiency ( $W_i$ , D) when grouped under small or large leaved genotype. Error ribbons represent mean  $\pm$  SE.  $n = 4-6$ . Letters represent the results of *Tukey's post-hoc* comparisons of group means.

To further characterize the response of net CO<sub>2</sub> assimilation ( $A$ ), stomatal conductance ( $g_s$ ) and intrinsic water use efficiency ( $W_i$ ), these parameters were integrated over the whole 12h day period to investigate levels of total daily  $g_s$ ,  $A$ , and  $W_i$  (Fig. 3.9). No significant differences in  $A$  integrated over a 12-hour period were observed between genotypes, although the Ge and NL large leaved genotypes displayed the lowest values (Fig. 3.9A). No significant differences were also observed in integrated daily  $g_s$  (Fig. 3.9B), however it should be noted that the IT genotype exhibited values of  $g_s$  (ca. 2.65 mol m<sup>-2</sup> Day<sup>-1</sup>) that were much higher than the other four genotypes over the course of the day, with the next highest value (NL; ca. 1.8 mol m<sup>-2</sup> Day<sup>-1</sup>) ca. 68% that of the value of the IT genotype. Intrinsic water use efficiency ( $W_i$ ) was significantly lower in the IT genotype compared with Sp, and was lower than all other genotypes (Fig. 3.9C). The lower value of  $W_i$  in the IT genotype was largely because of the large increase in  $g_s$ , whereas the highest value of  $W_i$  exhibited by the Sp genotype was driven by a combination of a

high integrated  $A$  and the lowest value of  $g_s$  over the diurnal period. When grouped together as either small leaved (Fr, Sp) or large leaved (IT, Ge, NL) genotypes, there was no significant difference between groups (Fig. 3.9D). However, it is noteworthy that small leaved genotypes exhibited a 43% increase in  $W_i$  compared with the large leaved genotypes (Fig. 3.9D).

### 3.3.6. Limitation of diurnal photosynthesis imposed by stomata

To investigate the potential limitation of net  $\text{CO}_2$  assimilation ( $A$ ) during the diurnal period ( $\text{Diur}_{\text{Limit}}$ ),  $A$  was predicted from the  $A/Q$  response curves (Fig. 3.4) assuming no stomatal limitation, and a maximized activation of the photosynthetic biochemistry. During the initial 2-3 hours of the diurnal light regime, all genotypes reached the predicted values of  $A$ . However, over the course of the rest of the diurnal measurement there was a tendency for measured values of  $A$  to be lower than the predicted from the model  $A$  response, especially at higher light levels (Fig. 3.10). The differences between expected and observed  $A$  integrated over the diurnal period were lowest for the three large leaved genotypes; IT genotype (11.67%); Ge (14.48%); NL (15.82%), whilst the two small leaved genotypes were both above 18%; Fr (18.19%); Sp (20.18%). Correlations between the limitation of  $A$  estimated from the  $A/C_i$  analysis ( $\text{ACi}_{\text{Limit}}$ ) and the limitation of  $A$  over the diurnal period estimated from  $A/Q$  analysis ( $\text{Diur}_{\text{Limit}}$ ) were shown to be positively correlated (Fig. 3.11A), highlighting that any limitation imposed by stomata (and leaf boundary layer) is conserved between methods and during different environmental responses. However, an offset between small leaved and large leaved genotypes is evident with small leaved genotypes displaying higher values of  $\text{Diur}_{\text{Limit}}$  compared to large leaved genotypes as previously shown (Fig. 3.10) but similar values of  $\text{ACi}_{\text{Limit}}$  (Fig. 3.7). Figure 3.11B highlights how the greater the limitation of  $A$  imposed by stomata over the diurnal period ( $\text{Diur}_{\text{Limit}}$ ), the higher the value of diurnal  $W_i$  over the same time period. This is expected, as a lower value of  $g_s$  (e.g. to conserve water) would also lead to a potentially greater limitation on  $A$ .

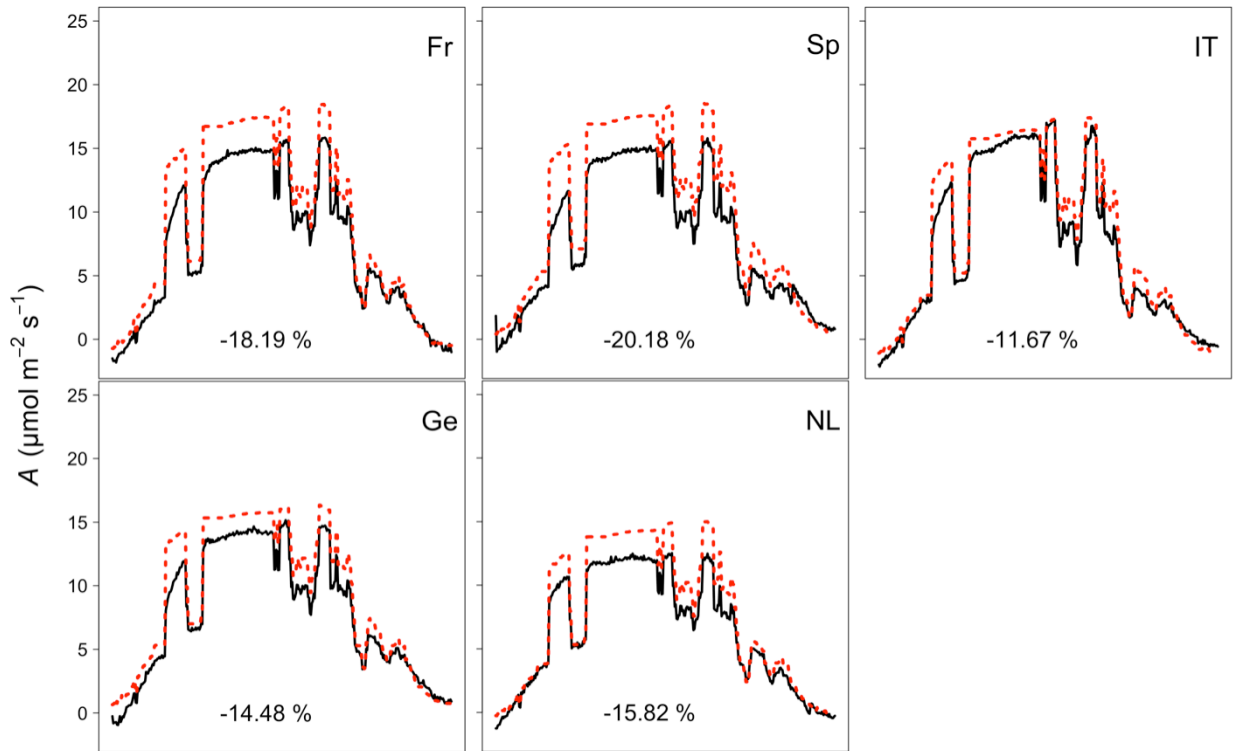


**Figure 3.10.** Diurnal measurements of observed net CO<sub>2</sub> assimilation (black line) and predicted net CO<sub>2</sub> assimilation modelled from the A/Q response curves (red dashed line) for the five selected genotypes. Percentage figure is the difference between observed and modeled values representing a loss in A through limitations in stomata, leaf boundary layer and biochemistry (Diur<sub>Limit</sub>). n = 4-6.

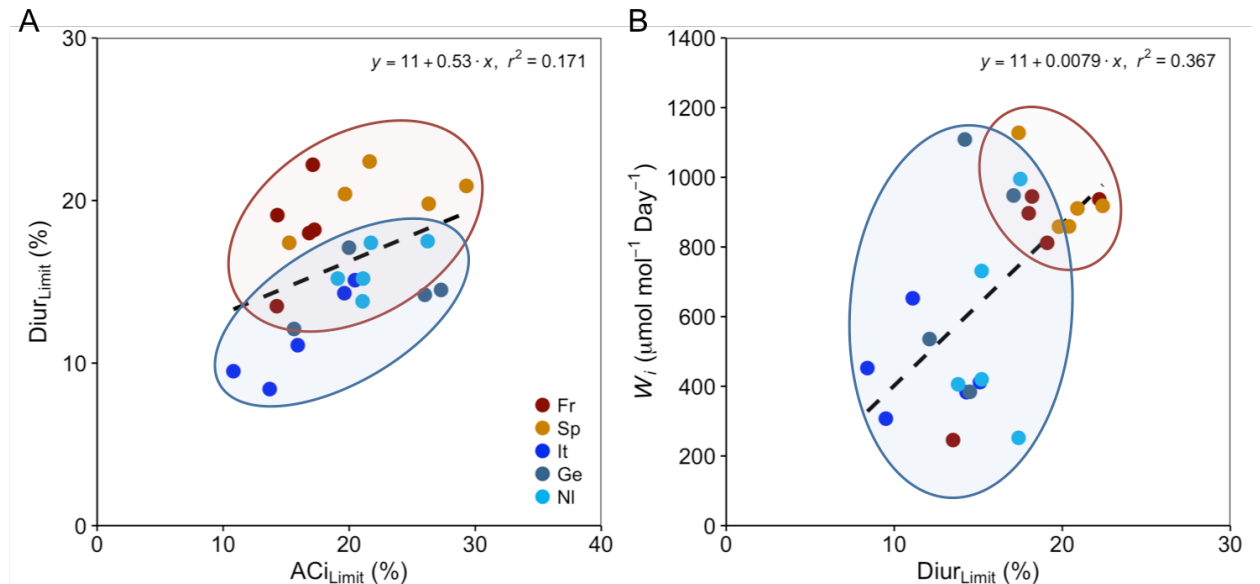


**Figure 3.11.** Correlation between the estimation of the limitation placed on net CO<sub>2</sub> assimilation by stomata and leaf boundary layer, calculated from the A/C<sub>i</sub> response curves (ACi<sub>Limit</sub>, Fig. 3.7) and the diurnal measurements (Diur<sub>Limit</sub>, Fig. 3.10) (A). Correlation between the limitation (Diur<sub>Limit</sub>) and daily intrinsic water use efficiency ( $W_i$ ) during the diurnal (B). Each data point represents an individual plant. Filled areas highlight small leaved (red) and large leaved (blue) genotypes, whilst black dotted line represents the trend in the data for all individuals.

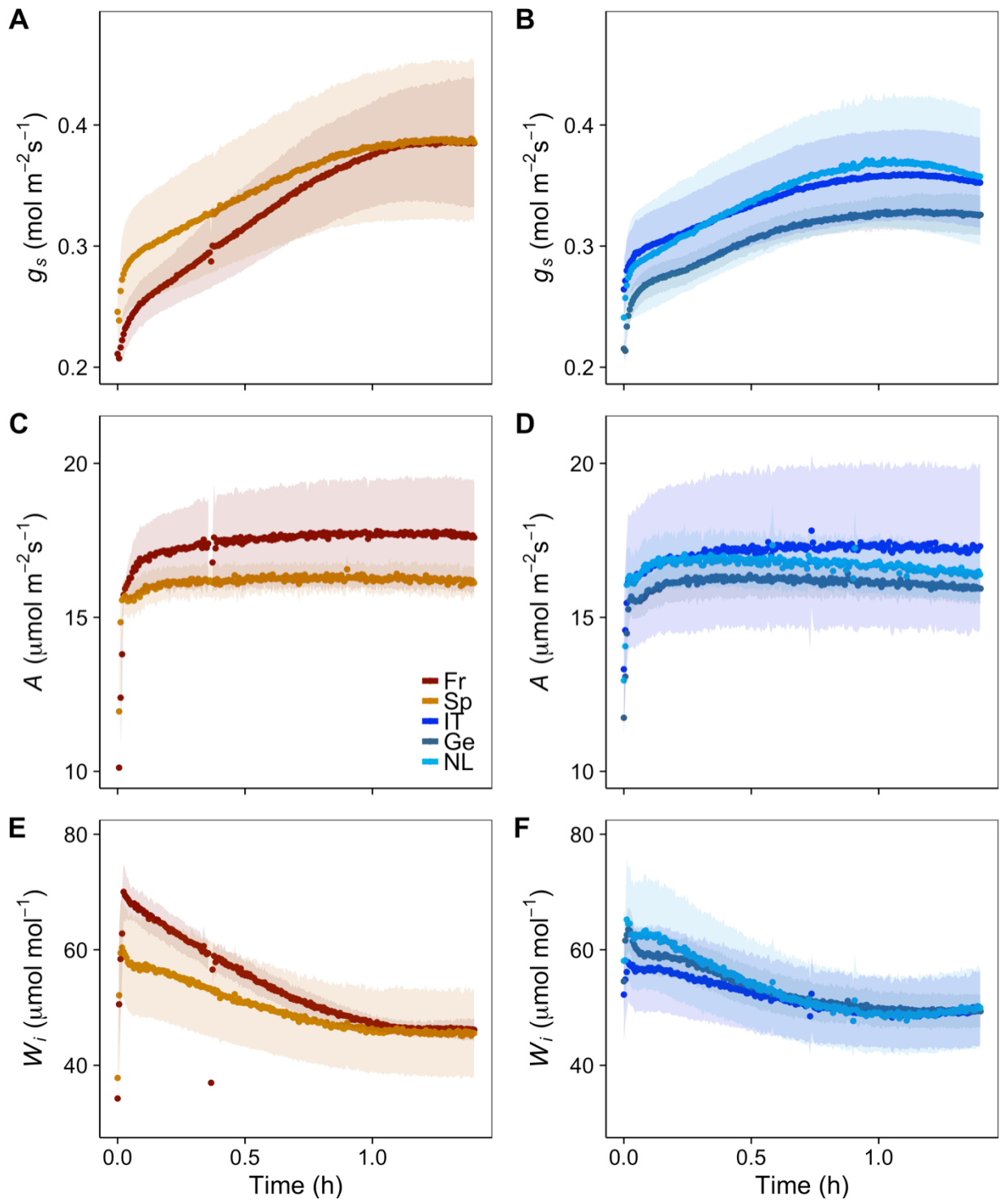


**Figure 3.12.** Temporal response of stomatal conductance ( $g_s$ ; A + B), net CO<sub>2</sub> assimilation ( $A$ ; C + D), and intrinsic water use efficiency ( $W_i$ ; E + F), to a step increase in light intensity (from 500 to 1500  $\mu\text{mol m}^{-2}\text{s}^{-1}$ ) for the five selected genotypes (one from each region). Gas exchange parameters ( $g_s$  and  $A$ ) were recorded at 20s intervals, leaf temperature maintained at 25°C, and leaf VPD at  $1 \pm 0.2$  KPa. Error ribbons represent mean  $\pm$  SE.  $n = 4-6$ .

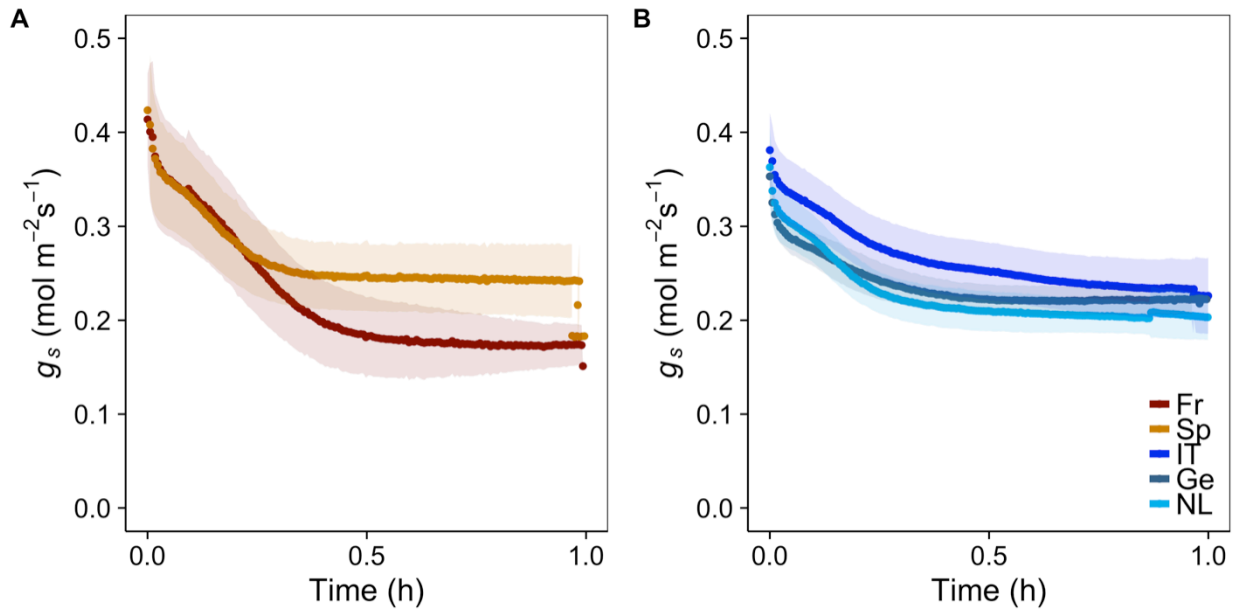


**Figure 3.13.** Temporal response of stomatal conductance ( $g_s$ ) to a step decrease in light intensity (from 1500 to 500  $\mu\text{mol m}^{-2} \text{s}^{-1}$ ) for the five selected genotypes (one from each region). Gas exchange parameters ( $g_s$ , and  $A$ ) were recorded at 20s intervals, leaf temperature maintained at 25°C, and leaf VPD at  $1 \pm 0.2$  KPa. Error ribbons represent mean  $\pm$  SE.  $n = 4-6$ .

### 3.3.7. Response of $g_s$ and $A$ to a step change in PPFD

To assess the difference in stomatal responses to light intensity, leaves from each genotype were subjected to a step increase in PPFD (500-1500  $\mu\text{mol m}^{-2} \text{s}^{-1}$ ) followed by a step decrease (1500-500  $\mu\text{mol m}^{-2} \text{s}^{-1}$ ), and the effect on  $A$  and  $g_s$  measured using gas exchange (Fig. 3.12). In all genotypes (Fr, Sp, IT, Ge, NL)  $g_s$  reached a new plateau within 90 minutes after the light was increased (Fig. 3.12A + B), however the large leaved genotypes reached a new plateau after only ca. 60 min, whilst the small leaved genotypes appear to take the entire 90 min. Following the increase in PPFD to 1500  $\mu\text{mol m}^{-2} \text{s}^{-1}$  an almost instantaneous increase in  $A$  occurred, which was in contrast with the slow increase in  $g_s$  (Fig. 3.12C + D). After the near instantaneous increase in  $A$ ,  $g_s$  continued to increase during the measurement period despite the fact that  $A$  had reached near steady state levels. Intrinsic water use efficiency ( $W_i$ ), decreased over the course of the step increase in light intensity (Fig. 3.12E + F), predominantly driven by the slow increase in  $g_s$  over the same time period.  $W_i$  calculated from the small leaved genotypes (Fr, Sp) was initially (first ten minutes) higher than the large leaved genotypes. However, by the end of the step increase  $W_i$  was lower in the small leaved genotypes than the large leaved, driven by the higher values of  $g_s$  at this time period. In all genotypes,  $g_s$  decreased when the light intensity was returned to 500  $\mu\text{mol m}^{-2} \text{s}^{-1}$  (Fig. 3.13). The highest final values of  $g_s$  at 500 PPFD were recorded in the Sp genotypes (ca. 0.24  $\text{mol m}^{-2} \text{s}^{-1}$ ), whilst Fr (ca. 0.17  $\text{mol m}^{-2} \text{s}^{-1}$ ) displayed the lowest values (Fig. 3.13A). Incidentally

the three large leaved genotypes displayed remarkably similar responses in  $g_s$  to a step decrease in light intensity (Fig. 3.13B).

### 3.3.8. Speed of $g_s$ response to a step change in PPFD

Stomatal responses to a step increase and decrease in PPFD were used to determine natural variation in the speed of  $g_s$  response to light amongst *Populus nigra* genotypes. Determined from the temporal response data were: time constants for stomatal opening ( $\tau_i$ , Fig. 3.14A); final values of  $g_s$  at 1500 PPFD ( $G_i$ , Fig. 3.14B) in response to a step increase in light; time constants for stomatal closure ( $\tau_d$ , Fig. 3.14C); final values of  $g_s$  at 500 PPFD for stomatal closure ( $G_d$ , Fig. 3.14D) in response to a step decrease in light; magnitude of change in  $g_s$  between steady state values at 500 PPFD to 1500 PPFD ( $\Delta G_i$ , Fig. 3.14E) and 1500 PPFD to 500 PPFD ( $\Delta G_d$ , Fig. 3.14F); the time constant for light saturated rate of carbon assimilation at 1500  $\mu\text{mol m}^{-2} \text{s}^{-1}$  PPFD ( $\tau_{ai}$ , Fig. 3.14G) and saturated rates of  $A$  at 1500 PPFD ( $A_i$ , Fig. 3.14H). Net CO<sub>2</sub> assimilation ( $A$ ) was deemed saturated at 1500 PPFD from analysis of light response curves on the same plants (Fig. 3.4). Time constants for stomatal opening ( $\tau_i$ , Fig. 3.14A) were significantly slower ( $P < 0.05$ ) in the small leaved genotypes (Fr, Sp) compared with the large leaved genotypes (IT, Ge, NL), with the three large leaved genotypes displaying remarkably similar values of  $\tau_i$ , despite no significant difference in final values of  $g_s$  at 1500 PPFD ( $G_i$ ; Fig. 3.13B). In contrast to stomatal opening, time constants for stomatal closure ( $\tau_d$ ) varied, with the Fr and Ge genotypes displaying significantly slower responses of  $g_s$  to a decrease in PPFD than the other three genotypes (Fig. 3.14C), with the Sp genotype showing the fastest response. Again, this does not correlate with final values of  $g_s$  at 500 PPFD as no significant difference was observed (Fig. 3.14D). The magnitude of change in  $g_s$  between steady state values at 500 PPFD to 1500 PPFD ( $\Delta G_i$ , Fig. 3.14E) and the magnitude of change in  $g_s$  between steady state values at 1500 PPFD to 500 PPFD ( $\Delta G_d$ , Fig. 3.14F) was higher in small leaved genotypes, and was significantly higher ( $P < 0.05$ ) in the Fr genotype compared to all three large leaved genotypes for both  $\Delta G_i$  and  $\Delta G_d$ . Time constants for light saturated  $A$  ( $\tau_{ai}$ , Fig. 3.14G) were significantly slower ( $P < 0.05$ ) in Ge compared to all other genotypes, with Sp displaying values of  $\tau_{ai}$  that were significantly faster ( $P < 0.05$ ) than all other genotypes. No significant differences in saturated rates of  $A$  at 1500 PPFD ( $A_i$ ; Fig. 3.14H) were observed between all five genotypes.

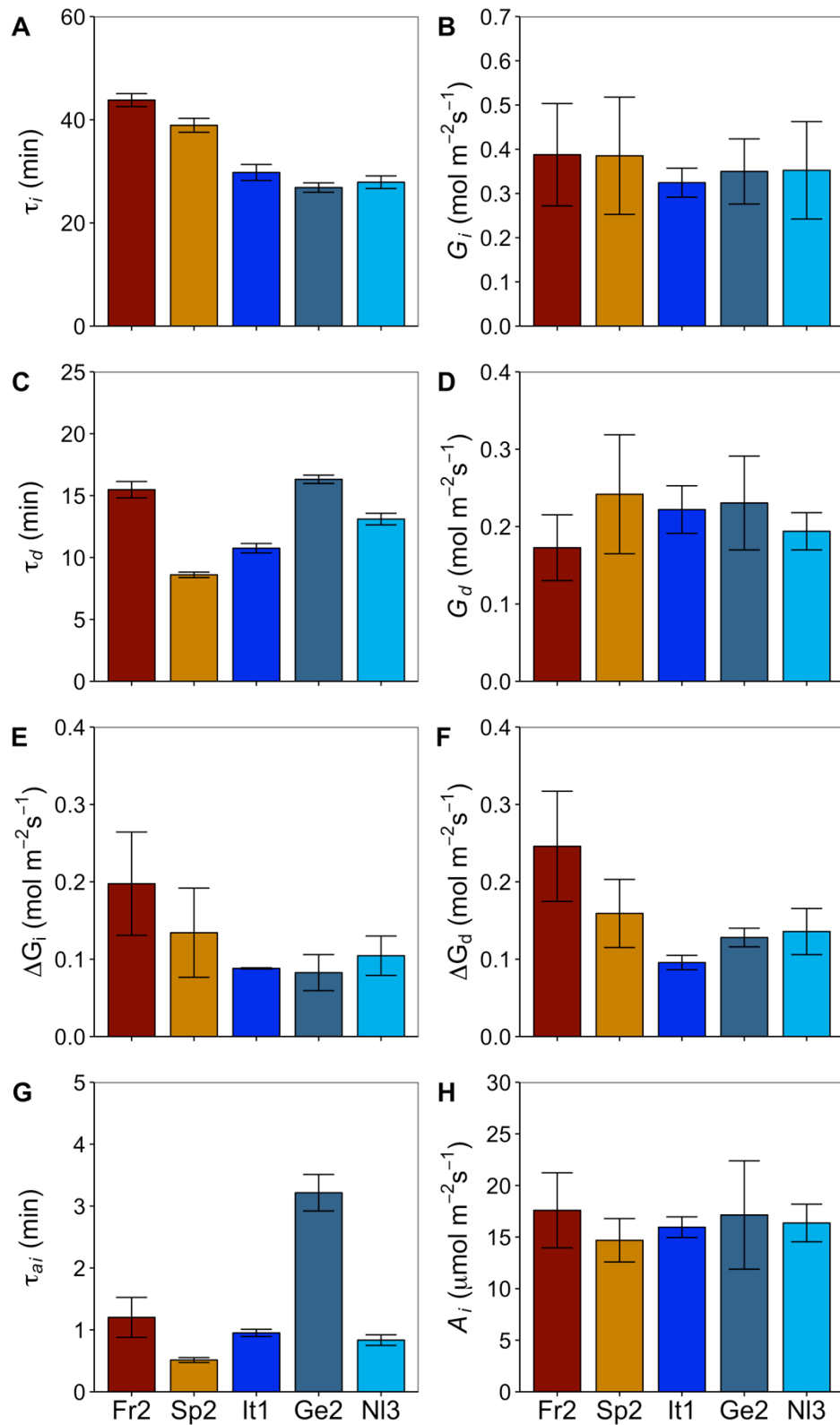


**Figure 3.14.** Time constant for stomatal opening ( $\tau_i$ , A), Final values of stomatal conductance at ( $1500 \mu\text{mol m}^{-2} \text{s}^{-1}$ ) after an increased step change in light intensity ( $G_i$ , B); time constant for stomatal closure ( $\tau_d$ , C), Final values of stomatal conductance at ( $500 \mu\text{mol m}^{-2} \text{s}^{-1}$ ) after a decreased step change in light intensity ( $G_d$ , D); difference in  $g_s$  at 500 and  $1500 \mu\text{mol m}^{-2} \text{s}^{-1}$  following the step increase ( $\Delta G_i$ , E) or decrease ( $\Delta G_d$ , F) in light intensity; light saturated rate of carbon assimilation ( $\tau_{ai}$ , G) to a step change in light intensity; and saturation of net  $\text{CO}_2$  assimilation at  $1500 \text{PPFD}$  ( $A_i$ , H). Error bars represent 95% confidence intervals.  $n=4-6$ .

### 3.3.9. Stomatal anatomy

Significant differences ( $P < 0.05$ ) were observed in abaxial stomatal density ( $SD_{Ab}$ ), with all four small leaved genotypes exhibiting significantly lower densities than all six large leaved genotypes (Fig. 3.15A). Fr2 had significantly lower ( $P < 0.05$ ) adaxial stomatal density than It1 and Ge2, with Ge2 also being significantly higher than the two Spanish genotypes (Sp1, Sp2) (Fig. 3.15B). Both French genotypes (Fr2, Fr4) had significantly lower ( $P < 0.05$ ) stomatal index than It1 (Fig. 3.15C), though no other differences were observed. No difference in stomatal ratio (Fig. 3.15D) or pore area (Fig. 3.15E) was observed between genotypes. Theoretical maximum of stomatal conductance ( $g_{smax}$ ; Fig. 3.15F) was significantly higher ( $P < 0.05$ ) in all six large leaved genotypes compared with the four small leaved, which was driven primarily by the large difference in stomatal density between these two groups.

### 3.3.10. Impact of stomatal density and speed of response on intrinsic water use efficiency

A negative relationship between abaxial stomatal density ( $SD_{Ab}$ ) and the time constant of stomatal opening to light ( $\tau_i$ ) was observed in all genotypes (Fig. 3.16A). In this case, as  $SD_{Ab}$  increased the time it took  $g_s$  to reach a new steady state after a step increase in light decreased. A negative relationship between  $SD_{Ab}$  and daily intrinsic water use efficiency during the diurnal ( $W_i$ ) was also observed between genotypes (Fig. 3.16B), where an increase in  $SD_{Ab}$  would lead to a decrease in  $W_i$ , as observed by the large leaved genotypes typically exhibiting higher densities and therefore lower  $W_i$ . It is interesting to note that this data lead to a positive relationship between the time constant for stomatal opening ( $\tau_i$ ) and daily intrinsic water use efficiency ( $W_i$ ) (Fig. 3.16C), where an increase in the time it took for stomatal conductance to reach a new steady state value would correspond to an increase in  $W_i$  over the diurnal period.

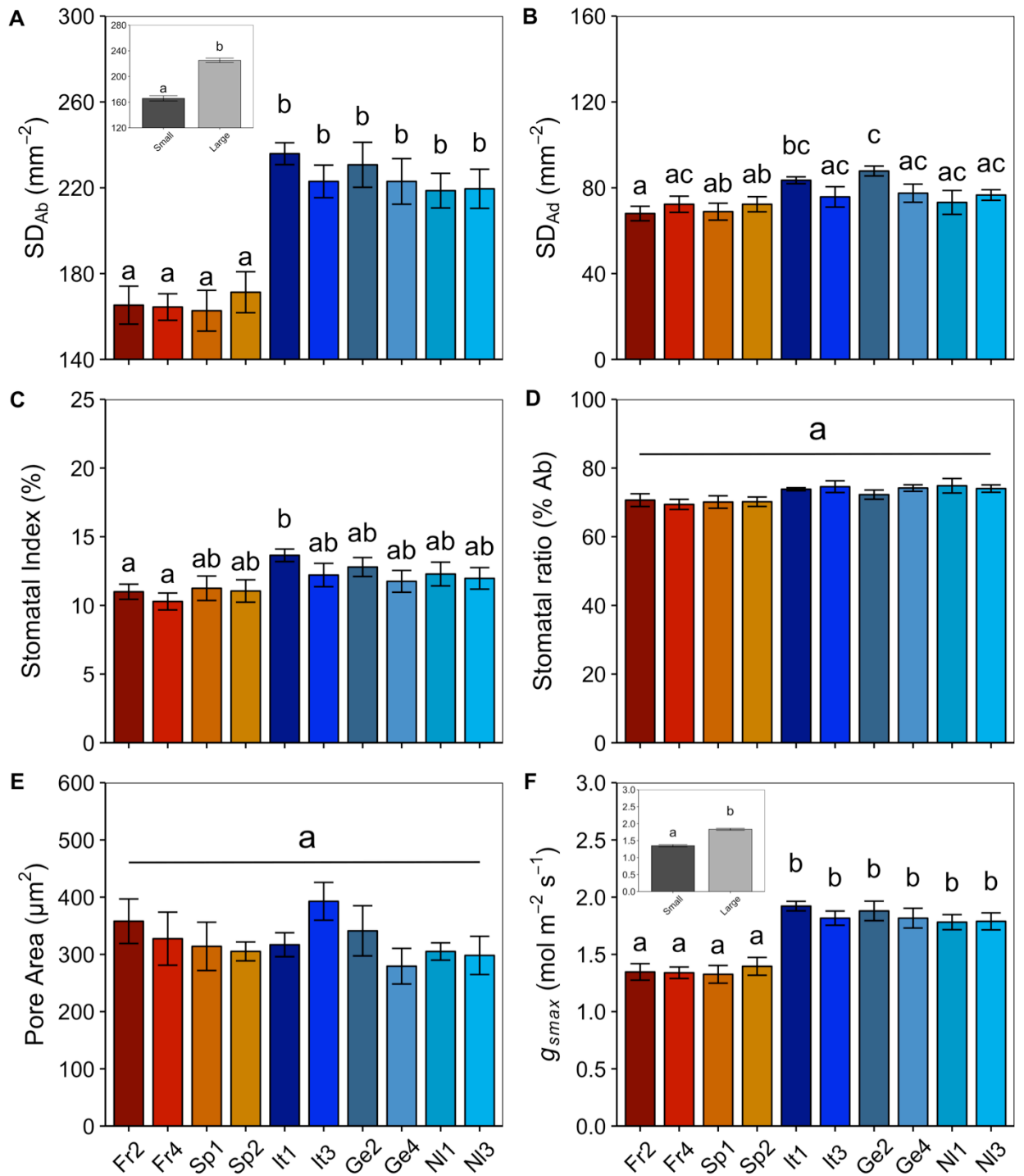


**Figure 3.15.** Stomatal anatomical characteristics including abaxial stomatal density ( $SD_{Ab}$ ; A); adaxial stomatal density ( $SD_{Ad}$ ; B); stomatal index (C); stomatal abaxial:adaxial ratio (D); abaxial stomatal pore area (E); maximum stomatal conductance ( $g_{smax}$ ; F) for the four small-leaved genotypes (red and orange), and the six large-leaved genotypes (Blue and turquoise). Inset graphs (A + F) highlight differences between grouped small and large leaf genotypes for  $SD_{Ab}$  and  $g_{smax}$ . Error bars represent mean  $\pm$  SE.  $n = 10$ . Letters represent the results of *Tukey's post-hoc* comparisons of group means.

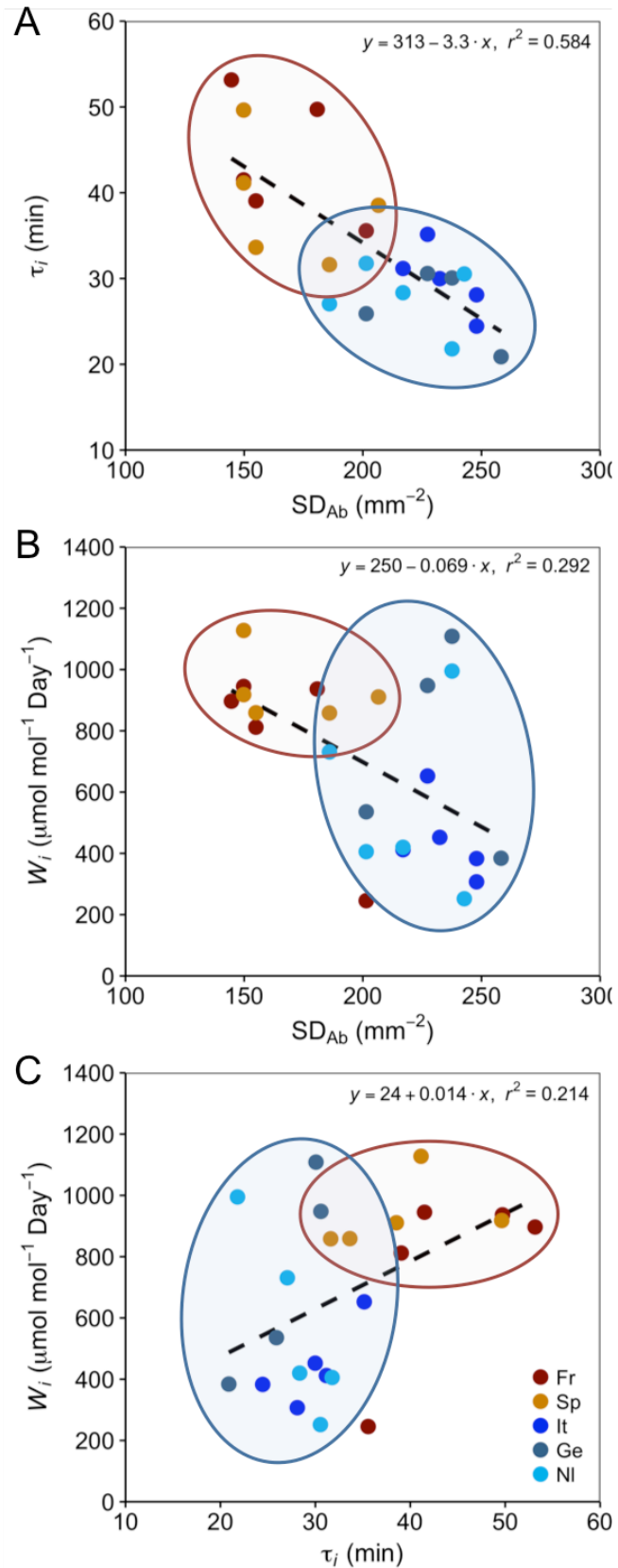


**Figure 3.16.** Correlations between abaxial stomatal density ( $SD_{Ab}$ ) and time constant for stomatal opening ( $\tau_i$ , A); daily intrinsic water use efficiency during the diurnal ( $W_i$ , B); and between  $\tau_i$  and  $W_i$  (C). Filled areas highlight small leaved (red) and large leaved (blue) genotypes, whilst black dotted line represents the trend in the data for all individuals.

### 3.4. Discussion

Plants regulate stomatal conductance to optimize carbon uptake and reduce water loss (Cowan 1977; Hetherington and Woodward, 2003; Ooba and Takahashi, 2003). A significant limitation in this process, is the speed and magnitude of the  $g_s$  response to light, which has been shown to vary widely between species (Cowan and Farquhar, 1977; Vico 2011; McAusland et al, 2016), with several studies highlighting large inter-specific variations in stomatal response through differences in stomatal anatomy (Hetherington and Woodward, 2003; Franks and Farquhar, 2007; McAusland et al, 2016) and biochemistry (McAusland et al, 2016). Despite this, the natural variation in stomatal responses to light intensity within a given species has received less attention as well as the potential acclimation to different environmental conditions. Previous research has focused on changes in  $g_s$  response associated with dynamic acclimation to sun and shade flecks in a controlled laboratory environment (Assmann and Grantz, 1990; Ooba and Takahashi, 2003; Vico et al, 2011; Drake et al, 2013).

In this study, a collection of *Populus nigra* (Black Poplar) genotypes from various locations of origin in Europe were assessed, to investigate natural variation in photosynthetic and stomatal traits, and the impact on intrinsic water use efficiency. Ten genotypes from five different locations (two from each) were chosen for analysis, and demonstrated large variation in leaf dimensions, stomatal anatomical traits, and phenotype.

Analysis of  $A/Q$  curves revealed higher  $A_{\text{sat}}$  values on an area basis in the small leaved genotypes, suggesting that plants acclimate to higher light intensities associated with their native environment (Chabot et al, 1979; Watling et al, 1997), as seen in the Spanish and French genotypes that had the highest Mean annual irradiance (Table 3.1). The higher  $A_{\text{sat}}$  values illustrated by the small leaved genotypes are characteristic of plants grown in high PPFD environments often related to a greater investment in photosynthetic compounds (Bailey et al, 2001). However, the thinner leaves exhibited by the large leaved genotypes along with higher values of  $A$  on a mass basis ( $A_{\text{mass}}$ ) suggests that these large leaved genotypes have a greater photosynthetic component (such as Rubisco) content per cell. This data was mirrored by the analysis of  $A/C_i$  response curves, suggesting that under well watered conditions plants will often adapt over the long term to maximise  $\text{CO}_2$  uptake (greater photosynthetic component per cell) and light capture (greater leaf area) at the expense of water use efficiency, this is consistent with previous work that has highlighted these potential adaptations both between and within species (Percy, 2007). Nevertheless, there was no difference in the maximum rates of carboxylation ( $V_{\text{cmax}}$ ) and electron transport ( $J_{\text{max}}$ ), and although there was a trend toward small leaved genotypes

having higher values of  $V_{cmax}$  and  $J_{max}$  the maximum rates may not be realised, as under ambient  $[CO_2]$  conditions and high light,  $CO_2$  would be more limiting than light availability (Allen and Pearcy, 2000; Pearcy, 2007). These observations suggest that small leaved genotypes invest in greater capacities for photosynthesis on an area basis due to the higher levels of irradiance and temperature in their native environment (see Table. 3.1) (Allen and Pearcy, 2000; Way and Pearcy, 2012).

Diurnal gas exchange under a fluctuating light regime, mimicking a light pattern that may be experienced by plants in the field, was used to examine the inter-specific variation in  $A$ ,  $g_s$ , and  $W_i$  over the diurnal period in different *Populus nigra* genotypes. In general, the two small leaved (Spanish and French) and the Italian genotypes displayed higher photosynthetic rates, which matched the findings from the  $A/Q$  curves. In the Italian genotype this was accompanied by a higher value of  $C_i$  over the diurnal period, indicating that there would have been a greater flux of  $CO_2$  from the atmosphere to the inside of the leaf. This is further supported by the lower value of the estimated limitation on  $A$  by stomata ( $Diur_{Limit}$ ) exhibited in this genotype, with the potential  $A$  over the diurnal period calculated from the  $A/Q$  response curves measured under conditions most favourable for photosynthesis, with theoretically maximised Rubisco activation and with no limitation on  $A$  imposed by stomata (Parsons et al, 1998). Interestingly in contrast to the Italian genotypes, the lower  $C_i$  levels observed in the small leaved genotypes (Spanish and French), indicate the possibility of a greater limitation in the flux of  $CO_2$  to the site of carboxylation, although this was not consistent with no change observed in  $V_{cmax}$ . This is interesting to note, as the estimations of diurnal limitations on photosynthesis ( $Diur_{Limit}$ ) would indicate that these genotypes have a greater limitation imposed on them by stomatal conductance. However, the limitation in  $A$  estimated from the diurnal measurements and  $A/Q$  curves were not coordinated with the limitation in  $A$  estimated from the  $A/C_i$  curves ( $ACi_{Limit}$ ), with the small leaved genotypes exhibiting the lowest levels of  $ACi_{Limit}$  but the highest  $Diur_{Limit}$ , suggesting that over the diurnal period all plants, even under well-watered conditions, will balance the need for  $CO_2$  uptake with the need to reduce water loss, depending on the current needs of the plant (Casson and Hetherington, 2010). The higher limitation of  $A$  along with the lower  $g_s$  values over the diurnal period observed in the small leaved genotypes, may indicate a water saving strategy that potentially balances  $CO_2$  uptake and water loss over the diurnal period to optimize the current needs of the plant, as revealed by the higher diurnal  $W_i$  in small-leaved genotypes (Lawson and Blatt, 2014; McAusland et al, 2016). Certainly, in areas where drought might be a constant constraint on performance, often maintaining water status is far more important than carbon gain, and as such represents a priority signal to which the plant must respond (Lawson and Morison, 2004; Lawson et al, 2010; Aasamaa and Söber, 2011). The high  $g_s$  response shown by the Italian genotype over the diurnal period potentially maximizes carbon capture, as highlighted by the lowest value of  $Diur_{Limit}$ , but this also leads to a reduction in  $W_i$ . This corresponds strongly with the

conditions at the origin site, where there is little limitation by water availability due to high precipitation levels and therefore no need to reduce stomatal aperture to conserve water (Hetherington and Woodward, 2003; Lawson and Blatt 2014), and with origin site air temperatures being high, there is a requirement to open stomata to maximize evaporative cooling (Caird et al, 2007; Hills et al, 2012; Schymanski et al, 2013).

The time taken to increase or decrease stomatal conductance ( $g_s$ ) to changes in environmental conditions plays a critical role in maximising carbon gain and conserving water (Cowan and Farquhar, 1977; Lawson et al, 2010; Vico et al, 2011; Lawson and Blatt, 2014), with considerable variation observed between species depending on growth environment and anatomy (Allen and Pearcy, 2000; Ooba and Takahashi, 2003; Vico et al, 2011; Drake et al, 2013; McAusland et al, 2016). Slower stomatal movement can often limit CO<sub>2</sub> diffusion for photosynthesis (Barradas et al, 1998; Barradas and Jones, 1996; Lawson et al, 1998; Kaiser and Kappen 2000; Vico et al, 2011), whilst faster responses and higher  $g_s$  can maximize carbon gain but at the expense of water use efficiency through increased transpiration (Barradas et al, 1994; Naumburg and Ellsworth, 2000; Lebaudy et al, 2008; McAusland et al, 2016). Considerable variation in the time taken for stomata to open or close to a step change in *PPFD* was observed between genotypes, with all genotypes taking longer to increase  $g_s$  than to decrease  $g_s$ , which is consistent with the theory that plants prioritise conservation of water over carbon gain (Ooba and Takahashi, 2003). Both the magnitude and rapidity of  $g_s$  response to a step change in *PPFD* differed between genotypes, primarily when grouped by leaf phenotype. Small leaved genotypes demonstrated the slowest  $g_s$  responses, which corresponded with them exhibiting the largest magnitude of change in  $g_s$  between steady state measurements. In contrast to the opening response, there was no relationship between the speed of stomatal closure and the magnitude of change in  $g_s$ . In fact, it has been hypothesised that the Spanish and French genotypes have developed smaller leaves to reduce total leaf surface area as an adaptation to drought conditions in their native environment (Viger et al, 2016). The slower  $g_s$  response by the Spanish and French genotypes may represent a negative impact on carbon gain but would reduce the chance of drought at the whole plant level (Meinzer and Grantz, 1990; Knapp, 1993), therefore benefitting genotypes adapted to environments more susceptible to drought (Hetherington and Woodward, 2003). The consequences for this adaptation are highlighted in the diurnal measurements, with the small leaved genotypes (Spanish and French) demonstrating the highest values of  $W_i$  and of the limitation in  $A$  imposed by stomata ( $Diur_{Limit}$ ), signifying that the speed of stomatal responses to perturbations in light is critical in determining CO<sub>2</sub> uptake and (as seen in the small leaved genotypes) water use efficiency over the course of the day (McAusland et al, 2016; Violet-Chabrand et al, 2016).

Stomatal density has been shown to increase with increasing growth light intensity (Gay and Hurd, 1975) and is related to maximising CO<sub>2</sub> diffusion for carbon assimilation, nutrient uptake and evaporative cooling (Schymanski et al, 2013). No major differences in stomatal index or pore area were observed between genotypes, indicating the lower values of  $g_{smax}$  observed in the small leaved genotypes was driven by stomatal density (Dow et al, 2014). The lower values of  $SD$  seen in the small leaved genotypes were consistent with the lower  $g_s$  values observed during the diurnal measurements compared with the Italian genotypes, which is consistent with the knowledge that growth light environment strongly influences these factors (Willmer and Fricker, 1996; Hetherington and Woodward, 2003; Franks and Beerling, 2009). However, these results do not correlate with the assumption that stomatal density increases with growth light, which may be due to other environmental factors playing a role during development, such as water availability (Gay and Hurd, 1975; Hetherington and Woodward, 2003; Lawson and Blatt, 2014), and CO<sub>2</sub> concentration (Tricker et al, 2005). It should also be noted that most of these studies have been carried out on annuals or crop species, and therefore may not be comparable to work on *Populus nigra*. The German and Netherlands genotypes also demonstrated lower  $g_s$  over the diurnal despite higher  $SD$ , which was unexpected but may be due to differences in guard cell signalling, light use efficiency, and other adaptive mechanisms (Chazdon and Pearcy, 1991; Kulheim et al, 2002; Bailey et al, 2004; Lawson et al, 2010; Drake et al, 2013).

It has been reported that higher stomatal densities promote more rapid  $g_s$  responses to changing light intensity (Drake et al, 2013; Franks and Farquhar, 2007; McAusland et al, 2016), which is consistent with the results shown here, as the higher stomatal densities observed in all individual plants was strongly correlated with the time constant for stomatal opening ( $\tau_i$ ). Intrinsic water use efficiency ( $W_i$ ) decreased with an increase in  $SD$  which was expected, as the greater magnitude in  $g_s$  promoted by higher  $SD$  did not necessarily come with a proportional increase in  $A$ . Interestingly, there was a trend toward slower time constants for stomatal opening ( $\tau_i$ ) correlating with higher  $W_i$ , with the small leaved genotypes exhibiting slower response times, higher  $W_i$  and demonstrating the highest values of stomatal limitation over the diurnal period. This is interesting to note as it has been theorised that slower stomatal opening responses are an adaptive mechanism in plants to reduce water loss and maintain leaf turgor (Lawson and Morison, 2004; McAusland et al, 2013, 2016) when facing conditions that may be water limited, again highlighting the strategy of prioritising water conservation over carbon gain in these genotypes (Lawson and Morison, 2004; Lawson et al, 2010; Aasamaa and Söber, 2011).

### 3.5. Main conclusions

In this chapter, natural variation in stomatal response to light was examined in a European *Populus nigra* population, to highlight differences in intra-specific photosynthetic and stomatal response and its impact on water use efficiency.

- Significant differences in the time taken for stomata to open to a step increase in light were observed between genotypes. The fastest rates were observed in the large leaved genotypes, which exhibited higher stomatal densities, suggesting the large leaved genotypes exhibit an adaptive mechanism to increase CO<sub>2</sub> uptake by maximizing stomatal conductance when conditions are ideal. Whilst the small leaved genotypes, that displayed the slowest rates of stomatal opening, lowest stomatal densities and were adapted to drier, high temperature environments, prioritize the conservation of water over the need for carbon gain.
- In all genotypes, an increase in stomatal density was positively correlated with faster  $g_s$  responses to an increase in light, and negatively correlated with intrinsic water use efficiency ( $W_i$ ) over the diurnal period. This led to the observation that slower  $g_s$  response times to an increase in light lead to higher  $W_i$  over the diurnal period. In fact, time constants for stomatal opening were greater than for closure in all genotypes, supporting observations in previous studies on crops that indicate a greater prioritization of conserving water over the need for greater carbon gain, by maintaining stomatal closure for longer.
- Over the diurnal period small leaved genotypes displayed higher levels of intrinsic water use efficiency ( $W_i$ ), driven largely by lower levels of stomatal conductance ( $g_s$ ) compared to large leaved genotypes. This would indicate that small leaved genotypes prioritize water conservation, however, as net CO<sub>2</sub> assimilation rates were comparable to the other genotypes, it would suggest that small leaved genotypes are able to change this priority to maintain high levels of carbon assimilation, depending on the current needs of the plant.
- Stomatal limitation of carbon assimilation estimated over the diurnal period was found to be higher in small leaved genotypes, which positively correlates with limitation in  $A$  estimated from the  $A/C_i$  response curves. This again suggests that the small leaved genotypes will prioritize water conservation over carbon gain even under well-watered conditions, by maintaining lower levels of stomatal conductance.

## CHAPTER 4

---

**Acclimation to growth light intensity impacts stomatal response, photosynthesis and water use efficiency in *Populus nigra***

## Transition Statement

In chapter 3, it was shown that considerable natural variation in stomatal and photosynthetic response exists with a European population of the model tree species *Populus nigra*. This population displayed large differences in the speed and magnitude of  $g_s$  response to instantaneous steps in light intensity and in behaviour over the diurnal period, greatly impacting photosynthesis and therefore water use efficiency. The diversity in adaptation observed in these genotypes to different native growth environmental conditions, highlights the need to consider the impact of different acclimation states on stomatal function and response. The majority of studies focused on growth light intensity have either been undertaken under constant light conditions, or on crops in an aim to investigate plant productivity.

In this chapter, assessment of the impact of growth light intensity on stomatal and photosynthetic acclimation in *Populus nigra*, was undertaken under dynamic light conditions on the roof at the University of Essex. This was in an attempt to characterize stomatal acclimation to growth light intensity under a real light environment, and investigate the impact on photosynthesis and water use efficiency.

## 4.1. Introduction

In nature, plants are subject to changes in light intensity that vary over the course of seconds, minutes, hours, days and during the entire growth period (Assmann and Wang, 2001), with the intensity of growth light impacting stomatal morphology and by extension the steady state values of stomatal conductance ( $g_s$ ) (Franks and Farquhar, 2001; Schlüter et al, 2003). Furthermore, stomatal anatomical characteristics, functional response, and behaviour are constantly adapting to changes in the light environment that plants experience through development (Percy, 2007; Alter et al, 2012), and as light is the main environmental driver of stomatal response and photosynthesis, it impacts dynamics of water use efficiency (Lawson and Blatt, 2014).

It is well known plants acclimate to differences in growth light intensity, with plants subject to higher light intensities often developing thicker leaves (Givnish, 1988; Evans and Poorter, 2001), higher photosynthetic rates per leaf area (Terashima et al, 2006), changes in biochemistry and morphology (Givnish, 1988; Weston et al, 2000; Bailey et al, 2001, 2004), and increases in stomatal density (Gay and Hurd, 1975; Hetherington and Woodward, 2003; Alter et al, 2012). Stomatal anatomy increases and decreases in response to changes in growth environment (Casson and Hetherington, 2010), with stomatal density often changing between leaves on the same plant, with mature leaves systemically signaling to developing leaves as conditions change through growth and development (Lake et al, 2001). Although many studies have shown that stomatal density changes with growth light intensity (Gay and Hurd, 1975), it is still unknown if and how stomatal function acclimates to growth light intensity especially under a dynamic growth light regime. The bulk of studies that have investigated stomatal acclimation to changes in light intensity, have done so on plants that have evolved in forest understory conditions (Chazdon and Percy, 1991; Tinoco-Ojanguren and Percy, 1993; Percy, 1994), or have revealed how these conditions impact stomatal anatomy (Knapp and Smith, 1987; 1988). As a consequence, acclimation of the functional response of stomata, both temporally and diurnally, has largely been overlooked (Lawson and Blatt, 2014), which fundamentally can have a profound impact on photosynthesis and water use efficiency, and the estimation of these parameters in predictive models.

Leaves experience short and long-term fluctuations in light intensity to which stomata respond, with the temporal response of stomatal conductance ( $g_s$ ) to these fluctuations, termed sunflecks, known to vary between species (Ooba and Takahashi, 2003; Vico et al, 2011; McAusland et al, 2016). In Chapter 3, I demonstrated how the temporal response varies within species that have developmentally acclimated to different environments. However, little is known about how changes in growth light intensity can

affect stomatal responses to sunflecks, at different light intensities and at different times of the day. Diurnal variation in stomatal behaviour and sensitivity to changes in light have been reported (Mencuccini et al, 2000; Tallman, 2004), and it has been highlighted that at certain times of the day  $g_s$  may restrict net CO<sub>2</sub> assimilation ( $A$ ) (Mencuccini et al, 2000; Poorter et al, 2016). Furthermore, stomatal acclimation to differences in growth light intensity will potentially influence the magnitude and temporal dynamics of  $g_s$  and  $A$  over the diurnal period, impacting daily patterns of photosynthesis and water use efficiency (Lawson and Blatt, 2014; Raven, 2014).

It is often shown that changes in stomatal traits, particularly stomatal density, can greatly impact intrinsic water use efficiency ( $W_i$ ) (Franks and Farquhar, 2007; Drake et al, 2013), however it is often the speed of  $g_s$  response at any given time point and over the diurnal period that is critical for carbon assimilation and water use (Kirschbaum and Pearcy, 1988; Lawson et al, 2010; McAusland et al, 2016). Despite this, little attention has been given to how stomatal behaviour acclimates to growth light, both in magnitude of  $g_s$  and the rate of response, and the impact this has on photosynthesis and water use. In order to assess the impact of growth light intensity on the kinetics and diurnal responses of stomatal conductance ( $g_s$ ), and the impact on photosynthesis ( $A$ ) and intrinsic water use efficiency ( $W_i$ ), bare root *Populus nigra* subsp. *Betulifolia* trees were grown on the roof at University of Essex under shade structures which reduced the light to 60 and 20% below that of ambient levels. As these plants were grown on the roof, they were still subject to natural fluctuations in light so any acclimation that occurred would be due to the average light intensity rather than any changes in the dynamics of growth light.

The aim of this chapter was to identify the impact of growth light intensity on the acclimation of stomatal conductance ( $g_s$ ) response and behavior over the diurnal period. This was assessed via the response of  $g_s$  to step changes in light at different intensities and at different times of the day, along with the measurement of  $g_s$  over a constant diurnal period. This was further evaluated by considering the impact changes in  $g_s$  response would have on carbon gain and intrinsic water use efficiency, the identification of which may lead to improved understanding of the dynamics of daily water use efficiency and how plants acclimate, both developmentally and dynamically, to differences in their growth light environment.

## 4.2. Materials and Methods

This section outlines methods specific to this chapter and modifications made to protocols outlined in Chapter 2 – “Materials and Methods”.

### 4.2.1. Plant material and growth conditions

Growth structures were built large enough to contain nine bare root trees, and covered in neutral density mesh to create growth light conditions approximately 60% and 20% that of ambient (Fig. 4.1). Measurements of photosynthetic photon flux density (PPFD) were periodically made throughout growth to make sure relative light levels were maintained under the mesh structures (Table. 4.1).

**Table 4.1.** Photosynthetic photon flux density (PPFD) measurements taken at ambient conditions and under the two shade covers. Six measurements per light treatment were taken weekly to make sure the light levels relative to ambient conditions remained the same under the shade covers during growth.

Date	Light – PPFD (% of Ambient)		
	Ambient	P60	P20
31-May	180±2.2	96.8±0.6 (54)	40.3±0.6 (22)
07-June	1706.7±9.1	1033.4±11.9 (61)	391.1±5.2 (23)
14-June	323.8±2.8	203.5±2.1 (63)	68.3±0.9 (21)
21-June	448.9±3.9	280.9±3.0 (62)	91.3±1.1 (20)
28-June	1621.2±7.6	987.5±7.5 (61)	352.1±4.2 (22)
05-July	446.4±4.3	293.1±3.6 (66)	92±1.7 (21)
12-July	1443.6±12.6	855.3±5.2 (59)	274.9±1.6 (19)
19-July	1835.7±8.4	1096.1±3.3 (60)	358.6±2.1 (20)
26-July	1150.2±11.2	677.1±7.2 (59)	231.2±3.7 (20)
02-August	489.7±4.1	295.6±3.9 (60)	98.5±1.6 (20)
<b>Mean % (of ambient)</b>	<b>100</b>	<b>60.3</b>	<b>20.7</b>

Bare root *Populus nigra* subsp. *betulifolia* plants were selected for this chapter as they are native to the UK, and represent a continuation of the species selected in chapter 3. They were planted directly in 15L

pots in Westland John Innes no.2 soil (Westland Horticulture, Dungannon, Northern Ireland) with rooting compound, and moved to the roof (University of Essex). Nine plants were placed directly in each shade structure with a further nine in the open at ambient conditions (Fig. 4.1). Plants were allowed to grow for four weeks before measurements took place, with the plants spaced at random and continuously rotated to reduce environmental error effects.

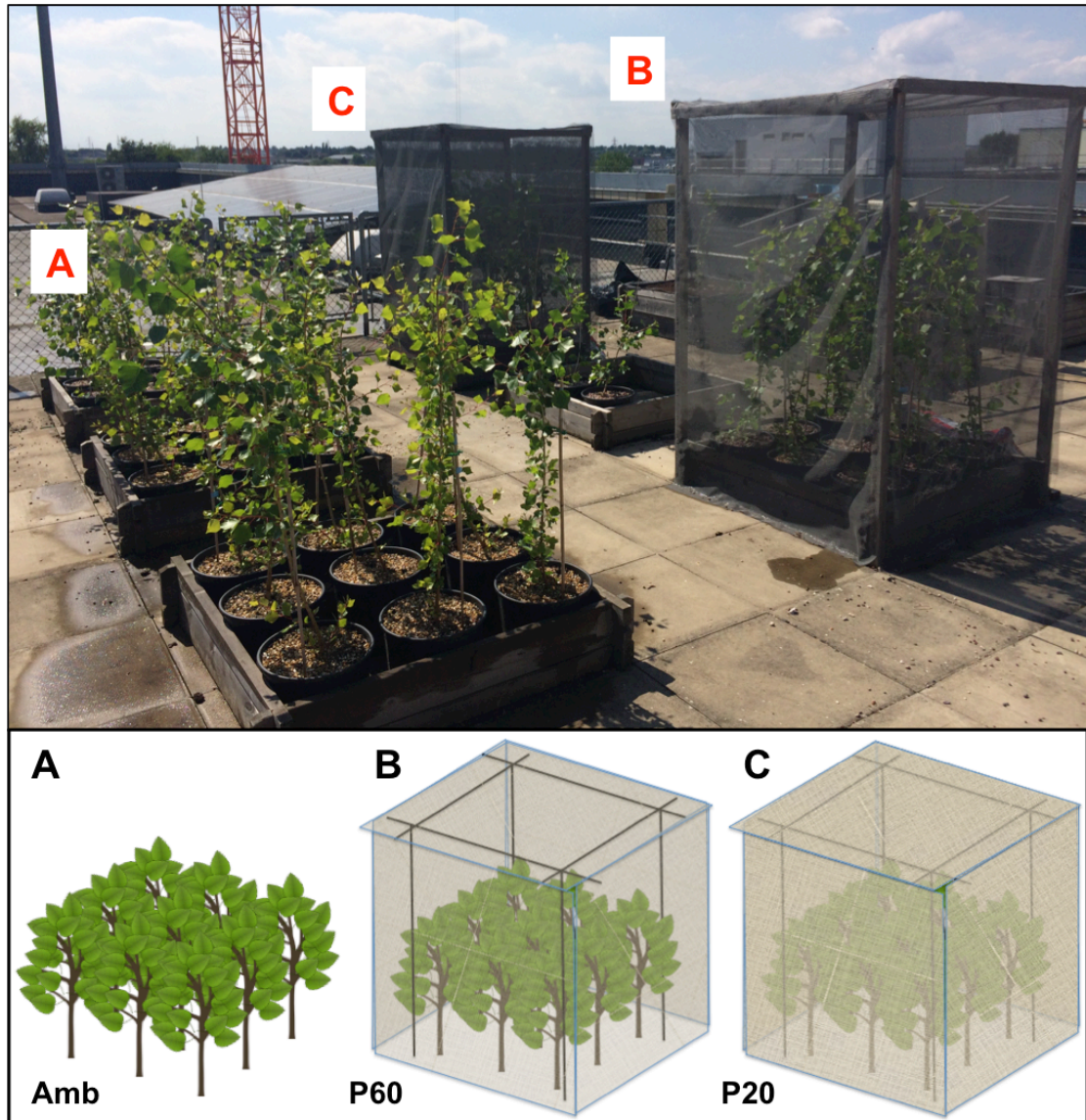


**Figure 4.1.** Structures built to create growth light conditions: at ambient under no mesh (A); ca. 60% of ambient (B); and ca. 20% of ambient (C). Each structure and ambient block held nine plants with minimal self-shading, with extra plants in ambient conditions in case any plants under any light condition showed abnormal growth and needed replacing.

## **4.2.2. Leaf gas exchange**

All gas exchange parameters, including net CO<sub>2</sub> assimilation ( $A$ ) and stomatal conductance ( $g_s$ ) were recorded and cuvette conditions maintained as laid out in Method 2.2, using a Li-Cor 6400XT portable gas exchange system (Li-Cor, Lincoln, Nebraska, USA). All measurements were taken between 9am and 3pm (to reduce time of day effects) using the youngest, fully expanded leaf, between leaves 5-8 as shown previously in Chapter 3, Figure 3.3.

### **4.2.2.1. $A/Q$ (net photosynthetic rate/PPFD) response curves**

The response of net CO<sub>2</sub> assimilation rate ( $A$ ) to photosynthetic photon flux density ( $PPFD$ ) was measured and recorded under cuvette conditions as described in method 2.2.1.

### **4.2.2.2. $A/C_i$ (net photosynthetic rate/intercellular CO<sub>2</sub> concentration) response curves**

The response of net CO<sub>2</sub> assimilation rate ( $A$ ) to intercellular CO<sub>2</sub> concentration ( $C_i$ ) was measured and recorded under cuvette conditions as described in method 2.2.2.

### **4.2.2.3. Temporal response of $A$ and $g_s$**

The response of net CO<sub>2</sub> assimilation rate ( $A$ ) and stomatal conductance ( $g_s$ ) to a step change in photosynthetic photon flux density ( $PPFD$ ), was carried out as described in method 2.2.3.

### **4.2.2.4. Diurnal measurements**

Diurnal gas exchange measurements of net CO<sub>2</sub> assimilation ( $A$ ) and stomatal conductance ( $g_s$ ) were carried out as described in method 2.2.4.

## **4.2.3. Modelling gas exchange parameters**

### **4.2.3.1. Determination of mass integrated net CO<sub>2</sub> assimilation**

Net CO<sub>2</sub> assimilation ( $A$ ) was converted to a mass integrated measurement using leaf mass area ( $LMA$ ) – see method 2.3.1.

#### **4.2.3.2. Estimating photosynthetic capacities**

Photosynthetic capacities ( $V_{C_{max}}$  and  $J_{max}$ ) were estimated from the  $A/C_i$  response curves using method 2.3.2.

#### **4.2.3.3. Assessing stomatal limitation from $A/C_i$ response curves**

The hypothetical  $A$  that would be obtained if the mesophyll had free access to the  $CO_2$  in the ambient air was calculated to quantify the limitation that the combined stomatal and boundary layer conductance impose on leaf  $CO_2$  uptake using the method described in section 2.3.3.

#### **4.2.3.4. Modelling net $CO_2$ assimilation rates**

Net  $CO_2$  assimilation ( $A$ ) as a function of light intensity ( $PPFD$ ) was modelled to simulate the maximum diurnal variations of  $A$  in absence of stomatal limitation under different light intensity conditions. For methods see 2.3.4.

#### **4.2.3.5. Determining the rapidity of stomatal conductance response**

The rapidity of the stomatal response following a step change in light intensity was assessed using method 2.3.5.

#### **4.2.3.6. Determining the rapidity of net $CO_2$ assimilation response**

The rapidity of the response of net  $CO_2$  assimilation following a step change in light intensity was assessed using method 2.3.6.

### **4.2.4. Leaf and stomatal characteristics**

#### **4.2.4.1. Stomatal anatomical measurements**

Stomatal density, pore area, index, ratio and theoretical maximum of stomatal conductance ( $g_{smax}$ ) were assessed by taking impressions of the surface of the leaf, following method 2.4.1, Chapter 2.

#### **4.2.4.2. Leaf anatomical measurements**

Total leaf area (cm<sup>2</sup>), dry weight (g), and specific leaf area (SLA, cm<sup>2</sup>/g), were measured on all poplar growth treatments and were taken using the youngest, fully expanded leaf, between leaves 5-8 as shown in Figure 3.3, Chapter 3.

#### **4.2.4.3. Leaf optical properties**

Measurements of transmittance and reflectance for each leaf was used to calculate absorbance, transmittance, and reflectance, and were measured on the youngest, fully expanded leaf, between leaves 5-8 as shown in Figure 3.3, Chapter 3. For method see 2.4.3.

## 4.3. Results

### 4.3.1. Photosynthetic response to photosynthetic photon flux density (PPFD)

The response of net CO<sub>2</sub> assimilation rate ( $A$ ) as a function of photosynthetic photon flux density (PPFD) ( $Q$ ) ( $A/Q$  curves, Fig. 4.2) was measured on poplar trees subjected to the three growth light treatments, to investigate differences in photosynthetic potential. Similar values of  $A$  at PPFDs below 400  $\mu\text{mol m}^{-2} \text{s}^{-1}$  were observed between all treatments (Fig. 4.2A), whereas at PPFD above this level there were noticeable differences in  $A$  between treatments, with plants grown at ambient conditions exhibiting higher  $A$  than the other treatments at all light levels above 500 PPFD. Plants grown at P60 (60% that of ambient) showed higher values of  $A$  than plants grown at P20 (20% that of ambient) at all light levels from 900 PPFD and above. At saturating light (ca. 1500  $\mu\text{mol m}^{-2} \text{s}^{-1}$ ),  $A_{\text{sat}}$  was found to be significantly higher ( $P < 0.05$ ) in plants grown in ambient conditions compared to the other two treatments, with  $A_{\text{sat}}$  also significantly higher ( $P < 0.05$ ) in P60 grown plants compared with P20 (Fig. 4.2C). To take into consideration photosynthesis per unit leaf volume,  $A$  was integrated by mass of dry leaf ( $A_{\text{mass}}$ ) calculated from measurements of leaf mass area (LMA), to highlight the impact of leaf thickness on measurements of  $A$ .  $A_{\text{mass}}$  was found to be similar between treatments throughout the  $A/Q$  curve (Fig. 4.2B), although at saturating PPFD  $A_{\text{mass-sat}}$  was significantly higher ( $P < 0.05$ ) in P60 grown plants compared to P20 (Fig. 4.2D). At low PPFD levels (ca. 200  $\mu\text{mol m}^{-2} \text{s}^{-1}$ ;  $A_{200}$ ) there was no significant difference between treatments (Fig. 4.2E), but when integrated by leaf dry mass ( $A_{\text{mass200}}$ ) both P60 and P20 treatments displayed significantly higher  $A$  ( $P < 0.05$ ) than plants grown at ambient conditions (Fig. 4.2F).

### 4.3.2. Leaf size and absorbance properties

Leaf area was measured on fully expanded mature leaves and was significantly higher ( $P < 0.05$ ) in plants grown under P20 conditions compared to the other two treatments with values ranging from ca. 80 cm<sup>2</sup> (P20) to ca. 44 cm<sup>2</sup> (Amb), with P60 grown plants also displaying significantly higher ( $P < 0.05$ ) areas than those grown at ambient conditions (Fig. 4.3A). Similar differences were found for leaf dry weight, with P20 grown plants showing significantly higher ( $P < 0.05$ ) values of dry weight than those grown at ambient conditions (Fig. 4.3B). The differences observed in leaf area and leaf dry weight led to significant differences in specific leaf area (SLA) (Fig. 4.3C), with P20 grown plants exhibiting significantly higher ( $P < 0.05$ ) specific leaf areas than those grown under the other two treatments, and P60 grown plants displaying significantly higher ( $P < 0.05$ ) values than those grown under ambient conditions.

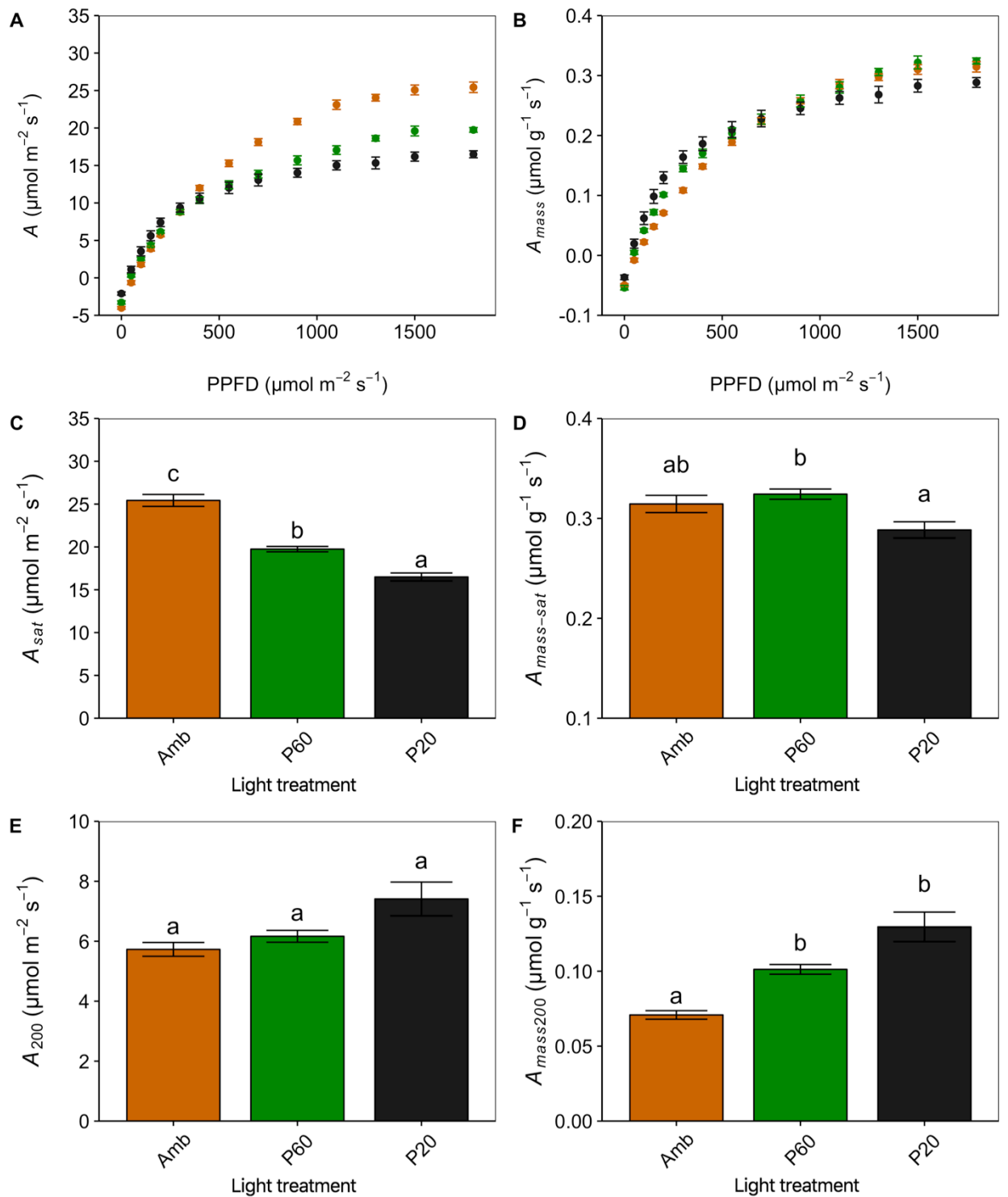


**Figure 4.2.** Photosynthesis as a function of light intensity (PPFD) for the three Poplar light treatments: Ambient (Orange); P60 (Green); P20 (Black). Net CO<sub>2</sub> assimilation on an area basis ( $A$ ; A); relative to leaf mass ( $A_{mass}$ ; B); light saturated rate of photosynthesis ( $A_{sat}$ ) on an area (C) and mass (D) basis; Photosynthesis at 200 PPFD ( $A_{200}$ ) on an area (E) and mass (F) basis. Error bars represent mean  $\pm$  SE.  $n = 5-6$ . Letters represent the results of *Tukey's post-hoc* comparisons of group means.

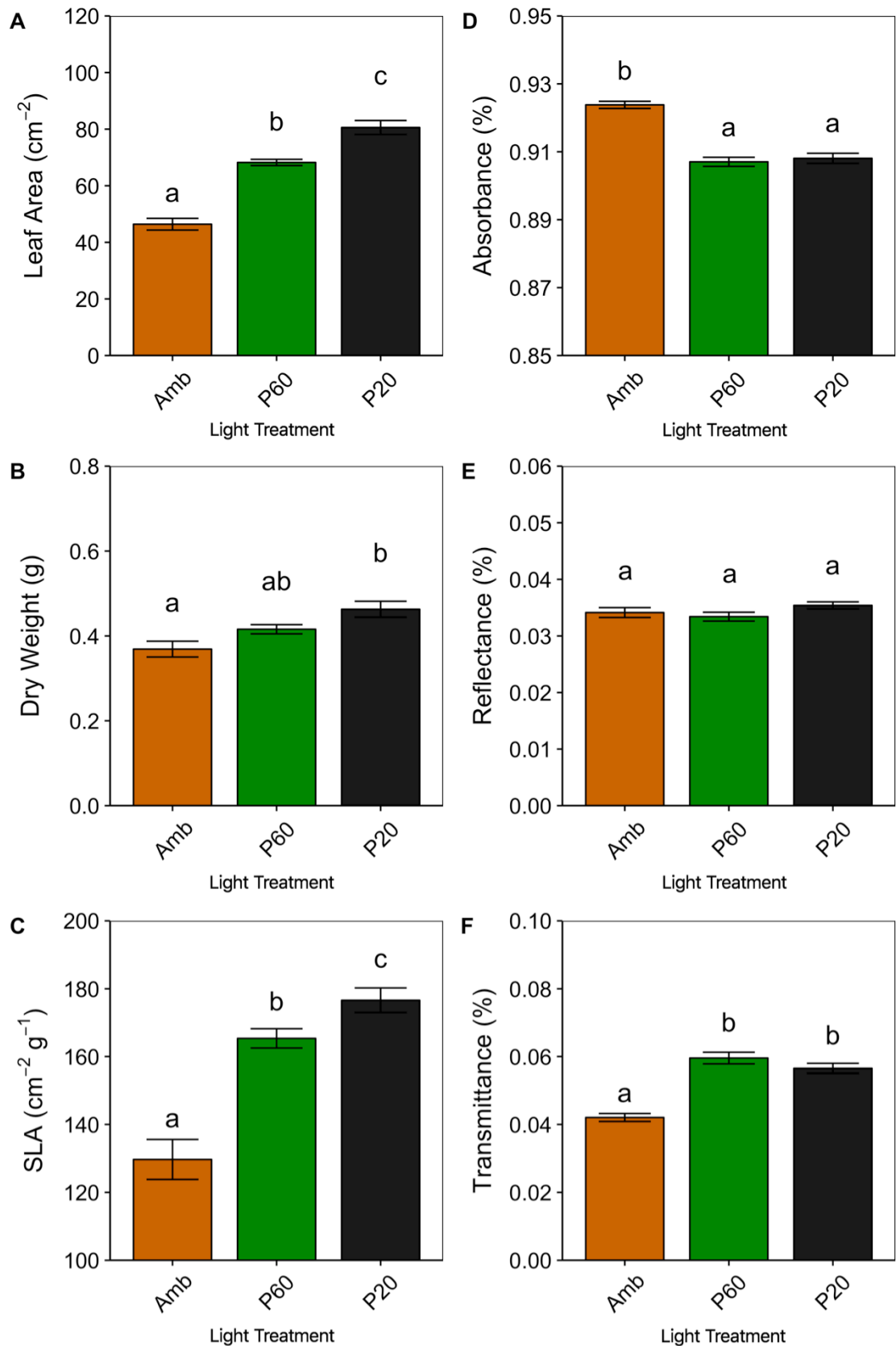


**Figure 4.3.** Leaf and Optical properties of the three Poplar light treatments; Ambient (Orange); P60 (Green); P20 (Black). Leaf area (A); Dry weight (B); Specific leaf area (SLA, C); Absorbance (D); reflectance (E); and transmittance (F) are shown. Error bars represent mean  $\pm$  SE.  $n = 6$ . Letters represent the results of Tukey's post-hoc comparisons of group means.

Plants grown under ambient light conditions (Amb) displayed significantly higher ( $P < 0.05$ ) values of leaf light absorption than those grown under the other two treatments (Fig. 4.3D). No significant differences were found between treatments for reflectance (Fig. 4.3E), although the higher values of absorbance in plants grown under ambient conditions led to a significantly lower ( $P < 0.05$ ) transmittance in these plants (Fig. 4.3F).

### 4.3.3. Variation in photosynthetic capacity between growth light treatments

Net CO<sub>2</sub> assimilation rate ( $A$ ) measured as a function of intercellular CO<sub>2</sub> ( $C_i$ ) on an area basis, was higher in plants grown under ambient conditions compared with the other two treatments at all atmospheric CO<sub>2</sub> concentrations ( $[CO_2]$ ) above 200 ppm (Fig. 4.4A). Plants grown at P60 also displayed higher  $A$  than P20 at all  $[CO_2]$  concentrations above this level. Interestingly, when integrated by mass ( $A_{mass}$ ) there was no difference between the three growth light treatments at any  $[CO_2]$  (Fig. 4.4B). Values of light and CO<sub>2</sub> saturated rates of photosynthesis ( $A_{max}$ ) were significantly higher ( $P < 0.05$ ) in plants grown under ambient light conditions compared to the other two treatments (Fig. 4.4C), with the P60 grown plants also displaying significantly higher ( $P < 0.05$ ) rates than those grown under P20. When light and CO<sub>2</sub> saturated rates of  $A$  are integrated by mass ( $A_{mass-max}$ ) there is seen to be no difference between growth light treatments (Fig. 4.4D). Values of light saturated rates of  $A$  at a CO<sub>2</sub> concentration of 400 ppm seen in the  $A/C_i$  curves ( $A_{400}$ ) were similar to light saturated rates observed in the  $A/Q$  analyses (Fig. 4.2), where plants grown under ambient conditions displayed significantly higher ( $P < 0.05$ ) values of  $A_{400}$  than those grown under the other light treatments (Fig. 4.4E). As observed with the  $A_{mass-max}$  values, no differences in the values of light saturated rates of  $A$  at 400 ppm when integrated by mass ( $A_{mass400}$ ) were observed (Fig. 4.4F). Differences in the maximum rate of carboxylation by Rubisco ( $V_{cmax}$ ) and the maximum electron transport rate for RuBP regeneration ( $J_{max}$ ) were found between treatments (Table 4.2). Plants grown under ambient conditions were found to have significantly higher ( $P < 0.05$ )  $V_{cmax}$  than P20 grown plants with values ranging from 108.2  $\mu\text{mol m}^{-2} \text{s}^{-1}$  (Amb) to 77.3  $\mu\text{mol m}^{-2} \text{s}^{-1}$  (P20), and significantly higher ( $P < 0.05$ )  $J_{max}$  than both the P60 and P20 treatments, values ranging from 161.1  $\mu\text{mol m}^{-2} \text{s}^{-1}$  (Amb) to 124.1 (P60) and 109.1  $\mu\text{mol m}^{-2} \text{s}^{-1}$  (P20).

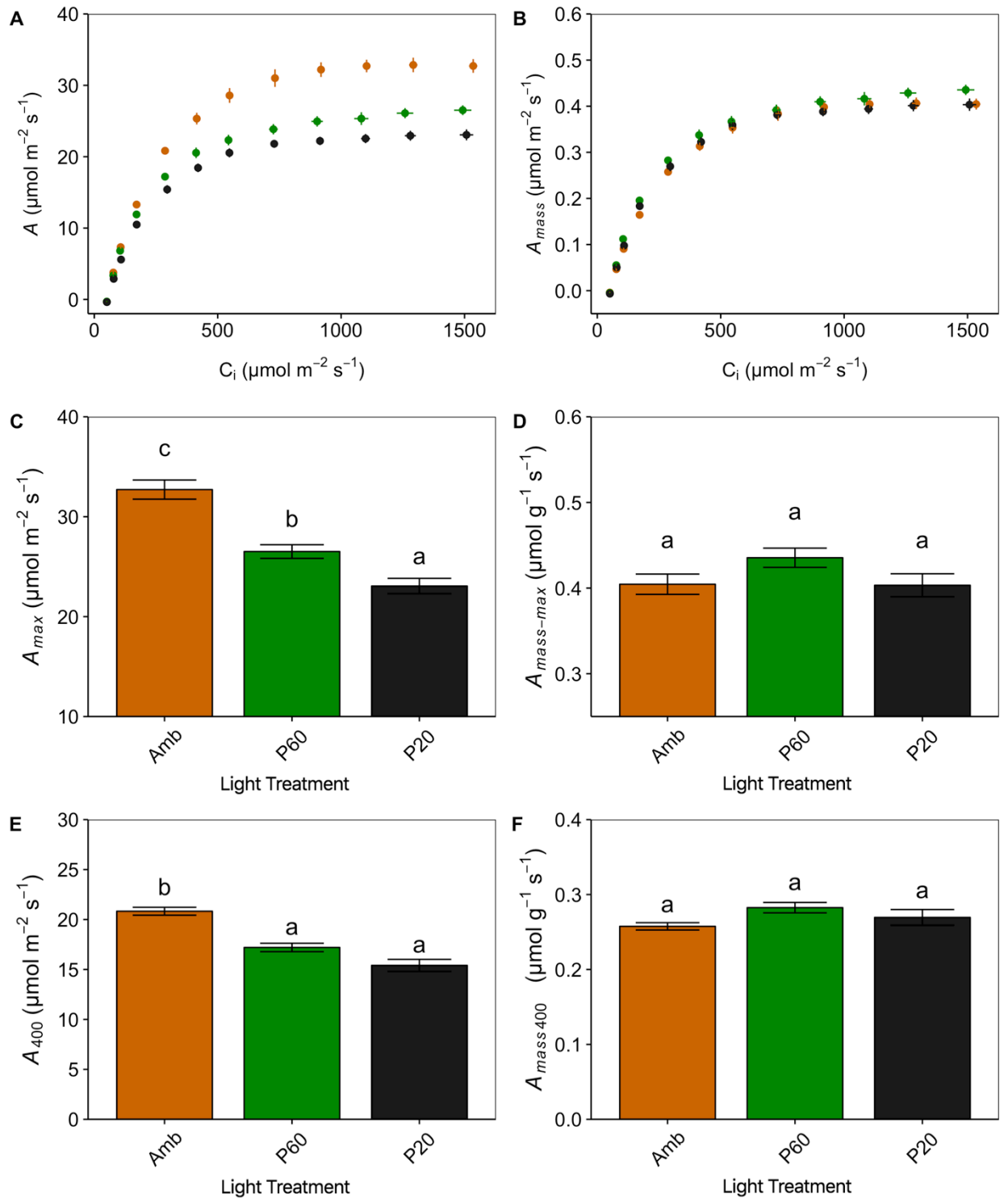


**Figure 4.4.** Photosynthesis as a function of intercellular CO<sub>2</sub> concentration (C<sub>i</sub>) for the three Poplar light treatments; Ambient (Orange); P60 (Green); P20 (Black). Net CO<sub>2</sub> assimilation on an area basis (A; A); relative to leaf mass (A<sub>mass</sub>; B); light and CO<sub>2</sub> saturated rate of photosynthesis (A<sub>max</sub>) on an area (C); and mass (D) basis; Light saturated Photosynthesis at ambient atmospheric CO<sub>2</sub> (400 ppm; A<sub>400</sub>) on an area (E) and mass (F) basis. Error bars represent mean ± SE. n = 5-6. Letters represent the results of *Tukey's post-hoc* comparisons of group means.

**Table 4.2.** Photosynthetic parameters ( $V_{cmax}$  and  $J_{max}$ ) estimated from the response of  $A$  to  $C_i$  of the three Poplar light treatments. Mean  $\pm$  SE. Letters represent the results of Tukey's post-hoc comparisons of group means.

Treatment	$V_{cmax}$	$J_{max}$
Amb	108.2 $\pm$ 5.12 <sup>a</sup>	161.1 $\pm$ 6.7 <sup>a</sup>
P60	91.5 $\pm$ 4.8 <sup>ab</sup>	124.1 $\pm$ 5 <sup>b</sup>
P20	77.3 $\pm$ 4.2 <sup>b</sup>	109.1 $\pm$ 3.7 <sup>b</sup>

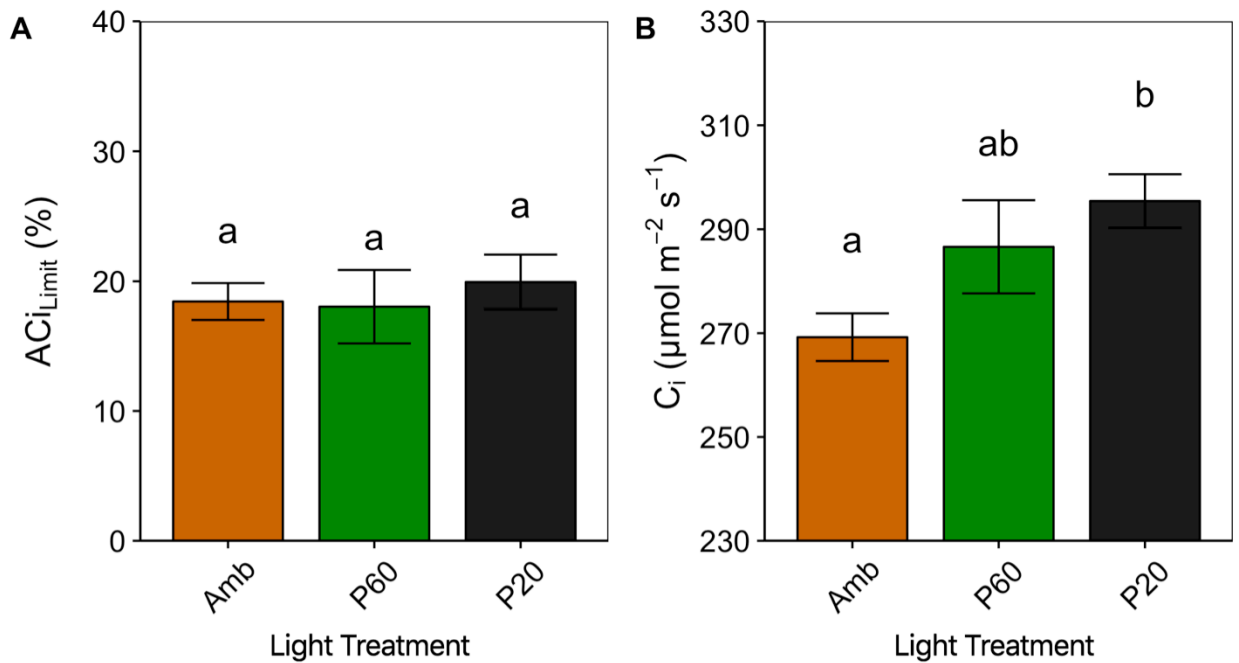


**Figure 4.5.** Estimation of the limitation ( $ACi_{Limit}$ ) placed on net  $\text{CO}_2$  assimilation by stomata and leaf boundary layer (A), calculated from the  $A/C_i$  response curves (Fig. 4.4), represented as the percentage (%) loss in  $A$  enforced by this limitation ( $ACi_{Limit}$ ). Also shown is the intercellular  $\text{CO}_2$  concentration ( $C_i$ ) at a reference  $\text{CO}_2$  of 400 ppm during the  $A/C_i$  response curves (B). Error bars represent mean  $\pm$  SE.  $n = 5-6$ . Letters represent the results of Tukey's post-hoc comparisons of group means.

#### 4.3.4. Limitation of $\text{CO}_2$ uptake (A) imposed by stomata conductance

$A/C_i$  curves were used to estimate the limitation imposed on  $A$  by stomata (and the leaf boundary layer), assuming hypothetically that  $A$  could be increased if the mesophyll had free access to  $\text{CO}_2$  in ambient air (therefore; intracellular  $\text{CO}_2$  ( $C_i$ ) = ambient  $\text{CO}_2$  ( $C_a$ )) (Farquhar and Sharkey, 1982). No differences in the limitation of  $A$  by stomata (and leaf boundary layer) as calculated from the  $A/C_i$  analyses ( $ACi_{Limit}$ ) were

observed between growth light treatments (Fig. 4.5A). Despite this, plants grown under ambient light conditions (Amb) exhibited significantly lower ( $P < 0.05$ ) values of intracellular  $\text{CO}_2$  concentration ( $C_i$ ) than those grown under P20 conditions (Fig. 4.5B), with P60 also displaying higher values of  $C_i$  than Amb though not to a significant level.

#### 4.3.5. Diurnal responses of $g_s$ , $A$ , and $W_i$ to a fluctuating pattern of light

To investigate stomatal and photosynthetic response over the diurnal period, and the implications for diurnal intrinsic water use efficiency, plants from the three growth light treatments were subjected to a diurnal fluctuating light regime (see FLH; Figure 2.1). Gas exchange parameters were measured continuously over the diurnal period, including: stomatal conductance ( $g_s$ ; Fig. 4.6A), net  $\text{CO}_2$  assimilation ( $A$ ; Fig. 4.6B), and intercellular  $\text{CO}_2$  concentration ( $C_i$ ; Fig. 4.6C), with intrinsic water use efficiency ( $W_i$ ; Fig. 4.6D) calculated from the values of  $A$  and  $g_s$  ( $W_i = A/g_s$ ). In general, the pattern of  $g_s$  response over the diurnal period was similar between growth light treatments. However, plants grown under ambient light conditions displayed higher magnitudes of the  $g_s$  response than the other treatments, reaching a peak value of  $g_s$  of ca.  $0.48 \text{ mol m}^{-2} \text{ s}^{-1}$ , whilst the P60 and P20 grown plants reached peaks of  $0.37$  and  $0.32 \text{ mol m}^{-2} \text{ s}^{-1}$  respectively (Fig. 4.6A). The pattern in the response of net photosynthesis ( $A$ ) was similar between growth treatments, though ambient grown plants (Amb) displayed higher peaks of  $A$  during the diurnal than the other two treatments (Fig. 4.6B), with peak values of  $A$  ranging from ca.  $27 \mu\text{mol m}^{-2} \text{ s}^{-1}$  for ambient grown plants, to ca.  $19$  and  $15 \mu\text{mol m}^{-2} \text{ s}^{-1}$  for the P60 and P20 grown plants respectively. Regarding the response of intercellular  $\text{CO}_2$  concentration ( $C_i$ ) there was no noticeable difference between treatments (Fig. 4.6C), with all plants displaying similar values of  $C_i$  throughout the diurnal measurement.  $W_i$  (measured as  $A/g_s$ ) was similar between treatments for most of the diurnal period (Fig. 4.6D), however, towards the end of the measurement (ca. 9-12 h into the diurnal) P20 grown plants displayed higher levels of  $W_i$  than both the P60 and Amb, with the P60 also showing higher values of  $W_i$  than the Amb grown plants during this period of the diurnal (Fig. 4.6D). In the P20 grown plants the higher values of  $W_i$  observed during this time of the diurnal, were largely driven by the lower values of  $g_s$  (Fig. 4.6A), as  $A$  (Fig. 4.6B) was similar between all treatments at this time of the measurement.

Stomatal conductance ( $g_s$ ), net  $\text{CO}_2$  assimilation ( $A$ ), and intrinsic water use efficiency ( $W_i$ ) were integrated over the whole 12h day period to further characterize and investigate levels of total daily  $g_s$ ,  $A$ , and  $W_i$  (Fig. 4.7). Plants grown under ambient light conditions displayed higher values of  $A$  integrated over a 12-hour period than plants grown under P60 and P20 conditions (Fig. 4.7A), with significant

differences ( $P < 0.05$ ) observed between the Amb and P20 plants. Ambient grown plants also exhibited significantly higher ( $P < 0.05$ ) values of  $g_s$  integrated over the diurnal period than plants grown under P20 conditions (Fig. 4.7B), though no differences were observed between P60 and P20 treatments. The similarity in the differences of daily  $A$  and  $g_s$  between growth treatments led to there being no significant differences in integrated daily  $W_i$  (Fig. 4.7C). However, it should be noted that  $W_i$  was slightly higher in P20 grown plants than P60 and Amb, which may be driven by the higher  $W_i$  observed in the P20 plants at the end of the diurnal period (Fig. 4.6D).

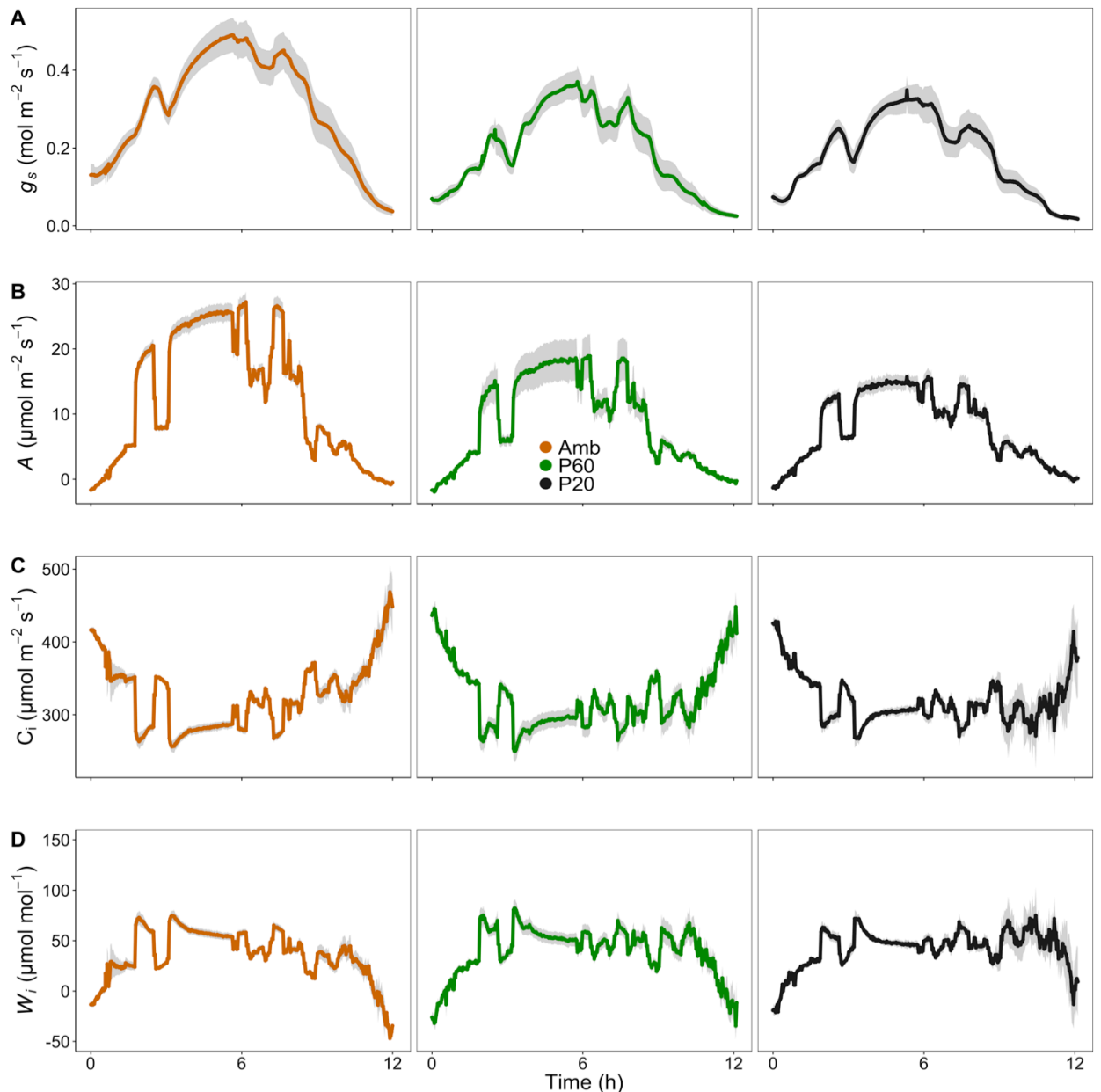


**Figure 4.6.** Diurnal measurements of gas exchange of stomatal conductance ( $g_s$ , A); net  $\text{CO}_2$  assimilation (A; B); internal  $\text{CO}_2$  concentration ( $C_i$ , C); and intrinsic water use efficiency ( $W_i$ , D) for the three Poplar light treatments. Error ribbons represent mean  $\pm$  SE.  $n = 4-6$ .

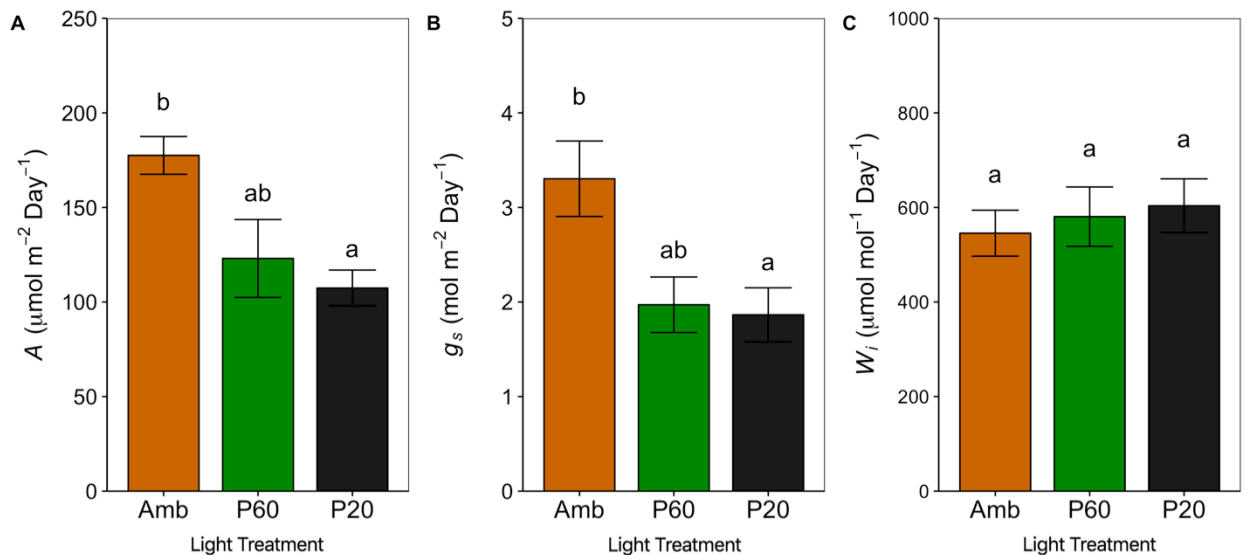


**Figure 4.7.** Integrated total daily net CO<sub>2</sub> assimilation ( $A$ ; A); stomatal conductance ( $g_s$ ; B); and intrinsic water use efficiency ( $W_i$ ; C), calculated from the diurnal measurements (Fig. 4.7) for the three Poplar light treatments. Error ribbons represent mean  $\pm$  SE.  $n = 4-6$ . Letters represent the results of *Tukey's post-hoc* comparisons of group means.

#### 4.3.6. Limitation of diurnal photosynthesis imposed by stomata

To investigate the potential limitation of net CO<sub>2</sub> assimilation ( $A$ ) during the diurnal period ( $\text{Diur}_{\text{Limit}}$ ),  $A$  was predicted from the  $A/Q$  response curves (Fig. 4.2) assuming no stomatal limitation, and a maximized activation of the photosynthetic biochemistry. During the first 2-3 hours of the diurnal regime, all treatments reached the predicted values of  $A$  (Fig. 4.8). However, over the course of the rest of the diurnal measurement there was a tendency, especially at higher light levels, for observed values of  $A$  to be lower than those predicted from the  $A/Q$  response curves. Differences between expected and observed values of  $A$  integrated over the day were lowest for plants grown under ambient conditions (Amb) and highest for P20 grown plants, with values ranging from 10.1% (Amb) to 14.7% (P20). Interestingly, later in the day (ca. 9-12 h into the diurnal) plants grown under P20 conditions displayed a tendency to reach predicted values of  $A$ , whilst those grown under P60 and Amb conditions failed to reach these values (Fig. 4.8). A positive correlation was observed between the limitation of  $A$  estimated from the  $A/C_i$  analysis ( $\text{ACi}_{\text{Limit}}$ ) and the limitation of  $A$  over the diurnal period estimated from the  $A/Q$  analysis ( $\text{Diur}_{\text{Limit}}$ ), with all treatments following this trend (Fig. 4.9A). This highlights that the limitation imposed by stomata (and any potential leaf boundary layer affect) is conserved between methods and under varying environmental responses. These data shows that when grown under low light conditions (P20) there is a trend toward greater stomatal limitation of  $A$ , as observed with the P20 grown plants exhibiting higher values of  $\text{Diur}_{\text{Limit}}$  and  $\text{ACi}_{\text{Limit}}$  (Fig. 4.9A). When comparing  $\text{Diur}_{\text{Limit}}$  to the diurnal  $W_i$

over the same time period, there is a noticeable trend toward plants that display higher values of  $Diur_{Limit}$  also showing higher values of  $W_i$  (Fig. 4.9B), this is highlighted by the fact that plants grown under ambient conditions (Amb) exhibited the lowest values of  $Diur_{Limit}$  and  $W_i$ .

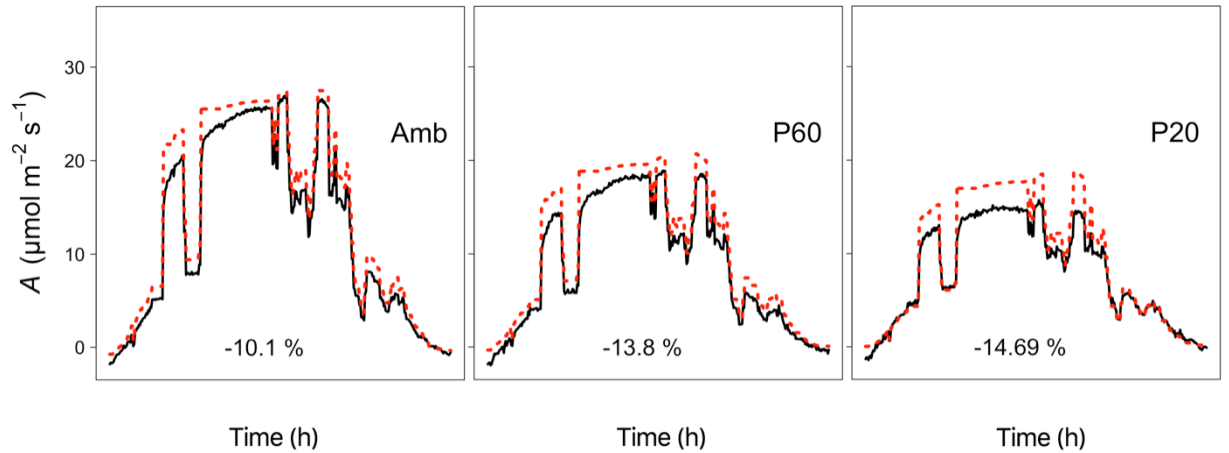


**Figure 4.8.** Diurnal measurements of observed net CO<sub>2</sub> assimilation (black line) and predicted net CO<sub>2</sub> assimilation modelled from the  $A/Q$  response curves (red dashed line) for the three Poplar light treatments. Percentage figure is the difference between observed and modeled values representing a loss in  $A$  through limitations in stomata, leaf boundary layer and biochemistry ( $Diur_{Limit}$ ).  $n = 4-6$ .

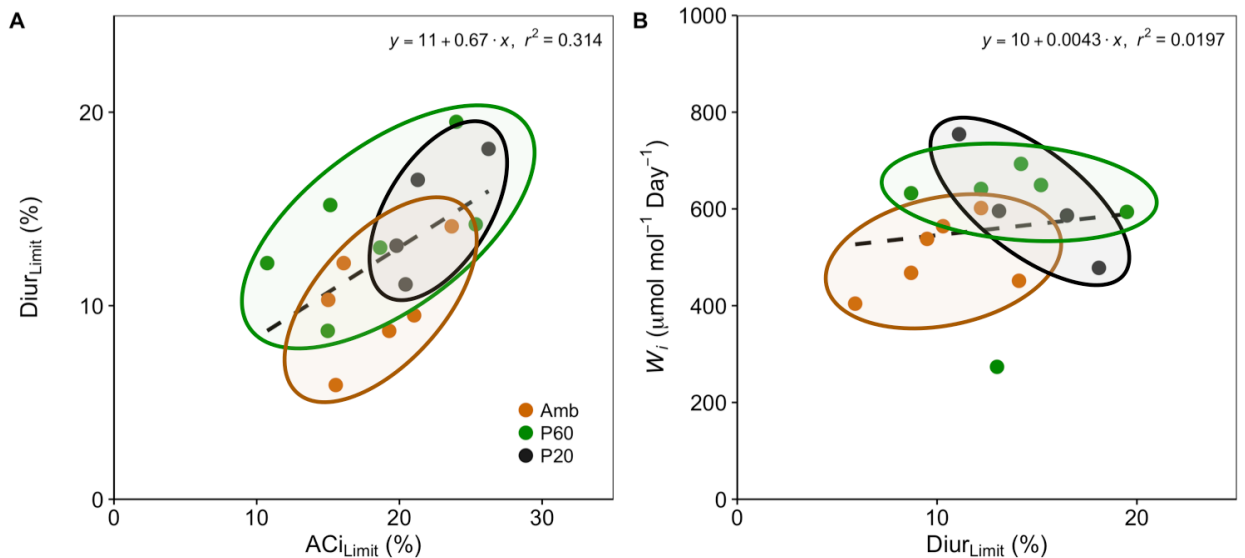


**Figure 4.9.** Correlation between the estimation of the limitation placed on net CO<sub>2</sub> assimilation by stomata and leaf boundary layer, calculated from the  $A/C_i$  response curves ( $ACi_{Limit}$ , Fig. 4.6) and the diurnal measurements ( $Diur_{Limit}$ , Fig. 4.8) (A). Correlation between the limitation ( $Diur_{Limit}$ ) and daily intrinsic water use efficiency ( $W_i$ ) during the diurnal (B). Each data point represents an individual plant. Filled areas highlight each light treatment, whilst the black dotted line represents the trend in the data for all individuals.

#### 4.3.7. Response of $g_s$ and $A$ to step changes at different $PPFD$ s

To assess the impact of growth light intensity on stomatal responses, leaves were subjected to step increases in  $PPFD$  (*Low*; 50-250  $\mu\text{mol m}^{-2} \text{s}^{-1}$ , *Mid*; 100-1000  $\mu\text{mol m}^{-2} \text{s}^{-1}$ , and *High*; 500-1500  $\mu\text{mol m}^{-2} \text{s}^{-1}$ ) followed by corresponding step decreases (*Low*; 250-50  $\mu\text{mol m}^{-2} \text{s}^{-1}$ , *Mid*; 1000-100  $\mu\text{mol m}^{-2} \text{s}^{-1}$ , and *High*; 1500-500  $\mu\text{mol m}^{-2} \text{s}^{-1}$ ), with the effect on  $A$  and  $g_s$  measured (Fig. 4.10). No differences in the response of  $g_s$  to a step increase in  $PPFD$  at *Low* light intensities (50-250  $\mu\text{mol m}^{-2} \text{s}^{-1}$ ) were observed between growth light treatments (Fig. 4.10A). Following a step increase in  $PPFD$  at *Mid* levels (100-1000  $\mu\text{mol m}^{-2} \text{s}^{-1}$ ) all three treatments reached a new plateau of  $g_s$  within 90 min after the increase in light, whilst all treatments failed to reach a new plateau of  $g_s$  within 90 min when subjected to an increase in  $PPFD$  at *High* light levels (500-1500  $\mu\text{mol m}^{-2} \text{s}^{-1}$ ) (Fig. 4.10A). Following the increase in  $PPFD$  a near instantaneous increase in  $A$  was observed in contrast with the slow initial increase in  $g_s$  in all growth light treatments, and at all step light intensities (Fig. 4.10B). In all treatments and during all three light intensity steps,  $g_s$  continued to increase despite the fact that  $A$  had reached a new steady state, this led to a continuous decrease in  $W_i$  through the 90 min measurement in all growth treatments and during all three light intensity steps (Fig. 4.10C). Despite all treatments displaying an uncoordinated temporal response of  $A$  and  $g_s$ , final values of  $A$  and  $g_s$  were strongly correlated during all three light intensity steps (Fig. 4.10A and B). This was particularly true for the *High* intensity step where plants grown under ambient conditions (*Amb*) exhibited the highest values of  $A$  and  $g_s$ , whilst the P20 plants displayed the lowest values of both parameters.  $W_i$  was largely unchanged between each light step and between each growth light treatment, although there was a tendency toward P20 and P60 grown plants to display slightly higher values of  $W_i$  than those grown under ambient conditions (*Amb*), especially during the *Mid* light step where  $W_i$  was ca. 30% greater in plants grown under P20 and P60 conditions during the first 30 min of the step increase in light (Fig. 4.10C). In all treatments, during the step decrease in light final values of  $g_s$  increased with an increase in the intensity of the light step (Fig. 4.11), with those subjected to a decrease in  $PPFD$  from 1500 to 500  $\mu\text{mol m}^{-2} \text{s}^{-1}$  displaying higher final values of  $g_s$  than those subject to a decrease from 250 to 50  $\mu\text{mol m}^{-2} \text{s}^{-1}$ . When subjected to a decrease in  $PPFD$  at *Low* light levels all treatments displayed similar responses, with P20 grown plants exhibiting the lowest final values of  $g_s$  (Fig. 4.11A). However, when exposed to decreases in  $PPFD$  at *Mid* and *High* light levels differences in  $g_s$  between treatments were more distinct, with plants grown under *Amb* conditions displaying the highest values of  $g_s$  and those grown under P20 conditions the lowest values (Fig. 4.11B and C).

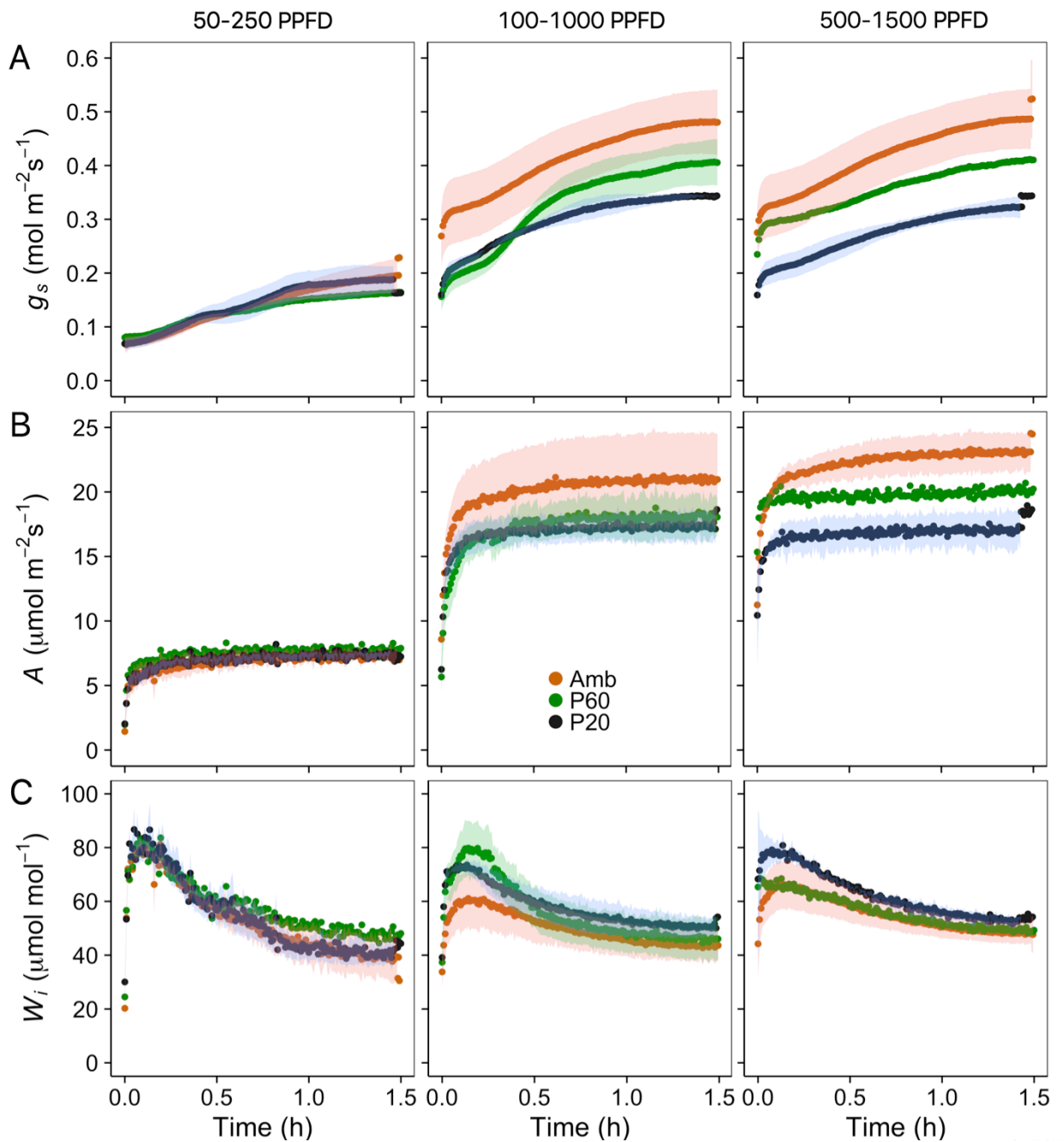


**Figure 4.10.** Temporal response of stomatal conductance ( $g_s$ , A), net  $\text{CO}_2$  assimilation ( $A$ , B), and intrinsic water use efficiency ( $W_i$ , C), to step increases in light intensity (50-250; 100-1000; and 500 to 1500  $\mu\text{mol m}^{-2} \text{s}^{-1}$  PPFD) for the three Poplar light treatments. Gas exchange parameters ( $g_s$  and  $A$ ) were recorded at 20s intervals, leaf temperature maintained at 25°C, and leaf VPD at  $1 \pm 0.2$  KPa. Error ribbons represent mean  $\pm$  SE.  $n = 4-6$ .

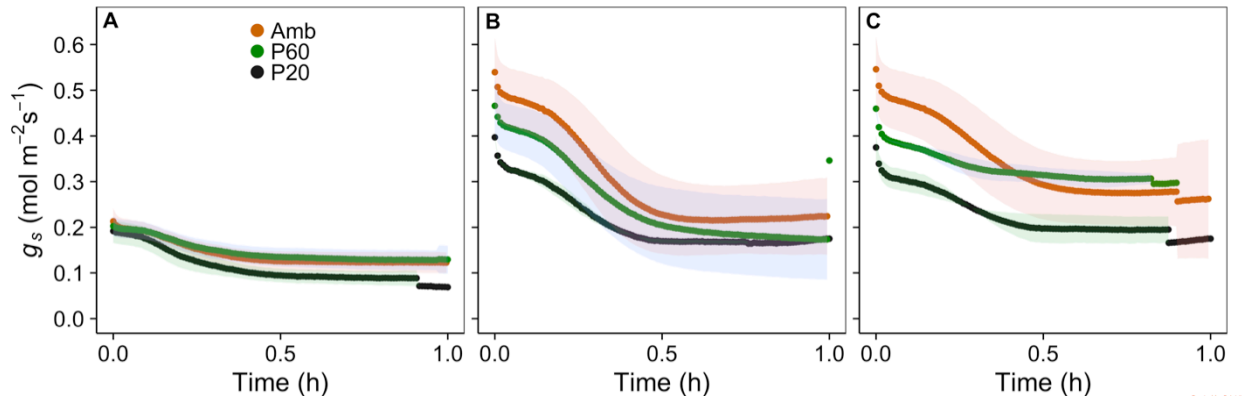


**Figure 4.11.** Temporal response of stomatal conductance ( $g_s$ ) to step decreases in light intensity (250-50 PPFD; A), (1000-100 PPFD; B), (1500 to 500 PPFD; C) for the three Poplar light treatments. Gas exchange parameters ( $g_s$ , and  $A$ ) were recorded at 20s intervals, leaf temperature maintained at 25°C, and leaf VPD at  $1 \pm 0.2$  KPa. Error ribbons represent mean  $\pm$  SE.  $n = 4-6$ .

#### 4.3.8. Speed of $g_s$ response to step changes at different PPFDs

Stomatal responses to a step increase in PPFD were used to determine the influence of growth light intensity on the speed of  $g_s$  response when subjected to different light intensity steps (*Low*; 50-250  $\mu\text{mol m}^{-2} \text{s}^{-1}$ , *Mid*; 100-1000  $\mu\text{mol m}^{-2} \text{s}^{-1}$ , and *High*; 500-1500  $\mu\text{mol m}^{-2} \text{s}^{-1}$ ). Time constants for stomatal opening ( $\tau_i$ , Fig. 4.12A) in response to a step increase in *Low* PPFD were significantly lower ( $P < 0.05$ ) in P60 grown plants compared with the other two treatments, with those grown under ambient conditions displaying the slowest responses. The slower response observed in Amb grown plants remained when subjected to a step increase in *Mid* PPFD, however the P20 grown plants exhibited significantly ( $P < 0.05$ ) faster responses in  $g_s$  than the other two treatments during this step (Fig. 4.12A). During a step increase at *High* PPFD, it was revealed that the Amb grown plants had the fastest  $g_s$  response, whilst the P60 grown plants displayed the slowest. In contrast to stomatal opening, time constants for stomatal closure ( $\tau_d$ ) were similar for all three treatments during step changes at *Low* and *High* light intensities (Fig. 4.12B). During decreases in light at *Mid* PPFD, P20 grown plants revealed significantly faster ( $P < 0.05$ )  $g_s$  responses than P60 and Amb treatments, although at *High* PPFD P20 plants were found to decrease  $g_s$  significantly slower ( $P < 0.05$ ) than the other two treatments.

The time constants for light saturated rates of carbon assimilation at each PPFD level ( $\tau_{a_i}$ , Fig. 4.12C) were determined from the temporal response data (Fig. 4.10), along with final values of  $g_s$  for stomatal opening ( $G_i$ , Fig. 4.12D), and stomatal closure ( $G_d$ , Fig. 4.12E), and final values of  $A$  ( $A_i$ , Fig. 4.12F) at each PPFD following a step change in light.

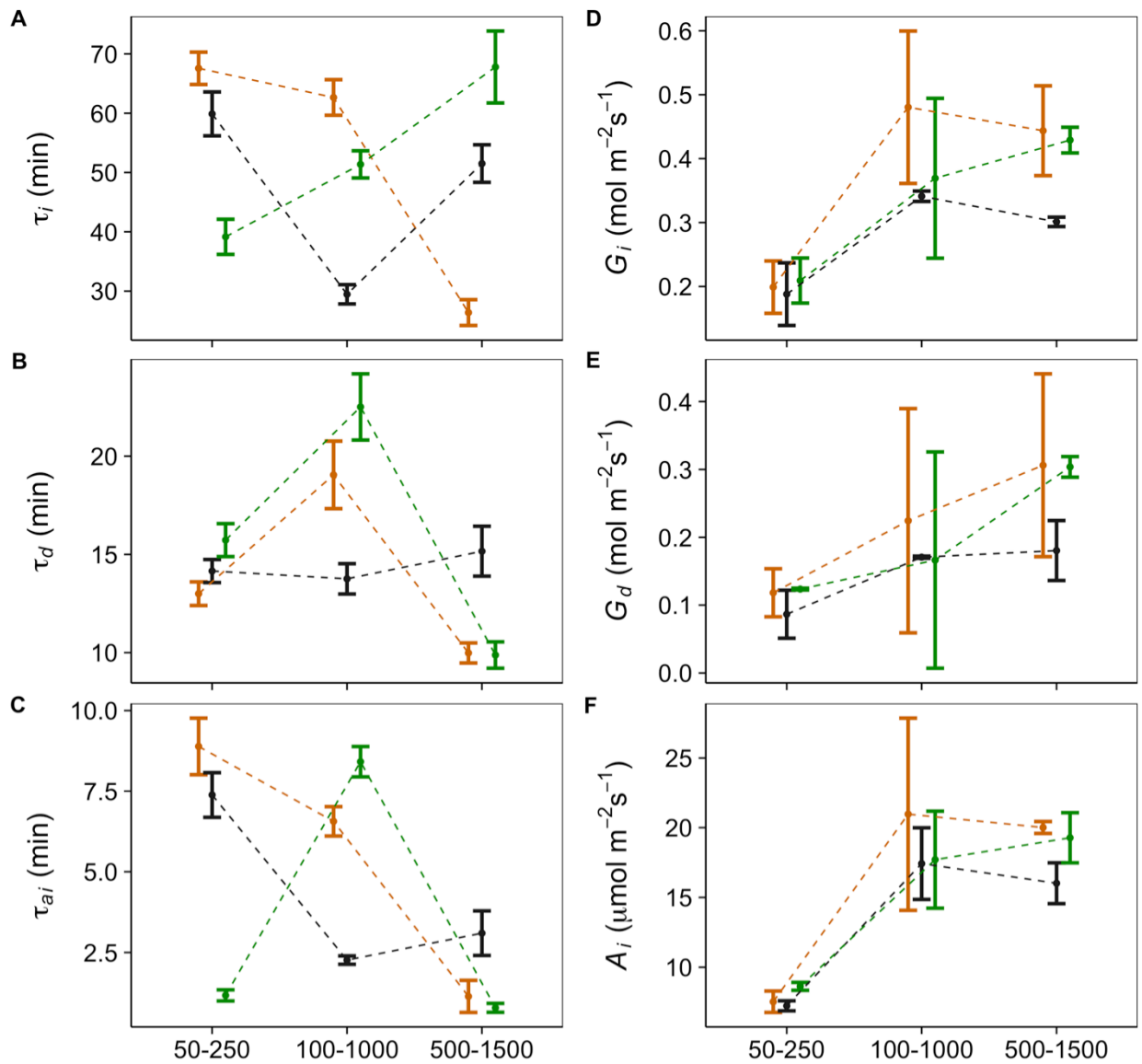


**Figure 4.12.** Time constant for stomatal opening ( $\tau_i$ , A), Final values of stomatal conductance after an increased step change in light intensity ( $G_i$ , B); time constant for stomatal closure ( $\tau_d$ , C), Final values of stomatal conductance after a decreased step change in light intensity ( $G_d$ , D); light saturated rate of carbon assimilation ( $\tau_{ai}$ , E) to a step change in light intensity; and saturation of net  $\text{CO}_2$  assimilation ( $A_i$ , F), at three different light steps (50-250, 100-1000, and 500-1500  $\mu\text{mol m}^{-2} \text{s}^{-1}$  PPFD) for the three Poplar light treatments: Ambient (Orange); P60 (Green); P20 (Black). Error bars represent 95% confidence intervals. n=4-6.

Time constants for light saturated A ( $\tau_{ai}$ , Fig. 4.12C) were significantly faster ( $P < 0.05$ ) in P60 grown plants compared to the other two treatments during *Low PPFD* steps. Conversely, during *Mid PPFD* steps in light P60 grown plants displayed significantly ( $P < 0.05$ ) slower responses of  $\tau_{ai}$  compared to P20 and Amb grown plants, with P20 presenting the fastest response times. During *High PPFD* light steps all treatments displayed similar time constants, although P20 grown plants were found to be significantly slower ( $P < 0.05$ ) than the other two treatments (Fig. 4.12C). No difference between the three growth

light treatments was observed in the final  $g_s$  values following a step increase in light ( $G_i$ , Fig. 4.12D) at *Low PPFd*. At *Mid PPFd* it was observed that plants grown at Amb conditions displayed significantly higher values of  $G_i$  compared to P20 grown plants. The difference in  $G_i$  between Amb and P20 remained at *High PPFd* steps, with P60 also showing significantly higher ( $P < 0.05$ )  $G_i$  than P20 grown plants (Fig. 4.12D). Final values of  $g_s$  following a step decrease in light ( $G_d$ , Fig. 4.12E) displayed similar trends to that of  $G_i$  in all treatments, irrespective of the *PPFD* intensity of the step change in light. No differences in  $G_d$  during *Low* and *Mid PPFd* step changes were observed between treatments, whilst at *High PPFds* P20 grown plants displayed significantly lower ( $P < 0.05$ ) values of  $G_d$  than P60 grown plants (Fig. 4.12E). No significant differences in the saturated rates of  $A$  ( $A_i$ ; Fig. 4.12F) were observed between treatment during step changes at *Low* and *Mid PPFds*, although as expected Amb grown plants displayed the highest values of  $A_i$  during *Mid PPFd* steps. However, after a step increase at *High PPFd*, plants grown at ambient conditions exhibited the highest values of  $A_i$  and were significantly higher ( $P < 0.05$ ) than P20 grown plants that in turn displayed the lowest values, which was to be expected.

#### 4.3.9. Response of $g_s$ and $A$ to a step change in *PPFD* as a function of time of day

To assess the impact of growth light intensity on stomatal responses at different times of the day, leaves were subjected to a step increase in *PPFD* ( $100\text{-}1000 \mu\text{mol m}^{-2} \text{s}^{-1}$ ) followed by a step decrease ( $1000\text{-}100 \mu\text{mol m}^{-2} \text{s}^{-1}$ ), and the effect on  $A$  and  $g_s$  measured (Fig. 4.13). In the morning period (8-10 am) P60 grown plants reached a new plateau of  $g_s$  within 90 min after the increase in light (Fig. 4.13A), whilst both the Amb and P20 treatments failed to reach a new plateau of  $g_s$  within this timeframe. In the midday (1-3pm) measurements  $g_s$  reached a new plateau in all light treatments (Fig. 4.13A), within 90 minutes. In the evening period (6-8pm) P20 and P60 treatments reached a new plateau of  $g_s$ , whilst the Amb treatments failed to reach a new plateau of  $g_s$  within the 90 minutes (Fig. 4.13A). Following the increase in *PPFD* to  $1000 \mu\text{mol m}^{-2} \text{s}^{-1}$ , a near instantaneous increase in  $A$  was observed in contrast with the slow initial increase in  $g_s$  in all treatments, during the morning and midday measurements (Fig. 4.13B). In the evening, the Amb and P60 grown plants displayed a slow increase in  $A$  that was synchronized with the response of  $g_s$  at the same time, indicating a potential limitation of  $A$  by  $g_s$ . In all treatments during the morning and midday measurement times,  $g_s$  continued to increase despite the fact that  $A$  had reached near steady state levels. Despite all treatments displaying a predominantly uncoordinated  $A$  and  $g_s$  temporal response, final values of  $A$  and  $g_s$  were strongly correlated, with plants grown under ambient conditions exhibiting the highest values of  $g_s$  and  $A$ , and P20 grown plants the lowest values (Fig. 4.13A and B). Intrinsic water use efficiency ( $W_i$ ) increased from morning to evening in all treatments (Fig. 4.13C). This was predominantly driven by the decrease in  $g_s$  values in the evening

(Fig. 4.13A), which led to lower values of  $A$  in all treatments (Fig. 4.13B).  $W_i$  was consistently higher in P60 grown plants compared to the other two treatments, at all times of day (Fig. 4.13C). This was mainly due to the fact that P60 plants displayed  $g_s$  values comparable to those of the P20 treatment, and values of  $A$  comparable to those of plants grown under ambient conditions that exhibited the highest  $A$  values.

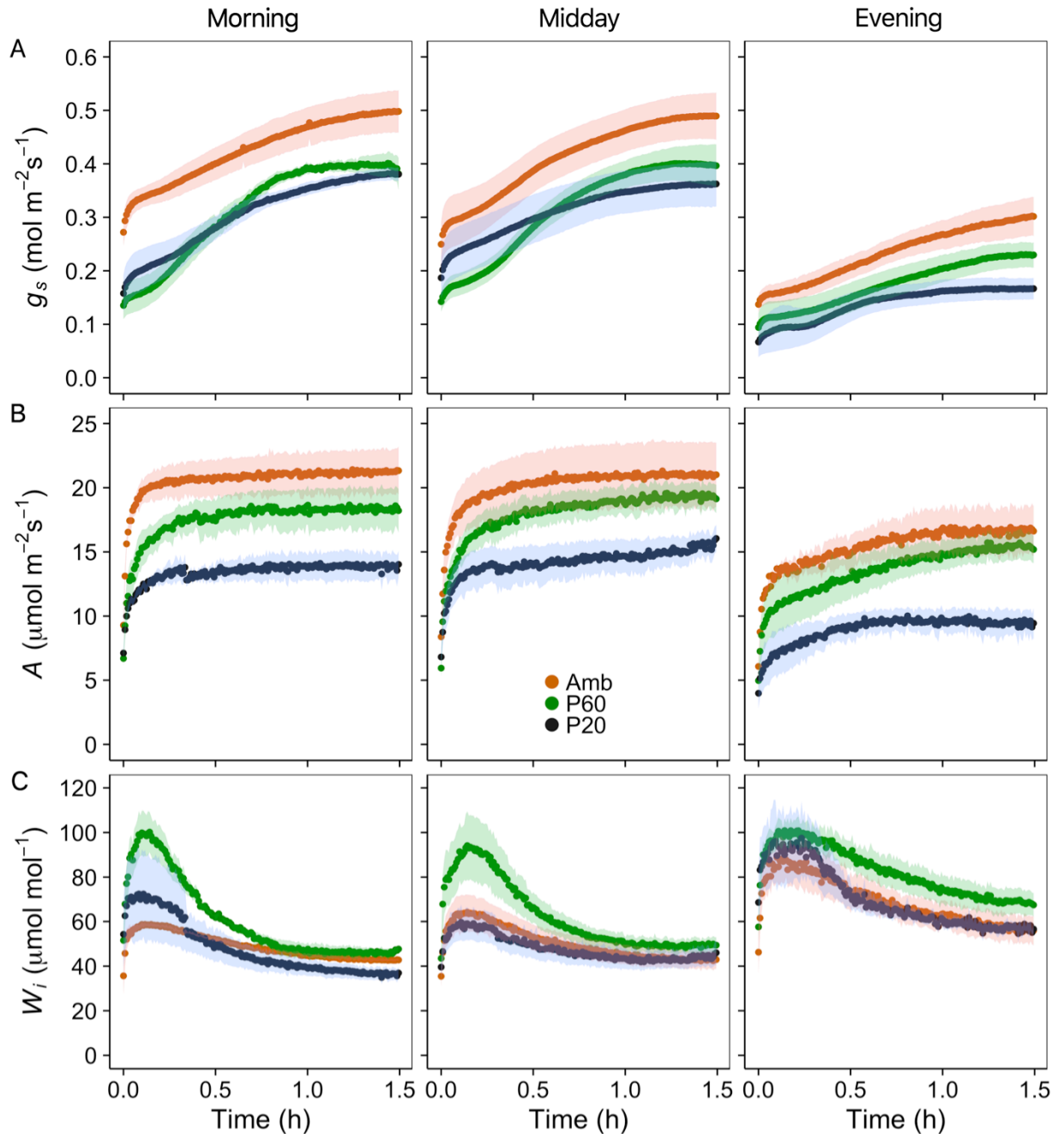


**Figure 4.13.** Temporal response of stomatal conductance ( $g_s$ , A), net  $\text{CO}_2$  assimilation ( $A$ , B), and intrinsic water use efficiency ( $W_i$ , C), to a step increase in light intensity ( $100\text{-}1000 \mu\text{mol m}^{-2} \text{s}^{-1}$  PPFD), at different times of day (Morning, Midday, and Evening) for the three Poplar light treatments. Gas exchange parameters ( $g_s$  and  $A$ ) were recorded at 20s intervals, leaf temperature maintained at  $25^\circ\text{C}$ , and leaf VPD at  $1 \pm 0.2$  KPa. Error ribbons represent mean  $\pm$  SE.  $n = 4\text{-}6$ .

In all treatments, final values of  $g_s$  decreased through the day (morning to evening) when subjected to a step decrease in  $PPFD$  from 1000 to 100  $\mu\text{mol m}^{-2} \text{s}^{-1}$  (Fig. 4.14). In the morning period the highest final values of  $g_s$  at 100  $PPFD$  were presented by Amb grown plants, whilst P60 and P20 treatments jointly displayed the lowest values (Fig. 4.14A), which correlated strongly with the final values of  $g_s$  at 1000  $PPFD$  (Fig. 4.13A). These values were maintained in all treatments during midday measurements (Fig. 4.14B), whilst in the evening period final values of  $g_s$  were decreased in all treatments (Fig. 4.14C), though Amb grown plants maintained the highest values of  $g_s$  with the P60 and P20 grown plants jointly displaying the lowest values.

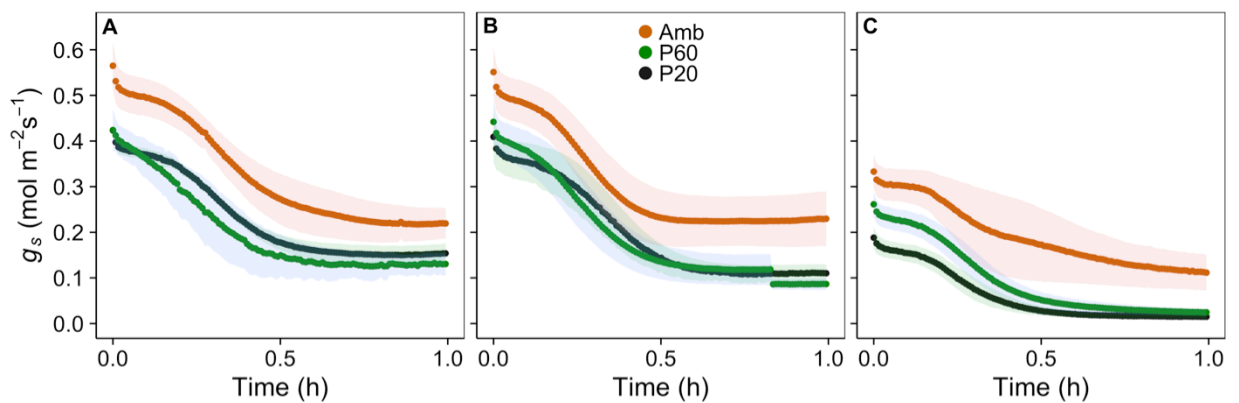


**Figure 4.14.** Temporal response of stomatal conductance ( $g_s$ ) to a step decrease in light intensity (1000-100  $\mu\text{mol m}^{-2} \text{s}^{-1}$   $PPFD$ ) at different times of day: Morning (A); Midday (B); Evening (C), for the three Poplar light treatments. Gas exchange parameters ( $g_s$ , and  $A$ ) were recorded at 20s intervals, leaf temperature maintained at 25°C, and leaf VPD at  $1 \pm 0.2$  KPa. Error ribbons represent mean  $\pm$  SE.  $n = 4-6$ .

#### 4.3.10. Speed of $g_s$ response to a step change in $PPFD$ as a function of time of day

Stomatal responses to a step increase in  $PPFD$  were used to determine the influence of acclimation to growth light regime and intensity on the speed of  $g_s$  response at different times of the day. Time constants for stomatal opening ( $\tau_i$ , Fig. 4.15A) in response to a step increase in light were significantly slower ( $P < 0.05$ ) in plants grown under ambient conditions compared with P60 and P20 grown plants when measured in the morning. Measurements at midday were comparable between all treatments, however  $\tau_i$  increased significantly ( $P < 0.05$ ) in the evening measurements in both Amb and P60 grown plants, with P20 plants significantly faster ( $P < 0.05$ ) than the other two treatments (Fig. 4.15A). In contrast to stomatal opening, time constants for stomatal closure ( $\tau_d$ ) significantly decreased ( $P < 0.05$ )

through the day (morning to evening) in all Amb and P20 treatments (Fig. 4.15B), although P60 grown plants maintained time constants throughout the day. The time constant for stomatal closure ( $\tau_d$ ) in the morning was significantly slower ( $P < 0.05$ ) in plants grown under ambient conditions, whilst P60 grown plants displayed the fastest responses. Conversely, in the evening the fastest responses of stomatal closure were exhibited by the Amb treatment, with time constants significantly faster ( $P < 0.05$ ) than the other two treatments (Fig. 4.15B). In general stomatal closure was much faster than stomatal opening in all treatments, and at all times of the day.

The time constant for light saturated rate of  $A$  at  $1000 \mu\text{mol m}^{-2} \text{s}^{-1}$  PPFD ( $\tau_{ai}$ , Fig. 4.15C) were determined from the temporal response data (Figs. 4.13), along with final values of  $g_s$  at  $1000$  PPFD for stomatal opening ( $G_i$ , Fig. 4.15D), stomatal closure ( $G_d$ , Fig. 4.15E), and saturated rates of  $A$  at  $1000$  PPFD ( $A_i$ , Fig. 6.10F). Net  $\text{CO}_2$  assimilation was deemed near saturation at  $1000$  PPFD from analysis of  $A/Q$  curves on the same plants (Fig. 4.2). Time constants for light saturated  $A$  ( $\tau_{ai}$ , Fig. 4.15C) were significantly lower ( $P < 0.05$ ) in Amb grown plants compared to P60 and P20 at morning and midday, with P20 grown plants displaying the highest values, whilst in the evening  $\tau_{ai}$  was significantly higher ( $P < 0.05$ ) in Amb compared with the other two treatments. The final value of  $g_s$  at  $1000 \mu\text{mol m}^{-2} \text{s}^{-1}$  ( $G_i$ , Fig. 4.15D), and following closure when light was reduced from  $1000$  to  $100 \mu\text{mol m}^{-2} \text{s}^{-1}$  ( $G_d$ , Fig. 4.15E) decreased significantly ( $P < 0.05$ ) through the day in all treatments. Final  $g_s$  at  $1000$  PPFD ( $G_i$ ) was significantly higher ( $P < 0.05$ ) in Amb compared with P20 grown plants in the morning and evening, with  $G_d$  also significantly higher in Amb compared with P20 although only during the evening step change in light (Fig. 4.15E). In general, final values of  $g_s$  at  $100$  PPFD ( $G_d$ ; Fig. 4.15E) displayed similar trends to that of  $G_i$  in all treatments, irrespective of the time of day. However, plants grown under ambient conditions always displayed higher values of  $G_d$  than the other two treatments at all times of day, with these values being significantly higher ( $P < 0.05$ ) than P20 grown plants in the evening. Saturated rates of  $A$  at  $1000$  PPFD ( $A_i$ ; Fig. 4.15F) remained constant from morning to midday in all treatments. In all light treatments there was a decrease in  $A_i$  from midday to evening, although this was only significant in P20 grown plants ( $P < 0.05$ ). Interestingly, a strong correlation was observed in all treatments between the final value of  $g_s$  ( $G_i$ ) and  $A$  ( $A_i$ ) under  $1000 \mu\text{mol m}^{-2} \text{s}^{-1}$  PPFD.

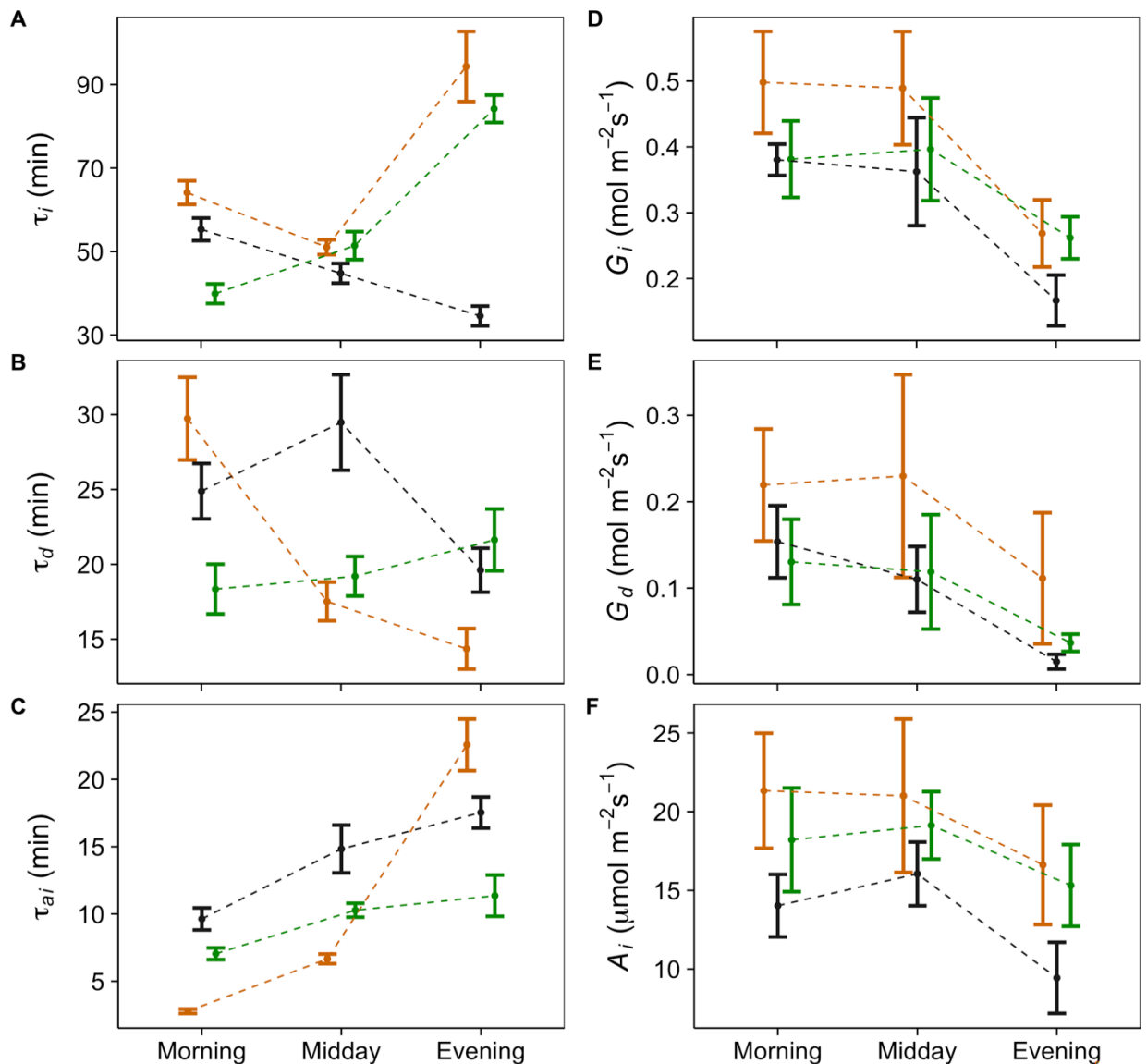


**Figure 4.15.** Time constant for stomatal opening ( $\tau_i$ , A); final values of stomatal conductance after an increased step change in light intensity ( $G_i$ , B); time constant for stomatal closure ( $\tau_d$ , C); final values of stomatal conductance after a decreased step change in light intensity ( $G_d$ , D); light saturated rate of carbon assimilation ( $\tau_{ai}$ , E) to a step change in light intensity; and saturation of net CO<sub>2</sub> assimilation ( $A_i$ , F), at different times of day (Morning, Midday, Evening) for the three Poplar light treatments: Ambient (Orange); P60 (Green); P20 (Black). Error bars represent 95% confidence intervals. n=4-6.

#### 4.3.11. Stomatal anatomy

Significant differences ( $P < 0.05$ ) in abaxial stomatal density ( $SD_{Ab}$ ) were observed between all three growth light treatments (Fig. 4.16A), with plants grown under ambient conditions exhibiting the highest and P20 the lowest values. Differences in adaxial stomatal density ( $SD_{Ad}$ ) matched those of  $SD_{Ab}$ , with significant differences observed between all three treatments (Fig. 4.16B). Stomatal index was also found to be significant between all treatments ( $P < 0.05$ ) (Fig. 4.16C), with Amb displaying the highest

values (ca. 16%) and P20 the lowest (ca. 10%). No differences in stomatal ratio between the abaxial and adaxial surface (Fig. 4.16D), or pore area (Fig. 4.16E) were observed between growth light treatments. The theoretical maximum of stomatal conductance ( $g_{smax}$ ; Fig. 4.16F) was significantly higher ( $P < 0.05$ ) in plants grown under ambient conditions (Amb) compared with the other two treatments, with P60 grown plants also significantly higher ( $P < 0.05$ ) than the P20. As there was no difference in pore area, anatomical  $g_{smax}$  was driven by the large differences observed in stomatal density in all treatments.

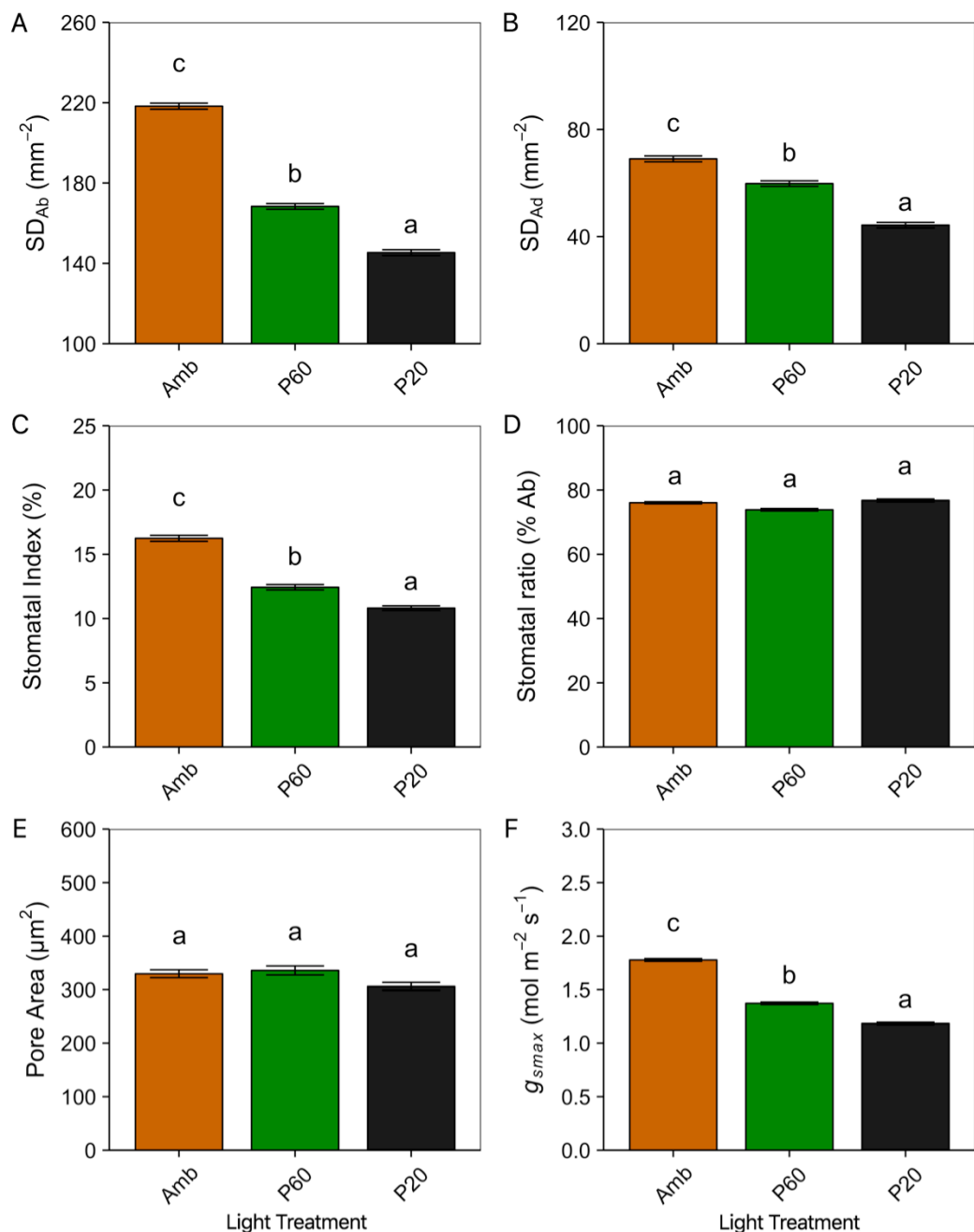


**Figure 4.16.** Stomatal anatomical characteristics including abaxial stomatal density ( $SD_{Ab}$ ; A); adaxial stomatal density ( $SD_{Ad}$ ; B); stomatal index (C); stomatal abaxial:adaxial ratio (D); abaxial stomatal pore area (E); maximum stomatal conductance ( $g_{smax}$ ; F) for the three Poplar light treatments. Error bars represent mean  $\pm$  SE.  $n = 10$ . Letters represent results of Tukey's post-hoc comparisons of group means.

#### 4.3.12. Impact of stomatal density and speed of response on intrinsic water use efficiency

A negative relationship between abaxial stomatal density ( $SD_{Ab}$ ) and daily intrinsic water use efficiency during the diurnal ( $W_i$ ) was observed between treatments (Fig. 4.17), where an increase in  $SD_{Ab}$  would lead to a decrease in  $W_i$ , as observed by the Amb treatment typically exhibiting higher stomatal densities and therefore lower  $W_i$ . A positive relationship was observed between  $SD_{Ab}$  and the time constant for stomatal opening ( $\tau_i$ ) after a step increase in  $PPFD$  from 50 to 250  $\mu\text{mol m}^{-2} \text{s}^{-1}$  (Fig. 4.18A), and from 100 to 1000  $\mu\text{mol m}^{-2} \text{s}^{-1}$  (Fig. 4.18B), with the Amb grown plants exhibiting the highest values of  $SD_{Ab}$  and the highest values of  $\tau_i$  during each light step. Interestingly, this became a strong negative relationship when  $SD_{Ab}$  was compared with the values of  $\tau_i$  during a step increase in  $PPFD$  from 500 to 1500  $\mu\text{mol m}^{-2} \text{s}^{-1}$  (Fig. 4.18C), with the Amb grown plants displaying the lowest values of  $\tau_i$  during this light step. There was no discernible relationship between the time constant for stomatal opening ( $\tau_i$ ) and the daily intrinsic water use efficiency ( $W_i$ ) measured from the diurnal measurements. However, there was a trend toward higher time constants for stomatal opening during *Low* (Fig. 4.18D) and *Mid* (Fig. 4.18E)  $PPFD$  step changes leading to lower values of  $W_i$ . Conversely, time constants for stomatal opening during *High*  $PPFD$  step changes showed a trend toward higher  $\tau_i$  values leading to higher values of  $W_i$  during the diurnal (Fig. 4.18F).

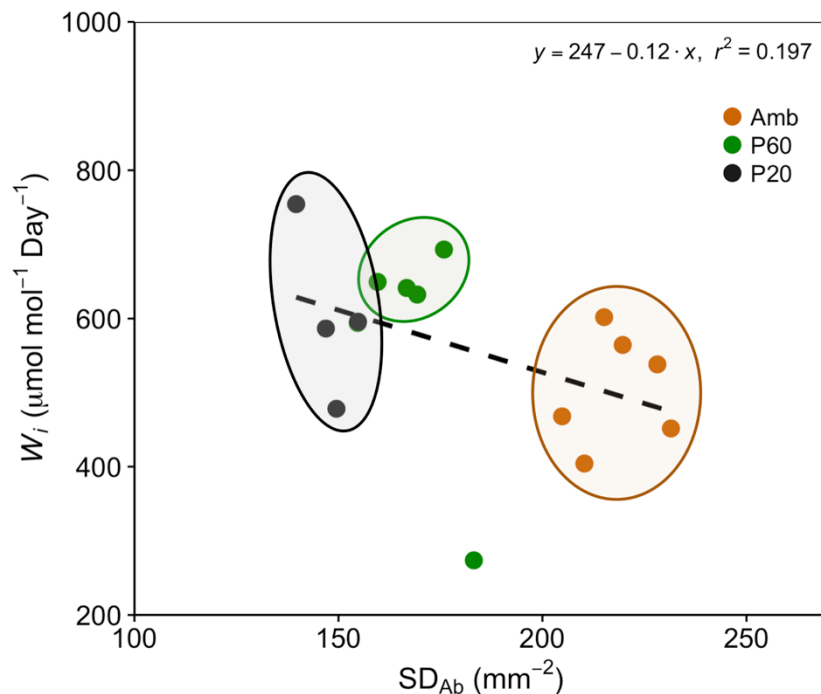


**Figure 4.17.** Correlation between abaxial stomatal density ( $SD_{Ab}$ ) and daily intrinsic water use efficiency during the diurnal ( $W_i$ ). Each data point represents an individual plant. Filled areas highlight the three light treatments: Ambient (Orange), 60% (P60; Green), 20% (P20; Black), whilst black dotted line represents the trend in the data for all individuals.

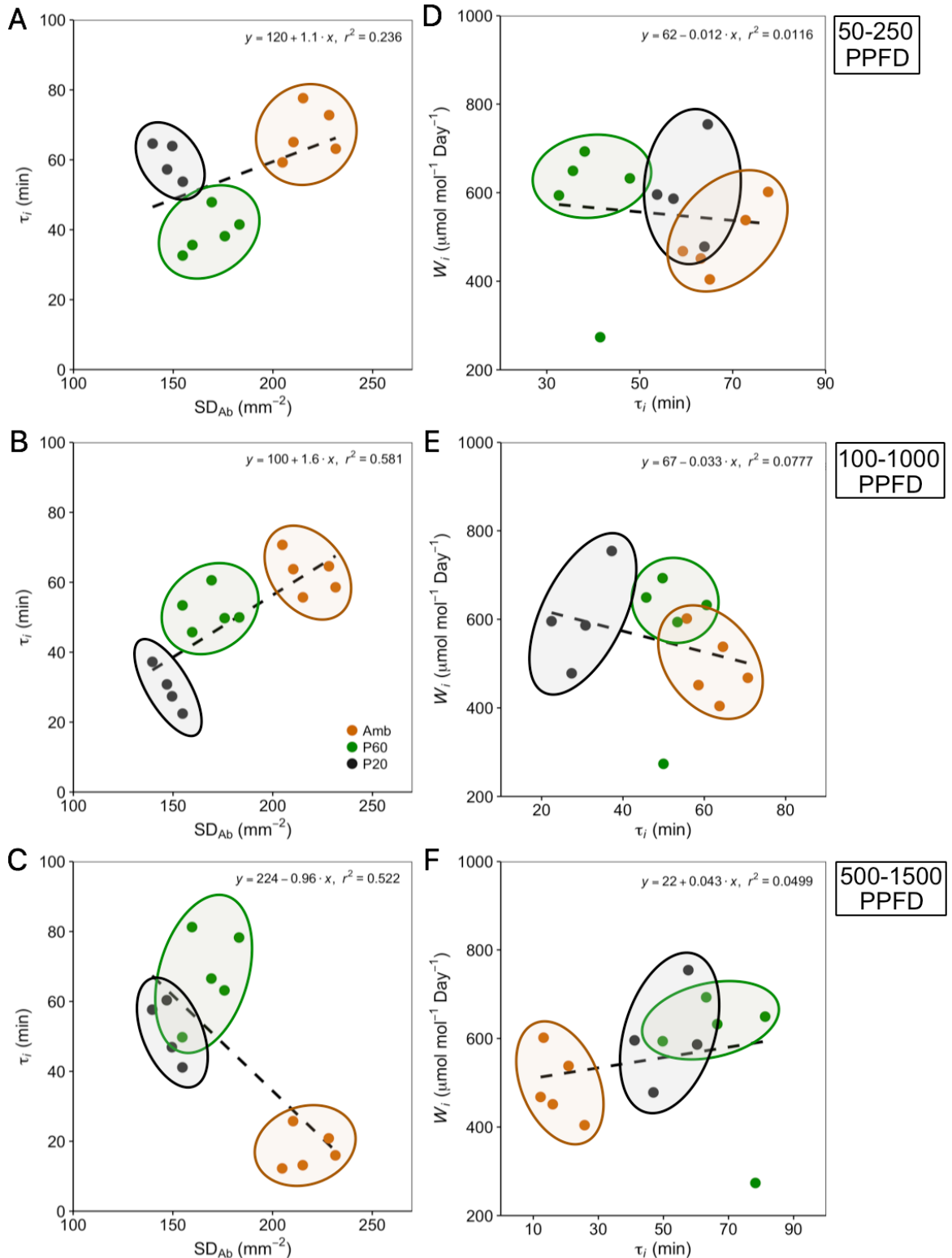


**Figure 4.18.** Correlations between abaxial stomatal density ( $SD_{Ab}$ ) and time constant for stomatal opening ( $\tau_i$ ) at three different light steps: 50-250 PPFD (A); 100-1000 PPFD (B); and 500-1500 PPFD (C), for the three Poplar light treatments. Correlations between time constant for stomatal opening to step increases in light intensity: 50-250 PPFD (D); 100-1000 PPFD (E); and 500-1500 PPFD (F) ( $\tau_i$ ) and daily intrinsic water use efficiency during the diurnal ( $W_i$ ), for the three Poplar light treatments. Each data point represents an individual plant. Filled areas highlight the three light treatments: Ambient (Orange), 60% (P60; Green), 20% (P20; Black), whilst black dotted line represents the trend in the data for all individuals.

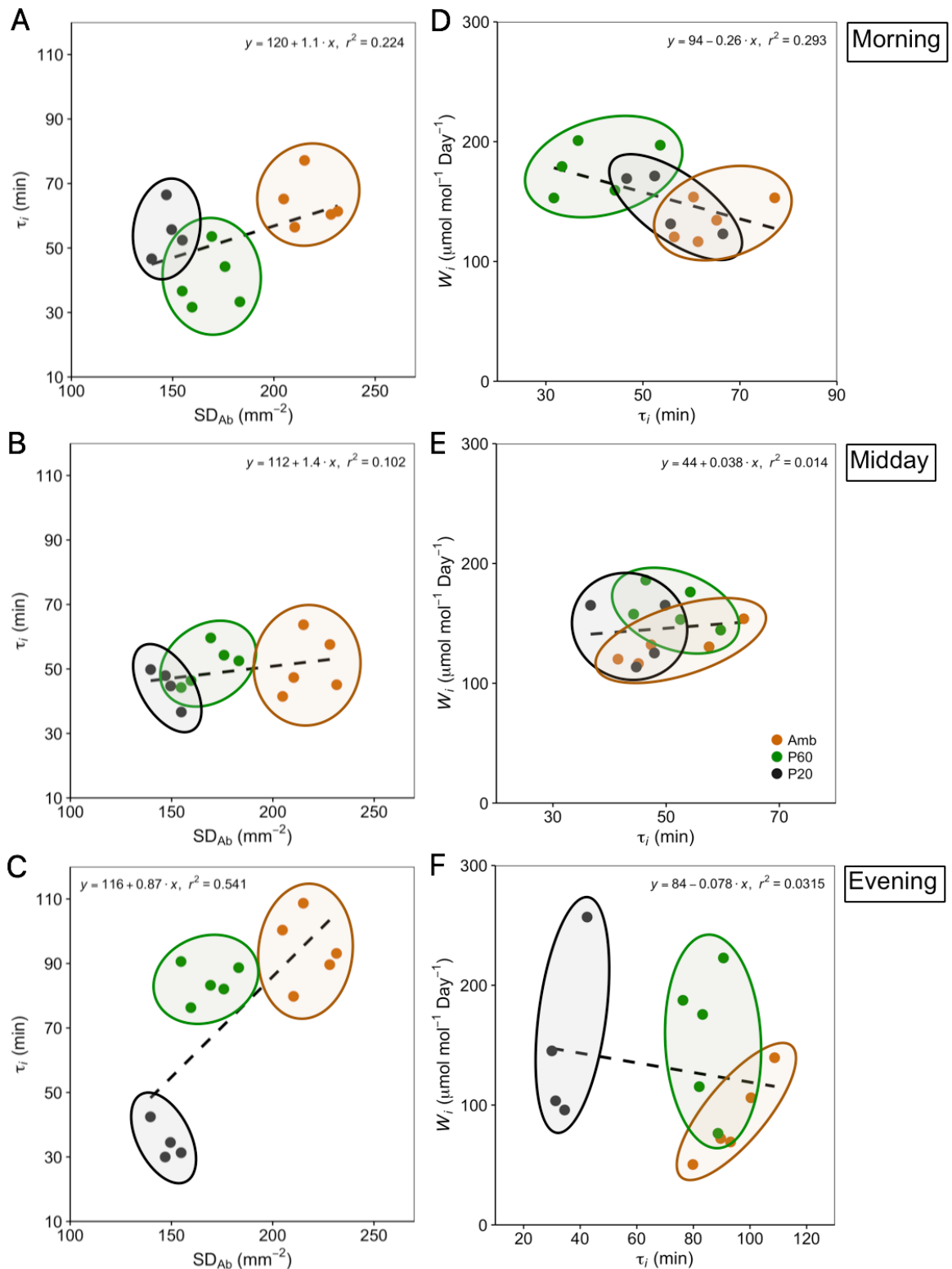


**Figure 4.19.** Correlations between abaxial stomatal density ( $SD_{Ab}$ ) and time constant for stomatal opening to a step increase in light ( $\tau_i$ ) at three different times of day: Morning (A); Midday (B); and Evening (C), for the three Poplar light treatments. Correlations between time constant for stomatal opening to a step increase in light intensity ( $\tau_i$ ) at different times of the day: Morning (D); Midday (E); and Evening (F) and daily intrinsic water use efficiency during the diurnal ( $W_i$ ). Three-hour periods were used to calculate  $W_i$  at times of the day: Morning (8-11am); Midday (12-3pm); Evening (4-7pm). Each data point represents an individual plant. Filled areas highlight the three light treatments: Ambient (Orange), 60% (P60; Green), 20% (P20; Black), whilst black dotted line represents the trend in the data.

Abaxial stomatal density ( $SD_{Ab}$ ), the time constant for stomatal opening following a step increase in  $PPFD$  from 100 to 1000  $\mu\text{mol m}^{-2} \text{s}^{-1}$  ( $\tau_i$ ), and intrinsic water use efficiency ( $W_i$ ) during the diurnal measurement were analyzed at different times of the day (Fig. 4.19). In the morning and evening a positive relationship between  $SD_{Ab}$  and  $\tau_i$  was observed, where the higher stomatal densities displayed by the Amb treatment lead to an increase in the time constant for stomatal opening (Fig. 4.19A and C), and the lower densities observed in the P20 treatment lead to the lowest values of  $\tau_i$ . However, at midday there was found to be no relationship between these two parameters (Fig. 4.19B). There was no relationship between the time constant for stomatal opening ( $\tau_i$ ) and the daily intrinsic water use efficiency ( $W_i$ ) measured from the diurnal measurements, at the different times of the day (Fig. 4.19D-F). However, there was a trend observed in the morning and evening that with an increase in the time constant for stomatal opening there was a corresponding decrease in  $W_i$  during the diurnal (Fig. 4.19D and F), with the Amb grown plants exhibiting the highest values for  $\tau_i$  and the lowest values of  $W_i$  at these times of the day.

## 4.4. Discussion

It was shown in Chapter 3 that there was significant intra-specific variation in the temporal response of stomatal conductance ( $g_s$ ), and that this varied greatly in magnitude; speed of response, and over the diurnal period. However, the aim of the work in this chapter was to investigate how this stomatal behaviour acclimate to changes in growth light intensity, and how this acclimation would impact the dynamics of photosynthesis ( $A$ ) and water use efficiency ( $W_i$ ) over the diurnal period. With previous research highlighting that dynamic acclimation to sun and shade flecks occurred in controlled environments (Assmann and Grantz, 1990; Ooba and Takahashi, 2003; Vico et al, 2011; Drake et al, 2013), it was important to investigate the impact of growth light intensity on the dynamic acclimation of stomatal behaviour in a natural light environment under different average daily light intensities.

In this Chapter, a collection of *Populus nigra* subsp. *Betulifolia* (native Black Poplar) bare root trees were evaluated, to investigate variation in stomatal and photosynthetic traits that occur through developmental acclimation of plants subject to growth in different light intensity treatments. Further assessment examined the impact on intrinsic water use efficiency over the course of the day. Three different light treatments were chosen, and demonstrated large differences in leaf anatomy, stomatal anatomical traits, stomatal behaviour and photosynthetic capacity.

Analysis of  $A/Q$  response curves revealed higher  $A_{sat}$  values in plants grown under ambient light conditions, followed by those grown under 60% that of ambient light (P60), demonstrating that plants photosynthetically acclimated to the average growth light intensity (Watling et al, 1997). Higher  $A_{sat}$  values observed in plants grown under ambient light conditions are characteristic of plants grown under high  $PPFD$  environments, and is often related to greater investments in photosynthetic components such as Rubisco and photosystem reaction centres (Bailey et al, 2001, 2004). Plants grown under 20% of ambient light (P20) demonstrated thinner leaves than the other treatments, which along with larger leaf areas is consistent with plants grown in shade conditions (Kirschbaum et al, 1988), and as they exhibited similar values of  $A$  on a mass basis ( $A_{mass}$ ) despite lower values on an area basis ( $A$ ), it suggests they may have a greater per cell content of photosynthetic components. These findings were reflected by the analysis of  $A/C_i$  response curves, which highlighted similar values of  $A_{mass}$  between treatments despite large differences in the light and  $CO_2$  saturated rates of photosynthesis ( $A_{max}$ ). This suggests that plants adapt even under different growth light conditions to maximise  $CO_2$  uptake by potentially increasing cell photosynthetic components (Pearcy, 2007; Weraduwege et al, 2015) or even enzyme (Rubisco) activation (Ernstsen et al, 1997). However, this may be at the expense of water use efficiency, especially under well-watered conditions when water availability is not limiting. On an area basis, differences in the maximum rates of carboxylation ( $V_{cmax}$ ) and electron transport ( $J_{max}$ ) were observed, with plants grown under higher light conditions exhibiting the highest values in both parameters. These observations suggest that plants grown under ambient light invest in increased photosynthetic capacities on an area basis due to the higher levels of  $PPFD$  experienced during growth (Allen and Pearcy, 2000a, 2000b; Pearcy, 2007; Way and Pearcy, 2012).

In order to investigate the acclimation of plants to growth light intensity and the impact this had on diurnal patterns of  $g_s$  response, photosynthesis and water use efficiency, plants were subjected to a fluctuating light regime (see FLH; Figure 2.1); mimicking a natural pattern of light that represented a typical day during growth. Plants grown under ambient light displayed higher photosynthetic rates, which matched the results from the  $A/Q$  analysis, along with significantly higher levels of stomatal conductance. The fact that these were accompanied by  $C_i$  values that were similar between all treatments, suggests that there may have been a greater flux of  $CO_2$  from the atmosphere to the site of carboxylation in this treatment. The lower values of  $Diur_{Limit}$  exhibited by the Amb treatment further support this theory, with the estimated limitation on  $A$  by stomata over the diurnal period lower in Amb grown plants, despite predicted values of the potential  $A$  (calculated from the  $A/Q$  response curves) being higher. However, the stomatal limitation in  $A$  estimated over the diurnal period was not coordinated with the stomatal limitation estimated from the  $A/C_i$  curves ( $ACi_{Limit}$ ), suggesting that over

the diurnal period all plants, even under well-watered conditions, will balance the need for CO<sub>2</sub> uptake with the need to reduce water loss, depending on the current needs of the plant (Casson and Hetherington, 2010). The lack of correlation between stomatal limitation methodologies may be due to the fact that during  $A/C_i$  measurements, plants were subjected to conditions most favourable for photosynthesis, in an attempt to maximise stomatal conductance to reduce stomatal limitation of  $A$ , and maximise the activation of photosynthetic enzymes (Ernstsen et al, 1997; Parsons et al, 1998). The high value of  $g_s$  over the diurnal period shown by plants grown under ambient conditions potentially increased carbon gain, as highlighted by the lower values of stomatal limitation during this period ( $Diur_{Limit}$ ), but led to a reduction in intrinsic water use efficiency ( $W_i$ ) despite these plants displaying higher values of  $A$ . Again, this highlights the fact that under well-watered conditions, there is a trend toward plants maximizing CO<sub>2</sub> uptake over the need to conserve water (Lawson and Morison, 2004; Aasamaa and Söber, 2011). As such, higher carbon assimilation rates would require greater transport (driven by higher  $g_s$ ) of nutrients (Hills et al, 2012; Schymanski et al, 2013). Interestingly, the higher levels of  $g_s$  exhibited by the high light treatment would also contribute to evaporative cooling, as plants grown under high light intensity are subject to higher leaf and air temperatures (Caird et al, 2007).

The time then for changes in stomatal conductance ( $g_s$ ) to alterations in the light environment is critical for maximize carbon uptake and limit water loss (Lawson et al, 2010; Vico et al, 2011; Lawson and Blatt, 2014; McAusland et al, 2016), with significant variation occurring between species and within species (see Chapter 3) depending on stomatal anatomy and acclimation to the growth environment (Ooba and Takahashi, 2003; Vico et al, 2011; Drake et al, 2013; McAusland et al, 2016). It has been well established that faster stomatal responses and higher magnitudes of  $g_s$  can improve carbon gain but will do so at the expense of water use efficiency (Barradas et al, 1994; Naumburg and Ellsworth, 2000; Lebaudy et al, 2008), whilst slower responses may limit CO<sub>2</sub> diffusion into the leaf and therefore photosynthesis (Barradas et al, 1998; Barradas and Jones, 1996; Kaiser and Kappen 2000; Vico et al, 2011; Lawson et al, 2012; Lawson and Blatt, 2014). Both rapidity and magnitude of  $g_s$  responses to a step change in  $PPFD$  were influenced by growth light intensity, with plants grown under ambient (High) conditions exhibiting greater magnitudes in  $g_s$  at *Mid* and *High* light levels. However, at *low* light steps no differences were observed, which is consistent with previously described data that shows that plants that are acclimated to different light environments may only show differences in  $A$  and  $g_s$  at higher light levels when light is less limiting (Yin and Johnson, 2000). Furthermore, plants grown under ambient conditions demonstrated the slowest  $g_s$  responses at all times of the day, and the highest magnitudes of change in  $g_s$ , however these differences lessened throughout the day. This reduction in the magnitude of  $g_s$  through the day has been described previously (Pfitch and Percy, 1989; Allen and Percy, 2000; Mencuccini et al, 2000), although primarily in the context of changes in leaf water status (Mencuccini et

al, 2000), with changes in the speed of response not reported. All treatments displayed considerable variation in the time for stomata to open or close in response to a step change in *PPFD*, with all treatments taking longer to increase than to decrease  $g_s$ , which is consistent with the proposed strategy that plants will prioritize water conservation over carbon gain (Ooba and Takahashi, 2003), whilst also representing a more conservative strategy in energy consumption such as reducing the cost of stomatal movement (Raven, 2014), and to potentially improve light use efficiency (Ooba and Takahasi, 2003).

The acclimation of the  $g_s$  response was impacted by the growth light intensity, with changes in the magnitude, rapidity, and diurnal response observed between treatments. Studies in forest (Percy, 2007; Eensalu et al, 2008) and crop canopies (Barradas et al, 1994, 1998; Qu et al, 2016) have demonstrated photosynthetic and stomatal acclimation to different growth light environments, highlighting the changes in anatomical and biochemical features that occur with leaves at different positions within the canopy, that receive varying degrees of light intensity (Barradas et al, 1998). Demonstrated here, is an acclimation to lower light that impacts the operational maximum of  $g_s$  throughout the day, and influences stomatal behavior when subjected to different step changes in light intensity. The consequences of this acclimation are that higher magnitudes and faster responses of  $g_s$  promote greater carbon gain, although often at the expense of water use efficiency ( $W_i$ ), whilst slower responses and lower magnitudes of  $g_s$  may conserve water but limit  $\text{CO}_2$  diffusion for  $A$  (Kirschbaum et al, 1988; Kaiser and Kappen 2000; Lawson et al, 2010, 2012; Vico et al, 2011; McAusland et al, 2016). However, as no differences in  $W_i$  were observed between treatments during the step changes in light or the diurnal measurements, it could be suggested that plants attempt to maintain the synchronicity between  $g_s$  and  $A$  to either maximize carbon gain or minimize water loss (Cowan, 1977; Hetherington and Woodward, 2003) depending on the current needs of the plant (Meinzer and Grantz, 1990; Medrano et al, 2015), irrespective of the acclimation state. Furthermore, this theory should be considered since the plants were well watered and therefore not limited by water availability.

It is well known that stomatal density increases with growth light intensity (Gay and Hurd, 1975; Lake et al, 2001), and the data reported here is consistent with previous studies findings. Anatomical stomatal acclimation occurred between treatments, with significantly higher stomatal densities (both abaxial,  $SD_{Ab}$ ; and adaxial,  $SD_{Ad}$ ) exhibited by plants grown under ambient light conditions. These differences are again consistent with the knowledge that higher maximum levels of  $g_s$  are strongly correlated with maximum levels of  $\text{CO}_2$  diffusion for carbon assimilation, evaporative cooling and nutrient uptake by the plant (Schymanski et al, 2013). The large differences observed between treatments in the magnitude of  $g_s$  in all measurements (step changes in *PPFD*, and diurnal), can be attributed to changes in the theoretical maximum of  $g_s$  ( $g_{smax}$ ). With no differences observed in pore area between treatments this

would indicate that values of  $g_{smax}$  were solely driven by stomatal density (Dow et al, 2014), which as is already known, is strongly influenced by growth light intensity (Willmer and Fricker, 1996; Hetherington and Woodward, 2003; Franks and Beerling, 2009).

Contrary to previous published work, higher stomatal densities did not necessarily promote faster  $g_s$  responses to changing light intensity (Franks and Farquhar, 2007; Drake et al, 2013; McAusland et al, 2016). In fact, at Low (50-250 *PPFD*) and Mid (100-1000 *PPFD*) light intensities, a lower stomatal density as seen in plants grown under low light, actually promoted faster responses in  $g_s$  to a step change in *PPFD*. A possible explanation for this may be that plants that develop lower stomatal densities, often develop larger stomata in an attempt to maintain stomatal conductance (Franks and Beerling, 2009; McAusland et al, 2016), however, no differences in pore area were observed between treatments. At High light intensities (500-1500 *PPFD*), stomatal density and speed of response was strongly correlated, which matches the data observed in Chapter 3. This suggests that under low light conditions, when light is most limiting, plants grown under ambient or high light conditions will conserve energy (Raven, 2014) and possibly water (Ooba and Takahashi, 2003), by reducing stomatal movement as carbon gain is maximised and therefore not limited by stomatal conductance. The energy conserved and water saved could then potentially be available later in the day when light intensities may increase (Mencuccini et al, 2000; Raven, 2014). Furthermore, plants acclimated to low light intensity displayed behaviour in contrast to those grown under high light, with faster responses occurring at low intensity light steps and slower responses occurring at high intensities. This strengthens the theory mentioned above that, as plants grown under low light rarely perceive high intensity light levels, they would maximise carbon capture at low light by increasing the rapidity of  $g_s$  response, whilst at high light levels that may never be realised during growth the response of  $g_s$  can be reduced (Raven, 2014; Lawson and Blatt, 2014). Indeed, the slower  $g_s$  responses observed at the end of the day in plants grown under high light conditions and with higher stomatal densities, may be due to changes in osmotic regulation that occur through the day (Mencuccini et al, 2000). Whilst decreases in the absolute values of  $A$  and  $g_s$  observed in all treatments over the course of the day, could be attributed to the accumulation of photosynthetic products or apoplastic sucrose in the guard cells, that may negatively feedback on the Calvin cycle and the rate of transpiration (Lu et al, 1997; Paul and Foyer, 2001; Paul and Pellny, 2003; Outlaw 2003; Kang et al, 2007; Kelly et al, 2013).

## 4.5. Main conclusions

In this chapter, the impact of growth light intensity on the acclimation of stomatal response and diurnal behavior was examined, using the model tree *Populus nigra*.

- Growth light intensity modified stomatal anatomy, specifically stomatal density and index, leading to significant changes in the theoretical maximum of stomatal conductance ( $g_{smax}$ ), which subsequently influences the magnitude of operational stomatal conductance ( $g_s$ ). This anatomical acclimation to growth light intensity greatly impacted the magnitude of stomatal conductance throughout the day and under different light intensities, whilst also increasing the potential for CO<sub>2</sub> diffusion into the leaf and therefore net CO<sub>2</sub> assimilation ( $A$ ).
- The intensity of growth light determined the rapidity and magnitude of  $g_s$  response and  $A$  over the diurnal period, with plants grown under high light exhibiting higher levels of both parameters. This increases the potential for carbon fixation but at the expense of water loss. The synchronicity between these two parameters was maintained between all light treatments, as highlighted by the similar values for intrinsic water use efficiency ( $W_i$ ). This represents an important strategy under well-watered (non-water limited) conditions, by maintaining carbon fixation, overall plant water status and therefore  $W_i$ .
- Plants grown under low light exhibited faster  $g_s$  responses than those grown under high light, when subjected to a step change at low light levels. Whilst the reverse is true at high light steps in  $PPFD$ , with plants grown under high light displaying faster  $g_s$  responses. This represents an interesting strategy, where plants acclimate by increasing  $g_s$  faster to light levels that they experience more often during growth and development, either as a way of maximizing carbon uptake or for the conservation of energy by limiting unnecessary stomatal movement.
- All growth light treatments displayed similar patterns of  $g_s$  response to a step change in light at different times of the day. With decreases in the absolute values of  $A$  and  $g_s$  evident throughout the day, in all treatments. The slower response and lower magnitudes of  $g_s$  and  $A$  observed at the end of the day in plants grown under high light, may be due to changes in osmotic regulation and the accumulation of photosynthetic products. As the rapidity of  $g_s$  response was maintained in low light grown plants throughout the day, it would suggest that accumulation of these products may not occur linearly between each acclimation state. This would impact the

estimation of the response of  $g_s$  and  $A$  in analytical models that would assume the response of these parameters not to change throughout the day.

- The research in this chapter highlights the need to understand the impact of different growth light intensities on stomatal function and response. With plants subjected to different growth light intensities displaying variation in stomatal and photosynthetic response, and therefore water use efficiency. This may lead to impacts on the prediction of carbon and water movement in models predicting ecosystem-atmospheric flux.

# CHAPTER 5

---

## Importance of fluctuations in light on plant photosynthetic acclimation in *Arabidopsis*

Violet-Chabrand, S., Matthews, J.S., Simkin, A.J., Raines, C.A. and Lawson, T., (2017) Importance of Fluctuations in Light on Plant Photosynthetic Acclimation. *Plant Physiology*, 173(4), pp.2163-2179.

### ***Plant Physiology***

(Doi: 10.1104/pp.16.01767)

#### **Acknowledgements and contributions to this chapter:**

I would like to thank Silvere Violet-Chabrand for help with performing model analysis, Andrew Simkin for carrying out immunoblotting and associated analysis, and Silvere Violet-Chabrand and Tracy Lawson for contributing to writing the finished published article.

## Transition Statement

In the previous two chapters, natural variation in photosynthetic and stomatal acclimation to growth environment and light intensity was explored in the model tree species *Populus nigra*. It was highlighted that growth light intensity has an effect not only on photosynthetic capacity and stomatal anatomy, but also on the dynamic response of stomatal conductance to changes in the light environment, and the impact this has on photosynthesis and water use efficiency. The acclimation of plants to light intensity has been studied extensively in crop and model species such as *Arabidopsis*, yet little is known about the effect of dynamic fluctuations in light on plant phenotype and acclimatory responses.

In this Chapter, natural fluctuations in light were mimicked over a diurnal period to examine the effect on photosynthetic processes and growth. Due to technical considerations with the programmable growth light environment, the model species *Arabidopsis thaliana* was used instead of *Populus nigra*, to maximise repetition number and reproducibility. High and low light intensities, delivered via a realistic dynamic fluctuating or square wave pattern were used to grow and assess the effect of fluctuating light on photosynthetic acclimation and response.

## 5.1. Introduction

In the natural environment plants experience a range of light intensities and spectral properties due to changes in sun angle and cloud cover in addition to shading from overlapping leaves and neighbouring plants. Leaves are therefore subjected to spatial and temporal gradients in incident light, which has major consequences for photosynthetic carbon assimilation (Pearcy, 1990; Chazdon and Pearcy, 1991; Pearcy and Way, 2012). As light is the key resource for photosynthesis, plants acclimate to the light environment under which they are grown to maintain performance and fitness. Light is one of the most dynamic environmental factors that directly impacts on plant performance, and it is therefore important to understand how plants acclimate to fluctuating light environments such as those experienced under field conditions.

Plant acclimation to changes in irradiance can be categorised as (i) dynamic acclimation which refers to a reversible biological process present within a given period of time (Walters and Horton, 1994; Murchie and Horton, 1997; Mullineaux, 2006; Okegawa et al, 2007; Athanasiou et al, 2010; Yin and Johnson, 2000; Tikkanen et al, 2010; Alter et al, 2012; Suorsa et al, 2012; Yamori, 2016); or (ii) developmental acclimation which is defined as changes in morphology (e.g. leaf thickness and density) resulting from a given growth light environment, and are largely irreversible (Weston et al, 2000; Murchie, 2005), and is the focus of this Chapter. The ability of plants to developmentally acclimate to a given light environment is particularly well-demonstrated in leaves grown in sun and shade conditions, which differ in photosynthetic efficiency, biochemistry (e.g. Rubisco content and change in Photosystem II and I ratio), anatomy (e.g. chloroplast size and distribution) and morphology (e.g. leaf mass area and thickness) (Givnish, 1988; Walters and Horton, 1994; Weston et al, 2000; Bailey et al, 2001; Bailey et al, 2004). Plants grown under high light intensity tend to develop thicker leaves than those grown under low light intensity (Evans and Poorter, 2001), which generally increases photosynthetic capacity per unit area improving the plant's ability to utilize light for carbon fixation (Terashima et al, 2006). Leaves acclimated to shade tend to have higher net photosynthetic rates at lower light levels compared to sun leaves (Givnish 1988). Previous studies investigating developmental acclimation have primarily focused on the effect of light intensity, with less emphasis given to the effect of dynamic light during growth, like that experienced under a natural environment. Fluctuations in light could have a significant impact on acclimation processes during growth, and need to be investigated alongside light intensity to assess the interaction between light regime and intensity.

Under natural environmental conditions, the random duration and intensity of fluctuating light from passing clouds or leaf movements (sun- and shade-flecks) result in incident light intensities below light saturation that reduce photosynthetic rates, whilst those intensities greater than saturated lead to excess excitation energy that can result in short potential “stress” periods and long term damage to leaf photosynthesis (Baker, 2008). Plants therefore employ mechanisms that enable them to deal with these changes in excitation pressure, including thermal dissipation of excitation energy. Such processes are termed non-photochemical quenching (NPQ) and are mainly associated with changes in the xanthophyll cycle (Demmig-Adams and Adams, 1992; Muller et al, 2001; Kulheim et al, 2002) and protonation of PSII antenna proteins (Li et al, 2000; 2004). Large diversity in light acclimation exists between individuals and species (Murchie and Horton, 1997), partly due to the random nature of light fluctuations and species-specific responses.

The majority of studies examining acclimation to fluctuating light conditions have been carried out on plants grown under constant intensities of light and swapped to a simple light pattern (consisting of one or more step changes in light intensity of different frequencies) (Yin and Johnson, 2000; Tikkanen et al, 2010; Alter et al, 2012; Suorsa et al, 2012; Yamori, 2016). Under these light conditions, acclimation responses have often been monitored over a period of several days (e.g. Alter et al, 2012; Athanasiou et al, 2010). Whilst this approach is powerful for studies on the mechanisms of dynamic light acclimation, it fails to recognise the importance of how plants developmentally acclimate to growth under fluctuating light intensities (Huxley, 1969), such as those found in the natural field environment (Frechilla et al, 2004). There are only a handful of studies that have examined the impact of “real” dynamic light environments on plant growth and performance (Kulheim et al, 2002; Yamori et al, 2016), however, none of these used a controlled environment to examine the direct impact of light.

In order to fully understand how plants integrate fluctuations in incident light, and how this influences acclimation and modifies plant growth, there was a need to grow plants in a controlled but dynamic environment that mimics a light regime that would be experienced in the field. How plants perform under these conditions and the differences in responses with those grown in square wave light regimes is important, as it will improve our understanding of how plants behave in “real” light environments, potentially improving model prediction.

The aim of this chapter is to identify whether there is a developmental acclimation to fluctuating light in the model species *Arabidopsis*, and if so how it may influence plant performance under dynamic light conditions. The work presented in this chapter may lead to greater understanding of plant acclimation to light, and potentially force us to rethink experimental growth conditions when drawing conclusions

on how plants will perform in the field. To address this, *Arabidopsis* plants were grown and measured under fluctuating and non-fluctuating (or square wave) light regimes at two different average intensities (high and low) (Fig. 5.1), and the performance of these plants evaluated.

## 5.2. Material and methods

*This section outlines methods specific to this chapter and modifications made to protocols outlined previously, if more detail is required please refer to Chapter 2 – “Materials and Methods”.*

### 5.2.1. Plant material and growth conditions

*Arabidopsis thaliana* (Columbia, Col-0) were grown in peat-based compost (Levingtons F2S, Everris, Ipswich, UK) in a controlled environment with growth conditions maintained at a relative humidity of 55-65%, air temperature of 21-22°C, and a CO<sub>2</sub> concentration of 400 μmol mol<sup>-1</sup>. Fluctuating light growth conditions were provided by a Heliospectra LED light source (Heliospectra AB, Göteborg, Sweden), with the light regime recreated from natural variations in light intensity recorded during a relatively clear day in July 2014 at the University of Essex (Fig. 5.1) and the assumption of a constant spectral distribution. The average light intensity was 460 μmol m<sup>-2</sup> s<sup>-1</sup> for high light conditions and 230 μmol m<sup>-2</sup> s<sup>-1</sup> for low light conditions. Plants were maintained under well-watered conditions, with the position under the growth light source randomized daily to remove any potential heterogeneity in the spectral quality and quantity. All gas exchange, chlorophyll fluorescence, and absorption measurements were taken on the youngest fully expanded leaf of 21-27 days old plants.

### 5.2.2. Growth Analysis

#### 5.2.2.1. Leaf anatomical measurements

Rosette area, taken as the area (cm<sup>2</sup>) of the visible rosette of the plant, was measured from when each plant was sown and placed under the lights (day 0) until the appearance of inflorescence (day 28-37). Total leaf area (cm<sup>2</sup>), total leaf dry weight (g), and specific leaf area (SLA, cm<sup>2</sup>/g), were measured on all

treatments at the same time once the first inflorescence had appeared on any treatment (*SQH* plants exhibited the first inflorescence after 28 days). All growth analysis measurements are a mean of 8-10 plants.

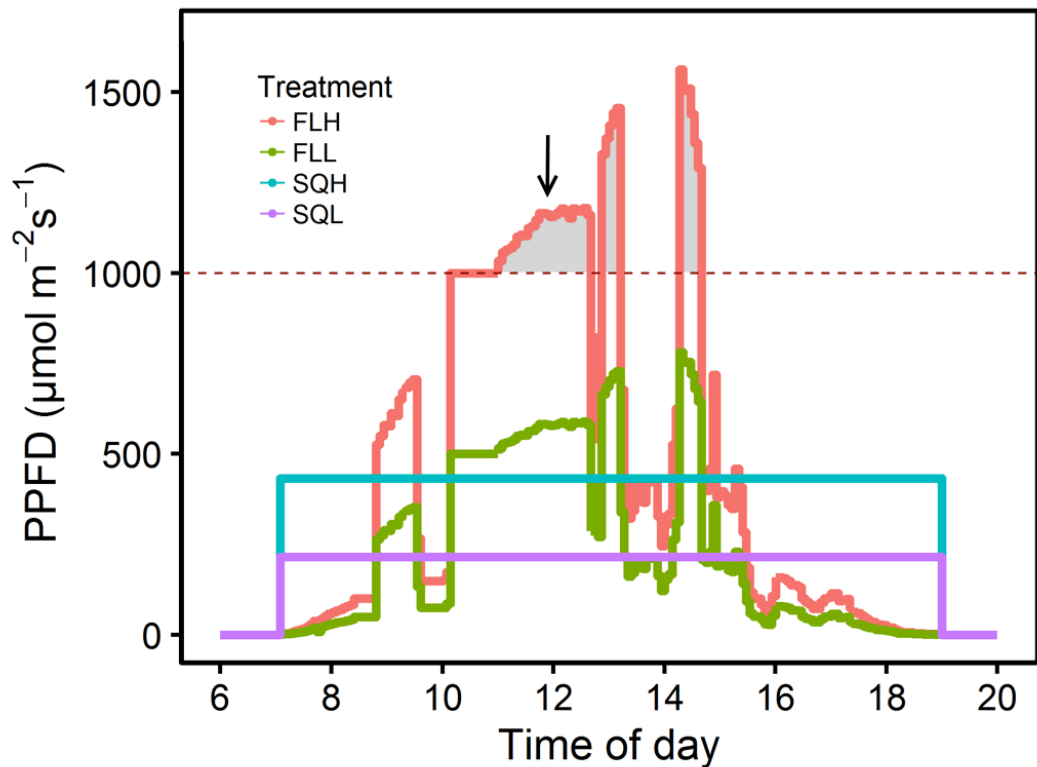


**Figure 5.1.** Diurnal light regimes used for plant growth and leaf level measurements of gas exchange. Areas under the curve represent the same average amount of light energy over the 12-h light regime depending on the light intensity: square wave high light (*SQH*) and fluctuating high light (*FLH*; mean =  $460 \mu\text{mol m}^{-2} \text{s}^{-1}$ ), square wave low light (*SQL*) and fluctuating low light (*FLL*; mean =  $230 \mu\text{mol m}^{-2} \text{s}^{-1}$ ). Arrow indicates time point (12pm) at which leaf discs were collected for protein and chlorophyll extraction.

### 5.2.2.2. Leaf optical properties

Measurements of transmittance and reflectance for each leaf was measured on the youngest, fully expanded leaf on each plant after 14, 21, and 28 days of growth and used to calculate absorbance. See method 2.4.3.

### 5.2.2.3. Analysis of photosynthetic pigments

To analyse changes in photosynthetic pigments, leaf samples were collected and analysed from intact leaves as described in method 2.4.4.

#### **5.2.2.4. Leaf cross-section analysis**

To investigate changes in leaf thickness, cell size and composition, the most recent fully expanded leaves were collected from plants after 28 days of growth, as described in method 2.4.5.

#### **5.2.2.5. Protein Extraction and Western Blotting**

Protein extraction was performed as described in method 2.4.6 to determine protein content and composition.

### **5.2.3. Leaf gas exchange**

All gas exchange ( $A$  and  $g_s$ ) parameters were recorded and cuvette conditions maintained as laid out in section 2.2, using a Li-Cor 6400XT portable gas exchange system (Li-Cor, Lincoln, Nebraska, USA). All measurements were taken using the youngest, fully expanded leaf.

#### **5.2.3.1. $A/Q$ (net photosynthetic rate/ $PPFD$ ) response curves**

The response of net  $CO_2$  assimilation rate ( $A$ ) to photosynthetic photon flux density ( $PPFD$ ) was measured and recorded under cuvette conditions as described in method 2.2.1.

#### **5.2.3.2. $A/C_i$ (net photosynthetic rate/intercellular $CO_2$ concentration) response curves**

The response of net  $CO_2$  assimilation rate ( $A$ ) to intercellular  $CO_2$  concentration ( $C_i$ ) was measured and recorded under cuvette conditions as described in method 2.2.2.

#### **5.2.3.3. Diurnal measurements**

Diurnal gas exchange measurements of  $A$  and  $g_s$  were carried out as described in method 2.2.4.

### **5.2.4. Modelling gas exchange parameters**

#### **5.2.4.1. Estimating photosynthetic capacities and limitations**

Photosynthetic capacities ( $V_{C_{max}}$  and  $J_{max}$ ) were estimated from the  $A/C_i$  response curves using method 2.3.2.

#### **5.2.4.2. Modelling net CO<sub>2</sub> assimilation rates**

Net CO<sub>2</sub> assimilation ( $A$ ) as a function of light intensity ( $PPFD$ ) was modelled to simulate the maximum diurnal variations of  $A$  in absence of stomatal limitation under different light intensity conditions. See method 2.3.4.

#### **5.2.4.3. Determination of mass integrated net CO<sub>2</sub> assimilation**

Net CO<sub>2</sub> assimilation ( $A$ ) was converted to a mass integrated measurement using leaf mass area ( $LMA$ ) – see method 2.3.1.

#### **5.2.5. Light use efficiency**

Daily light use efficiency was calculated as the ratio between the predicted daily-integrated photosynthesis (g) and the daily-absorbed light intensity (MJ), as laid out in method 2.5.1. Light use efficiency ( $LUE$ ) was calculated as the ratio between leaf dry mass (g) and absorbed light intensity (MJ), as described in method 2.5, see Chapter 2.

#### **5.2.6. Statistical analysis**

On each parameter derived from the diurnal measurement, a one-way ANOVA with light treatment as a factor and corrected for unequal variance (White's adjustment), was applied on each recorded time. When significant differences were observed, a Tukey post-hoc test was used to compare the different light treatments. All other stats were applied as laid out in method 2.6.

## 5.3. Results

### 5.3.1. Photo-acclimation of plants grown under different light regimes

Light response curves in which net CO<sub>2</sub> assimilation rate ( $A$ ) was measured as a function of photosynthetic photon flux density ( $PPFD$ ) ( $Q$ ) ( $A/Q$  curves, Fig. 5.2A) revealed similar  $A$  values at  $PPFD$ s below 250  $\mu\text{mol m}^{-2} \text{s}^{-1}$  in plants grown under all the different light regimes: square wave high ( $SQH$ ) and low ( $SQL$ ) and fluctuating high ( $FLH$ ) and low ( $FLL$ ) light intensity. Measurements of  $A$  at  $PPFD$  above this value and light saturated assimilation rate ( $A_{sat}$ , Table 5.1), were significantly greater in plants grown under high light intensity compared with those grown under low light, independently of the light regime (Fig. 5.2A).

Commonly, photosynthesis is measured per unit leaf area, however this area also represents a volume of photosynthetic tissues that can differ among plants (e.g. different leaf thickness). To take into consideration photosynthesis per unit leaf volume, we integrated  $A$  by mass of dry leaf ( $A_{mass}$ ). There was significantly greater  $A_{mass}$  in plants grown under fluctuating light regimes compared to those grown under square wave light regimes (Fig. 5.2B), and as expected a tendency for plants grown under high light regimes to have greater rates of  $A_{mass}$  compared to plants grown under low light regimes.

Dark respiration, derived from the  $A/Q$  curve ( $R_{d\text{-model}}$ ) was significantly higher in plants grown under  $SQH$  and there was a general tendency for higher respiration in plants grown in square wave light intensity regimes compared with fluctuating regimes (Table. 5.1) in  $R_{d\text{-model}}$  as well as those measured during diurnals ( $R_{d\text{-diurnal}}$ ). However, it should be noted that,  $R_{d\text{-diurnal}}$  measured at the start of the diurnal was lower than that  $R_{d\text{-model}}$  determined from the  $A/Q$  analysis. Plants grown under  $SQH$  also had a significantly higher light compensation point ( $\Gamma$ ) compared to plants grown under fluctuating light regimes (Table 5.1).

The large differences observed in the response of  $A$  to  $PPFD$  between plants grown under low and high light intensity, was less noticeable for Photosystem II (PSII) operating efficiency ( $F_q'/F_m'$ ) (Fig. 5.2C). The decrease in  $F_q'/F_m'$  with increasing  $PPFD$  was mainly driven by changes in the PSII efficiency factor ( $F_q'/F_v'$ ) (Fig. 5.2D).  $F_q'/F_m'$  was also affected, although to a lower extent, by the maximum efficiency of PSII ( $F_v'/F_m'$ ) which was higher in plants grown under high  $PPFD$  (Fig. 5.2E), with low values illustrating greater non-photochemical quenching. In general plants grown under fluctuating regimes had a higher  $F_v'/F_m'$  compared with those grown under square wave, particularly when measured under high  $PPFD$ s. Plants grown under  $SQL$  showed the lowest values in both quenching parameters:  $F_q'/F_v'$  and  $F_v'/F_m'$ . Non-photochemical quenching ( $NPQ$ ) increased more rapidly at low light intensity in plants grown under

SQL compared to plants grown in the other lighting regimes, and in general *NPQ* had a tendency to be lower in plants grown under fluctuating light (Fig. 5.2F).

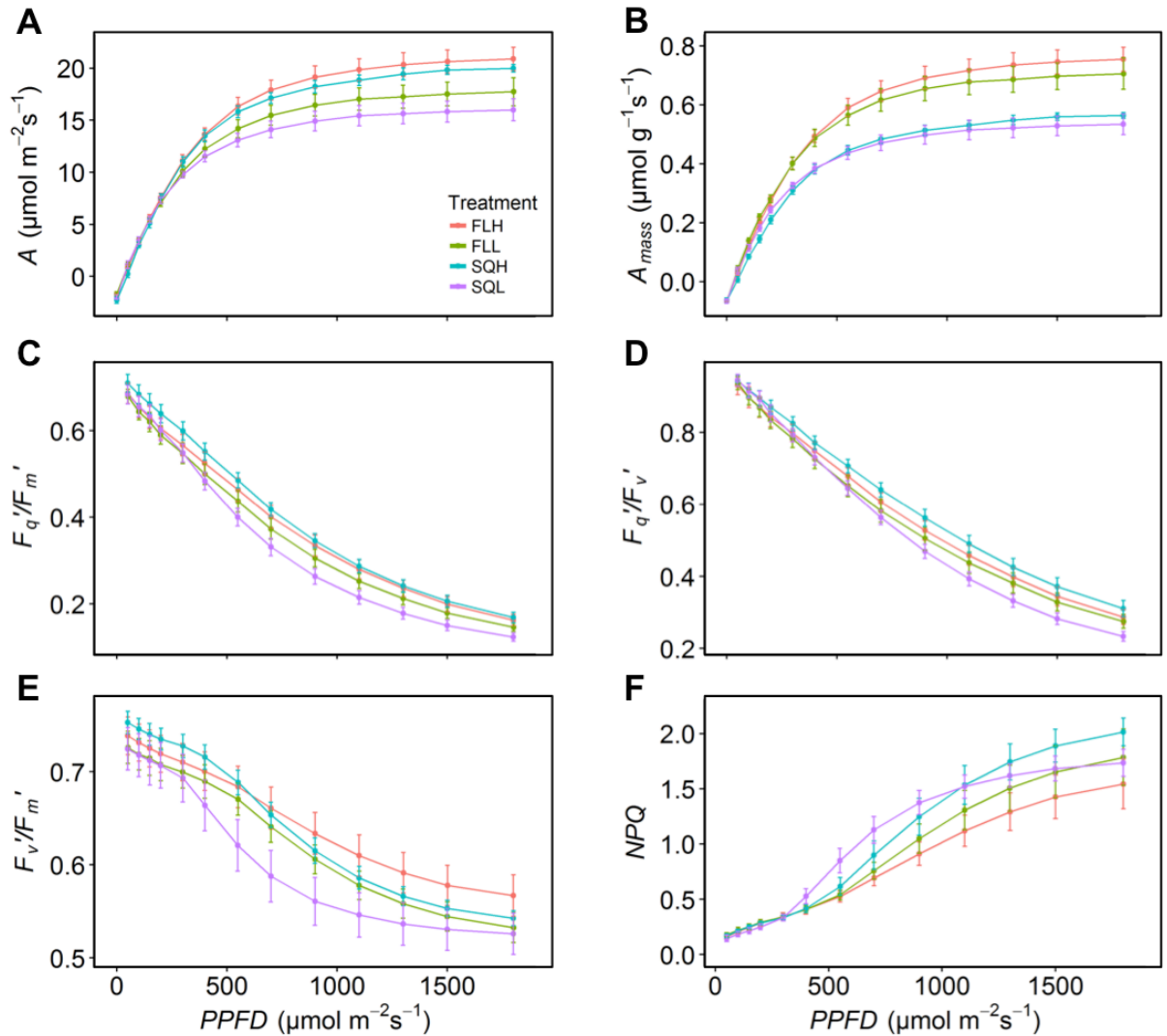


**Figure 5.2.** Photosynthesis as a function of light intensity (*PPFD*) of plants grown under the four light regimes square wave high light (*SQH*); fluctuating high light (*FLH*); square wave low light (*SQL*) and fluctuating low light (*FLL*). Net CO<sub>2</sub> assimilation on an area basis ( $A$ ; A); relative to leaf mass ( $A_{\text{mass}}$ ; B); and chlorophyll fluorescence parameters  $F_q'/F_m'$  (C);  $F_q'/F_v'$  (D);  $F_v'/F_m'$  (E) and *NPQ* (F). Error bars represent confidence interval at 95%. n= 5.

**Table 5.1.** Parameter values (mean±SE) estimated from the response of *A* to light intensity, from plants grown under the four light regimes: *SQH*; *FLH*; *SQL*; *FLL*.  $A_{sat}$ : maximum net CO<sub>2</sub> assimilation at saturating light;  $\alpha$ : quantum yield of photosynthesis;  $\theta$ : curvature parameter;  $\Gamma$ : light compensation point. Two values of dark respiration were estimated: the first from the model (" $R_{d-model}$ ") and the second at the beginning of the diurnal period (" $R_{d-diurnal}$ "). Letters represent the results of Tukey's post-hoc comparisons of group means.

	FLH	FLL	SQH	SQL
$A_{sat}$	22.48±0.2 <sup>a</sup>	18.78±0.21 <sup>b</sup>	21.38±0.07 <sup>a</sup>	17.38±0.19 <sup>b</sup>
$R_{d-model}$	1.77±0.03 <sup>b</sup>	1.59±0.04 <sup>b</sup>	2.37±0.05 <sup>a</sup>	1.95±0.05 <sup>ab</sup>
$R_{d-diurnal}$	0.89±0.22 <sup>ab</sup>	0.41±0.04 <sup>b</sup>	1.39±0.17 <sup>a</sup>	1.03±0.11 <sup>ab</sup>
$\alpha$	0.053±0.0004 <sup>a</sup>	0.054±0.0007 <sup>a</sup>	0.057±0.0007 <sup>a</sup>	0.062±0.001 <sup>a</sup>
$\theta$	0.78±0.01 <sup>a</sup>	0.71±0.01 <sup>ab</sup>	0.78±0.01 <sup>a</sup>	0.63±0.02 <sup>b</sup>
$\Gamma$	33.77±0.52 <sup>b</sup>	30.31±0.57 <sup>b</sup>	42.87±0.83 <sup>a</sup>	33.02±0.87 <sup>b</sup>

### 5.3.2. Leaf properties in plants acclimated to different light regimes

Leaf absorbance (measured after 28 days of growth) was significantly different between plants grown in the different light regimes ( $P<0.05$ ) ranging from 0.88 (*FLL*) to 0.93 (*SQH*) (Fig. 5.3A). Plants grown under fluctuating light regimes had significantly lower absorbance values ( $P<0.05$ ) compared with those grown under square wave regimes, with a smaller but also significant difference between high and low light treatments. The only difference in leaf reflectance was observed between the fluctuating treatments, with a higher value shown by *FLL* grown plants (Fig. 5.3B), whilst transmittance was generally higher in fluctuating light treatments compared to square wave grown plants and in plants grown at lower light intensities (Fig. 5.3C).

Differences in leaf thickness depended on both intensity and light regime (Fig. 5.4A), with significantly thinner leaves ( $P<0.05$ ) for plants grown under low light and fluctuating light compared to square wave grown plants. A difference in leaf thickness was primarily driven by differences in the thickness of the mesophyll palisade layer in all treatments (Fig. 5.4B). Thickness of the palisade mesophyll layer was significantly ( $P<0.05$ ) higher in square wave grown plants, and in plants subjected to a higher intensity of light. The layer of spongy mesophyll cells was significantly thinner ( $P<0.05$ ) in plants grown under fluctuating light, whilst also being thinner in *FLH* compared with *FLL* (Fig. 5.4C).

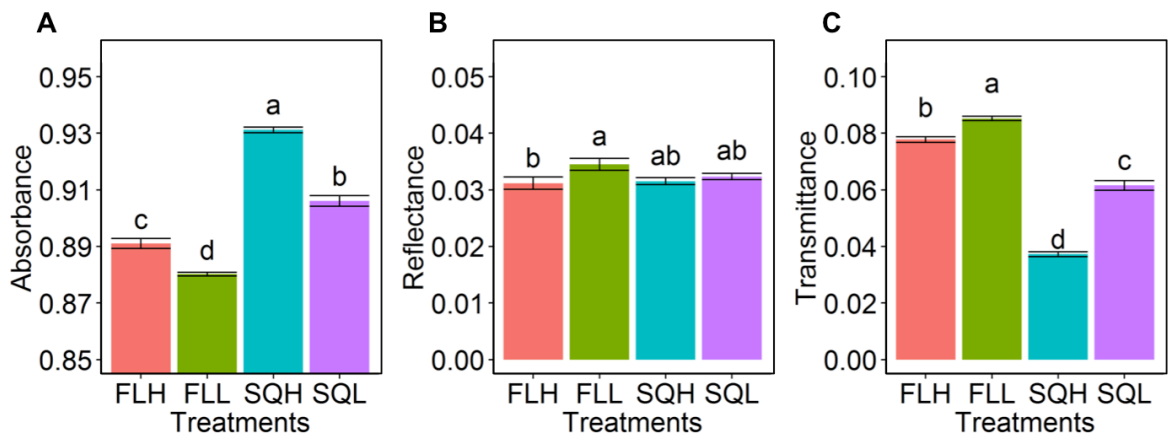


**Figure 5.3.** Optical properties including absorbance (A); transmittance (B) and reflectance (C) of leaves grown under the four different light regimes square wave high light (SQH); fluctuating high light (FLH); square wave low light (SQL) and fluctuating low light (FLL). Error bars represent mean  $\pm$  SE.  $n = 10$ . Letters represent the results of Tukey's post-hoc comparisons of group means.

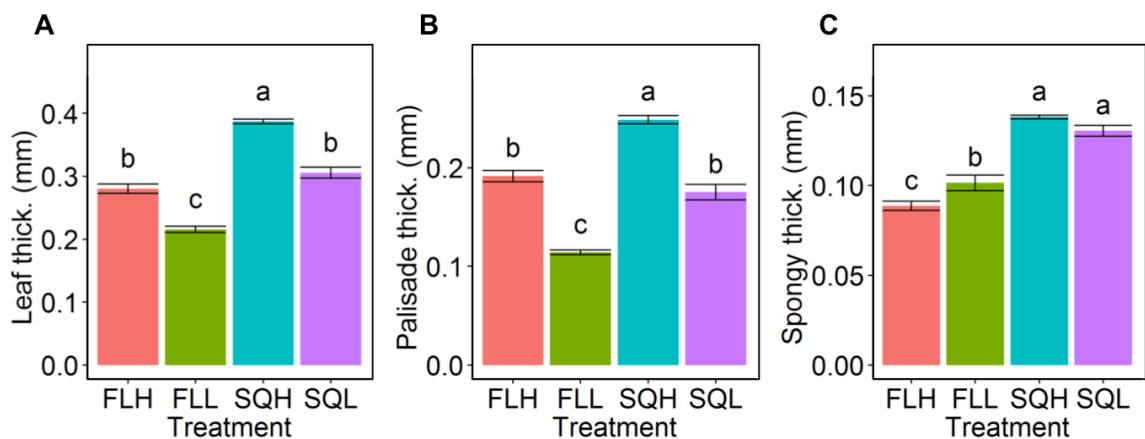


**Figure 5.4.** Leaf anatomical properties including total thickness (A); palisade layer thickness (B) and Spongy layer thickness (C) of plants grown under the four light treatments; square wave high light (SQH); fluctuating high light (FLH); square wave low light (SQL) and fluctuating low light (FLL). Error bars represent mean  $\pm$  SE.  $n = 6$ . Letters represent the results of Tukey's post-hoc comparisons of group means.

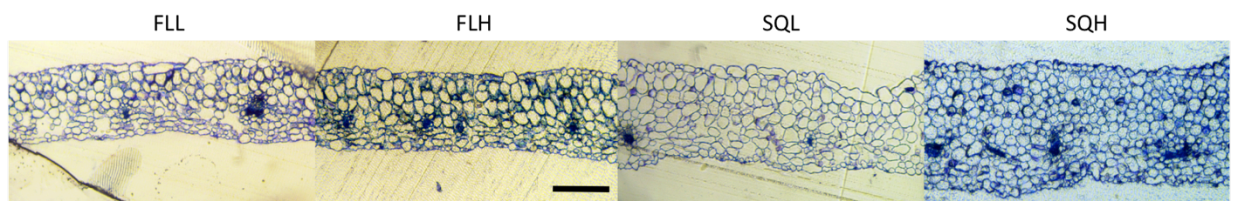


**Figure 5.5.** Cross section of leaves grown under the four light treatments square wave high light (SQH); fluctuating high light (FLH); square wave low light (SQL) and fluctuating low light (FLL). Leaves collected after 28 days growth under the light regime. Bar indicates 200  $\mu\text{m}$ .

As a result of the increased leaf thickness in plants grown under square wave treatments, there was a tendency for a higher number of cells (as observed in Fig. 5.5) with more circular cell shape in the palisade mesophyll compared to fluctuating treatments, measured by the length/width ratio ( $P=0.06$ , Table 5.2). Despite thicker leaves and a greater number of cells in square wave grown plants, there was no significant difference in total protein content between treatments.

The only significant differences observed in chlorophyll a/b ratio between plants grown under fluctuating or square wave light regimes was the lower ratio in *FLL* compared to *SQL* (Table 5.3). Plants grown under *SQL*, *FLL* and *FLH* had significantly lower total carotenoid/total chlorophyll ratio compared to plants grown under *SQH* ( $P<0.05$ ).

**Table 5.2.** Cell size (width, length) and shape (length/width) (mean $\pm$ SE) from leaf tissues of plants grown under the four light treatments. Epidermal Abaxial (EpiAb); Epidermal Adaxial (EpiAd).

Tissue	Treatment	Width (mm)	Length (mm)	L/W
EpiAb	FLH	0.024 $\pm$ 0.004	0.018 $\pm$ 0.002	0.828 $\pm$ 0.061
	FLL	0.026 $\pm$ 0.005	0.016 $\pm$ 0.002	0.691 $\pm$ 0.059
	SQH	0.031 $\pm$ 0.006	0.021 $\pm$ 0.002	0.918 $\pm$ 0.22
	SQL	0.031 $\pm$ 0.003	0.02 $\pm$ 0.002	0.696 $\pm$ 0.074
EpiAd	FLH	0.048 $\pm$ 0.009	0.024 $\pm$ 0.003	0.607 $\pm$ 0.114
	FLL	0.049 $\pm$ 0.01	0.026 $\pm$ 0.003	0.661 $\pm$ 0.092
	SQH	0.04 $\pm$ 0.005	0.032 $\pm$ 0.002	0.934 $\pm$ 0.149
	SQL	0.045 $\pm$ 0.009	0.027 $\pm$ 0.003	0.712 $\pm$ 0.077
Palisade	FLH	0.04 $\pm$ 0.002	0.053 $\pm$ 0.004	1.353 $\pm$ 0.115
	FLL	0.034 $\pm$ 0.003	0.048 $\pm$ 0.003	1.453 $\pm$ 0.131
	SQH	0.039 $\pm$ 0.003	0.045 $\pm$ 0.003	1.155 $\pm$ 0.041
	SQL	0.043 $\pm$ 0.003	0.048 $\pm$ 0.003	1.137 $\pm$ 0.066
Spongy	FLH	0.037 $\pm$ 0.005	0.025 $\pm$ 0.002	0.739 $\pm$ 0.069
	FLL	0.036 $\pm$ 0.004	0.023 $\pm$ 0.002	0.685 $\pm$ 0.068
	SQH	0.048 $\pm$ 0.003	0.033 $\pm$ 0.002	0.728 $\pm$ 0.068
	SQL	0.039 $\pm$ 0.004	0.027 $\pm$ 0.003	0.741 $\pm$ 0.081

**Table 5.3.** Chlorophyll a/b ratio (Chl a/b) and total carotenoid:total chlorophyll ratio (Car/Chl) of plants grown under the four light treatments. n = 8. Letters represent the results of Tukey's post-hoc comparisons of group means.

Treatment	Chl a/b	Car/Chl
FLH	3.86±0.16 <sup>ab</sup>	0.36±0.01 <sup>a</sup>
FLL	3.69±0.12 <sup>a</sup>	0.32±0.02 <sup>a</sup>
SQH	4.32±0.18 <sup>ab</sup>	0.44±0.02 <sup>b</sup>
SQL	4.22±0.13 <sup>b</sup>	0.31±0.02 <sup>a</sup>

### 5.3.3. Impact of growth light on photosynthetic capacity

Assimilation rate measured as a function of intercellular [CO<sub>2</sub>] ( $C_i$ ) was higher in plants grown under *SQH* (Fig. 5.6A), and generally greater in plants grown under high light intensity regimes. The light and CO<sub>2</sub> saturated rate of photosynthesis  $A_{max}$  was highest in plants grown under square wave regimes compared to plants grown under fluctuating light regimes irrespective of light intensity, with *SQH* grown plants >15% higher than all other growth treatments. In contrast, the light and CO<sub>2</sub> saturated rate of  $A_{mass}$  ( $A$  integrated by mass) was significantly higher in plants grown under fluctuating light regimes compared with square wave light regimes (Fig. 5.6B). Nevertheless, the differences in  $A_{mass}$  between fluctuating and square wave light regimes were smaller than those observed in the  $A/Q$  curves (Fig. 5.2B). The maximum rate of carboxylation by Rubisco ( $V_{Cmax}$ ) and the maximum electron transport rate ( $J_{max}$ ) for ribulose 1,5-bisphosphate (RuBP) regeneration (Fig. 5.6A), were highest in plants grown under square wave conditions, and those grown under high light intensities (Table 5.4). Estimates of mesophyll conductance ( $g_m$ ) ranged from 0.154 to 0.927 mol m<sup>-2</sup> s<sup>-1</sup>, however the only significant difference was the high values in the *SQH* plants (Table 5.4).

The operating efficiency of PSII photochemistry ( $F_q'/F_m'$ ) was significantly higher in plants grown under the *SQH* regime compared to those grown under the other light regimes at all CO<sub>2</sub> concentrations measured (Fig. 5.6C). Plants grown under the other three light regimes (*FLH*, *FLL* and *SQL*) showed no significant difference at high CO<sub>2</sub>, but the  $C_i$  concentration where the switch between the Rubisco- and RuBP regeneration-limited  $A$  occurs ( $C_{ic}$ ), was significantly higher in plants grown under square wave light regimes compared to fluctuating light conditions (Fig. 5.6C).

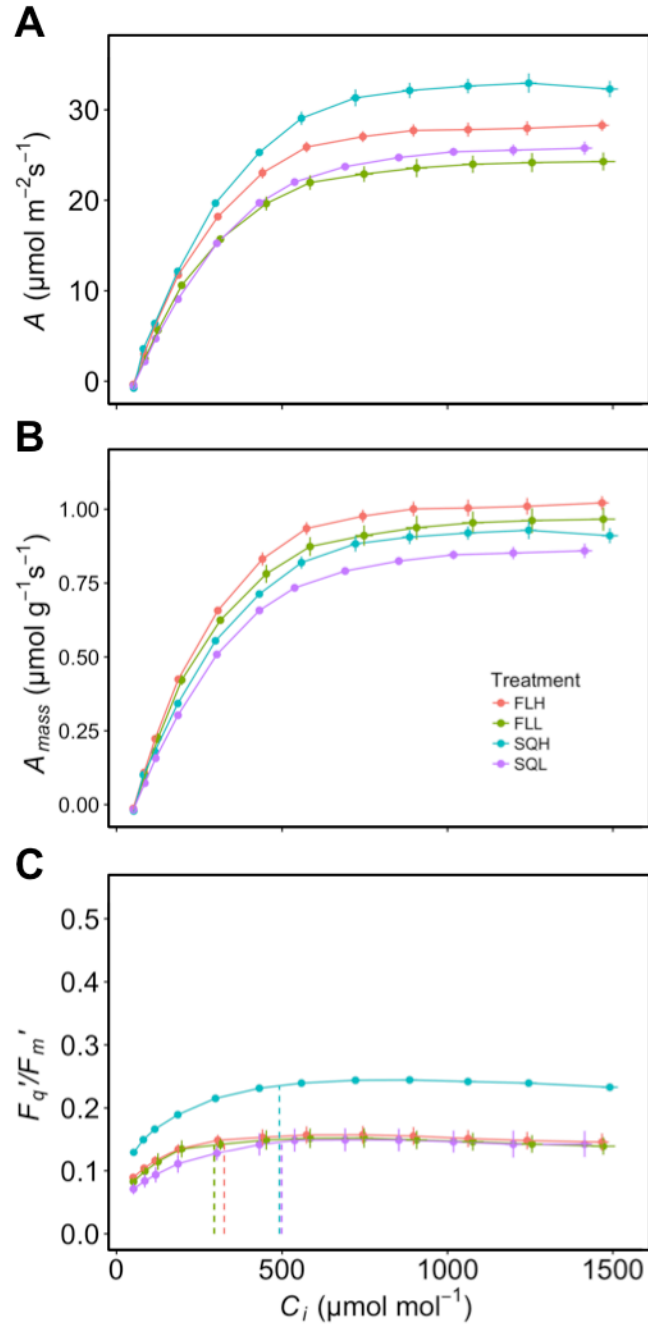


**Figure 5.6.** Photosynthesis as a function of intercellular CO<sub>2</sub> concentration ( $C_i$ ) of plants grown under the four light treatments square wave high light (SQH); fluctuating high light (FLH); square wave low light (SQL) and fluctuating low light (FLL). Net CO<sub>2</sub> assimilation on an area basis ( $A$ ; A); relative to leaf mass ( $A_{mass}$ ; B); and the operating efficiency of PSII photochemistry ( $F_q'/F_m'$ ; C). Error bars represent mean  $\pm$  SE.  $n = 6$ . Dotted line shows the  $C_i$  at the point where the switch between RuBisCO and RuBP regeneration-limited  $A$  occurs.

**Table 5.4.** Photosynthetic parameters (mean  $\pm$  SE) estimated from the response of  $A$  to  $C_i$  of plants grown under the four light regimes: square wave high light (*SQH*); fluctuating high light (*FLH*); square wave low light (*SQL*) and fluctuating low light (*FLL*). Letters represent the results of Tukey's post-hoc comparisons of group means.

Treatment	$V_{C_{max}}$	$J_{max}$	$g_m$	$R_{day}$
<b>FLH</b>	62.2 $\pm$ 1.8 <sup>bc</sup>	126.9 $\pm$ 3.3 <sup>b</sup>	0.570 $\pm$ 0.14 <sup>ab</sup>	0.6 $\pm$ 0.1 <sup>a</sup>
<b>FLL</b>	51.3 $\pm$ 1.9 <sup>a</sup>	105.2 $\pm$ 3.1 <sup>a</sup>	0.154 $\pm$ 0.02 <sup>b</sup>	0.7 $\pm$ 0.2 <sup>a</sup>
<b>SQH</b>	68.8 $\pm$ 2.0 <sup>c</sup>	148.2 $\pm$ 4.6 <sup>c</sup>	0.927 $\pm$ 0.07 <sup>a</sup>	0.9 $\pm$ 0.4 <sup>a</sup>
<b>SQL</b>	55.8 $\pm$ 1.5 <sup>ab</sup>	118.8 $\pm$ 1.7 <sup>b</sup>	0.464 $\pm$ 0.17 <sup>ab</sup>	1.4 $\pm$ 0.3 <sup>a</sup>

Although significant differences in  $V_{C_{max}}$  were found between high and low light treatments, there was no significant difference in Rubisco content or the contents of the Calvin-Benson cycle proteins fructose 1,6-bisphosphate aldolase (FBPA) or transketolase (TK) between light treatments (Fig. 5.7). Furthermore, compared to *FLL* grown plants, we observed a small significant increase in protein levels of the photosystem I (PSI) protein PsaA in *SQL* grown plants. Interestingly, we did observe a significant increase in the level of three key proteins of the cytochrome *b<sub>6</sub>f* complex, Cyt *f*, Cyt *b<sub>6</sub>* and Rieske FeS in plants grown under *SQL* compared to *FLL*, as well as for the PSI type I chlorophyll a/b-binding protein (Lhca1), matching the observed differences in  $J_{max}$  (Table. 5.4). A similar tendency for these proteins was found between high light treatments with higher protein levels in *SQH* grown plants compared to *FLH*. A significant increase in protein level was observed in *FLH* grown plants compared to *FLL* plants for Lhca1, proteins of the cytochrome *b<sub>6</sub>f* complex and ATP synthase. The level of PsbD (D2), which forms the reaction centre of PSII was higher under high light treatments but only significantly between *SQL* and *SQH* grown plants (Fig. 5.7).

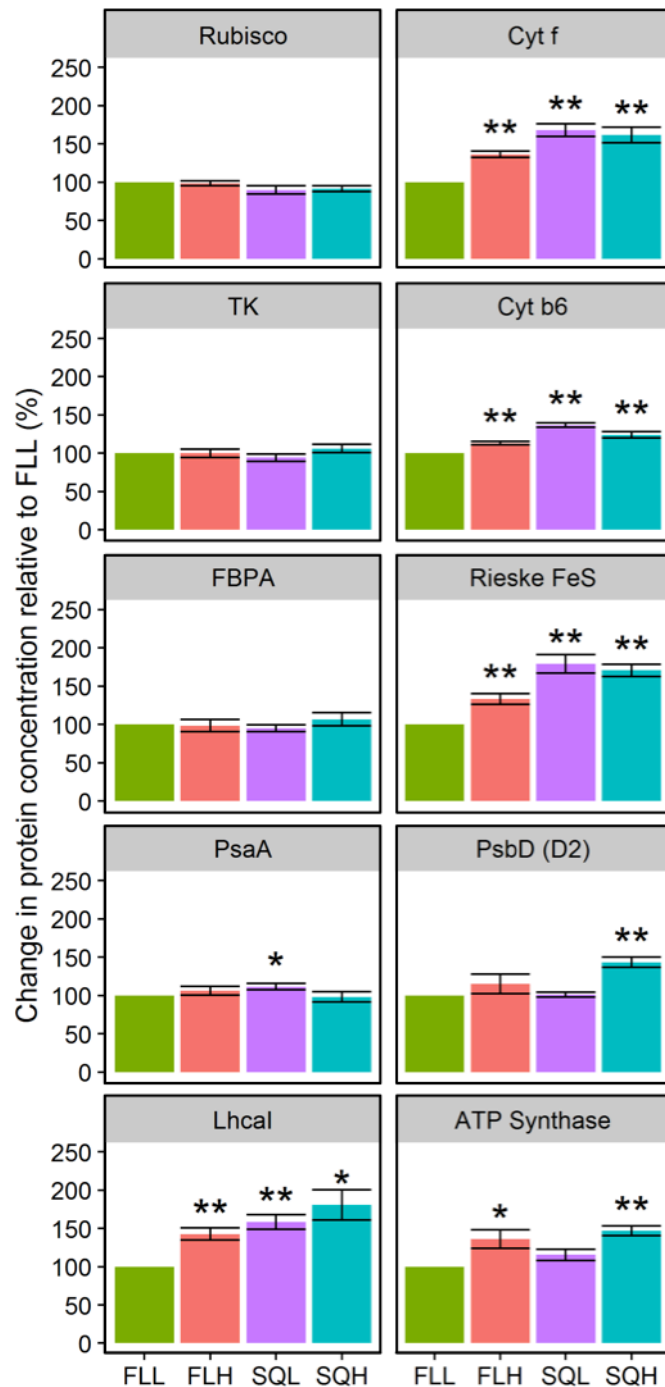


**Figure 5.7.** Percentage of change in protein concentration relative to *FLL* treatment determined from 4 replicate immunoblot analysis of leaves grown under the four light treatments. Rubisco, the Calvin-Benson cycle proteins Transketolase (TK), FBPA aldolase (FBPA) were probed along with the electron transport cytochrome *b<sub>6</sub>f* complex proteins *cyt f*, *cyt b<sub>6</sub>*, and Rieske FeS, the photosystem I Lhca1 and PsaA proteins, the Photosystem II PsbD/D2 proteins, and ATP synthase. Treatments were statistically analysed against *FLL* grown plants using a one-sample t-test (\*  $p < 0.05$ , \*\*  $p < 0.01$ ).

### 5.3.4. Diurnal leaf level responses of gas exchange and chlorophyll fluorescence

#### 5.3.4.1. Measurements under diurnal high light fluctuating conditions ( $DF_{high}$ )

To determine the impact of acclimation to different growth light regimes on operational rates of photosynthesis ( $A$ ), plants were measured under a diurnal fluctuating high light regime ( $DF_{high}$ ). Infra-red gas exchange measurements of  $A$ ,  $C_i$  and  $g_s$  were recorded every 2 minutes along with chlorophyll fluorescence parameters  $F_q'/F_m'$ ,  $F_v'/F_m'$  and  $F_q'/F_v'$  in plant from all experimental growth conditions. In general, plants grown under fluctuating conditions had the greatest net photosynthetic rates on an area ( $A$ ) basis through the majority of the diurnal, however these differences were only significant at specific light periods (indicated by letters in Fig. 5.8A). Photosynthesis measured on a mass integrated ( $A_{mass}$ ) basis was highest in plants grown under fluctuating light compared with square wave grown plants, however differences were only significant (for all light levels during the diurnal) in high light grown plants (Fig. 5.8B). This matched with a higher  $F_q'/F_m'$  compared with plants grown under square wave conditions irrespective of light intensity. Despite a generally lower photosynthetic rates, stomatal conductance to water vapour ( $g_s$ ) in plants grown under  $SQH$  regime was significantly higher than those grown under low light conditions (Fig. 5.8C), particularly at the beginning and the end of the diurnal period. Despite the differences in  $A$  and  $g_s$ , no differences in  $C_i$  were observed between the treatments for most of the  $DF_{high}$  period (Fig. 5.8D).

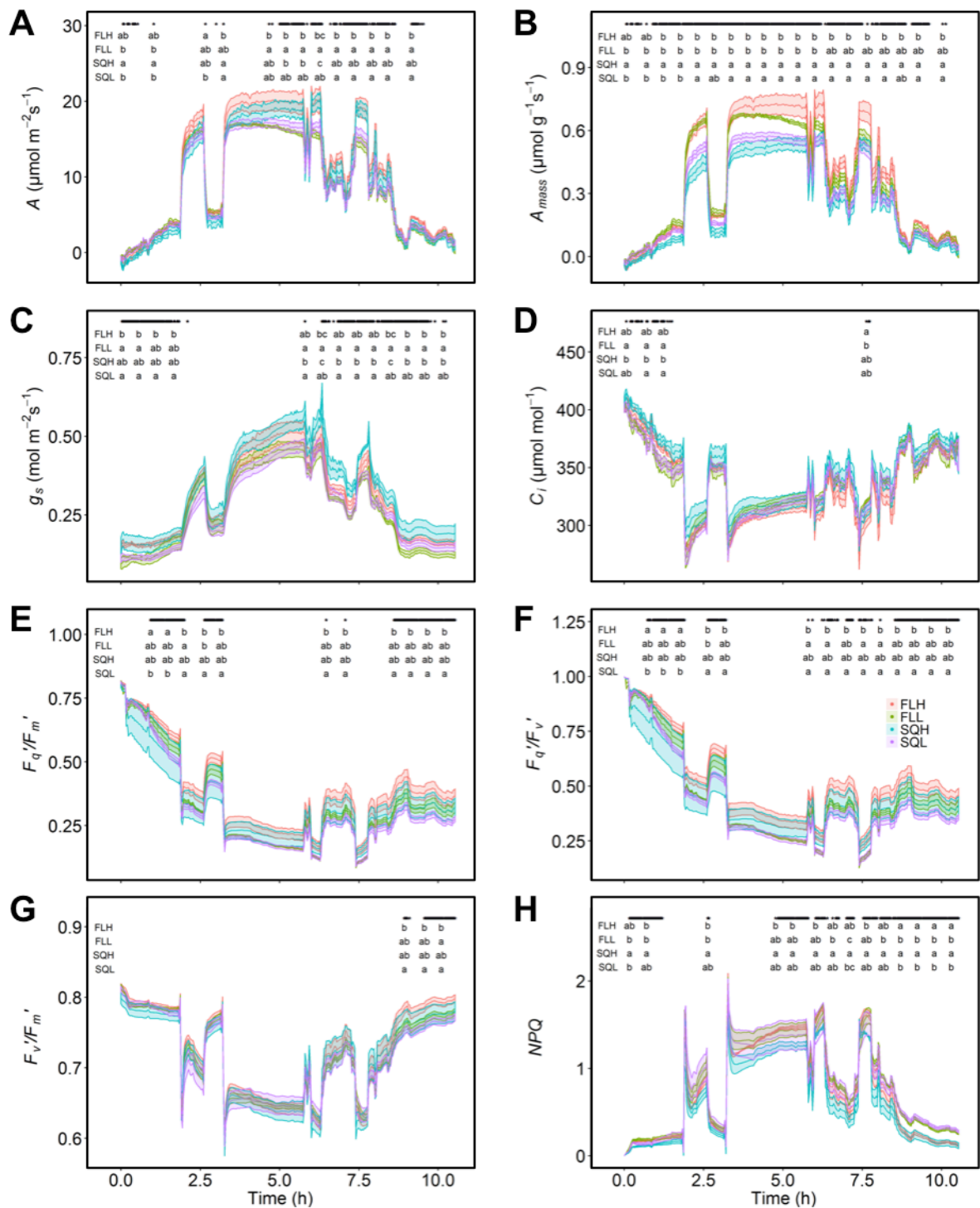


**Figure 5.8.** Diurnal measurements of gas exchange of net CO<sub>2</sub> assimilation on an area basis ( $A$ ; A); net CO<sub>2</sub> assimilation on a leaf mass basis ( $A_{mass}$ ; B); stomatal conductance ( $g_s$ , C); internal CO<sub>2</sub> concentration ( $C_i$ , D); and chlorophyll fluorescence parameters  $F_q'/F_m'$  (E);  $F_q'/F_v'$  (F);  $F_v'/F_m'$  (G) and  $NPQ$  (H) estimated under fluctuating high light ( $DF_{high}$ ) in all four light regimes square wave high light (SQH); fluctuating high light (FLH); square wave low light (SQL) and fluctuating low light (FLL). Error bars represent mean  $\pm$  SE. Stars above the curves denote a significant difference between the light regimes using a one-way ANOVA with unequal variance.  $n = 5$ . Letters represent the results of Tukey's post-hoc comparisons of group means.

During these measurements it was noted that after approximately 4h into the light of the  $DF_{high}$  period and under saturating light conditions, the plants grown under low light regimes ( $FLL$  and  $SQL$ ) started to display a decrease in  $A$  that was not correlated with a decrease in  $g_s$ , in contrast to plants grown under high light regimes which maintained a high level of  $A$  throughout the diurnal period. The decrease in  $A$  observed in plants grown under low light regimes continued through the day and during periods of saturating light intensities ( $>1000 \mu\text{mol m}^{-2} \text{s}^{-1}$ ) at approximately 6h and 8h into the light period, more pronounced decreases in  $A$  were detected compared to plants grown under high light regimes ( $P < 0.05$ ). The kinetics of  $A_{mass}$  did not change but in general  $A_{mass}$  was significantly higher in plants grown under fluctuating light regimes (similar to the  $A/Q$  analysis; see Fig. 5.2) ( $P < 0.05$ ; +50%  $A_{mass}$ ) compared to plants grown under square wave light regimes over the majority of the diurnal period (Fig. 5.8B).

At periods of low light intensity ( $<300 \mu\text{mol m}^{-2} \text{s}^{-1}$ ), PSII operating efficiency ( $F_q'/F_m'$ ) displayed significantly higher values in plants grown under  $FLH$  regime compared to the other growing conditions (Fig. 5.8E). In all treatments,  $F_q'/F_m'$  decreased through the  $DF_{high}$  period with significantly lower values at the end of the diurnal compared to the beginning even under comparable  $PPFDs$ . This difference in  $F_q'/F_m'$  was mostly driven by changes in PSII efficiency factor ( $F_q'/F_v'$ ) which mirrored  $F_q'/F_m'$  through the  $DF_{high}$  period (Fig. 5.8F). No differences in the maximum efficiency of PSII ( $F_v'/F_m'$ ) were observed until the end of the diurnal period with the highest values observed in the  $FLH$  grown plants (Fig. 5.8G). On the other hand, measurements of non-photochemical quenching ( $NPQ$ ) showed significant differences between  $FLH$  and  $SQH$  grown plants (Fig. 5.8H) during most of the  $DF_{high}$  period. At the end of the  $DF_{high}$  period, significantly lower  $NPQ$  was observed in plants grown under high light intensity compared to low light growing conditions.

#### 5.3.4.2. Measurements under diurnal low light fluctuating conditions ( $DF_{low}$ )

To further investigate the interaction of fluctuating light intensity on the dynamic response of photosynthesis, plants grown under the different treatments were measured under the same fluctuating pattern but applied at the lower light intensity ( $DF_{low}$ ). For large periods of the  $DF_{low}$ , plants grown under high light regimes ( $FLH$  and  $SQH$ ) showed significantly higher  $A$  compared to those grown under low light regimes ( $P < 0.05$ ), with the highest values of  $A$  recorded in plants grown under  $FLH$  regime (Fig. 5.9A). However, this difference in  $A$  between the measurements of plants grown under the different conditions was only apparent at  $PPFDs$  above  $300 \mu\text{mol m}^{-2} \text{s}^{-1}$ . In contrast to the observations made for  $A$ , a significant difference in  $A_{mass}$  was observed between the fluctuating and square wave light treatments with the highest values observed in  $FLH$  grown plants, approximately 50% higher than in plants grown under  $SQH$  (Fig. 5.9B).

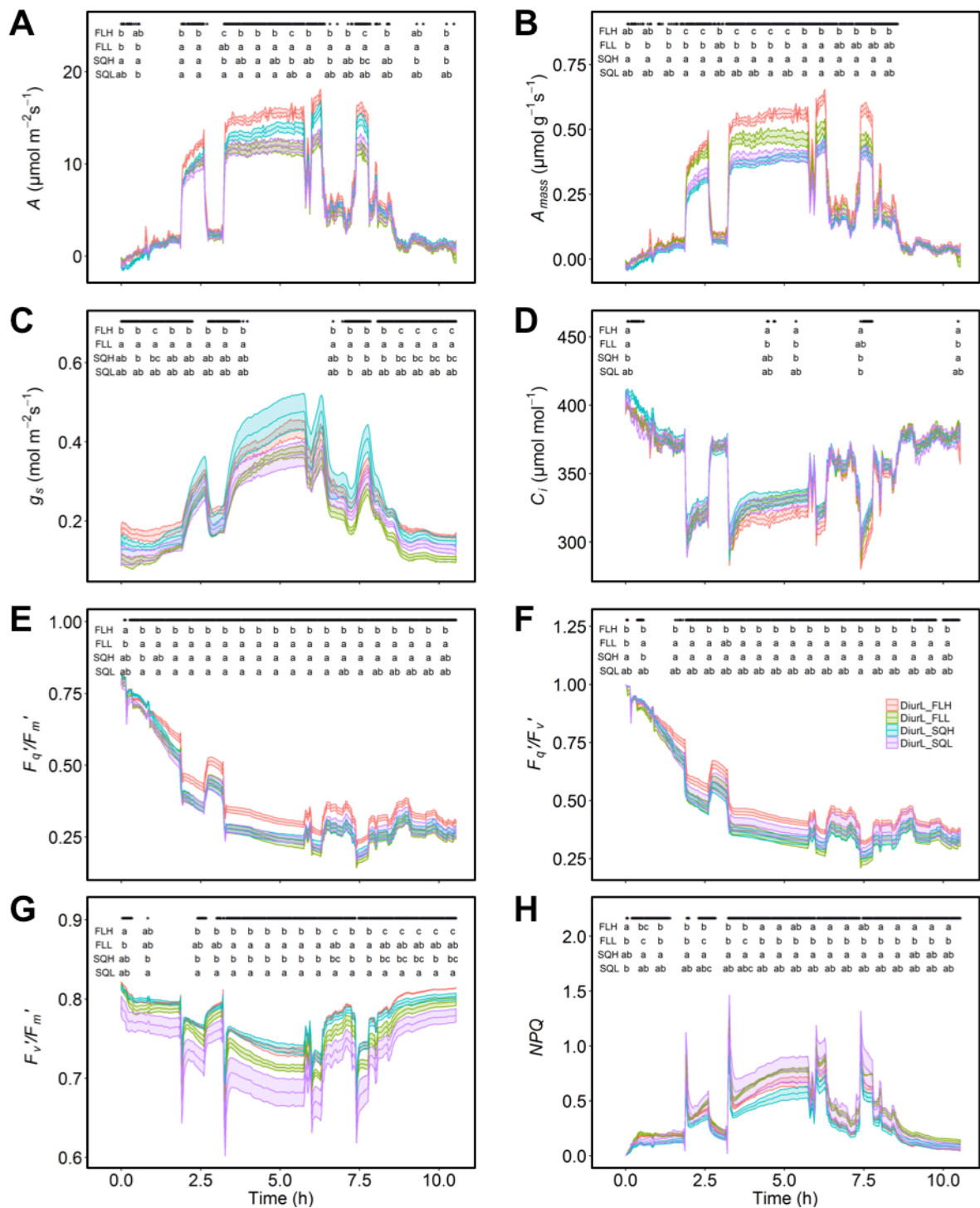


**Figure 5.9.** Diurnal measurements of gas exchange of  $A$  (A),  $A_{mass}$  (B),  $g_s$  (C),  $C_i$  (D), and chlorophyll fluorescence parameters  $F_q'/F_m'$  (E);  $F_q'/F_v'$  (F);  $F_v'/F_m'$  (G) and  $NPQ$  (H) estimated under fluctuating low light ( $DF_{low}$ ) in all four light regimes SQH, FLH, SQL, FLL. Error bars represent mean  $\pm$  SE. Stars above the curves denote a significant difference between the light regimes using a one-way ANOVA with unequal variance.  $n = 5$ . Letters represent the results of *Tukey's post-hoc* comparisons of group means.

Plants grown under high light intensity (*FLH* and *SQH*) also displayed significantly higher  $g_s$  during large periods of  $DF_{low}$  compared to plants grown under low light intensity (*FLL* and *SQL*) (Fig. 5.9C). During periods of higher light intensity ( $>500 \mu\text{mol m}^{-2} \text{s}^{-1}$ ), the  $g_s$  of *SQH* grown plants was generally higher than the other treatments. Similar to the results of plants measured under  $DF_{high}$ ,  $C_i$  was not significantly different between treatments (Fig. 5.9D).

As observed under  $DF_{high}$ , the operating efficiency of PSII photochemistry ( $F_q'/F_m'$ ) decreased significantly through the  $DF_{low}$  period.  $F_q'/F_m'$  (Fig. 5.9E) and  $F_q'/F_v'$  (Fig. 5.9F) were significantly higher in *FLH* grown plants over the entire  $DF_{low}$  period. The PSII maximum efficiency ( $F_v'/F_m'$ ) showed significantly higher values in plants grown under high light intensity regimes (*FLH* and *SQH*) compared to low light conditions, through the entire diurnal period (Fig. 5.9G). As predicted plants grown under low light intensity showed a significantly higher *NPQ* compared with high light grown plants with the lowest values observed in *SQH* grown plants (Fig. 5.9H). In comparison to  $DF_{high}$  measurements,  $DF_{low}$  measurements showed a significantly higher  $F_v'/F_m'$  in high light intensity grown plants.

### 5.3.5. Comparison of measured diurnal photosynthesis with predicted from A/Q analysis

To reveal the potential limitation of net  $\text{CO}_2$  assimilation ( $A$ ) during the diurnal period,  $A$  was predicted from the  $A/Q$  response curves assuming no  $g_s$  limitation, and a maximized activation of the biochemistry associated with photosynthesis. During the initial 4-6 hours of  $DF_{high}$  (Fig. 5.10A-D), all plants irrespective of their growing conditions reached the predicted  $A$ . However, after this period, there was a general tendency for measured  $A$  to be lower than that predicted from the model  $A$  response. The difference between expected and observed  $A$  values integrated over the diurnal period was 18.8% for *FLH* grown plants but more than 22% in all other treatments.

Surprisingly, none of the plants measured under  $DF_{low}$  reached the predicted  $A$  values at any point over the diurnal regimes (Fig. 5.10E-H). The lowest integrated differences between predicted and measured  $A$  values were observed for plants grown under high light regimes ( $< 26.4\%$ ) with the lowest values for *FLH* grown plants (19.8%). Differences of more than 30% were observed in plants grown under low light regimes. In general, measurements under  $DF_{low}$  regimes showed a larger difference between predicted and observed  $A$  values but were able to maintain levels of  $A$  throughout the diurnal period, compared to measurements under  $DF_{high}$  that showed a continuous increase in the divergence between observed and predicted  $A$ .

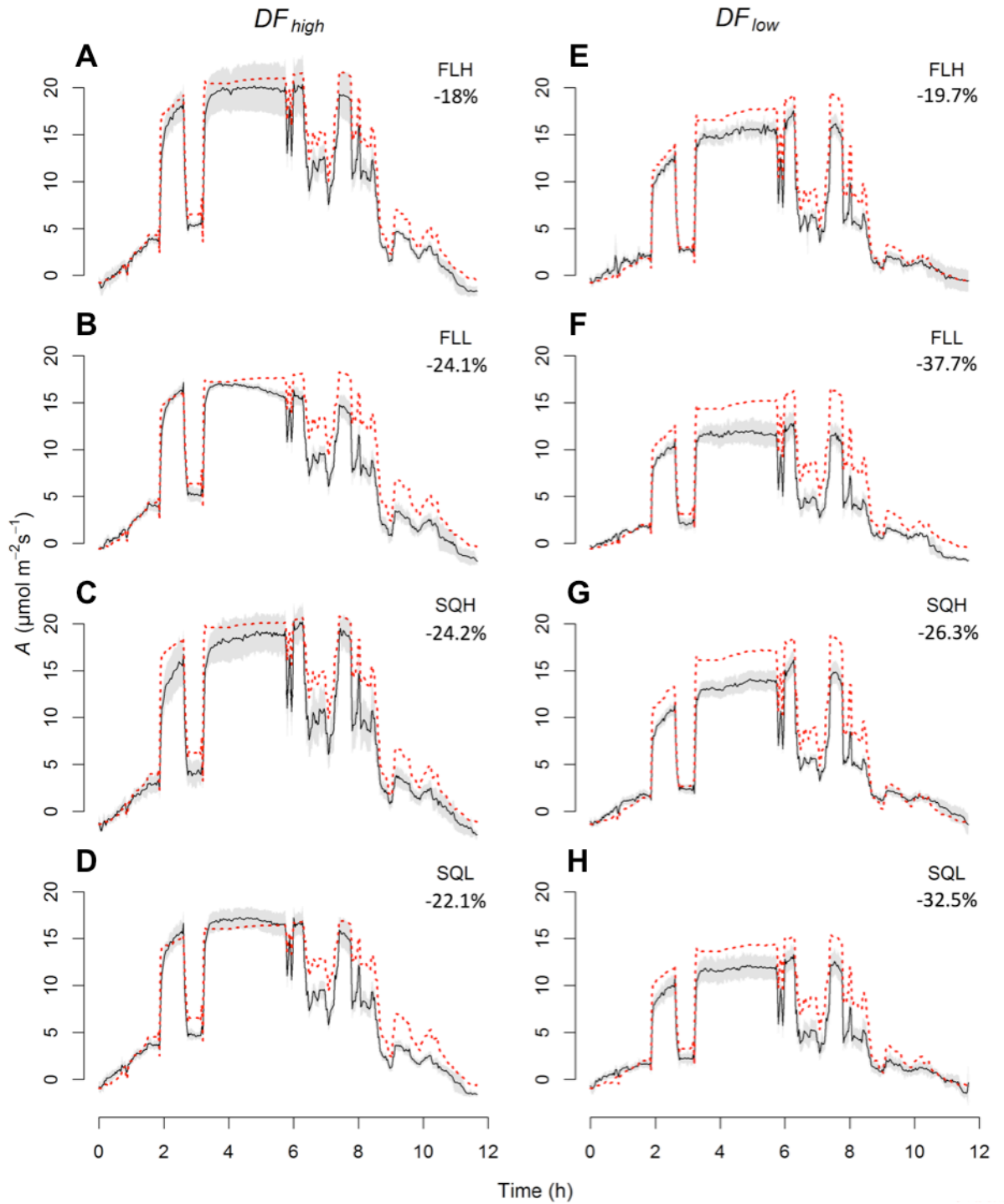


**Figure 5.10.** Diurnal measurements of observed net CO<sub>2</sub> assimilation (black line) and predicted net CO<sub>2</sub> assimilation modelled from the  $A/Q$  responses (see Eq. 6) (red dashed line) of the four light regimes square wave high light (SQH); fluctuating high light (FLH); square wave low light (SQL) and fluctuating low light (FLL) over diurnal periods of  $DF_{high}$  (A-D) and  $DF_{low}$  (E-H).  $n = 5$ . Grey shading is error bars represent confidence interval at 95%.

### 5.3.6. Influence of growth light regimes on plant development

The increase in rosette area as a function of time was modelled using a sigmoidal curve (Fig. 5.11A and Table 5.5) and revealed a higher initial growth rate in plants grown under square wave light regimes compared to those grown under fluctuating light, commencing day 10 until day 28 (Fig. 5.11A). After this period of time, plants grown under fluctuating light regimes caught up with plants grown under square wave light regimes. It is interesting to note that the plants grown under square wave light regimes flowered approximately 6 days before those grown under fluctuating light regimes, irrespective of the light intensity (Fig. 5.11A).

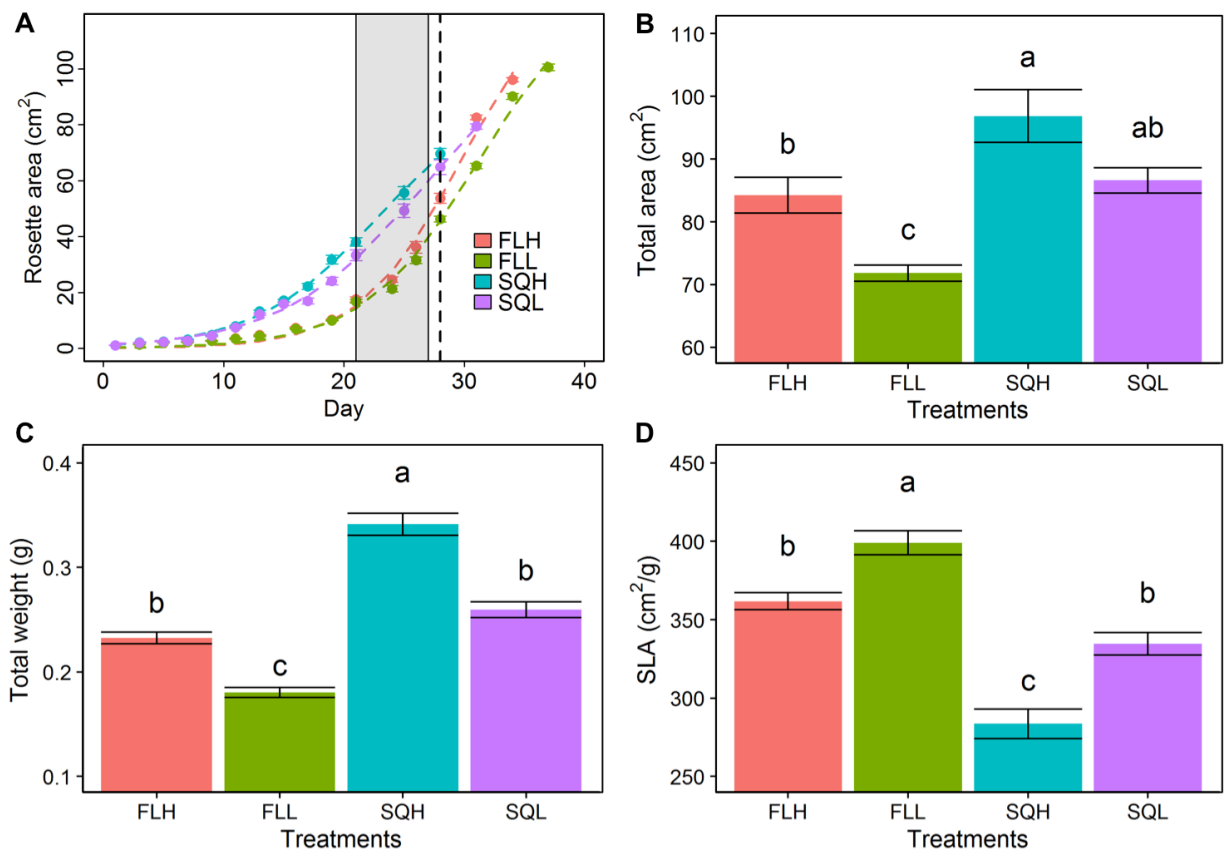


**Figure 5.11.** Growth analysis of plants grown under the four light regimes, square wave high light (SQH); fluctuating high light (FLH); square wave low light (SQL) and fluctuating low light (FLL). Shown is the kinetics of the increase in rosette area (A), with each point representing a mean of 10 plants. Grey area represents the period during which gas exchange measurements were taken. Dotted line indicates time of harvest for all treatments. The last point of each curve was measured upon appearance of first inflorescence. Also shown; total leaf area of each plant (B); total above ground dry mass (C) and specific leaf area (D). Error bars represent mean  $\pm$  SE. n = 8-10. Letters represent the results of Tukey's post-hoc comparisons of group means.

Plants grown under square wave light regimes (*SQH* and *SQL*) had significantly greater total leaf areas at 28 days of growth, compared to plants grown under fluctuating light regimes (*FLH* and *FLL*) (Fig. 5.11B). In general, high light grown plants had a higher total leaf area, and plants grown under fluctuating light regimes were significantly higher than square wave. Plants grown under square wave light regimes had greater total leaf mass than those grown in fluctuating light regimes (Fig. 5.11C). Specific leaf area (*SLA*) was significantly lower in plants grown under square wave light regimes and under high light intensity (Fig. 5.11D), resulting mainly from a change in leaf thickness (Fig. 5.5) (thinner leaves for plants grown under fluctuating light intensity regime).

**Table 5.5.** Parameters ( $\pm$ SE) describing the increase in area of the rosette as a function of time (days after germination) using a sigmoidal model:  $a/(1 + e^{-b * (Day-c)})$ .

Treatment	a	b	c
FLH	134.63 $\pm$ 14.2	0.236 $\pm$ 0.023	29.72 $\pm$ 1.04
FLL	132.42 $\pm$ 8.8	0.210 $\pm$ 0.014	31.05 $\pm$ 0.77
SQH	94.03 $\pm$ 4.9	0.196 $\pm$ 0.009	22.83 $\pm$ 0.63
SQL	119.14 $\pm$ 8.9	0.169 $\pm$ 0.008	26.94 $\pm$ 0.97

The differences in rosette area and leaf absorbance described previously, influenced the total average light absorbed by the plants grown under the different light regimes, with a significantly higher light absorbed in plants grown under square wave light regimes compared to plants grown under fluctuating light regimes (Fig. 5.12A). The predicted net CO<sub>2</sub> assimilation (*A*) and dark respiration (*R<sub>d-model</sub>*) (from the *A/Q* curves) integrated over the course of a 24h period revealed a significantly higher integrated carbon assimilation in plants grown under square wave light regimes, and higher light intensities (Fig. 5.12B). It should also be noted that the integrated daily carbon gain (Fig.5.12B) is determined from the integrated daily net photosynthetic rate minus respiratory losses in the dark, which can represent a cost between 20-40% of total daily carbon gain (Fig. 5.12B). Overall, the amount of carbon lost to respiration in the dark was higher in square wave grown plants; although this represented a smaller proportion of the total carbon gain over 24h compared to fluctuating grown plants, irrespective of light intensity. Daily light use efficiency (*Daily LUE*), the ratio of the daily-integrated carbon assimilation and absorbed light, describes how efficiently the plants convert the light absorbed into biomass (Fig. 5.12C). *Daily LUE* was significantly higher in plants grown under square wave light regimes independently of the light intensity. Long term *LUE* calculated over 28 days of growth gave a different picture, with a significantly higher *LUE*

in plants grown under low light intensity as well as in plants grown under fluctuating light intensities (Fig. 5.12D). The long term *LUE* is the sum of the *Daily LUE* and therefore includes the variation through time as well as the heterogeneity between and within leaves.

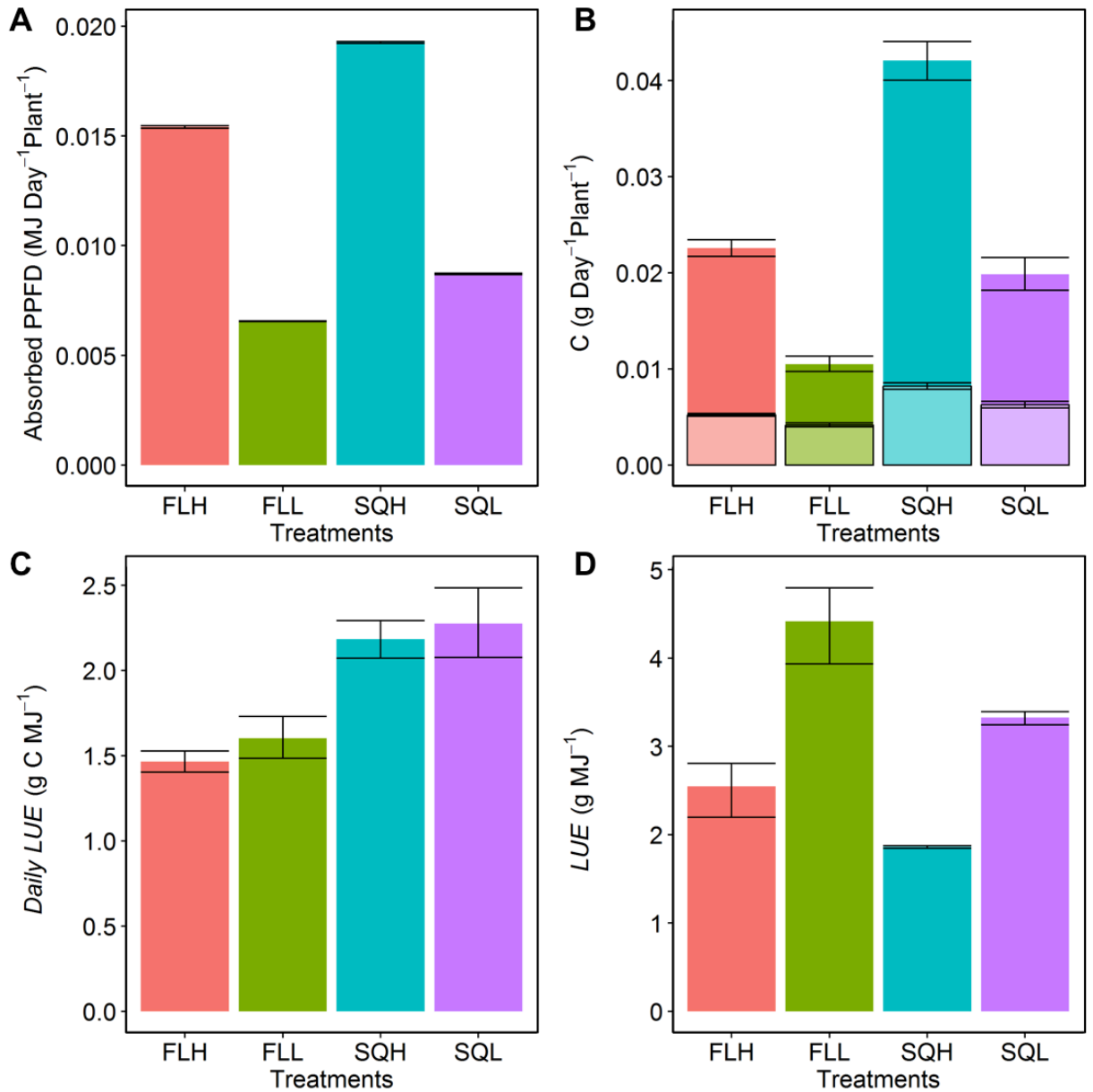


**Figure 5.12.** Total daily absorbed light (A), net carbon gain (darker colours) and carbon loss by dark respiration (lighter colours) (B), modelled *Daily* light use efficiency (*LUE*) (C) and overall long term light use efficiency (D) of plants grown under the four light treatments square wave high light (*SQH*); fluctuating high light (*FLH*); square wave low light (*SQL*) and fluctuating low light (*FLL*). Error bars represent 95% confidence interval. n = 8.

## 5.4. Discussion

Most of our knowledge regarding photo-acclimation during development in *A. thaliana* has been gained from growing plants under high or low square wave light regimes in a controlled environment (Yin and Johnson, 2000; Tikkanen et al, 2010; Alter et al, 2012; Suorsa et al, 2012; Yamori, 2016), or focused on plants grown in glasshouses with natural fluctuations in light intensity, but with uncontrolled and often un-reproducible environmental conditions (Athanasίου et al, 2010; Kulheim et al, 2002). The aim of the research presented in this chapter was to mimic natural fluctuations in light intensity in a controlled manner, to study light acclimation response of *Arabidopsis* in order to further our understanding of how plants operate in a realistic field environment. As a first step toward understanding how fluctuating light intensities influence photosynthesis and development of *A. thaliana*, the effect of the growth light regimes on photo-acclimation was examined, with the phenotype and performance of plants grown under fluctuating and square wave light regimes compared.

Analysis of  $A/Q$  response curves revealed higher  $A_{sat}$  values, in plants grown under high light, irrespective of whether this was delivered in a square or fluctuating light regime, suggesting minimal limitation of photosynthetic rates by Rubisco and demonstrating that plants acclimate to the average light intensity (Chabot et al, 1979; Watling et al, 1997), rather than a maximum or minimum light value. Photosynthetic capacity has also been reported to depend on the pattern of switching between high and low light intensity (Yin and Johnson, 2000; Retkute et al, 2015). Higher  $A_{sat}$  values observed in high light grown plants are often related to the amount of photosynthetic components including Rubisco, cytochrome f, H<sup>+</sup>-ATPase and reaction centres (Bailey et al, 2001). Although Rubisco content (on leaf area basis) did not change between treatments, the difference in leaf thickness and cell number suggests a greater Rubisco content per cell in plants grown under fluctuating light, (although this does not necessarily correlate with Rubisco activity). This higher Rubisco concentration per cell in thinner leaves enabled plants grown under fluctuating light to achieve similar  $A_{sat}$  values to square wave grown plants on a leaf area basis, and a higher  $A_{sat}$  value on a mass basis. Compared to plants grown under square wave conditions, those grown under fluctuating light were more limited by RuBP regeneration, as illustrated by the lower  $J_{max}$  values estimated from  $A/C_i$  response curves. However, plants grown under fluctuating light will not necessarily benefit from an increase in  $J_{max}$ , as under ambient conditions, [CO<sub>2</sub>] will be more limiting than regeneration of RuBP under periods of high light such as those encountered under the fluctuating regimes (Percy, 2007). Additionally, higher  $J_{max}$  values and the higher operating efficiency of PSII photochemistry ( $F_q'/F_m'$ ) at saturating light and high [CO<sub>2</sub>] in plants grown under *SQH* conditions, suggests higher potential electron transport rates than plants grown

under low or fluctuating light treatments. The higher content of Lhca1, PsbD and electron transport proteins (Cyt *f*, Cyt *b<sub>6</sub>*, RieskeFeS, ATP synthase) in square wave grown plants, would also facilitate greater light absorption and enhanced capacity to process light. All of these observations together suggest that *SQH* grown plants have the ability and resources to invest in greater capacity for photosynthesis on an area basis, even if the potential to fully utilise this investment is not realised on a day-to-day basis (as shown in the diurnal responses; Figs. 5.8 and 5.9).

In order to examine the impact of developmental acclimation to growth irradiance the ability of the plants to operate in fluctuating light environments was assessed by gas exchange and chlorophyll fluorescence under a diurnal fluctuating high ( $DF_{high}$ ) or low ( $DF_{low}$ ) light regime in plants from all growth treatments (see Fig. 5.8 and Fig. 5.9). In general plants grown under fluctuating light regimes had higher photosynthetic rates and photosynthetic efficiency than their square wave grown counterparts, which was particularly evident when measured under the  $DF_{low}$  lighting regimes. The significantly higher  $F_q'/F_m'$  along with higher  $F_q'/F_v'$  illustrates that the greater PSII operating efficiency in these plants was due to an ability to utilize the products of linear electron transport (Baker, 2008). The greater capacity to utilize light for processes down stream of PSII in the fluctuating plants was not accompanied by a significantly higher  $g_s$  or greater  $C_i$  indicating that greater CO<sub>2</sub> flux from the atmosphere to inside the leaf could not account for these differences.

When measured under fluctuating light regimes ( $DF_{high}$  and  $DF_{low}$ ), the differences in dissipation of excess absorbed energy ( $NPQ$ ) between plants grown under fluctuating and square wave regimes, illustrated differences in photo-protective strategies and developmental acclimation (particularly when measured under  $DF_{low}$ ) (Alter et al, 2012). As expected, irrespective of the regime, plants grown under low light exhibited a greater  $NPQ$  over most of the diurnal period, compared to those grown under high light conditions as these plants were acclimated to a lower level of light (Demmig-Adams and Adams, 1992). Despite slightly higher  $A$  during  $DF_{low}$  and  $DF_{high}$ , plants grown under *FLH* regimes also displayed higher  $NPQ$  than those grown under *SQH* regimes, suggesting that *FLH* plants have greater capacity to tolerate high light stress associated with these conditions. The response of  $NPQ$  through the diurnal period was in contradiction with the observations from the  $A/Q$  curves (which illustrated reduced  $NPQ$  in plants grown under fluctuating light conditions), revealing a more complex nature of the regulation of excess energy dissipation than the one observed in steady state. Furthermore, there is a temporal component of the  $NPQ$  response that is not observed during an  $A/Q$  curve, illustrated by the difference in  $NPQ$  at the start and end of the diurnal period when light intensities are similar. A possible explanation for this increase in  $NPQ$ , towards the end of the light period is the development of photoinhibition following exposure to high light levels towards the middle of the photoperiod. This is

also supported by the fact that smaller difference in  $NPQ$  between the started and end of the photoperiod are evident when measured under the low ( $DF_{low}$ ) light regime.

During these diurnal measurements all plants displayed a decrease in  $A$  after 4h into the diurnal period, despite the fact that stomatal conductance ( $g_s$ ) increased over the same period and  $C_i$  was not limiting. The decrease in  $F_q'/F_v'$  along with  $A$  suggests this was due mainly to a decrease in sink capacity for the end products of electron transport, namely ATP and NADPH (Murchie and Lawson, 2013). These results suggests that there is a process that slows down Calvin cycle activity later in the diurnal period, which for example, could be sugar accumulation in the leaf applying a feedback control on photosynthesis (Paul and Foyer, 2001; Paul and Pellny, 2003). An alternative explanation has been proposed by Yamori (2016), who stated that under fluctuating light the electron transport system accumulates excess reducing power, which cannot be dissipated as heat and may lead to photoinhibition of PSI or PSII, and a decrease in  $CO_2$  assimilation.

A comparison was made between the measured leaf level gas exchange values and the predicted values of assimilation rate (determined from  $A/Q$  analyses) measured under  $DF_{high}$  and  $DF_{low}$  conditions, to examine the effect of fluctuating light on photosynthetic processes over the diurnal period. It is interesting that none of the plants measured under  $DF_{low}$  were able to achieve the predicted  $A$  irrespective of their growth light regimes. One possible explanation for this is that predicted  $A$  is based on the  $A/Q$  response curves that are conducted under conditions maximizing processes such as Rubisco activation (Ernstsen et al, 1997; Carmo-Silva and Salvucci, 2013), and ensuring no stomatal limitation of  $A$  (Parsons et al, 1998). For example, the  $A/Q$  response curves were initiated by stabilizing a leaf in a cuvette for 30-60 min at saturating light to ensure that  $g_s$  and  $A$  were maximal, after which light was rapidly decreased and  $A$  recorded when a new steady state value was reached (1-3 min). The short delay between each measurement was not long enough for  $g_s$  and the activation of Rubisco to reduce, consequently each measurement was recorded when the conditions were most favourable for photosynthesis. During the diurnal,  $C_i$  values did not indicate a  $g_s$  limitation of  $A$ , but the slow increase in light and the rapid fluctuations could prevent full activation of Rubisco during the diurnal and may be a possible explanation for the differences observed, as the assumption is that under  $A/Q$  curve conditions photosynthetic activation is maximised (Carmo-Silva and Salvucci, 2013; Meacham et al, 2017).

To assess the impact of light regime on plant growth efficiency, daily light use efficiency (*Daily LUE*) was determined on mature leaves (between 21 and 28 days old), along with long term light use efficiency (*LUE*) over the entire growth period (28 days), to examine instantaneous values of plant performance to convert absorbed light into carbon as well as the long term *LUE*.

Under both light intensities, *LUE* was higher in plants grown under fluctuating light regimes, suggesting a specific adaptation to maximise the light utilised for carbon fixation, facilitated by their improved light saturated rate of photosynthesis (on a mass basis) and lower cost of maintenance (illustrated by lower respiration rates). Plants grown under square wave regimes (and high light intensity) absorbed more light, had a greater daily carbon gain and a greater biomass compared to fluctuating and low light grown plants, despite having lower light use efficiencies (*LUE*). The lower *LUE* efficiency in square wave grown plants could be the result of greater investment in cells, metabolic components and leaf structure relative to the carbon gained by this investment (Weraduwage et al, 2015). Compared to low light grown plants, the lower *LUE* in plants grown under high light could be the result of an increase in the energy dissipated through processes such as *NPQ* associated with the higher growth light intensity, reducing the amount of carbon fixed relative to the amount of light absorbed (Porcar-Castell et al, 2012). In general, plants grown under square wave light regimes had higher photosynthetic capacity on an area basis, but this was not sufficient to fully utilise the absorbed light for carbon fixation, resulting in a reduction in *LUE*. This suggests that under fluctuating (high) light, plants balance acclimation between the increase in photosynthetic capacity and the increase in dissipation of excess energy (Givnish, 1988).

At leaf level, daily light use efficiency (*Daily LUE*) represents the efficiency of the plant to convert the incident light into carbon over a 24h diurnal period (Medlyn, 1998). For example, a decrease in *Daily LUE* can be explained during periods of high light intensity that may occur in a fluctuating environment, by the fact that plants cannot utilize all the available light for carbon fixation. This is illustrated in Fig. 5.1, which shows the light intensity that saturates photosynthesis in *FLH* grown plants (dotted line) and the shaded areas the proportion of light that is higher than saturation for photosynthesis and light above this intensity will not drive additional carbon fixation in these plants. This theoretically decreases the average growth light intensity *FLH* plants were grown in. *Daily LUE* was lowest in plants grown under fluctuating light regimes, due to a smaller rosette area early in development. In plants grown under fluctuating light, the greater investment in photosynthetic capacity by area along with the greater proportion of daily respiration in the dark induced an extra cost to growth, which could explain the slow development of these leaves at early stages (Percy, 2007). After the initial period of slow growth, the rosette area of plants grown under fluctuating light regimes increased rapidly as the light absorbed by these plants was converted more efficiently into biomass, as illustrated by the increased long term *LUE*. These results seem contradictory, but one explanation could be that the partitioning of the carbon fixed at different growth stages was not the same between treatments, with generally more carbon invested in processes other than growth (such as photo-protection) early in development, in plants grown under fluctuating light compared to square wave light regimes.

## 5.5. Main conclusions

In this chapter, the impact of dynamic growth light regimes on photosynthetic acclimation and plant growth was examined.

- Plants grown under fluctuating light showed a previously undescribed phenotype, exhibiting thinner leaves, with a lower light absorption compared to square wave grown plants, yet similar photosynthetic rates per unit leaf area and greater values when considered on a leaf mass basis. The fluctuating growth light phenotype described here enabled these plants to perform more effectively in dynamic environments than square wave grown plants, with greater rates of photosynthesis along with lower  $g_s$ , potentially increasing water use efficiency.
- Although  $A/Q$  analyses were useful to characterise the difference in photosynthetic capacity, in this case they failed to accurately predict assimilation rates over the diurnal period, overestimating these by up to 38% particularly under low light. This may suggest an activation of photosynthesis during the light response curves that may not be present during diurnal measurements if high light levels are not achieved, putting in to question how we view these analyses (light response curves) as representations of every day plant behaviour.
- The diurnal data shown in this chapter revealed a negative feedback on photosynthesis that resulted in an approximate 20% decrease of the predicted total daily carbon assimilated, without a corresponding decrease in stomatal conductance. This potentially leads to major impacts on predictions of daily water use and carbon gain, and therefore models of ecosystem-atmosphere carbon and water budgets.
- The research in this chapter highlights that growing plants under laboratory conditions and square wave illumination does not fully represent plant development under a natural environment, with significant variation in leaf anatomy, biochemistry and performance between growth light treatments. This stresses the importance of considering fluctuations in incident light in future experiments that aim to infer plant productivity under natural conditions in the field.

# CHAPTER 6

---

## Acclimation to fluctuating light impacts the rapidity of response and diurnal rhythm of stomatal conductance in *Arabidopsis*

**Matthews, J.S., Vialet-Chabrand, S.R. and Lawson, T., (2018)** Acclimation to fluctuating light impacts the rapidity of response and diurnal rhythm of stomatal conductance. *Plant Physiology*, 176(3), pp.1939-1951.

### ***Plant Physiology***

(Doi: 10.1104/pp.17.01809)

#### **Acknowledgements and contributions to this chapter:**

I would like to thank Silvere Vialet-Chabrand for help with performing model analysis, and Silvere Vialet-Chabrand and Tracy Lawson for contributing to writing the finished published article.

## Transition Statement

In the previous chapter, it was revealed that growth under dynamic fluctuating light influenced the photosynthetic acclimation and development of the model plant *Arabidopsis thaliana*, irrespective of the average daily growth light intensity. In fact, plants subjected to fluctuating light had thinner leaves and lower photosynthetic capacities, despite displaying photosynthetic rates per unit leaf area that were comparable to those grown under square wave light. Plants grown under fluctuating light also displayed slower growth rates early in development than square wave grow plants, likely due to not being able to fully utilize the absorbed light energy at high light levels for carbon fixation. The majority of light acclimation studies have focused on light intensity and photo-acclimation, with few exploring the impact of dynamic growth light on stomatal acclimation and behavior.

In this chapter, assessment of the impact of growth light regime on stomatal acclimation was undertaken, with plants grown under the same light regimes used in Chapter 5, with the addition of a third treatment (sinusoidal regime at high and low light intensities), to assess the effect of light regime dynamics on gas exchange and water use efficiency.

## 6.1. Introduction

In order to maintain an optimal balance between  $A$  and  $g_s$ , stomata continually adjust aperture to external environmental cues (e.g. PPFD) and internal signals, which can include hormonal (e.g. ABA; Mencuccini et al, 2000; Tallman, 2004), circadian (Gorton et al, 1989; Dodd et al, 2005; Hubbard and Webb, 2015; Hassidim et al, 2017) and/or a currently unidentified 'mesophyll signal' (Lee and Bowling, 1992; Mott et al, 2008; Fujita et al, 2013). Many studies have reported a strong correlation between  $A$  and  $g_s$  (e.g. Wong et al, 1979) and it has been theorized that synchronicity exists to optimize the trade-off between photosynthesis and water loss (Buckley 2017). However, this synchronicity is often inhibited by the temporal stomatal response (Lawson and Blatt, 2014); the speed at which stomata open and close to changing environmental cues, such as those experienced in a dynamic field environment (Lawson et al, 2010; Jones, 2013). Stomatal responses to changing environmental cues are often an order of magnitude slower than those observed in  $A$ , resulting in lags in stomatal behaviour and a temporal disconnect between  $A$  and  $g_s$ , with implications for water use efficiency and crop productivity (Tinoco-Ojanguren and Pearcy, 1993; Lawson and Blatt, 2014; McAusland et al, 2016).

The close relationship between  $A$  and  $g_s$  has often been reported under steady state conditions and has been used by many models to predict diurnal time courses of  $g_s$  (Damour et al, 2010), such as the widely used Ball-Berry model (Ball et al, 1987) and its offshoots. The use of steady state models under fluctuating environmental conditions, can lead to inaccurate predictions of the diurnal response of  $g_s$ , as these models do not really take into account the slow temporal response of stomata (Violet-Chabrand et al, 2013). Moreover, the lack in temporal synchronicity between  $A$  and  $g_s$  that cannot be predicted by these models, has important implications for carbon gain and water use when integrated over the diurnal period and/or entire growing season. Furthermore, as measurements of  $g_s$  in the field are highly variable they correlate poorly with those measured under steady state conditions in the laboratory (Poorter et al, 2016), which are often taken in the middle of the day to maximize photosynthetic activation and reduce potential stomatal limitation on  $A$ .

In addition to the temporal responses outlined above, diurnal variation in sensitivity and temporal kinetics to various stimuli, have been reported for both stomatal behavior and photosynthesis. For example, there is evidence to suggest that the rapidity of stomatal responses may change at different times of day (Mencuccini et al, 2000; Tallman, 2004). Additionally, changes in  $g_s$  to fluctuations in water status have been shown to restrict  $A$  depending on the time of day, and stomata have been reported to be more responsive to ABA in the morning compared with the afternoon (Mencuccini et al, 2000). It has

been recognized that the circadian clock at least in part controls these diurnal modifications in  $A$  and  $g_s$  responses over the diurnal period (e.g. Dodd et al, 2005; Hassidim et al, 2017), through regulating the temporal patterns of transcription in photosynthesis, stomatal opening and other physiological processes (Gorton et al, 1989, 1993; Hubbard and Webb, 2015). Adjustment of the circadian clock to environmental cues such as light or temperature is fundamental for synchronizing plant biological processes with growth environment (Yin and Johnson, 2000; de Dios et al, 2016), which is important for photosynthesis and plant growth (Dodd et al, 2005; Caldeira et al, 2014). Although the mechanisms behind diurnal regulation of  $A$  and  $g_s$  and the impact on water use efficiency are not fully understood, these studies highlight the need for a greater understanding of the impact of temporal stomatal response over the entire diurnal period, as these will have important implications for cumulative  $A$  and water loss as well as model predictions.

The speed and magnitude of the temporal response of  $g_s$  is known to vary between species (McAusland et al, 2016), although little is known about how growth light conditions may affect stomatal responses at different times of the day. In the natural environment the response of  $A$  and  $g_s$  is dominated by photosynthetic photon flux density (PPFD) (Pearcy, 1990; Way and Pearcy, 2012), which varies temporally over the course of seconds, minutes, days and seasons (Assmann and Wang, 2001), due to changes in cloud cover, sun angle, and shading from neighboring leaves and plants (Pearcy, 1990; Chazdon and Pearcy, 1991; Way and Pearcy, 2012). Leaves therefore experience short and long-term fluctuations in light (sun/shade flecks) to which  $g_s$  and  $A$  respond. Although it is well established that photosynthesis and to some extent stomatal behavior (including  $g_s$  kinetics) acclimate to growth light intensity, in Chapter 5 acclimation of photosynthesis to the pattern of growth irradiance as well as intensity was demonstrated, with fluctuating light having a large impact on photosynthetic performance (Kulheim et al, 2002; Alter et al, 2012; Suorsa et al, 2012; Yamori 2016; Kaiser et al, 2016). However, it is not currently known if fluctuations in light impact stomatal acclimation and potentially influence the magnitude and temporal dynamics of  $g_s$  and  $A$  over the diurnal period, and how it may affect water use efficiency.

In order to assess the influence of dynamic light on temporal kinetics and diurnal responses of  $g_s$  and  $A$ , gas exchange in *Arabidopsis* plants (Col-0) grown under dynamic light regimes that mimic the 'field' environment, were compared with plants grown under square wave light regimes, representative of 'laboratory' growth conditions. Plants were grown under three light regimes; fluctuating with a fixed pattern of light, fluctuating with a randomized pattern of light (sinusoidal), and non-fluctuating (square wave), to assess the effect of light pattern on gas exchange. Two different average light intensities (high

and low) were used, to separate the effect of light intensity from light pattern on stomatal acclimation and response.

The aim of this chapter was to evaluate the impact of growth light conditions on the acclimation of  $g_s$  response and diurnal behavior, with the response of  $g_s$  to a step change in light as well as the diurnal response of  $g_s$  under constant light assessed. This allowed the quantification of the periodicity, magnitude and rapidity of the response of  $g_s$ , and determines if these processes significantly impact stomatal behavior over the course of the day. To separate the response of  $g_s$  from environmental/external and non-environmental/internal signals, gas exchange measurements of  $A$  and  $g_s$  were captured over a 12h period under a constant square wave light regime. As a result, any variation in the response of  $g_s$  will be due to the acclimatory response of internal signals to the pattern of growth light. When used in conjunction with current steady state models of  $g_s$ , a better understanding of the  $g_s$  response to internal signals could greatly improve their predictive power under a dynamic light environment.

## 6.2. Material and Methods

*This section outlines methods specific to this chapter and modifications made to protocols outlined previously, if more detail is required please refer to Chapter 2 – “Materials and Methods”.*

### 6.2.1. Plant material and growth conditions

Fluctuating and square wave light growth conditions were delivered via a Heliospectra LED light source (Heliospectra AB, Göteborg, Sweden). A fluctuating light regime ( $FL_{High}$ ) was recreated from a natural light regime recorded at the University of Essex during a relatively clear day in July (see Fig. 6.1) (with the assumption of a constant spectral distribution). The average light intensity over the 12h fluctuating regime was calculated as  $460 \mu\text{mol m}^{-2} \text{s}^{-1}$  and was used as the light intensity for the square wave high light treatment ( $SQ_{High}$ ). This value was then halved to  $230 \mu\text{mol m}^{-2} \text{s}^{-1}$  for the fluctuating ( $FL_{Low}$ ) and square wave ( $SQ_{Low}$ ) low light conditions.

Plants (*Arabidopsis thaliana*, Col-0) were grown in peat-based compost (Levingtons F2S, Everris, Ipswich, UK) and were maintained under well-watered conditions in a controlled environment, with growth conditions maintained at a relative humidity of 55-65%, air temperature of 21-22°C, and a CO<sub>2</sub> concentration of 400 μmol mol<sup>-1</sup>. The position of the plants under the light source was changed daily at random to remove any effect of potential heterogeneity in the light quality and quantity.

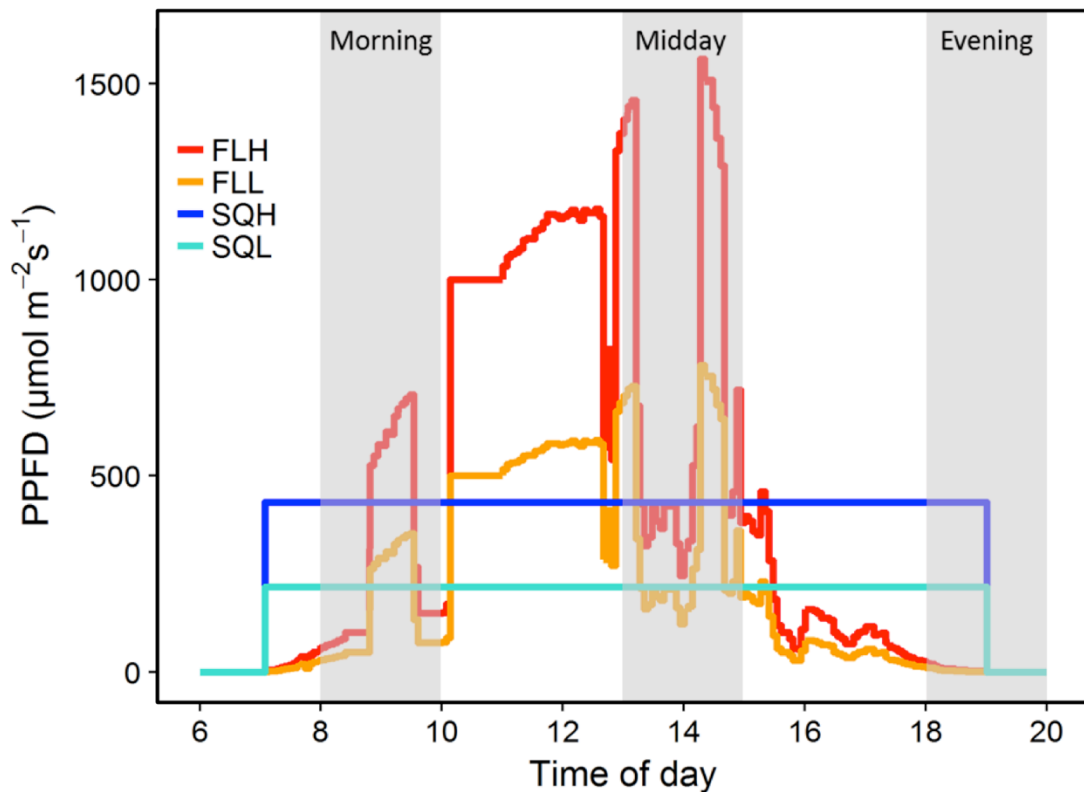


**Figure 6.1.** Diurnal light regimes used for plant growth conditions and leaf level gas exchange measurements. Each diurnal represents the same average amount of light energy over the 12-hour light regime for *SQ* (square wave) and *FL* (fluctuating) treatments depending on the light intensity, *SQH* (square wave high light) and *FLH* (fluctuating high light) (mean = 460 μmol m<sup>-2</sup> s<sup>-1</sup>), *SQL* (square wave low light) and *FLL* (fluctuating low light) (mean = 230 μmol m<sup>-2</sup> s<sup>-1</sup>). Shaded areas represent periods at which measurements were taken for time of day effects (Morning; 8-10 am, Midday; 1-3 pm, Evening; 6-8 pm).

### 6.2.1.1. Simulating daily light fluctuations for sinusoidal growth light regime.

The sinusoidal growth light regime was simulated with random variations in light, and was constrained to maintain the daily amount of light intensity (*PPFD*) constant during the growth, with each day exhibiting different random fluctuations in light (Fig. 6.2). As with the other light treatments described above, average light intensities of 460 μmol m<sup>-2</sup> s<sup>-1</sup> for the sinusoidal high light treatment (*SN<sub>High</sub>*) and

230  $\mu\text{mol m}^{-2} \text{s}^{-1}$  for the sinusoidal low light treatment ( $SN_{Low}$ ) were used. For more details, see method 2.1.

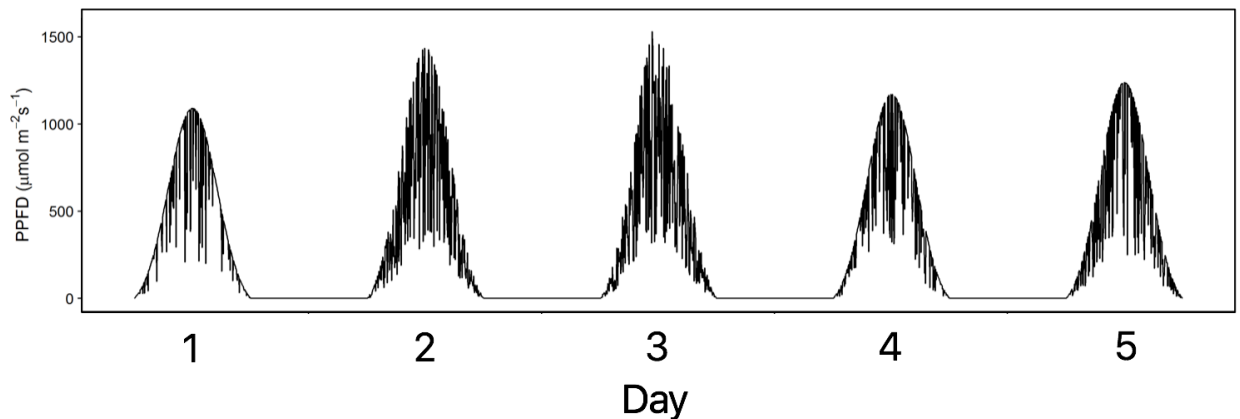


**Figure 6.2.** First five days of the simulated sinusoidal high light regime ( $SN_{High}$ ), highlighting the random fluctuations in light intensity unique to each day.

### 6.2.2. Leaf gas exchange

All gas exchange ( $A$  and  $g_s$ ) parameters were recorded and cuvette conditions maintained as laid out in Method 2.2, using a Li-Cor 6400XT portable gas exchange system (Li-Cor, Lincoln, Nebraska, USA). All measurements were taken using the youngest, fully expanded leaf.

#### 6.2.2.1. Measurements and modelling of diurnal stomatal conductance under constant light

To investigate the acclimation of diurnal stomatal response in plants grown under the six light treatments, all plants were subjected to a square wave light regime corresponding to their growth light intensity ( $SQ_{High}$ : high light treatments;  $SQ_{Low}$ : low light treatments), with net  $\text{CO}_2$  assimilation ( $A$ ) and stomatal conductance ( $g_s$ ) measured continuously over the diurnal period. See method 2.2.5.

#### 6.2.2.2. Temporal response of $A$ and $g_s$

The response of net  $\text{CO}_2$  assimilation rate ( $A$ ) and stomatal conductance ( $g_s$ ) to a step change in photosynthetic photon flux density ( $PPFD$ ), was carried out as described in method 2.2.3.

### **6.2.3. Modelling gas exchange parameters**

#### **6.2.3.1. Determining the rapidity of stomatal conductance response**

The rapidity of the stomatal response following a step change in light intensity was assessed using method 2.3.5.

#### **6.2.3.2. Determining the rapidity of net CO<sub>2</sub> assimilation response**

The rapidity of the photosynthesis response following a step change in light intensity was assessed using method 2.3.6.

### **6.2.4. Including diurnal stomatal behaviour in the Ball-Berry model for predicting $g_s$**

An addition was made to the original Ball-Berry model (Ball et al, 1987) to take into consideration the time of the day effect on  $g_s$ : two versions (with and without the Gaussian response of  $g_s$ ) were adjusted on an independent dataset described previously in Chapter 5. The difference between observed and modelled data for both models was assessed. See method 2.3.7.

### **6.2.5. Stomatal anatomical measurements**

Stomatal density, pore area, index, ratio, theoretical maximum of stomatal conductance ( $g_{smax}$ ), and Nocturnal conductance (referred to here as  $g_{s\text{ night}}$ ) were assessed by taking stomatal impressions of the surface of the leaf, for more details see method 2.4.1.

## 6.3. Results

### 6.3.1. Diurnal responses of $g_s$ , $A$ , and $W_i$ to a square wave pattern of light

To investigate the acclimation of diurnal stomatal response in plants grown under the six light treatments (FLH, Fluctuating high light; SNH, Sinusoidal high light; SQH, Square high light; FLL, Fluctuating low light; SNL, Sinusoidal low light; SQL, Square low light), all treatments were subjected to the square wave light regime corresponding to their growth light intensity ( $SQ_{High}$ : high light treatments;  $SQ_{Low}$ : low light treatments), with net CO<sub>2</sub> assimilation ( $A$ ; Fig. 6.3A), stomatal conductance ( $g_s$ ; Fig. 6.3B), and intrinsic water use efficiency ( $W_i$ ; Fig. 6.3C) measured continuously over the diurnal period.

When integrated over the entire diurnal period,  $A$  was higher in SQH grown plants compared to FLH and significantly higher ( $P < 0.05$ ) in SQH compared to SNH grown plants (Fig. 6.3A), although there was no difference between plants under low light treatments. After approx. 5h into the light regime,  $A$  started to decrease in all high light grown plants and this decrease continued to the end of the light period (Fig. 6.3A). In all low light treatments a continuous slow decrease in  $A$  was observed throughout the entire diurnal light period. In all growth light treatments  $g_s$  responses were not coordinated with  $A$ , and displayed a Gaussian pattern of response (Fig. 6.3B), whilst  $A$  displayed a more square wave response (Fig. 6.3A). FLH, SQH and SNH grown plants displayed similar patterns of  $g_s$  but differed in the maximum  $g_s$  achieved, and the time at which peak  $g_s$  occurred over the diurnal period. Initial levels of  $g_s$  ca. 1h after the light was turned on were comparable between all treatments depending on light intensity, whilst maximum values of  $g_s$  in all treatments were reached approx. 4.5-6h into the diurnal period (Fig. 6.3B). In the evening (6-8pm)  $g_s$  decreased to a value approximately 0.06 mol m<sup>-2</sup> s<sup>-1</sup> lower than the initial value observed in the morning in SQH and FLH treatments (ca. 0.3 to 0.24 mol m<sup>-2</sup> s<sup>-1</sup>, morning and evening respectively), although this was not the case in SNH (0.27 to 0.26 mol m<sup>-2</sup> s<sup>-1</sup>) grown plants. The maximum value of  $g_s$  reached during the diurnal period was higher in FLH (0.38 mol m<sup>-2</sup> s<sup>-1</sup>) and SNH (0.375 mol m<sup>-2</sup> s<sup>-1</sup>) compared to SQH (0.32 mol m<sup>-2</sup> s<sup>-1</sup>) grown plants (Fig. 6.3B). FLL and SNL showed higher levels of  $g_s$  than SQL grown plants throughout the day, with the maximum  $g_s$  reached significantly higher ( $P < 0.05$ ) in FLL (0.27 mol m<sup>-2</sup> s<sup>-1</sup>) and SNL (0.275 mol m<sup>-2</sup> s<sup>-1</sup>) compared to SQL (0.19 mol m<sup>-2</sup> s<sup>-1</sup>) grown plants (Fig. 6.3B). Intrinsic water use efficiency ( $W_i$ ) was greater in SQ grown plants compared to FL and SN treatments across the entire diurnal light period, in both high and low light grown plants measured under their respective light intensities (Fig. 6.3C). In high light treatments  $W_i$  remained relatively constant between morning and evening, assisted by the fact that the decrease in  $A$  toward the end of the day was accompanied by a decrease in  $g_s$ . In low light treatments  $W_i$  decreased through the

day driven by the continuous slow decrease in  $A$ . All six treatments experienced a drop in  $W_i$  at midday due to the increase of  $g_s$  at this time with little or no change in  $A$  (Fig. 6.3C).

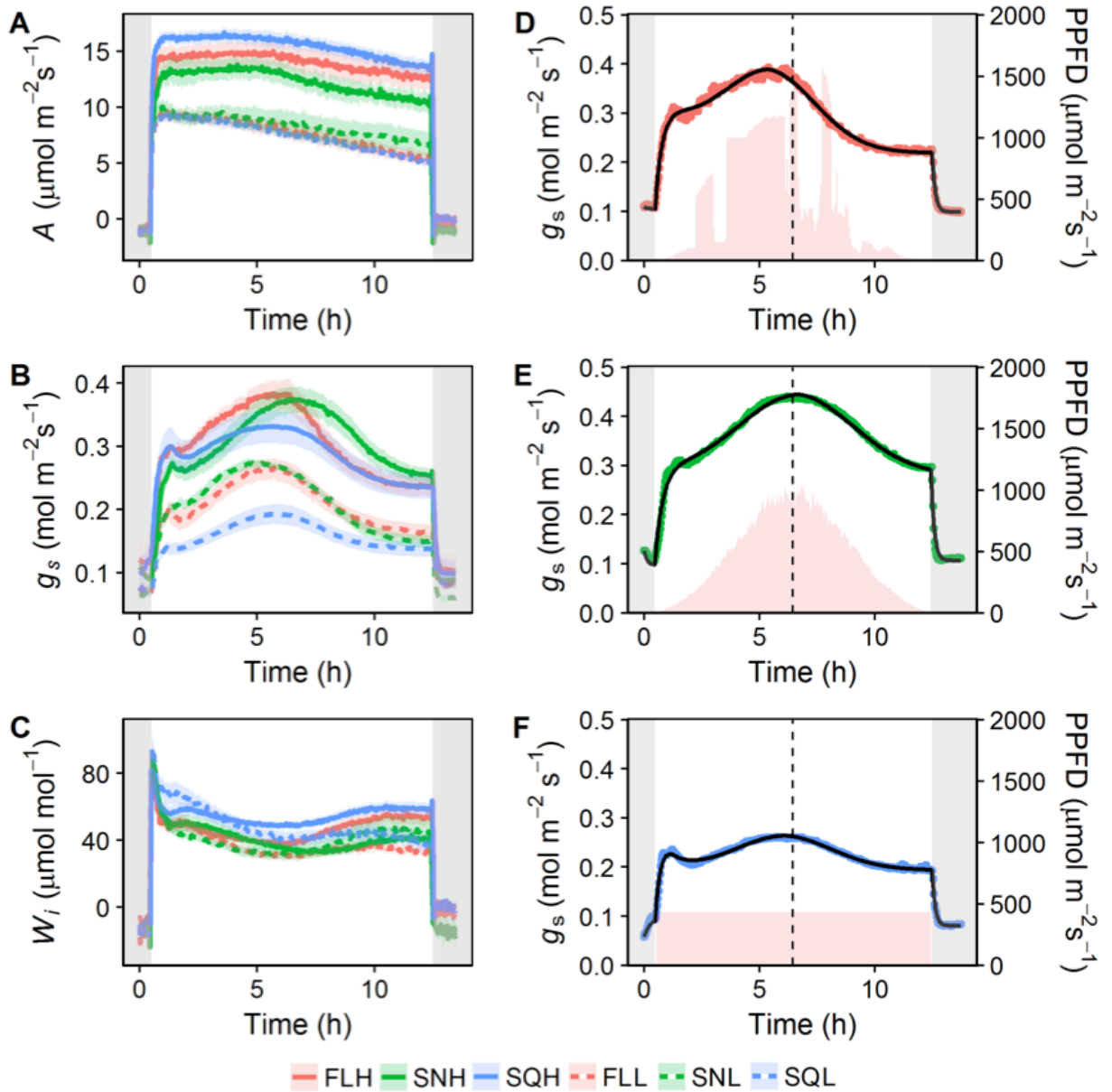


**Figure 6.3.** Diurnal measurements of gas exchange; net CO<sub>2</sub> assimilation ( $A$ ; A); stomatal conductance ( $g_s$ , B); Intrinsic water use efficiency ( $W_i$ ; C), measured under square wave regimes of light. *FLH*, *SNH* and *SQH* treatments were measured under square wave high light regime ( $SQ_{High}$ ); *FLL*, *SNL* and *SQL* treatments were measured under square wave low light regime ( $SQ_{Low}$ ). Error bars represent mean  $\pm$  SE,  $n = 5-7$ . Grey shaded areas indicate when light source is off. Represented are examples of *FLH* (D), *SNH* (E) and *SQH* (F) to highlight fit of the temporal response exponential model (black line). Pink shaded areas illustrate growth light regimes for *FLH* (D), *SNH* (E) and *SQH* (F).

The temporal response of  $g_s$  to external and internal cues was modeled using an exponential equation (See Method 2.2.5), Figures 6.3D-F display examples of the model fit on individuals of each high light treatment (FLH, SNH, and SQH respectively).  $R^2$  and  $rmse$  of the relationship between observed and predicted data were as follows for all treatments ( $R^2$ ,  $rmse$  respectively): FLH (0.99, 0.008), SNH (0.99, 0.008), SQH (0.99, 0.005), FLL (0.99, 0.006), SNL (0.99, 0.006), SQL (0.99, 0.002).

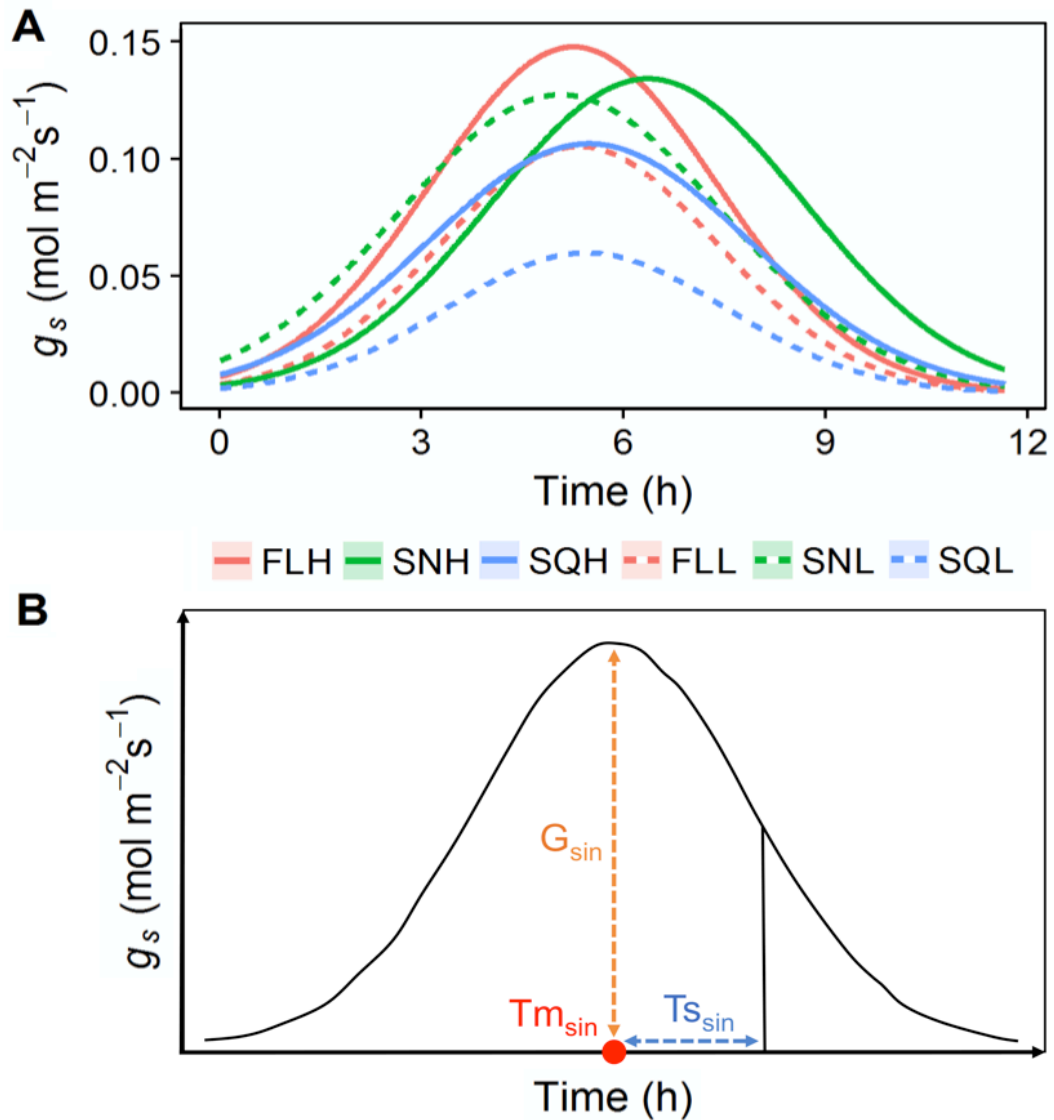


**Figure 6.4.** Gaussian signal of stomatal conductance ( $g_s$ ) during diurnal measurements of square wave light (A). Shown is a diagrammatic example highlighting the parameters extracted from the data (B); relative percentage of Gaussian driven  $g_s$  ( $R_{sin}$ ); the time at which peak  $g_s$  occurs ( $Tm_{sin}$ ); the width of the peak ( $Ts_{sin}$ ); and magnitude ( $G_{sin}$ ), during the diurnal signal of  $g_s$ . FLH, SNH and SQH treatments were measured under square wave high light regime ( $SQ_{High}$ ); FLL, SNL and SQL treatments were measured under square wave low light regime ( $SQ_{Low}$ ).

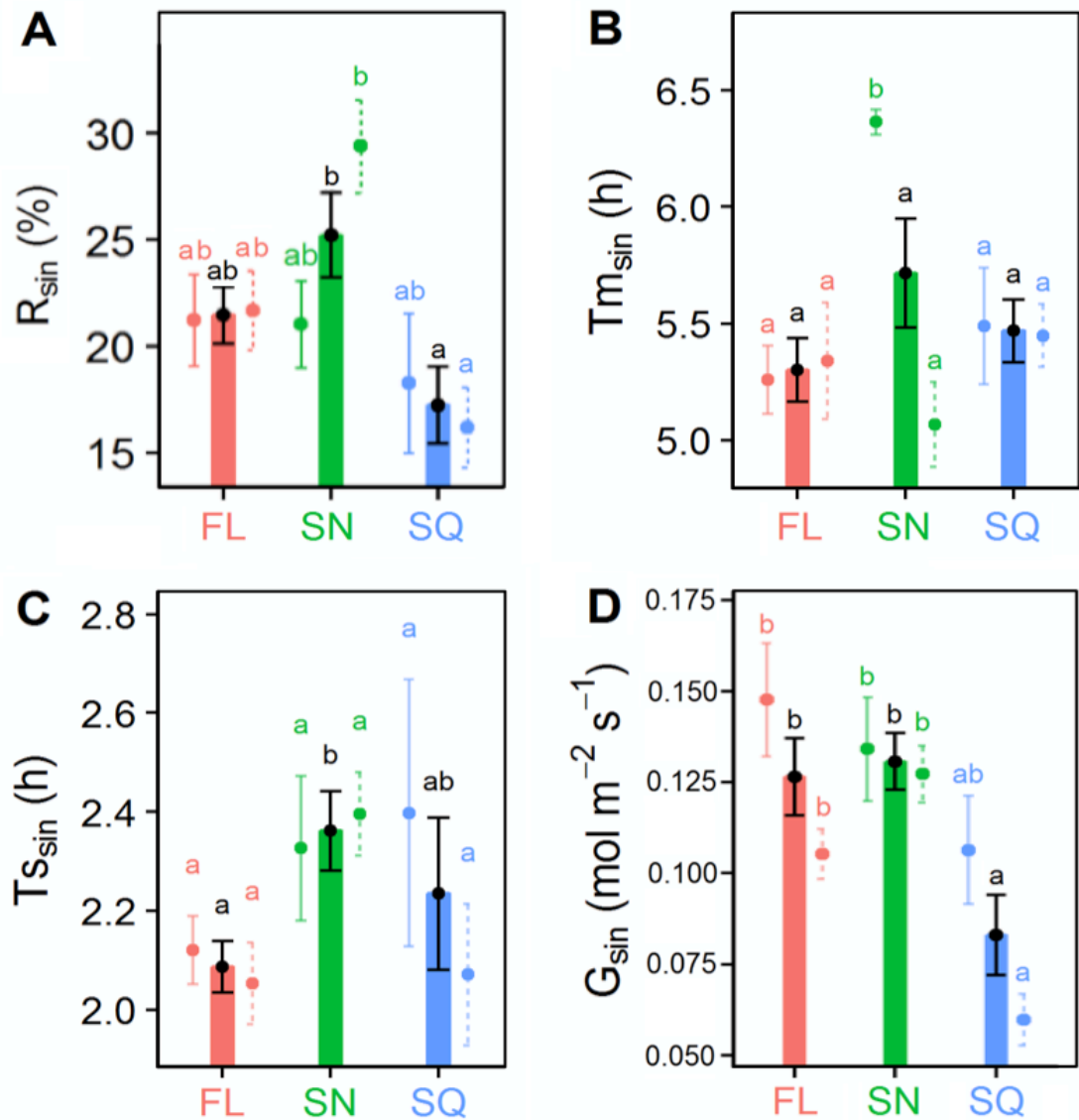


**Figure 6.5.** Parameters extracted from the gaussian signal of stomatal conductance ( $g_s$ ) during diurnal measurements of square wave light. Shown is the relative percentage of Gaussian driven  $g_s$  ( $R_{sin}$ , A); the time at which peak  $g_s$  occurs ( $Tm_{sin}$ , B); the width of the peak ( $Ts_{sin}$ , C); and magnitude ( $G_{sin}$ , D), during the diurnal signal of  $g_s$ . *FLH*, *SNH* and *SQH* treatments were measured under square wave high light regime ( $SQ_{High}$ ); *FLL*, *SNL* and *SQL* treatments were measured under square wave low light regime ( $SQ_{Low}$ ). Colored bars are combined data from high and low light treatments. Error bars represent mean  $\pm$  SE,  $n = 5-7$ . Letters represent the results of Tukey's posthoc comparisons of group means.

To further characterize the importance of the Gaussian response of  $g_s$  relative to the diurnal variation, a descriptive model was used to dissect the data into parameters that relate to variation of the leaf internal signals. Using this model, the Gaussian element of the diurnal response of  $g_s$  was separated from the response to change in light intensity (Fig. 6.4A), and separated into descriptive parameters (Fig. 6.4B). The percentage of Gaussian driven  $g_s$  ( $R_{sin}$ , Fig. 6.5A), the time at which peak  $g_s$  occurs ( $Tm_{sin}$ , Fig. 6.5B), the width of the peak ( $Ts_{sin}$ , Fig. 6.5C), and magnitude ( $G_{sin}$ , Fig. 6.5D) were determined from the

descriptive model. Significant differences in the proportion of the Gaussian driven  $g_s$  ( $R_{sin}$ ; Fig. 6.5A) were observed between plants grown under different light regimes ( $P < 0.05$ ), with the lowest values ca. 16% observed in SQL grown plants, and the highest ca. 30% in SNL. When the results were grouped according to light regime (not divided into intensity), a significant difference in  $R_{sin}$  was observed between SQ and SN grown plants ( $P < 0.05$ ), with SQ (ca. 17%) lower than both FL (ca. 21%) and SN (25%) treatments (Fig. 6.5A). There was no significant difference in the time at which peak  $g_s$  occurred ( $T_{m_{sin}}$ ) between treatments irrespective of light intensity and treatment (Fig. 6.5B), except for SNH that took ca. 1h longer to reach a maximum value of  $g_s$  than all other treatments. Although there was a noticeable trend of FL treatments having lower values of  $T_{s_{sin}}$  than SN (irrespective of light intensity; Fig. 6.5C), no significant differences were observed, however  $T_{s_{sin}}$  was significantly lower in FL (ca. 2.1h) than SN (ca. 2.35h) when grouped by light regime ( $P < 0.05$ ; Fig. 6.5C). Large variation in the magnitude of the Gaussian element ( $G_{sin}$ ; Fig. 6.5D) was observed between and within treatments, with values ranging from ca.  $0.06 \text{ mol m}^{-2} \text{ s}^{-1}$  in SQL to ca.  $0.15 \text{ mol m}^{-2} \text{ s}^{-1}$  in FLH. SQ grown plants exhibited lower values of  $G_{sin}$  than FL and SN under both light intensities, with SQL significantly lower ( $P < 0.05$ ) than all other treatments. When light intensities were grouped together, SQ (ca. 0.08) grown plants were significantly lower ( $P < 0.05$ ) than FL (ca. 0.125) and SN (ca. 0.13) treatments (Fig. 6.5D).

### 6.3.2. Response of $g_s$ and $A$ to a step change in PPFD as a function of time of day

To assess the impact of growth light regimes on stomatal responses, leaves were subjected to a step increase in PPFD ( $100\text{-}1000 \text{ } \mu\text{mol m}^{-2} \text{ s}^{-1}$ ) followed by a step decrease ( $1000\text{-}100 \text{ } \mu\text{mol m}^{-2} \text{ s}^{-1}$ ), and the effect on  $A$  and  $g_s$  measured using gas exchange (Figs. 6.6 and 6.7). In the morning period (8-10am) both high and low intensity fluctuating light treatments (FLH and FLL) and sinusoidal light treatments (SNH and SNL) reached a new plateau of  $g_s$  within 90 min after the light increase (Figs. 6.6A and 6.7A), whilst both the square wave treatments; SQH (Fig. 6.6A) and SQL (Fig. 6.7A), failed to reach a new plateau of  $g_s$  within this timeframe. In the midday (1-3pm) and evening (6-8pm) measurements,  $g_s$  reached a plateau in all light treatments (High; Fig. 6.6A and Low; Fig. 6.7A), within 90 minutes. Following the increase in PPFD to  $1000 \text{ } \mu\text{mol m}^{-2} \text{ s}^{-1}$  a near instantaneous increase in  $A$  was observed in contrast with the slow initial increase in  $g_s$  in all treatments, and at all times of day (Fig. 6.6B and Fig. 6.7B). In all treatments and three measurement times,  $g_s$  continued to increase during the measurement period despite the fact that  $A$  had reached near steady state levels.

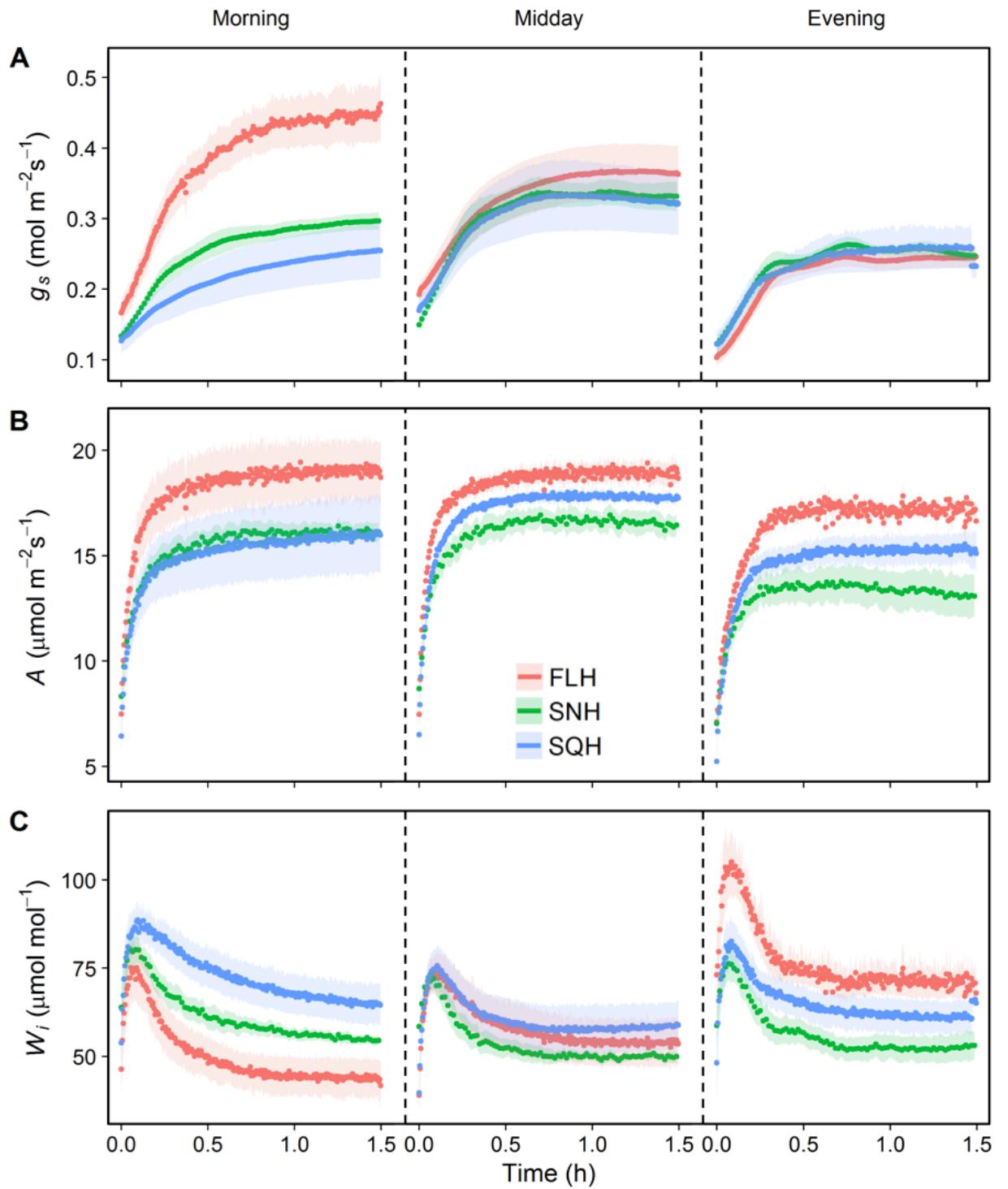


**Figure 6.6.** Temporal response of stomatal conductance ( $g_s$ , A), net CO<sub>2</sub> assimilation (A, B), and intrinsic water use efficiency ( $W_i$ , C), to a increased step change in light intensity (from 100 to 1000  $\mu\text{mol m}^{-2} \text{s}^{-1}$ ), at different times of the day. Gas exchange parameters ( $g_s$ , A and  $W_i$ ) were recorded at 20s intervals, leaf temperature maintained at 25°C, and leaf VPD at  $1 \pm 0.2$  KPa. Plants grown under the three high light treatments; fluctuating (FLH); sinusoidal (SNH); square wave (SQH). Error ribbons represent mean  $\pm$  SE. n = 5-6.

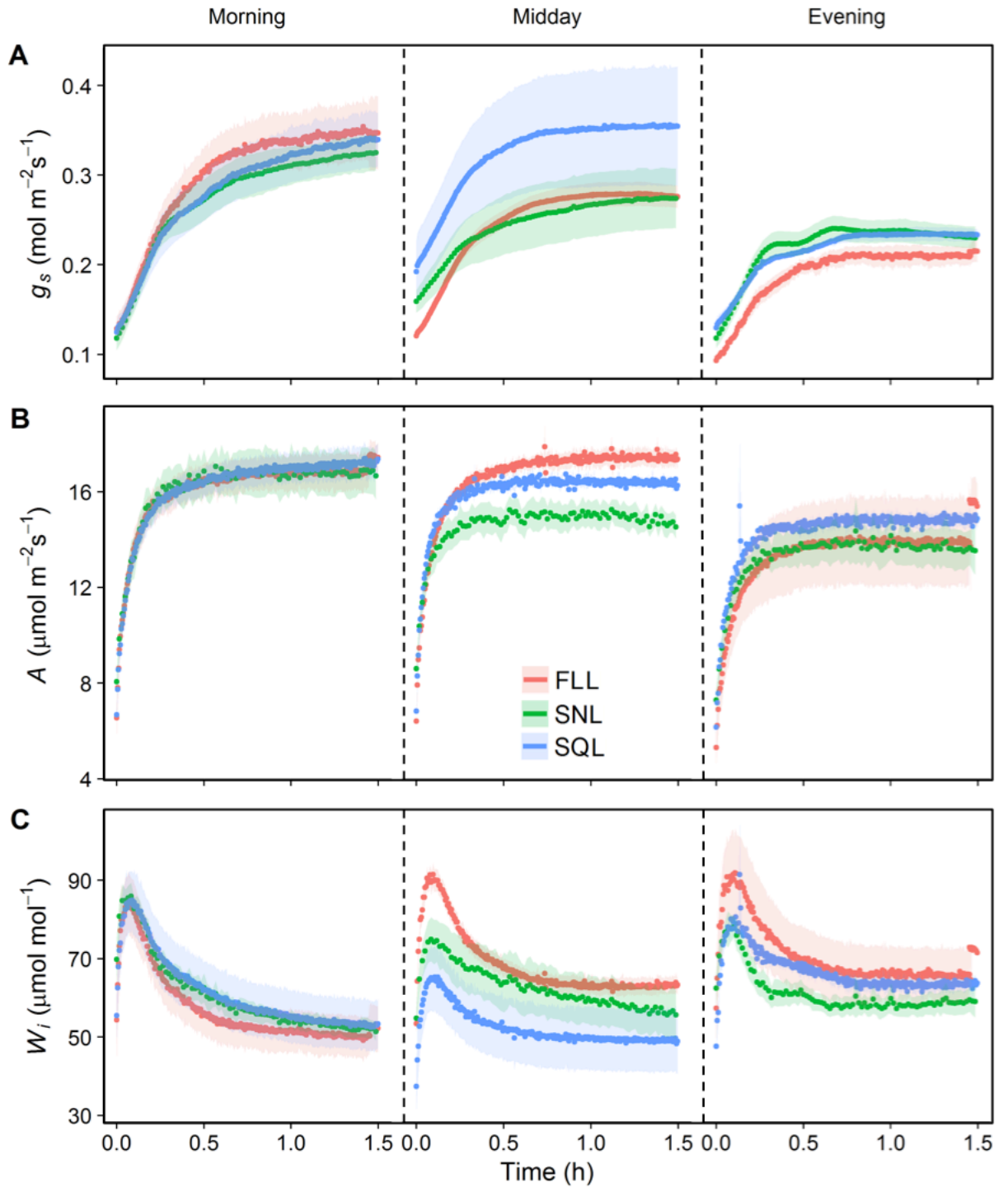


**Figure 6.7.** Temporal response of stomatal conductance ( $g_s$ , A), net CO<sub>2</sub> assimilation ( $A$ , B), and intrinsic water use efficiency ( $W_i$ , C), to a increased step change in light intensity (from 100 to 1000  $\mu\text{mol m}^{-2} \text{s}^{-1}$ ), at different times of the day.  $g_s$ ,  $A$  and  $W_i$  were recorded at 20s intervals, leaf temperature maintained at 25°C, and leaf VPD at  $1 \pm 0.2$  KPa. Plants grown under the three low light treatments; fluctuating (FLL); sinusoidal (SNL); square wave (SQL). Error ribbons represent mean  $\pm$  SE.  $n = 5$ .

Although all treatments displayed a predominantly uncoordinated  $A$  and  $g_s$  temporal response, final values of  $A$  and  $g_s$  were strongly correlated, especially in the morning where FLH exhibited the highest levels of operational maximum  $g_s$  and  $A$ , whilst SQH displayed the lowest values in each category (Fig. 6.6A and 6.6B). Intrinsic water use efficiency ( $W_i$ ), measured as  $A/g_s$ , increased over the day in FL grown plants (Fig. 6.6C), predominantly driven by the decrease in  $g_s$  values over this period (Fig. 6.6A).  $W_i$  measured in SQ and SN grown plants changed little between morning and evening, although SQ grown plants always exhibited higher values than SN plants.  $W_i$  values were higher in the morning for SQ and SN grown plants compared to FL treatments irrespective of light intensity (Fig. 6.6C and Fig. 6.7C), driven largely by the lower  $g_s$  values (Fig. 6.6A). In the evening the inverse was evident with FL treatments displaying higher levels of  $W_i$ , driven by the higher  $A$  values in FLH grown plants (Fig. 6.6B) and the lower final  $g_s$  values in FLL grown plants (Fig. 6.7A). In all treatments, final values of  $g_s$  decreased through the day (morning to evening) when subjected to a step decrease in PPFD from 1000 to 100  $\mu\text{mol m}^{-2} \text{s}^{-1}$  (Fig. 6.8). In the morning period the highest final values of  $g_s$  at 100 PPFD were shown by FLH (ca.  $0.26 \text{ mol m}^{-2} \text{s}^{-1}$ ) grown plants, whilst SNH ( $0.14 \text{ mol m}^{-2} \text{s}^{-1}$ ) displayed the lowest values (Fig. 6.8A), which correlated strongly with the final values of  $g_s$  at 1000 PPFD (Fig. 6.6A). In the evening period final values of  $g_s$  were comparable between all treatments (Fig. 6.8).

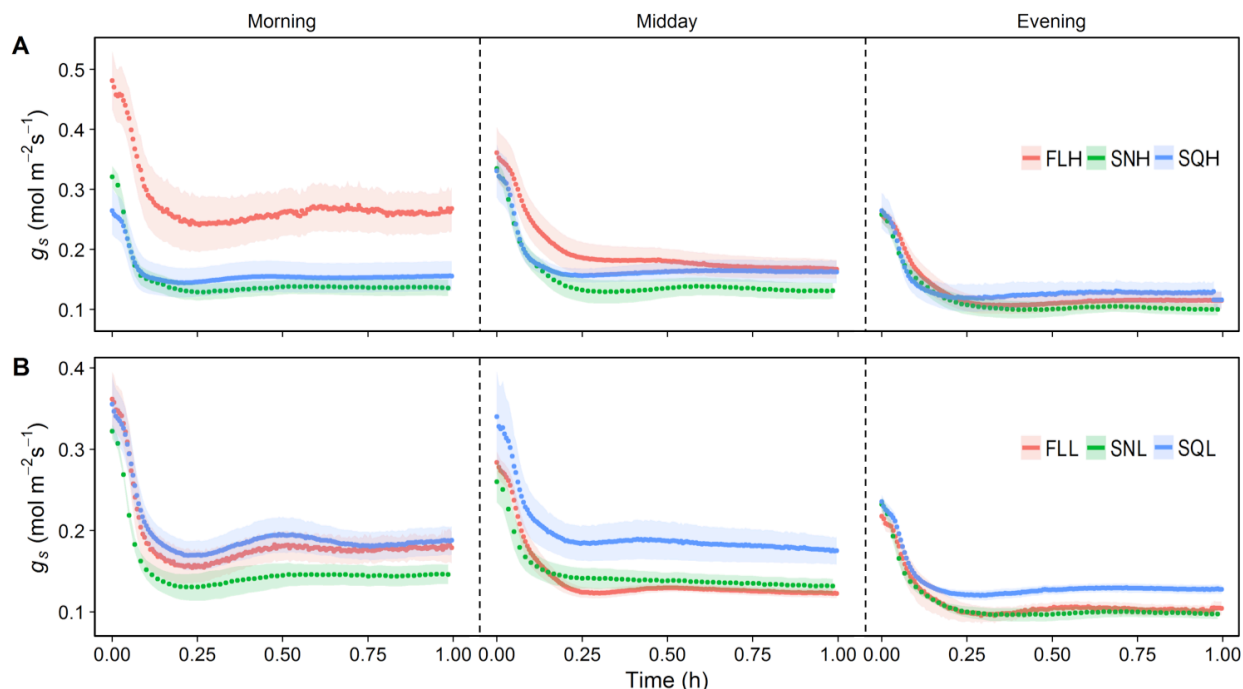


**Figure 6.8.** Temporal response of stomatal conductance ( $g_s$ ), to a step decreased in light intensity (from 1000 to 100  $\mu\text{mol m}^{-2} \text{s}^{-1}$ ), at different times of the day. Stomatal conductance ( $g_s$ ) was recorded at 20s intervals, leaf temperature maintained at 25°C, and leaf VPD at  $1 \pm 0.2$  KPa. Plants grown under the three high light treatments (A) and three low light treatments (B); fluctuating (*FLH and FLL*); sinusoidal (*SNH and SNL*); square wave (*SQH and SQL*). Error ribbons represent mean  $\pm$  SE. n = 5-6.

### 6.3.3. Speed of $g_s$ response to a step change in PPFD

Stomatal responses to a step increase in PPFD were used to determine the influence of acclimation to growth light regime and intensity on the speed of  $g_s$  response at different times of the day.

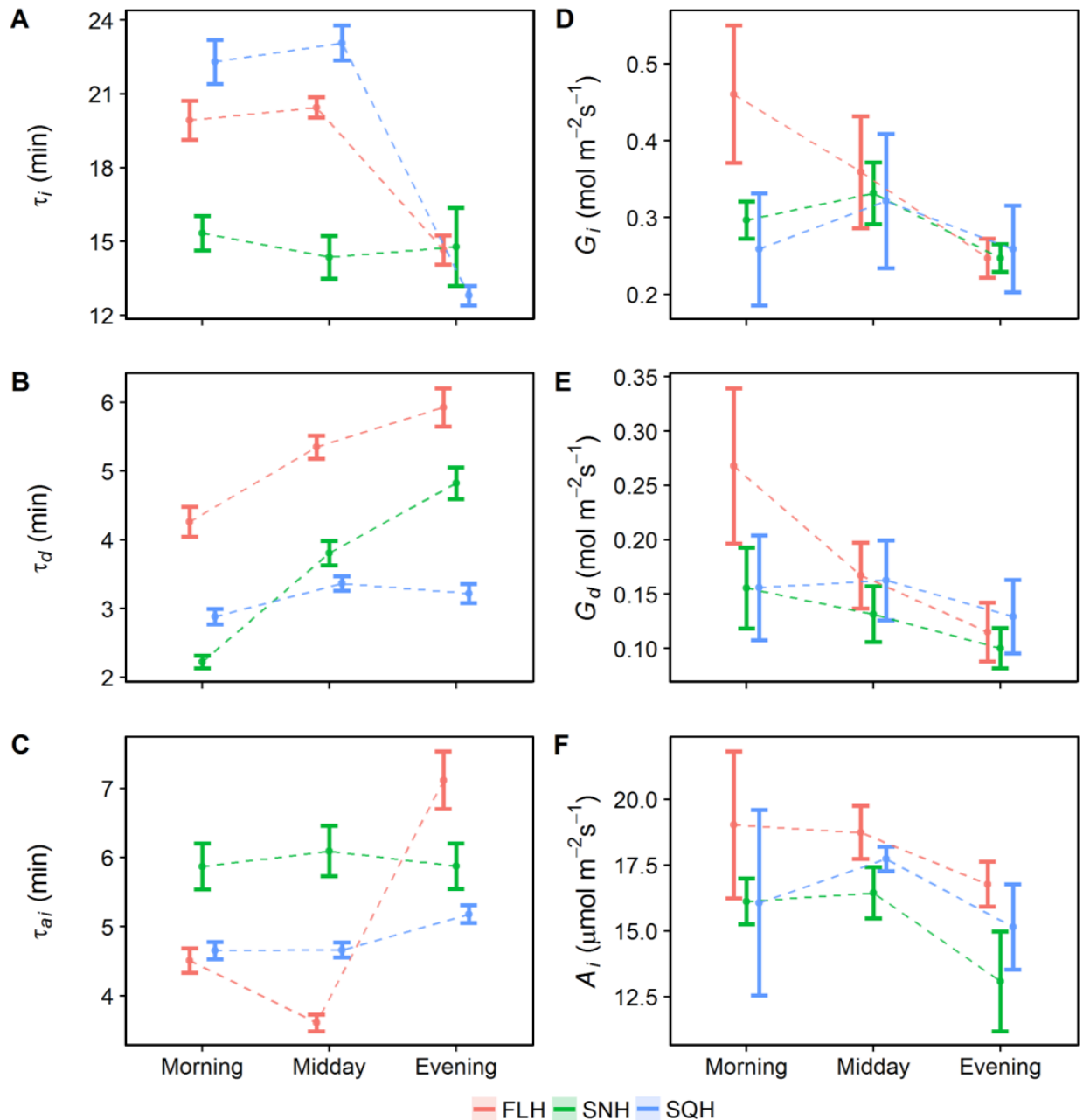


**Figure 6.9.** Time constants for stomatal opening ( $\tau_i$ , A), stomatal closure ( $\tau_d$ , B), and light saturated rate of carbon assimilation ( $\tau_{ai}$ , C) to a step change in light intensity (from 100 to 1000  $\mu\text{mol m}^{-2} \text{s}^{-1}$ ; and from 1000 to 100  $\mu\text{mol m}^{-2} \text{s}^{-1}$  respectively). Final values of stomatal conductance after an increased step change in light intensity ( $G_i$ , D); after a decreased step change in light intensity ( $G_d$ , E); and saturation of net CO<sub>2</sub> assimilation at 1000  $\mu\text{mol m}^{-2} \text{s}^{-1}$  ( $A_i$ , F), at different times of the day (Morning, Midday, Evening). Plants grown under the three high light treatments; fluctuating (FLH); sinusoidal (SNH); square wave (SQH). Error bars represent 95% confidence intervals. n = 5-6.

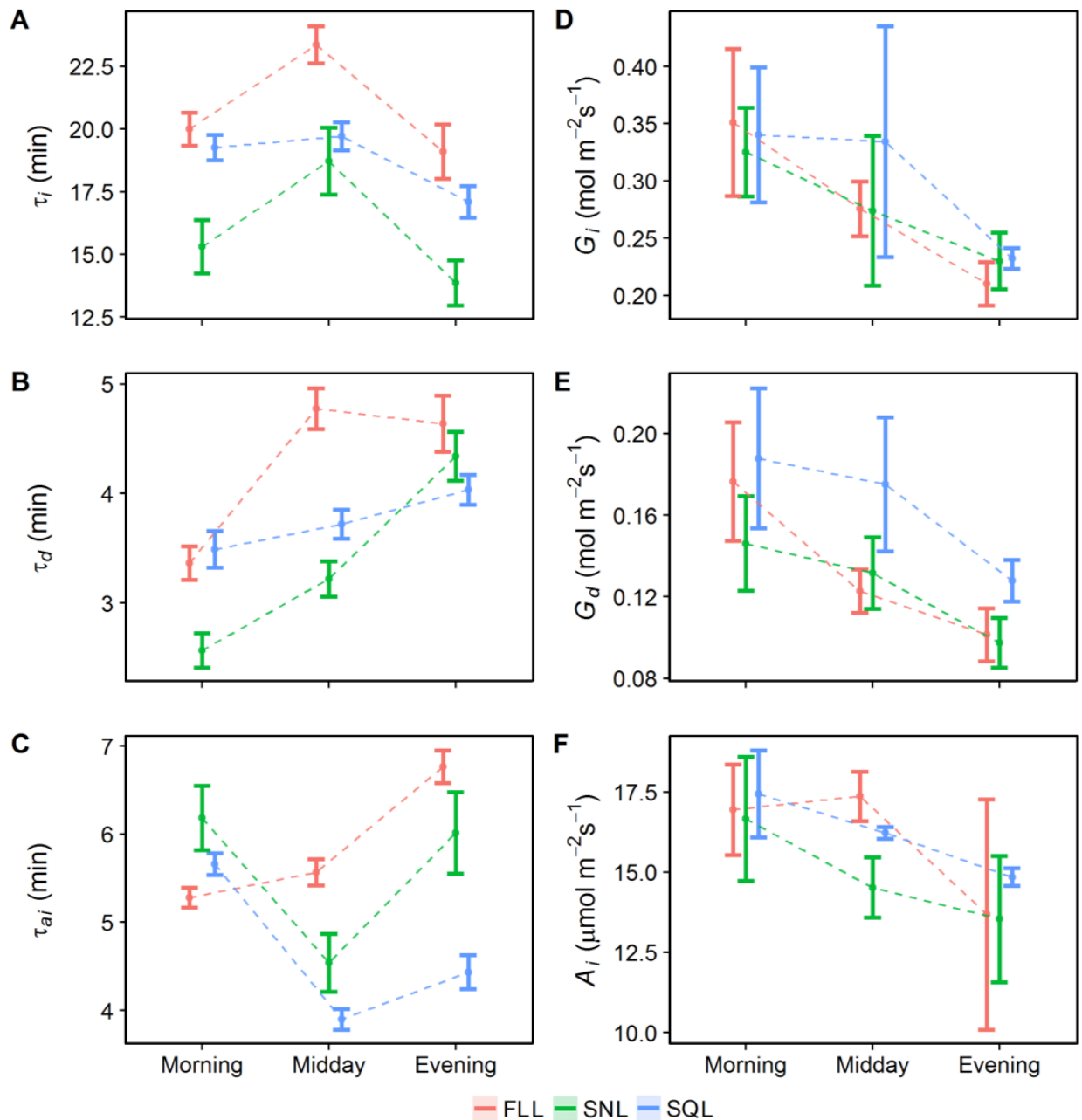


**Figure 6.10.** Time constants for stomatal opening ( $\tau_i$ , A), stomatal closure ( $\tau_d$ , B), and light saturated rate of carbon assimilation ( $\tau_{ai}$ , C) to a step change in light intensity (from 100 to 1000  $\mu\text{mol m}^{-2} \text{s}^{-1}$ ; and from 1000 to 100  $\mu\text{mol m}^{-2} \text{s}^{-1}$  respectively), at different times of the day. Final values of stomatal conductance after (1000  $\mu\text{mol m}^{-2} \text{s}^{-1}$ ) an increased step change in light intensity ( $G_i$ , D); after (100  $\mu\text{mol m}^{-2} \text{s}^{-1}$ ) a decreased step change in light intensity ( $G_d$ , E); and saturation of net CO<sub>2</sub> assimilation at 1000  $\mu\text{mol m}^{-2} \text{s}^{-1}$  ( $A_i$ , F), at different times of the day (Morning, Midday, Evening). Plants grown under the three low light treatments; fluctuating (FLL); sinusoidal (SNL); square wave (SQL). Error bars represent 95% confidence intervals. n = 5-6.

Time constants for stomatal opening ( $\tau_i$ , Fig. 6.9A) in response to a step increase in light were significantly lower ( $P < 0.05$ ) in SNH grown plants compared with FLH and SQH grown plants when measured in the morning. The slower responses observed in the FLH and SQH grown plants remained at

the midday measurement period, however  $\tau_i$  dropped significantly ( $P < 0.05$ ) in the evening measurements in both FLH and SQH indicating a faster response similar to that observed for SNH throughout the day (Fig. 6.9A). In low light treatments  $\tau_i$  was significantly faster in SNL grown plants ( $P < 0.05$ ) compared to FLL and SQL at all times of day (Fig. 6.10A), with time constants decreasing at midday in all treatments before returning in the evening to levels comparable to the morning. In contrast to stomatal opening, time constants for stomatal closure ( $\tau_d$ ) increased significantly ( $P < 0.05$ ) through the day (morning to evening) in all FL and SN treatments irrespective of light intensity (Fig. 6.9B and Fig. 6.10B), although SN grown plants were significantly faster ( $P < 0.05$ ) than FL at all times of day. The time constant for stomatal closure ( $\tau_d$ ) was maintained at all times of day in SQ grown plants irrespective of light intensity, whilst in both FL and SN treatments  $\tau_d$  significantly increased ( $P < 0.05$ ) from morning to evening. In general stomatal closure was much slower in plants grown under FL than in SN and SQ, with SN  $g_s$  responses slower than SQ in the evening.

The time constant for light saturated rate of carbon assimilation at 1000  $\mu\text{mol m}^{-2} \text{s}^{-1}$  PPFD ( $\tau_{ai}$ , Fig. 6.9C and Fig. 6.10C) were determined from the temporal response data (Figs. 6.6 and 6.7), along with final values of  $g_s$  at 1000 PPFD for stomatal opening ( $G_i$ , Fig. 6.9D and Fig. 6.10D), stomatal closure ( $G_d$ , Fig. 6.9E and Fig. 6.10E), and saturated rates of A at 1000 PPFD ( $A_i$ , Fig. 6.9F and Fig. 6.10F). Net  $\text{CO}_2$  assimilation was deemed saturated at 1000 PPFD from analysis of light response curves on the same plants (see Chapter 5, Fig. 5.2). Time constants for light saturated A ( $\tau_{ai}$ , Fig. 6.9C) were significantly higher ( $P < 0.05$ ) in SNH compared to SQH and FLH at morning and midday, whilst in the evening  $\tau_{ai}$  was significantly higher ( $P < 0.05$ ) in FLH. In low light treatments (Fig. 6.10C)  $\tau_{ai}$  significantly decreased ( $P < 0.05$ ) from morning to midday in SQL and SNL, and significant decreased ( $P < 0.05$ ) in all low light treatments from midday to evening. The final  $g_s$  at 1000  $\mu\text{mol m}^{-2} \text{s}^{-1}$  ( $G_i$ , Fig. 6.9D and Fig. 6.10D), and following closure when light was reduced from 1000 to 100  $\mu\text{mol m}^{-2} \text{s}^{-1}$  ( $G_d$ , Fig. 6.9E and Fig. 6.10E) differed significantly through the day. Final  $g_s$  at 1000 PPFD ( $G_i$ ) decreased significantly ( $P < 0.05$ ) from morning to evening in FLH grown plants (ca. 0.46 to 0.25  $\text{mol m}^{-2} \text{s}^{-1}$ , respectively; Fig. 6.9D), whereas SQH and SNH treatments remained constant throughout the day displaying a trend of increased  $G_i$  at midday. All low light treatments (FLL, SQL, SNL) displayed similar trends in  $G_i$  throughout the day, with a significant decrease ( $P < 0.05$ ) from morning to evening; ca. 0.35 to 0.21  $\text{mol m}^{-2} \text{s}^{-1}$  in FLL; ca. 0.34 to 0.23  $\text{mol m}^{-2} \text{s}^{-1}$  in SQL; and ca. 0.33 to 0.23  $\text{mol m}^{-2} \text{s}^{-1}$  in SNL (morning and evening respectively, Fig. 6.10D). Final values of  $g_s$  at 100 PPFD ( $G_d$ ; Fig. 6.9E and Fig. 6.10E) displayed similar trends to that of  $G_i$  in all treatments, irrespective of light intensity.  $G_d$  significantly decreased ( $P < 0.05$ ) from morning to evening in FLH grown plants (ca. 0.27 to 0.11  $\text{mol m}^{-2} \text{s}^{-1}$ ; Fig. 6.9E), though remained constant in SQH and SNH treatments at all times of day. In all low light treatments,  $G_d$  significantly decreased ( $P < 0.05$ ) from morning to evening (Fig. 6.10E); ca. 0.17 to 0.1  $\text{mol m}^{-2} \text{s}^{-1}$  in FLL; ca. 0.19 to 0.13  $\text{mol m}^{-2} \text{s}^{-1}$  in SQL; and

ca. 0.15 to 0.1 mol m<sup>-2</sup> s<sup>-1</sup> in SNL (morning and evening respectively, Fig. 6.10E). Saturated rates of  $A$  at 1000 PPFD ( $A_i$ ; Fig. 6.9F and Fig. 6.10F) remained constant from morning to midday in all treatments, irrespective of light intensity. In all light treatments there was a decrease in  $A_i$  from midday to evening, although this was only significant in SNH and SQL treatments ( $P < 0.05$ ). A strong correlation was observed in all treatments between the final value of  $g_s$  ( $G_i$ ) and  $A$  ( $A_i$ ) under 1000  $\mu\text{mol m}^{-2} \text{s}^{-1}$  PPFD.

#### 6.3.4. Stomatal anatomy

With regard to stomatal anatomy, significant differences ( $P < 0.05$ ) in stomatal density ( $SD$ ) were observed between plants grown under high and low light intensity, though no difference was observed between plants grown under the different patterns of growth light of the same average intensity (Fig. 6.11). FLH, SNH, and SQH grown plants had significantly higher ( $P < 0.05$ ) abaxial stomatal density than SQL, with SNH also significantly higher than FLL grown plants (Fig. 6.11A). No difference in adaxial stomatal density (Fig. 6.11B), abaxial pore area (Fig. 6.11C), or adaxial pore area (Fig. 6.11D) was observed between treatments. Maximum stomatal conductance ( $g_{s\text{max}}$ ) was greater in all high light compared to low light treatments, but was only significantly higher ( $P < 0.05$ ) in FLH, SNH, and SQH grown plants compared to FLL (Fig. 6.11E), and no difference was observed between the different patterns of growth light. Similar to  $g_{s\text{max}}$ , nocturnal conductance ( $g_{s\text{night}}$ ) was higher in all high light treatments than low light grown plants, yet was only significantly different ( $P < 0.05$ ) between SNH and SNL, with no difference observed between pattern of growth light. It should be noted that there was a strong positive correlation between  $g_{s\text{max}}$  and  $g_{s\text{night}}$ , with all the low light treatments exhibiting lower  $g_{s\text{max}}$  and  $g_{s\text{night}}$  values compared to the high light treatments (Fig. 6.12).

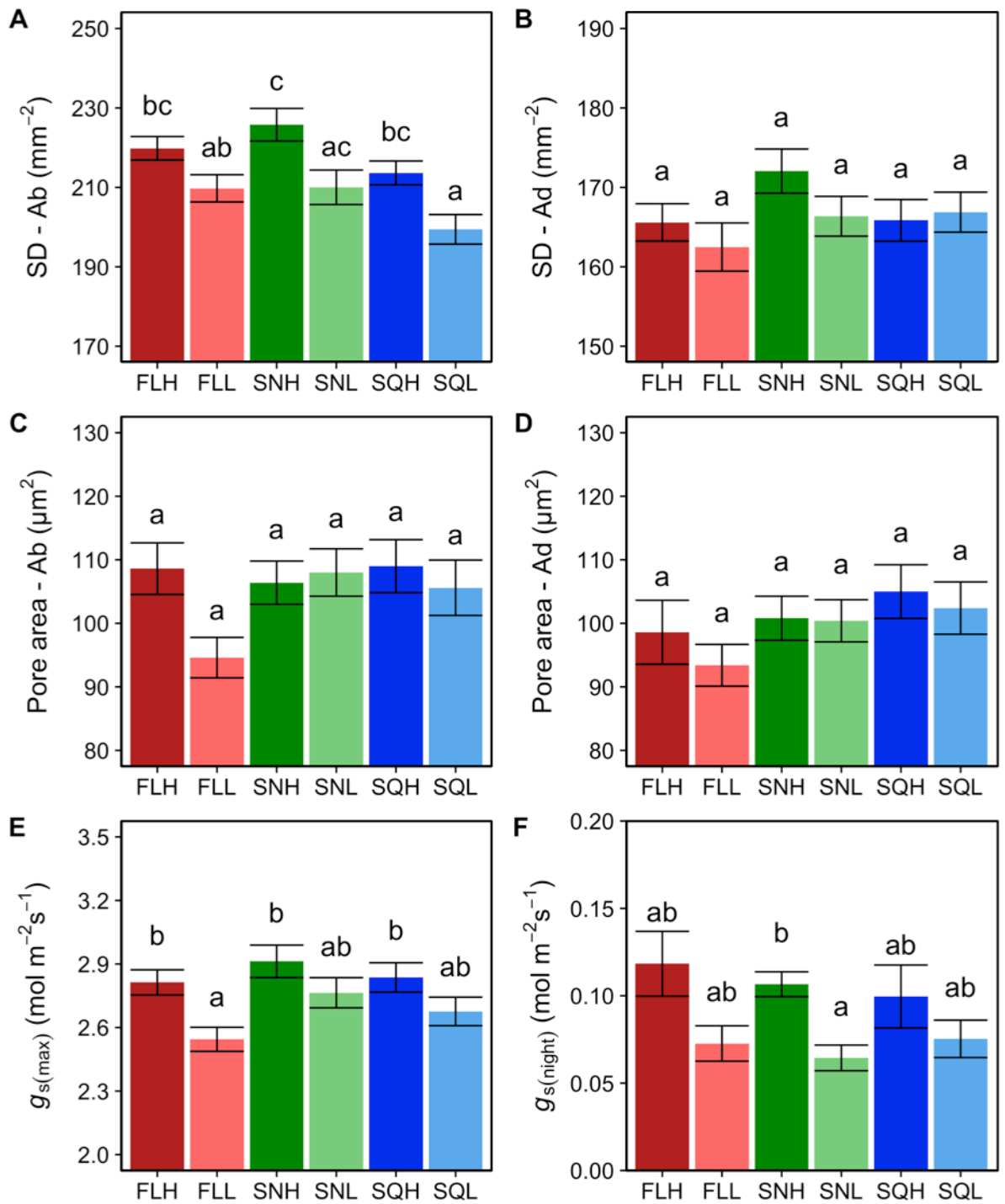


**Figure 6.11.** Stomatal anatomical characteristics including abaxial stomatal density (SD – Ab; A); adaxial stomatal density (SD – Ad; B); abaxial stomatal pore area (C); adaxial stomatal pore area (D); maximum stomatal conductance ( $g_{s(\text{max})}$ ; E); nocturnal stomatal conductance ( $g_{s(\text{night})}$ ; F) of plants grown under the six light treatments; fluctuating high and low light (FLH, FLL); sinusoidal high and low light (SNH, SNL); and square wave high and low light (SQH, SQL). Error bars represent mean  $\pm$  SE.  $n = 20$  (A-E),  $n = 5-7$  (F). Letters represent the results of *Tukey's post-hoc* comparisons of group means.

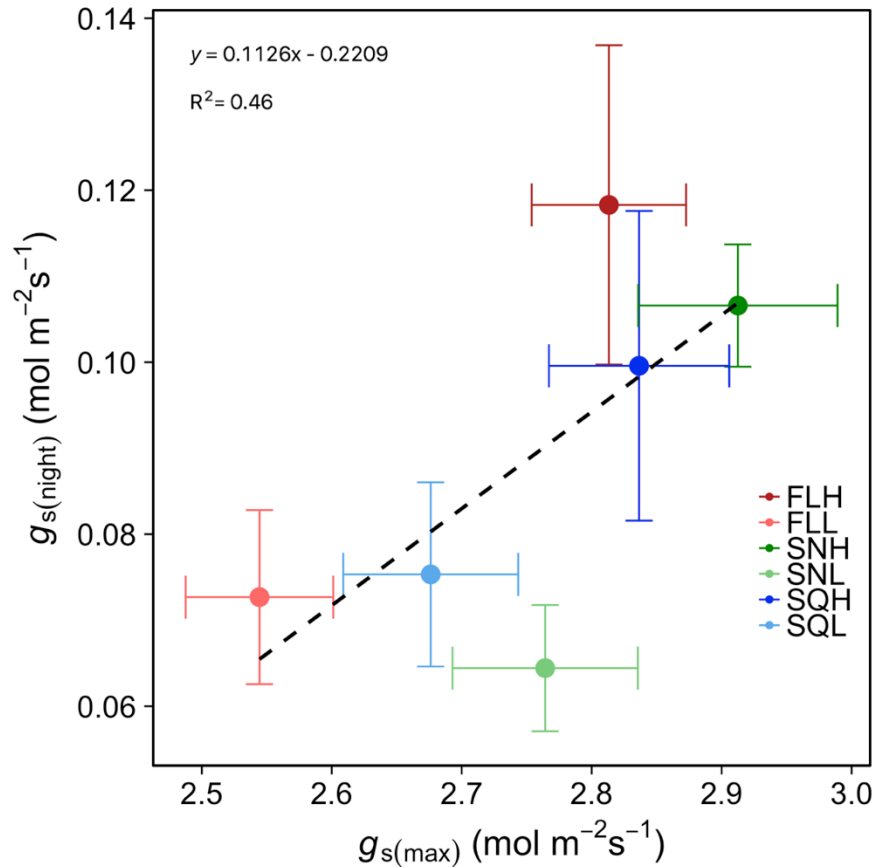


**Figure 6.12.** Correlation between stomatal conductance characteristics; maximum stomatal conductance ( $g_{s(max)}$ ) and nocturnal stomatal conductance ( $g_{s(night)}$ ) of plants grown under the six light treatments; fluctuating high and low light (FLH, FLL); sinusoidal high and low light (SNH, SNL); and square wave high and low light (SQH, SQL). Error bars represent mean  $\pm$  SE.  $n = 20$  ( $g_{s(max)}$ ),  $n = 5-7$  ( $g_{s(night)}$ ).

### 6.3.5. Impact of diurnal stomatal behaviour on predictive models of $g_s$ in a dynamic environment

Based on the findings of  $g_s$  response over the diurnal period, an addition of the time of day effect was made to the Ball-Berry model to investigate whether adding this Gaussian element would improve predictive power and model fit when trying to predict  $g_s$  under different light regimes and intensities. To demonstrate the improvements in predictive power, and display an example of the fit of the two models (with and without the Gaussian element), a completely independent data set measured under a dynamic light environment previously described in (Chapter 5) was used. Figure 6.13A shows the difference between measured and predicted  $g_s$  values using the Ball-Berry model without (Fig. 6.13B) and with (Fig. 6.13C) a Gaussian element. The new model that had the addition of a Gaussian element, displayed improvements in the prediction of  $g_s$  at all times of day, especially at periods of high and low

light where the original Ball-Berry model failed to accurately predict the full range of variation in the data (Fig. 6.13A). Under all light conditions the best model fit was always that with the addition of the Gaussian element, as  $R^2$  of the relationship between observed and predicted data increased by over 10% (0.837 to 0.941, respectively), and  $rmse$  was improved by ca. 40% (0.0527 to 0.0317, respectively) indicating a significant improvement in predictive power. This indicates that with the addition of a Gaussian element performance significantly improves, especially under a dynamic light environment.

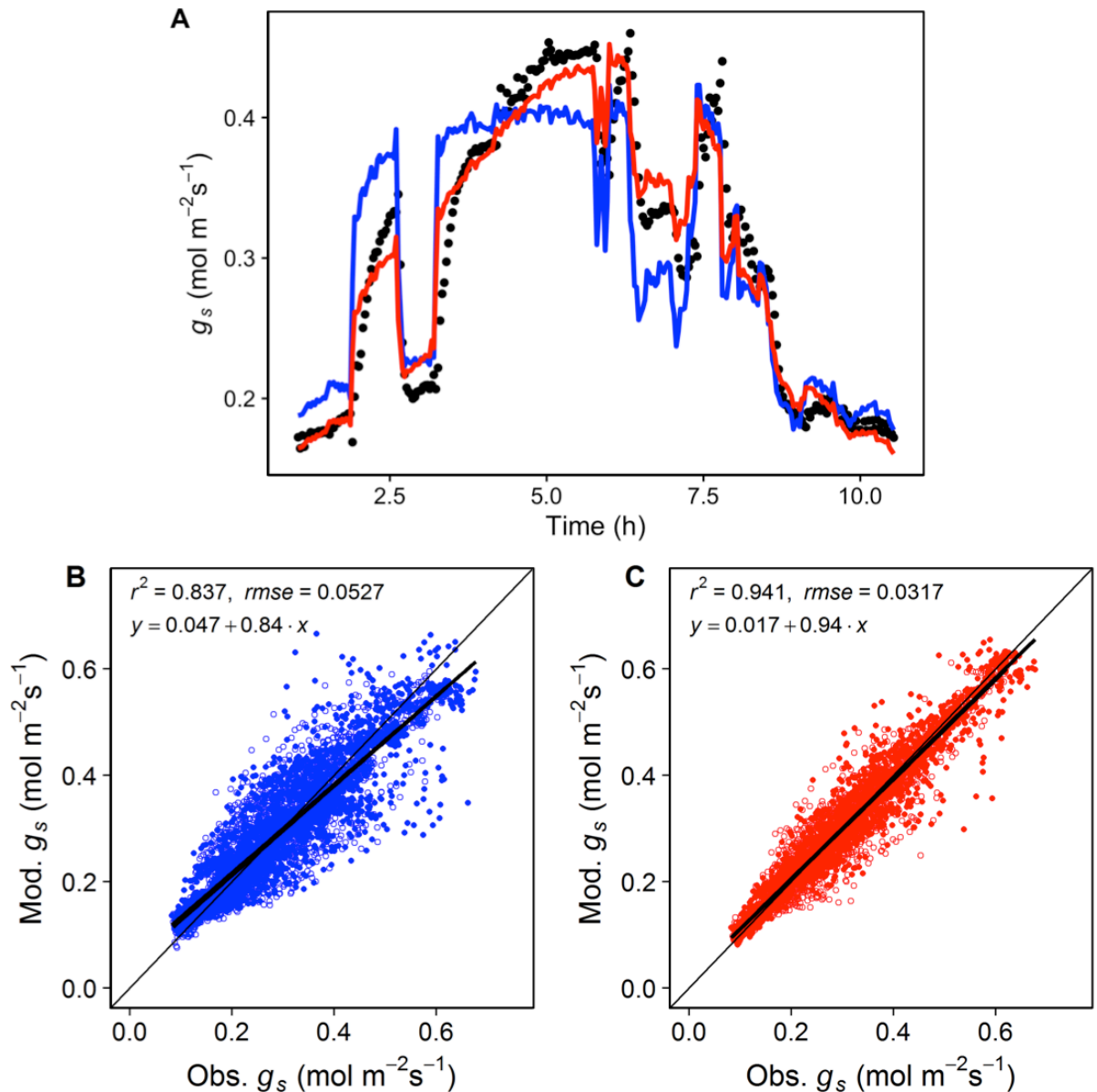


**Figure 6.13.** An example of adjustment made on an existing independent data set (black circles) measured under a dynamic light environment (A; see Chapter 5), for the Ball-Berry model without (blue line) and with (red line) a Gaussian element. Shown are the comparisons between measured and predicted  $g_s$  values using the Ball-Berry model without (B; Blue dots) and with (C; Red dots) a Gaussian element. Open and closed circles are the Fluctuating and Square-wave treatments respectively, from the independent data set.

## 6.4. Discussion

It was shown in Chapter 5 that photosynthesis and to some extent stomatal conductance acclimates to the pattern and intensity of growth irradiance; however, the aim of the research in this chapter was to investigate how acclimation to fluctuating growth light influences the magnitude and temporal dynamics of  $g_s$  over the diurnal period. The impact of fluctuating growth lighting regimes on stomatal behaviour was examined, with the acclimatory response of stomata anatomy, the rapidity of response, and the magnitude of  $g_s$  stomatal responses over the day highlighted. Also shown is an internally driven diurnal signal (referred to as the 'internal signal') that uncouples  $g_s$  from  $A$ , the magnitude and shape of which were modified by both light intensity and light pattern.

Similar to previously published work (Gay and Hurd, 1975; Lake et al, 2001), there was anatomical stomatal acclimation to light intensity, with significantly higher stomatal density ( $SD$ ) under high light. However, as there was no change in  $SD$  between growth treatments of the same intensity, the physiological differences observed, would potentially be the result of alterations to stomatal guard cell biochemistry, sensitivity or signaling rather than any increases in the potential anatomical maximum of  $g_s$  (Lawson and Blatt, 2014).

Both the rapidity and magnitude of  $g_s$  responses to a step change in PPFD were influenced by growth light regimes, and this was particularly evident at the start of the day. Plants grown under dynamic (fluctuating and sinusoidal) high light showed a faster response and in general a greater magnitude of change, however these differences in stomatal responses diminished throughout the day. This has also been described previously by Mencuccini et al. (2000), but not in the context of light acclimation. These authors used detached leaves and pressurized them to simulate different levels of leaf water status, and hypothesized that the magnitude of  $g_s$  responses observed at different times of the day were driven by changes in the osmotic regulation that altered stomatal aperture. Others have also described a reduction in the magnitude of the  $g_s$  response through time (Pfitch and Pearcy, 1989; Allen and Pearcy, 2000), however faster responses towards the end of the day were not reported. In contrast to opening, a slower closing response was observed in plants grown under dynamic light, with slower time constants for closure in the evening compared to the morning. This strategy was described previously by Ooba and Takahashi (2003), and it is believed to improve light use efficiency by maintaining open stomata under fluctuating light, reducing the limitation of  $A$  by  $g_s$ . This may also represent a more conservative strategy in energy (e.g. cost of stomatal movements; Raven, 2014) under fluctuating light regimes.

The decrease over the course of the day in the absolute values of both  $A$  and  $g_s$  (observed in both the measurements following the step increase in light and over the diurnal period) could be attributed to the accumulation of photosynthetic products, resulting in a negative feedback on the Calvin cycle (Paul and Foyer, 2001; Paul and Pellny, 2003), or an increase in apoplastic sucrose that accumulates in the guard cells, regulated by the rate of transpiration (Lu et al, 1997; Outlaw 2003; Kang et al, 2007; Kelly et al, 2013; Lawson et al, 2014; Daloso et al, 2016). However, no significant acclimation of the slow decrease in  $A$  and  $g_s$  through the day by growth light intensity and pattern was observed in this experiment.

The acclimation of the rapidity of  $g_s$  response was sensitive to light intensity as well as pattern. Previous studies in forest (e.g. Pearcy, 2007) and crop canopies (Barradas et al, 1994; Qu et al, 2016) have reported stomatal acclimation to different light environments with leaves at different heights or positions within the canopy receiving varying degrees of light intensity (Barradas et al, 1998), resulting in different anatomical and biochemical features (Givnish, 1988; Pearcy, 2007). In general under lower light maximum  $g_s$  throughout the day is reduced and the speed of the  $g_s$  response is dependent on species and growth environment (Allen and Pearcy, 2000; Ooba and Takahashi, 2003; Vico et al, 2011; Drake et al, 2013; Vialet-Chabrand et al, 2013; McAusland et al, 2016). Quantified here is the impact of growth light on the acclimation of the rapidity of the  $g_s$  response at different times of the day. The results show that estimates of the rapidity of  $g_s$  depend on the micro-environment experienced by the chosen leaf and the time at which the measurement was captured.

As stomatal responses to changing light are an order of magnitude slower than photosynthetic responses (Jones 1998, 2013; Lawson et al, 2010), slower stomata can limit  $\text{CO}_2$  diffusion for  $A$  (Barradas et al, 1998; Kaiser and Kappen, 2000; McAusland et al, 2016; Vico et al, 2011), whilst higher  $g_s$  can be at the expense of  $W_i$ . The different growth light regimes clearly produced different acclimation responses, with plants grown under fluctuating light regimes showing the greatest variation in  $W_i$  throughout the day as observed in the light step measurements.  $W_i$  was lowest in the morning in plants grown under fluctuating light and increased towards the evening. A possible explanation for this could be that although these plants receive the same amount of light as the other treatments throughout the day, the majority of this light was delivered earlier in the day. This suggests that the pattern of light distribution leads to an acclimation that will determine the kinetics and magnitude of the  $g_s$  response at different times of day. Although the stomatal acclimation described in this chapter in plants subjected to fluctuating light may show a reduction in the efficiency of water use earlier in the day, it may be important for light utilization of sun/shade flecks for photosynthesis, as previously shown in Chapter 5 when these plants were measured under their growth light regime. The variation in  $W_i$  over the diurnal

period may represent a more conservative strategy that potentially balances CO<sub>2</sub> uptake and water loss over the diurnal period to optimize the current needs at the whole plant level (Meinzer and Grantz, 1990; Medrano et al, 2015).

Diurnal gas exchange under constant light revealed an internally driven diurnal  $g_s$  response that was not only disconnected from  $A$ , but also strongly influenced by the patterns of growth light regime and to a smaller extent the average light intensity. This diurnal  $g_s$  was unexpected and represented ca. 25% of the total daily  $g_s$ , and could be considered detrimental, as significant water is lost for no extra carbon gain, however it may also play a valuable role in translocation of photosynthates, nutrient uptake, and/or maintenance of optimal leaf temperature through transpirational cooling (Caird et al, 2007; Hills et al, 2012). Although measured under constant light, all plants showed a sinusoidal pattern of response of  $g_s$  over the diurnal period, irrespective of growth light regime. What is novel about these findings is that  $g_s$  was not only partially uncoupled from  $A$  over a substantial part of the day, but that the characteristics (magnitude and period) of this  $g_s$  response are acclimating to the growth light intensity *and* the pattern of the lighting regime.

Plants grown under dynamic light regimes showed a higher magnitude of  $g_s$  response under constant light conditions, which highlights the importance of growth light pattern on the acclimation of this internal signal. Interestingly, the duration of the  $g_s$  response to the internal signal was also dependent on growth light regime. These large changes in  $g_s$  over the course of the day represent a significant loss in water with little variation in CO<sub>2</sub> assimilation over the same period, resulting in significantly reduced plant  $W_i$ . This emphasizes the importance of the growth light regime as it potentially influences the regulation of  $g_s$  over the course of the day. It has been reported that diurnal oscillations in  $g_s$ , such as those seen here, may be due to circadian rhythms, as it is well established that regulation of temporal transcription patterns by the circadian clock play an important role in rhythms of photosynthesis and stomatal opening (Dodd et al, 2004, 2005; Hubbard and Webb, 2015; de Dios et al, 2016; Hassidim et al, 2017). However, characterization of this response as circadian would require continuous measurements over multiple days (3+ days) in a constant low light environment to show if the rhythm persists in each diurnal time period (Dodd et al. 2005). Some other hypotheses involving ABA concentration (Mencuccini et al, 2000; Tallman et al, 2004), and the level of sucrose and calcium signaling (Dodd et al, 2006; Haydon et al, 2017) have been put forward to explain internally driven diurnal variations in  $g_s$ .

Demonstrated in this chapter is that the addition of an equation describing the 'internal' signal to the widely used Ball-Berry model (Ball et al, 1987) greatly improves the predictive power of the model, when estimating  $g_s$  under a dynamic light environment. Using an independent data set from Chapter 5,

there was seen to be an improvement in both the  $R^2$  (ca. 10%) and a reduction in the error (*rmse*; ca. 40%) between observed and predicted data, highlighting the importance of this added element under dynamic fluctuating light. Although integration of a diurnal signal to the Ball-Berry model was first attempted by de Dios et al (2016) and also showed an improvement in the prediction of  $g_s$ , the results shown here were at a higher time resolution which enabled the capture of rapid variations in  $g_s$  when subjected to fluctuating light regimes. To further improve the model prediction, a dynamic model that can integrate other results such as those described in this chapter will be required, that not only includes the diurnal regulation of  $g_s$  but also the altered  $g_s$  kinetics at different times of day.

## 6.5. Main conclusions

In this chapter, the impact of dynamic growth light regimes on stomatal acclimation and diurnal behavior was examined.

- Growth light environment modified stomatal kinetics at different times of the day, with differences in the rapidity and magnitude of the response of  $g_s$  to a step change in light demonstrated between treatments. This time of day effect on stomatal response is important to consider when attempting to compare stomatal behaviour between species and within populations, and the impact this may have on photosynthetic measurements and therefore water use efficiency.
- Both the intensity and pattern of growth light determined the acclimation of the rapidity of  $g_s$  and the response of  $g_s$  over the diurnal period. This represents an important strategy for maintaining carbon fixation and overall plant water status by conditioning the plant to respond appropriately to future diurnal variations in light.
- The different growth light treatments produced distinctly different acclimation responses in intrinsic water use efficiency ( $W_i$ ), with plants grown under fluctuating light exhibiting lower  $W_i$  in the morning and higher  $W_i$  in the evening, which was predominantly driven by changes in stomatal conductance. This variation in  $W_i$  over the diurnal period may represent a more conservative strategy that potentially balances  $\text{CO}_2$  uptake and water loss over the diurnal period to optimize the current needs at the whole plant level.

- The diurnal response of  $g_s$  was quantified, and the characteristics of which found to be modified by growth light environment. The importance of this diurnal response was demonstrated by improvements in the prediction of  $g_s$  when a diurnal element was added to the widely used Ball-Berry model of stomatal conductance.
- A dynamic model of  $g_s$  that includes the internally driven response of  $g_s$  over the diurnal period will help improve the prediction of  $g_s$ , even under a dynamic environment such as that experienced by plants in the field. This was illustrated by the improvement in predicted  $g_s$  from plants acclimated to different light environments and measured under dynamic regimes.

# CHAPTER 7



## General discussion

## 7.1. Overview

Despite stomatal behaviour occurring at the micro-scale, it is important to recognize the impact they have on the global carbon and water cycles. Although stomata typically occupy only a small portion of the leaf surface (0.3-5%), they account for up to 95% of all gaseous flux of CO<sub>2</sub> and water vapour in terrestrial ecosystems, with estimations that 60% of all precipitation that falls on the terrestrial biosphere is taken up by plants and transpired through stomatal pores (Morison, 2003; Katul et al, 2012). Therefore, the acclimation of stomatal behaviour to growth light has large effects on photosynthetic CO<sub>2</sub> fixation and water loss through leaf, whole plant and canopy levels, with major consequences for carbon and hydrological cycles at global scales (Hetherington and Woodward, 2003; Keenan et al, 2012, 2013).

At the onset of this work most studies that have investigated plant acclimation to growth light, primarily focused on photosynthetic acclimation in the form of adjustments to leaf morphology and photosynthetic apparatus stoichiometry (e.g. see, Terashima et al, 2006; Athanasiou et al, 2010; Kono and Terashima, 2014). Whilst studies that examined stomatal acclimation have focused on anatomical changes such as stomatal density, size and index (Willmer and Fricker, 1996; Lake et al, 2001; Hetherington and Woodward, 2003), often ignoring the impact on the functional response of stomata. It is well known that during growth and development, plants experience a range of light intensities and spectral qualities, and therefore, leaves are subjected to spatial and temporal gradients in incident light, to which stomata respond to maximise CO<sub>2</sub> uptake or reduce water loss. Despite this, current models that incorporate  $g_s$  as a factor in carbon and water fluxes across scales, use predicted steady state values of  $g_s$  that presume instantaneous changes in  $g_s$  at each observed light level (Damour et al, 2010). These models are ultimately limited in accurately predicting variations in  $g_s$ , as they neglect to incorporate the temporal aspect of stomatal response at a given time and over the diurnal period. It is therefore essential to understand the impact of growth light on stomata behaviour, and to create a more substantial data profile for use by the community to develop improved predictive models.

The aims of this thesis were to determine how acclimation to growth light environment would impact stomatal behaviour and diurnal response, and how stomatal conductance ( $g_s$ ), and net CO<sub>2</sub> assimilation ( $A$ ), influence water use efficiency ( $W_i$ ). On identifying differences in the natural variation in stomatal response to light in the model tree species *Populus nigra*, an experiment was set up to assess the impact of stomatal acclimation to growth light intensity on the response of  $g_s$ ,  $A$  and  $W_i$ . Additionally, the model species *Arabidopsis thaliana* was subjected to dynamic growth light conditions, to separate the

influence of light intensity and fluctuations in light on stomatal and photosynthetic acclimation. Through the assessment of the response of  $g_s$  to different light conditions, like those experienced by plants in the field, the work in this study aims to potentially improve the prediction of stomatal conductance in vegetation-climate models, and facilitate greater understanding of ecosystem response to changing climatic conditions.

## 7.2. Influence of dynamic growth light on the temporal response of $g_s$

When analyzing the influence of growth light on the temporal response of  $g_s$  and  $A$ , and therefore  $W_i$ , it was apparent that acclimation of the  $g_s$  response was altered by both the intensity and the pattern of growth light. This acclimation led to changes in the speed of  $g_s$  response as well as altering the magnitude of change in  $g_s$  before and after light was applied. The time taken to increase or decrease  $g_s$  to changes in  $PPFD$  plays a critical role in maximising carbon gain and conserving water, with faster responses and higher magnitudes of  $g_s$  improving carbon gain but often at the expense of water use efficiency through increased transpiration (Barradas et al, 1994; Naumburg and Ellsworth, 2000; Lebaudy et al, 2008; McAusland et al, 2016). The data in Chapter 3 demonstrated that changes in the speed of  $g_s$  response may well be due to developmental acclimation to conditions at the native site of origin, with the slowest rates of response occurring in genotypes acclimated to drier, high temperature environments. This may represent a negative impact on carbon gain but would reduce the chance of drought at the whole plant level (Meinzer and Grantz, 1990; Knapp, 1993), therefore benefitting genotypes adapted to environments more susceptible to drought (Hetherington and Woodward, 2003), by prioritizing the conservation of water over carbon gain (Ooba and Takahashi, 2003). In contrast, it would appear that *Populus nigra* genotypes that are adapted to more favourable conditions (lower temperatures, higher precipitation), exhibit an adaptive mechanism to increase  $CO_2$  uptake by maximizing stomatal conductance under well-watered conditions. Interestingly, when a single genotype of *Populus nigra* was subjected to changes in growth light intensity, as shown in Chapter 4, it became apparent that adaptive strategies were in place by which plants would acclimate the rapidity of  $g_s$  response to maximize performance under a given intensity of growth light. Highlighted in Chapter 4, was the fact that plants grown under high light intensities exhibited faster  $g_s$  responses than those grown under low light, when subjected to a step change at high light levels. Conversely, those grown under low light displayed the fastest  $g_s$  responses when subjected to low intensity step changes in light. This is in conjunction with previous work that has shown developmental acclimation to shade conditions; highlighting the importance of acclamatory responses in maximizing carbon gain in light-limited

environments (Pearcy, 2007; Way and Pearcy, 2012). Potentially, this represents an interesting strategy, where plants acclimate by increasing the rapidity of the  $g_s$  response to light levels experienced most often during growth and development, either as a way of maximizing carbon uptake or for the conservation of energy for use later in the day, by limiting unnecessary stomatal movement (Mencuccini et al, 2000; Raven, 2014).

It should be noted that when plants (both *Populus* and *Arabidopsis*) were subjected to step changes in light at different times of the day, it was revealed that there were significant differences in the rapidity and magnitude of  $g_s$  response. In Chapter 4, *Populus nigra* plants subjected to different growth light intensities displayed a reduction in the magnitude and speed of  $g_s$  responses toward the end of the day, although as this was accompanied by similar reductions in  $A$ ,  $W_i$  remained constant throughout. The synchronicity of these parameters was maintained in all treatments, representing an important strategy under well-watered (non-water limited) conditions (Wong et al, 1979), to optimize the trade off between photosynthesis and water loss (Buckley, 2017), and maintain overall plant water status and therefore  $W_i$ . The data disclosed in Chapter 6, showed similar  $g_s$  responses through the day in *Arabidopsis* when subjected to different fluctuating or square-wave light intensity regimes. However, the differences observed in the magnitude and speeds of  $g_s$  response were far greater than those observed in the intensity treatments alone (see Chapter 4). This would indicate that the acclimation of the rapidity of  $g_s$  response was sensitive to the intensity as well as the pattern of growth light. This is in line with previous studies that have reported stomatal acclimation to different light environments, with leaves at different heights or positions within the canopy receiving varying degrees of light intensity (Barradas et al, 1994; Barradas et al, 1998; Qu et al, 2016). However, as growth light was not quantified in these studies, the data shown in this thesis potentially provides stronger evidence of the direct impact of growth light on the acclimation of the dynamic response of stomata.

Highlighted in this study, the importance of the temporal response of  $g_s$  is largely unknown and underestimated, whilst understanding this variation will aid in the development of future scaling efforts to scale from individual stomata to leaf and canopy levels. At this point in time, what is obvious is that there is a lack of quantitative data on the rapidity of stomatal response under different environmental and growth conditions. This lack of information makes it difficult to assess the impact of uncoordinated responses of  $A$  and  $g_s$  on leaf level gas exchange, and to potentially describe the mechanisms of guard cell movement.

### 7.3. Diurnal variation in stomatal response: impact on water use efficiency

In nature, environmental conditions are rarely stable and lead to complex patterns in plant response over the day. Stomatal conductance ( $g_s$ ) and photosynthetic rate ( $A$ ) are continuously responding to changes in light and a strong correlation between these two parameters is often observed (Wong et al, 1979; Farquhar and Sharkey, 1982; Mansfield et al, 1990; Buckley and Mott, 2013). In all Chapters, a fluctuating light regime, mimicking a pattern of light that may be experienced by plants in the field, was used to examine diurnal gas exchange, the coordination of  $A$  and  $g_s$  and the impact on water use efficiency ( $W_i$ ) over the course of the day. All plant types displayed similar responses of  $g_s$ ,  $A$  and  $W_i$  over the diurnal period but differed in the magnitude of these parameters. Presented In Chapter 3, was how genotypes of *Populus nigra* that were adapted to warmer, drier climates displayed lower levels of  $g_s$  over the diurnal period whilst maintaining similar levels of  $A$ , which led to increases in daily  $W_i$  in these genotypes. These findings are supported by previous studies that found that when subject to drought conditions, plants would often prioritize the signal to maintain leaf water status over the need to fix carbon from the atmosphere (Lawson and Morison, 2004; Aasamaa and Söber, 2011). The data observed in Chapter 4 revealed that  $W_i$  was largely comparable in all plants, even when subjected to different intensities of growth light. This was because the photosynthetic and stomatal acclimatory responses led to increases in  $A$  and  $g_s$  over the diurnal period, which was in conjunction with an increase in the intensity of growth light. It has been suggested that the coordination between  $A$  and  $g_s$  can be seen as a plant acclimatory response to control  $g_s$  in a way that will maximize  $A$  and minimize transpiration over a typical diurnal light pattern (Cowan and Farquhar, 1977; Buckley, 2017), thereby maintaining a near constant  $W_i$ .

Interestingly, Chapters 5 and 6 revealed interesting results regarding acclimation to fluctuating light. It would appear, at least in the model species *Arabidopsis*, that growth under fluctuating light has an effect on the acclimation of stomatal response and photosynthesis, that is at least comparable if not more than the effect from growth light intensity. The data revealed that plants grown under fluctuating light displayed a previously undescribed phenotype, which enabled these plants to perform more efficiently in dynamic light environments. Over the diurnal period, these plants displayed greater rates of photosynthesis whilst maintaining similar, if not lower levels of stomatal conductance, which led to improvements in daily water use efficiency. The diurnal data in Chapter 5 also showed a potential negative feedback on photosynthesis through the day in all light treatments, which resulted in ca. 20% decrease in the daily total carbon gain. It has been suggested that this may be due to a slowing down of Calvin cycle activity later in the diurnal period, leading to sugar accumulation applying a feedback

control on photosynthesis (Paul and Foyer, 2001; Paul and Pellny, 2003). Despite this reduction in photosynthesis there was no corresponding decrease in  $g_s$ , impacting the total daily water use efficiency of the plant.

Crucially in Chapter 6, the impact of dynamic growth light regimes on stomatal acclimation and diurnal behaviour was examined. It was revealed that there was an internally driven response of  $g_s$  that essentially uncouples  $A$  and  $g_s$  over the diurnal period, with characteristics that are modified by the growth light environment. The magnitude of the response of  $g_s$  when subject to a square-wave pattern of light was higher in plants that were not only subjected to higher intensities of growth light, but also if they were subject to fluctuations in growth light. In fact, fluctuations in light had a greater impact on the diurnal  $g_s$  response than light intensity. These large changes in  $g_s$  over the course of the day potentially represent a significant loss in water with little variation in  $A$  over the same period, resulting in significantly reduced plant  $W_i$ . The importance of this signal on diurnal  $g_s$  response was demonstrated by the inclusion of the Gaussian element describing the internal signal, which greatly improved the prediction of  $g_s$  from the widely used Ball-Berry model (Ball et al, 1987). Quantification of the components of the internal signal potentially provides a tool for assessing diurnal patterns of stomatal behavior. A dynamic model of  $g_s$  that includes these components will be able to describe the contribution of each element to the diurnal response of  $g_s$ , even under a dynamic environment such as that experienced by plants in the field. Critically, the acclimation of diurnal stomatal response and photosynthesis described in Chapters 5 and 6, revealed important strategies in plants for maintaining carbon fixation and overall plant water status by conditioning the plant to respond efficiently to future diurnal variations in light. Furthermore, these strategies led to major effects on daily water use and carbon gain, and therefore will impact model prediction of ecosystem-atmosphere carbon and water budgets.

#### **7.4. Conclusions and further investigation**

Dynamic stomatal behaviour plays a key role in regulating the flux of carbon and water through the soil-plant-atmosphere continuum, and represents an important factor in scaling leaf level measurements of photosynthesis and therefore water use efficiency through to whole plant and canopy levels (Weyers et al, 1997). Over the diurnal period, fluctuations in light drive the temporal and spatial dynamics of carbon gain and water loss. It is therefore essential to consider the speed of stomatal response to fluctuations in light, when assessing carbon uptake and water use (Lawson and Blatt, 2014). The findings in this study

highlight the variation in  $g_s$  response, photosynthesis, and water use efficiency that can occur in plants when subjected to different growth light conditions. This information illustrates the impact of growing plants in dynamic light regimes, similar to those experienced by plants in the natural environment, on the phenotype and physiology of model species *Populus nigra* and *Arabidopsis thaliana*. Potentially providing a first step toward understanding how dynamic growth light influences stomatal dynamic response, water use, and plant growth. Furthermore, it emphasizes that growing plants under laboratory conditions and square-wave illumination does not accurately represent plant acclimation and development under a natural environment. Highlighting the need to potentially rethink how we grow plants as a community if we are to infer results from the lab to the field.

The spatial and temporal aspects of stomatal behaviour have often been ignored, with most descriptive and predictive models neglecting to consider the impact of this variation in  $g_s$  on gas exchange. Data from this study suggests that the addition of stomatal dynamics to existing models, may reveal the extent to which  $g_s$  has been inaccurately predicted by steady-state models (Damour et al, 2010). It should be noted that in the future, greater focus in modeling efforts should be given to the integration of temporal stomatal dynamics to fluctuations in environmental signals (Vico et al, 2011; Vialet-Chabrand et al, 2013). This would be in an attempt to predict the impact of large-scale heterogeneity in stomatal traits caused by different acclimatory states, on the flux of carbon and water through the canopy, ecosystem, and global scales. Furthermore, as stomata are subjected to constant fluctuations in environmental conditions over the diurnal period, it is often the speed of  $g_s$  response that is critical in determining CO<sub>2</sub> uptake and transpiration dynamics over the course of the day (Vialet-Chabrand et al, 2016; McAusland et al, 2016).

Further development in dynamic models of guard cell movement and stomatal behaviour is limited by the lack of quantitative data on the rapidity and diurnal response of  $g_s$  to different environmental conditions. Following the results of the research presented here, it is important to consider that improvements and further validation of current models of gas exchange would only be possible through the collection as a community, of more quantitative data on diurnal and temporal responses of  $g_s$ . With specific attention given to the impact of spatial variation in gas exchange on scaling efforts, triggered by alterations in stomatal development and acclimation to environmental growth conditions.

In conclusion, the findings herein emphasize that an abundance of variation in  $g_s$  responses to light exists within species, and that acclimation to different light environments can bring about stark changes in this response, greatly influencing photosynthesis and therefore water use efficiency. Acclimation to growth light impacts the dynamic response of  $g_s$  over the diurnal period, and can produce significant

variation in the magnitude and rate of  $g_s$  response to light, outlining the potential for heterogeneity across scales. Finally, this study highlights the importance of considering plant acclimation to growth light, and the impact this has on the functional response of stomata, when attempting to model the response of  $g_s$  across leaf to ecosystem and global scales.

# CHAPTER 8



## References

## References

- Aasamaa K, Söber A** (2011) Responses of stomatal conductance to simultaneous changes in two environmental factors. *Tree Physiol* **31**: 855–864
- Allen MT, Percy RW** (2000) Stomatal behavior and photosynthetic performance under dynamic light regimes in a seasonally dry tropical rain forest. *Oecologia* **122**: 470–478
- Allen MT, Percy RW** (2000) Stomatal versus biochemical limitations to dynamic photosynthetic performance in four tropical rainforest shrub species. *Oecologia* **122**: 479–486
- Alter P, Dreissen A, Luo FL, Matsubara S** (2012) Acclimatory responses of *Arabidopsis* to fluctuating light environment: comparison of different sunfleck regimes and accessions. *Photosynth Res* **113**: 221–237
- Arve LE, Kruse OMO, Tanino KK, Olsen JE, Futsæther C, Torre S** (2017) Daily changes in VPD during leaf development in high air humidity increase the stomatal responsiveness to darkness and dry air. *J. Plant Physiol* **211**: 63–69
- Assmann SM, Grantz DA** (1990) Stomatal response to humidity in sugarcane and soybean: effect of vapour pressure difference on the kinetics of the blue light response. *Plant, Cell Environ* **13**: 163–169
- Assmann SM, Wang XQ** (2001) From milliseconds to millions of years: guard cells and environmental responses. *Curr Opin Plant Biol* **4**: 421–8
- Athanasίου K, Dyson BC, Webster RE, Johnson GN** (2010) Dynamic acclimation of photosynthesis increases plant fitness in changing environments. *Plant Physiol* **152**: 366–373
- Bailey S, Walters RG, Jansson S, Horton P** (2001) Acclimation of *Arabidopsis thaliana* to the light environment: the existence of separate low light and high light responses. *Planta* **213**: 794–801
- Bailey S, Horton P, Walters RG** (2004) Acclimation of *Arabidopsis thaliana* to the light environment: the relationship between photosynthetic function and chloroplast composition. *Planta* **218**: 793–802
- Baker NR** (2008) Chlorophyll fluorescence: a probe of photosynthesis in vivo. *Annu Rev Plant Biol* **59**: 89–113
- Baldocchi D** (2014) Measuring fluxes of trace gases and energy between ecosystems and the atmosphere - the state and future of the eddy covariance method. *Glob Chang Biol* **20**: 3600–3609
- Ball JT, Berry JA** (1982)  $C_i/C_s$  ratio: a basis for predicting stomatal control of photosynthesis. Year B. Carnegie Inst. Wash.
- Ball JT, Woodrow IE, Berry JA** (1987) A model predicting stomatal conductance and its contribution to the control of photosynthesis under different environmental conditions. In J Biggins, ed, *Prog. Photosynth. Res.* Springer Netherlands, pp 221–224
- Barman R, Jain AK, Liang M** (2014) Climate-driven uncertainties in modeling terrestrial energy and water fluxes: a site-level to global-scale analysis. *Glob Chang Biol* **20**: 1885–900

- Baroli I, Price GD, Badger MR, Caemmerer S Von** (2008) The contribution of photosynthesis to the red light response of stomatal conductance [OA]. **146**: 737–747
- Barradas VL, Jones HG, Clark JA** (1994) Stomatal responses to changing irradiance in *phaseolus vulgaris* L. *J Exp Bot* **45**: 931–936
- Barradas VL, Jones HG** (1996) Responses of CO<sub>2</sub> assimilation to changes in irradiance: laboratory and field data and a model for beans (*Phaseolus vulgaris* L.). *J Exp Bot* **47**: 639–645
- Barradas VL, Jones HG, Clark, JA** (1998) Sunfleck dynamics and canopy structure in a *Phaseolus vulgaris* L. canopy. *International Journal of Biometeorology* **42**(1): 34-43
- Bernacchi CJ, Kimball BA, Quarles DR, Long SP, Ort DR** (2007) Decreases in stomatal conductance of soybean under open-air elevation of [CO<sub>2</sub>] are closely coupled with decreases in ecosystem evapotranspiration. *Plant Physiol* **143**: 134–144
- Blatt MR** (2000) Cellular signaling and volume control in stomatal movements in plants. *Annu Rev Cell Dev Biol* **16**: 221–241
- Blom-Zandstra M, Pot CS, Maas FM, Schapendonk AHCM** (1995) Effects of different light treatments on the nocturnal transpiration and dynamics of stomatal closure of two Rose cultivars. *Sci Hortic (Amsterdam)* **61**: 251–262
- Bonan GB, Williams M, Fisher RA, Oleson KW** (2014) Modeling stomatal conductance in the earth system: linking leaf water-use efficiency and water transport along the soil–plant–atmosphere continuum. *Geosci Model Dev* **7**: 2193–2222
- Brodribb TJ, McAdam SAM** (2017) Evolution of the stomatal regulation of plant water content. *Plant Physiol* **174**: 639-649
- Buckley TN, Mott KA, Farquhar GD** (2003) A hydromechanical and biochemical model of stomatal conductance. *Plant, Cell Environ* **26**: 1767–1785
- Buckley TN, Mott KA** (2013) Modelling stomatal conductance in response to environmental factors. *Plant, Cell Environ* **36**: 1691–1699
- Buckley TN** (2017) Modeling stomatal conductance. *Plant Physiol* **174**: 572-582
- Caird MA, Richards JH, Donovan LA** (2007) Nighttime stomatal conductance and transpiration in C<sub>3</sub> and C<sub>4</sub> plants. *Plant Physiol* **143**: 4–10
- Caldeira CF, Jeanguenin L, Chaumont F, Tardieu F** (2014) Circadian rhythms of hydraulic conductance and growth are enhanced by drought and improve plant performance. *Nat Comms* **5**: 5365
- Carmo-Silva AE, Salvucci ME** (2013) The regulatory properties of Rubisco activase differ among species and affect photosynthetic induction during light transitions. *Plant Physiol* **161**: 1645–1655
- Casson SA, Hetherington AM** (2010) Environmental regulation of stomatal development. *Curr Opin Plant Bio* **13**: 90–95

- Chabot BF, Jurik TW, Chabot JF** (1979) Influence of instantaneous and integrated light-flux density on leaf anatomy and photosynthesis. *Am J Bot* **66**: 940–945
- Chater C, Kamisugi Y, Movahedi M, Fleming A, Cuming AC, Gray JE, Beerling DJ** (2011) Regulatory mechanism controlling stomatal behavior conserved across 400 million years of land plant evolution. *Curr Biol* **21**: 1025–9
- Chazdon RL** (1988) Sunflecks and their importance to forest understorey plants. *Adv Ecol Res* **18**: 1–63
- Chazdon RL, Pearcy RW** (1991) The importance of sunflecks for forest understorey plants. *Bioscience* **41**: 760–766
- Chen ZH, Hills A, Bätz U, Amtmann A, Lew VL, Blatt MR** (2012) Systems dynamic modeling of the stomatal guard cell predicts emergent behaviors in transport, signaling, and volume control. *Plant Physiol* **159**: 1235–1251
- Cowan IR, Troughton JH** (1971) The relative role of stomata in transpiration and assimilation. *Planta* **97**: 325–36
- Cowan IR** (1977) Stomatal behaviour and environment. In *Advances in botanical research*, Academic press **4**: 117–228.
- Cowan IR, Farquhar GD** (1977) Stomatal function in relation to leaf metabolism and environment. *Symp Soc Exp Biol* **31**: 471–505
- Daloso DM, Dos Anjos L, Fernie AR** (2016) Roles of sucrose in guard cell regulation. *New Phytol* **211**: 809–818
- Damour G, Simonneau T, Cochard H, Urban L** (2010) An overview of models of stomatal conductance at the leaf level. *Plant, cell & Environ* **33**: 1419–1438
- de Dios VR, Goulden ML, Ogle K, Richardson AD, Hollinger DY, Davidson EA, Alday JG, Barron-Gafford GA, Carrara A, Kowalski AS, et al** (2012) Endogenous circadian regulation of carbon dioxide exchange in terrestrial ecosystems. *Glob Chang Biol* **18**: 1956–1970
- de Dios VR, Gessler A, Ferrio JP, Alday JG, Bahn M, del Castillo J, Devidal S, García-Muñoz S, Kayler Z, Landais D, Martín-Gómez P, Milcu A, Piel C, Pirhofer-Walzl K, Ravel O, Salekin S, Tissue DT, Tjoelker MG, Voltas J, Roy J** (2016) Circadian rhythms have significant effects on leaf-to-canopy scale gas exchange under field conditions. *GigaSci* **5**(1): 43
- De Kauwe MG, Kala J, Lin YS, Pitman AJ, Medlyn BE, Duursma RA, Abramowitz G, Wang YP, Miralles DG** (2015) A test of an optimal stomatal conductance scheme within the CABLE land surface model. *Geosci Model Dev* **8**: 431–452
- Demmig-Adams B, Adams WW** (1992) Photoprotection and other responses of plants to high light stress. *Annu Rev Plant Physiol Plant Mol Biol* **43**: 599–626
- Dewar RC, Franklin O, Mäkelä A, McMurtrie RE, Valentine HT** (2009) Optimal function explains forest responses to global change. *Bioscience* **59**: 127–139
- Dickmann DI, Kuzovkina J**, (2014) Poplars and willows of the world, with emphasis on silviculturally important species. *Poplars and willows: trees for society and the environment* **22**(8)

- Dodd AN, Parkinson K, Webb AA** (2004) Independent circadian regulation of assimilation and stomatal conductance in the *ztl-1* mutant of *Arabidopsis*. *New Phytologist* **162**(1): 63-70
- Dodd AN, Salathia N, Hall A, Kévei E, Tóth R, Nagy F, Hibberd JM, Millar AJ, Webb AA** (2005) Plant circadian clocks increase photosynthesis, growth, survival, and competitive advantage. *Science* **309**: 630-633
- Dodd AN, Jakobsen MK, Baker AJ, Telzerow A, Hou SW, Laplaze L, Barrot L, Scott Poethig R, Haseloff J, Webb AA** (2006) Time of day modulates low-temperature Ca<sup>2+</sup> signals in *Arabidopsis*. *The Plant Journal* **48**(6): 962-973
- Doheny-Adams T, Hunt L, Franks PJ, Beerling DJ, Gray JE, Berry JA, Beerling DJ, Franks PJ, Farquhar GD, Sharkey TD, et al** (2012) Genetic manipulation of stomatal density influences stomatal size, plant growth and tolerance to restricted water supply across a growth carbon dioxide gradient. *Philos Trans R Soc Lond B Biol Sci* **367**: 547–555
- Doi M, Kitagawa Y, Shimazaki K** (2015) Stomatal Blue Light Response Is Present in Early Vascular Plants. *Plant Physiol* **169**: 1205–1213
- Dow GJ, Berry JA, Bergmann DC** (2014) The physiological importance of developmental mechanisms that enforce proper stomatal spacing in *Arabidopsis thaliana*. *New Phytol* **201**: 1205–1217
- Drake PL, Froend RH, Franks PJ** (2013) Smaller, faster stomata: scaling of stomatal size, rate of response, and stomatal conductance. *J Exp Bot* **64**: 495–505
- Eensalu E, Kupper P, Sellin A, Rahi M, Sober A, Kull O** (2008) Do stomata operate at the same relative opening range along a canopy profile of *Betula pendula*? *Func Plant Bio* **35**(2): 103-110
- Ernstsen J, Woodrow IE, Mott KA** (1997) Responses of Rubisco activation and deactivation rates to variations in growth-light conditions. *Photosynth Res* **52**: 117–125
- Evans JR, Poorter H** (2001) Photosynthetic acclimation of plants to growth irradiance: the relative importance of specific leaf area and nitrogen partitioning in maximizing carbon gain. *Plant, Cell Environ* **24**: 755–767
- Farquhar GD, Raschke K** (1978) On the resistance to transpiration of the sites of evaporation within the leaf. *Plant Physiol* **61**: 1000–1005
- Farquhar GD, Caemmerer S Von, Berry JA** (1980) A biochemical model of photosynthesis CO<sub>2</sub> fixation in leaves of C<sub>3</sub> species. *Planta* **149**: 78–90
- Farquhar GD, Sharkey TD** (1982) Stomatal conductance and photosynthesis. *Annu Rev Plant Physiol* **33**: 317–345
- Farquhar GD, Wong SC** (1984) An empirical model of stomatal conductance. *Funct Plant Biol* **11**: 191–210
- Fischer RA, Rees D, Sayre KD, Lu Z-M, Condon AG, Saavedra AL** (1998) Wheat yield progress associated with higher stomatal conductance and photosynthetic rate, and cooler canopies. *Crop Sci* **38**(6): 1467-1475

- Foyer FH, Nurmi A, Dulieu H, Parry MAJ** (1993) Analysis of two Rubisco-deficient tobacco mutants, h7 and sp25; evidence for the production of rubisco large subunits in the sp25 mutant that form clusters and are inactive. *J Exp Bot* **44**: 1445-1452
- Franks PJ, Farquhar GD** (2001) The effect of exogenous abscisic acid on stomatal development, stomatal mechanics, and leaf gas exchange in *Tradescantia virginiana*. *Plant Physiol* **125**: 935–942
- Franks PJ, Farquhar GD** (2007) The mechanical diversity of stomata and its significance in gas-exchange control. *Plant Physiol* **143**: 78–87
- Franks PJ, Beerling DJ** (2009) Maximum leaf conductance driven by CO<sub>2</sub> effects on stomatal size and density over geologic time. *Proc Natl Acad Sci U S A* **106**: 10343–10347
- Franks PJ, W. Doheny-Adams T, Britton-Harper ZJ, Gray JE** (2015) Increasing water-use efficiency directly through genetic manipulation of stomatal density. *New Phytol* **207**: 188–195
- Frechilla S, Talbott LD, Zeiger E** (2004) The blue light-specific response of *Vicia faba* stomata acclimates to growth environment. *Plant Cell Physiol* **45**: 1709–1714
- Fujita T, Noguchi K, Terashima I** (2013) Apoplastic mesophyll signals induce rapid stomatal responses to CO<sub>2</sub> in *Commelina communis*. *New Phytol* **199**: 395–406
- Gay AP, Hurd RG** (1975) The influence of light on stomatal density in the tomato. *New Phytologist* **75**(1): 37-46
- Gerardin T, Douthe C, Flexas J, Brendel O** (2018) Shade and drought growth conditions strongly impact dynamic responses of stomata to variations in irradiance in *Nicotiana tabacum*. *Environ Exp Bot*
- Givnish TJ** (1988) Adaptation to sun and shade: a whole-plant perspective. *Aust J Plant Physiol* **15**: 63–92
- Gorton HL, Williams WE, Binns ME, Gemmell CN, Leheny EA, Shepherd AC** (1989) Circadian stomatal rhythms in epidermal peels from *Vicia faba*. *Plant Physiol* **90**(4): 1329-1334.
- Gorton HL, Williams WE, Assmann SM** (1993) Circadian rhythms in stomatal responsiveness to red and blue light. *Plant Physiol* **103**(2): 399-406
- Harrison EP, Willingham NM, Lloyd JC, and Raines CA** (1998) Reduced sedoheptulose-1,7-bisphosphatase levels in transgenic tobacco lead to decreased photosynthetic capacity and altered carbohydrate accumulation. *Planta* **204**: 27-36
- Hassidim M, Dakhiya Y, Turjeman A, Hussien D, Shor E, Anidjar A, Goldberg K, Green RM** (2017) CIRCADIAN CLOCK ASSOCIATED 1 (CCA1) and the circadian control of stomatal aperture. *Plant physiol* **175**: 1864-1877
- Haydon MJ, Mielczarek O, Frank A, Román Á, Webb AA** (2017) Sucrose and ethylene signaling interact to modulate the circadian clock. *Plant physiol* **175**: 947-958
- Hedrich R, Marten I** (1993) Malate-induced feedback regulation of plasma membrane anion channels could provide a CO<sub>2</sub> sensor to guard cells. *EMBO J* **12**: 897–901
- Hedrich R, Marten I, Lohse G, Dietrich P, Winter H, Lohaus G, Heldt HW** (1994) Malate sensitive anion channels enable guard cells to sense changes in the ambient CO<sub>2</sub> concentration. *Plant J* **6**: 741–748

- Henkes S, Sonnewald U, Badur R, Flachmann R, and Stitt M** (2001) A small decrease of plastid transketolase activity in antisense tobacco transformants has dramatic effects on photosynthesis and phenylpropanoid metabolism. *Plant Cell* **13**: 535–551
- Hetherington AM, Woodward FI** (2003) The role of stomata in sensing and driving environmental change. *Nature* **424**: 901–8
- Hills A, Chen ZH, Amtmann A, Blatt MR, Lew VL** (2012) OnGuard, a computational platform for quantitative kinetic modeling of guard cell physiology. *Plant Physiol* **159**: 1026–1042
- Hubbard KE, Webb AAR** (2015) Circadian rhythms in stomata: Physiological and molecular aspects. In: Mancuso S, Shabala S, eds. *Rhythms in Plants*. Switzerland: Springer International Publishing, pp 231–55
- Huxley PA** (1969) The effect of fluctuating light intensity on plant growth. *J Appl Ecol* **6**: 273–276
- Inoue S-I, Kinoshita T** (2017) Blue light regulation of stomatal opening and the plasma membrane H<sup>+</sup>-ATPase. *Plant Physiol* **174**: 531–538
- Jones HG** (1998) Stomatal control of photosynthesis and transpiration. *J Exp Bot* **49**: 387–398
- Jones HG** (2013) *Plants and microclimate: a quantitative approach to environmental plant physiology*. Cambridge university press
- Kaiser H, Kappen L** (1997) In situ observations of stomatal movements in different light-dark regimes: The influence of endogenous rhythmicity and long-term adjustments. *J Exp Bot* **48**: 1583–1589
- Kaiser H, Kappen L** (2000) In situ observation of stomatal movements and gas exchange of *Aegopodium podagraria* L. in the understorey. *J Exp Bot* **51**: 1741–1749
- Kaiser H, Kappen L** (2001) Stomatal oscillations at small apertures: indications for a fundamental insufficiency of stomatal feedback-control inherent in the stomatal turgor mechanism. *J Exp Bot* **52**: 1303–1313
- Kaiser E, Morales A, Harbinson J, Heuvelink E, Prinzenberg AE, Marcelis LFM** (2016) Metabolic and diffusional limitations of photosynthesis in fluctuating irradiance in *Arabidopsis thaliana*. *Sci Rep* **6**: 31252
- Kang Y, Outlaw WH Jr, Andersen PC, Fiore GB** (2007) Guard-cell apoplastic sucrose concentration: a link between leaf photosynthesis and stomatal aperture size in the apoplastic phloem loader *Vicia faba* L. *Plant Cell Environ* **30**: 551–558
- Katul GG, Oren R, Manzoni S, Higgins C, Parlange MB** (2012) Evapotranspiration: A process driving mass transport and energy exchange in the soil-plant-atmosphere-climate system. *Rev. Geophys.* **50**(3)
- Keenan TF, Davidson E, Moffat AM, Munger JW, Richardson AD** (2012) Using model-data fusion to interpret past trends, and quantify uncertainties in future projections, of terrestrial ecosystem carbon cycling. *Glob Chan Bio* **18**: 2555–2569
- Keenan TF, Hollinger DY, Bohrer G, Dragoni D, Munger JW, Schmid HP, Richardson AD** (2013) Increase in forest water-use efficiency as atmospheric carbon dioxide concentrations rise. *Nature* **499**: 324–7

- Keenan TF, Gray J, Friedl MA, Toomey M, Bohrer G, Hollinger DY, Munger JW, O’Keefe J, Schmid HP, Wing IS, Yang B, Richardson AD** (2014) Net carbon uptake has increased through warming-induced changes in temperature forest phenology. *Nat Clim Chan* **4**: 598-604
- Kelly G, Moshelion M, David-Schwartz R, Halperin O, Wallach R, Attia Z, Belausov E, Granot D** (2013) Hexokinase mediates stomatal closure. *Plant J* **75**: 977–988
- Kirschbaum MU, Pearcy RW** (1988) Gas exchange analysis of the relative importance of stomatal and biochemical factors in photosynthetic induction in *Alocasia macrorrhiza*. *Plant Physiol* **86**: 782–785
- Kirschbaum MUF, Gross LJ, Pearcy RW** (1988) Observed and modelled stomatal responses to dynamic light environments in the shade plant *Alocasia macrorrhiza*. *Plant, Cell Environ* **11**: 111–121
- Knapp AK, Smith WK** (1987) Stomatal and photosynthetic responses during sun/shade transitions in subalpine plants: influence on water use efficiency. *Oecologia* **74**: 62–67
- Knapp AK, Smith WK** (1988) Effect of water stress on stomatal and photosynthetic responses in subalpine plants to cloud patterns. *Am J Bot* **75**: 851
- Knapp AK** (1993) Gas exchange dynamics in C<sub>3</sub> and C<sub>4</sub> grasses: consequence of differences in stomatal conductance. *Plant Physiol* **74**: 113–123
- Kono M, Terashima I** (2014) Long-term and short-term responses of the photosynthetic electron transport to fluctuating light. *J Photochem Photobiol B Biol* **137**: 89–99
- Külheim C, Agren J, Jansson S** (2002) Rapid regulation of light harvesting and plant fitness in the field. *Science* **297**: 91–93
- Lake JA, Quick WP, Beerling DJ, Woodward FI** (2001) Plant development: signals from mature to new leaves. *Nature* **411**(6834): 154
- Lawson T, James W, Weyers J** (1998) A surrogate measure of stomatal aperture. *J Exp Bot* **49**: 1397–1403
- Lawson T, Weyers J** (1999) Spatial and temporal variation in gas exchange over the lower surface of *Phaseolus vulgaris* L. primary leaves. *J Exp Bot* **50**: 1381–1391
- Lawson T, Oxborough K, Morison JIL, Baker NR** (2003) The responses of guard and mesophyll cell photosynthesis to CO<sub>2</sub>, O<sub>2</sub>, light, and water stress in a range of species are similar. *J Exp Bot* **54**: 1743–1752
- Lawson T, Morison J IL** (2004) Stomatal function and physiology. *Evol. Plant Physiol.* Elsevier, pp 217–242
- Lawson T, Lefebvre S, Baker NR, Morison JIL, Raines CA** (2008) Reductions in mesophyll and guard cell photosynthesis impact on the control of stomatal responses to light and CO<sub>2</sub>. *J Exp Bot* **59**: 3609–3619
- Lawson T** (2009) Guard cell photosynthesis and stomatal function. *New Phytol* **181**: 13–34

- Lawson T, von Caemmerer S, Baroli I** (2010) Photosynthesis and stomatal behaviour. *In* UE Lüttge, W Beyschlag, B Büdel, D Francis, eds, *Prog. Bot.* Springer, Berlin, Heidelberg, pp 265–304
- Lawson T, Kramer DM, Raines CA** (2012) Improving yield by exploiting mechanisms underlying natural variation of photosynthesis. *Curr Opin Biotechnol* **23**: 215–220
- Lawson T, Blatt MR** (2014) Stomatal size, speed, and responsiveness impact on photosynthesis and water use efficiency. *Plant Physiol* **164**: 1556–70
- Lawson T, Simkin AJ, Kelly G, Granot D** (2014) Mesophyll photosynthesis and guard cell metabolism impacts on stomatal behaviour. *New Phytol* **203**: 1064–1081
- Leakey ADB, Scholes JD, Press MC** (2005) Physiological and ecological significance of sunflecks for dipterocarp seedlings. *J Exp Bot* **56**: 469–482
- Lebaudy A, Vavasseur A, Hosity E, Dreyer I, Leonhardt N, Thibaud J-B, Véry A-A, Simonneau T, Sentenac H** (2008) Plant adaptation to fluctuating environment and biomass production are strongly dependent on guard cell potassium channels. *Proc Natl Acad Sci U S A* **105**: 5271–5276
- Lee J, Bowling DJF** (1992) Effect of the mesophyll on stomatal opening in *Commelina communis*. *J Exp Bot* **43**: 951–957
- Lee JS, Bowling DJF** (1995) Influence of the mesophyll on stomatal opening. *Funct Plant Biol* **22**: 357–363
- Lee M, Choi Y, Burla B, Kim Y-Y, Jeon B, Maeshima M, Yoo J-Y, Martinoia E, Lee Y** (2008) The ABC transporter AtABC14 is a malate importer and modulates stomatal response to CO<sub>2</sub>. *Nat Cell Biol* **10**: 1217–1223
- Li XP, Björkman O, Shih C, Grossman AR, Rosenquist M, Jansson S, Niyogi KK** (2000) A pigment-binding protein essential for regulation of photosynthetic light harvesting. *Nature* **403**: 391–5
- Li XP, Gilmore AM, Caffarri S, Bassi R, Golan T, Kramer D, Niyogi KK** (2004) Regulation of photosynthetic light harvesting involves intrathylakoid lumen pH sensing by the PsbS protein. *J Biol Chem* **279**: 22866–22874
- Li T, Kromdijk J, Heuvelink E, van Noort FR, Kaiser E, Marcelis LFM** (2016) Effects of diffuse light on radiation use efficiency of two *Anthurium* cultivars depend on the response of stomatal conductance to dynamic light intensity. *Front Plant Sci* **7**: 1–10
- López-Juez E, Jarvis RP, Takeuchi A, Page AM, Chory J** (1998) New Arabidopsis *cue* mutants suggest a close connection between plastid- and phytochrome regulation of nuclear gene expression. *Plant Physiol* **118**: 803–815
- Lu P, Zhang SQ, Outlaw WH, Riddle KA** (1995) Sucrose: a solute that accumulates in the guard-cell apoplast and guard-cell symplast of open stomata. *FEBS Lett* **362**: 180–184
- Lu P, Outlaw WH Jr, Smith BG, Freed GA** (1997) A new mechanism for the regulation of stomatal aperture size in intact leaves: accumulation of mesophyll-derived sucrose in the guard-cell wall of *Vicia faba*. *Plant Physiol* **114**: 109–118

- Lugassi N, Kelly G, Fidel L, Yaniv Y, Attia Z, Levi A, Alchanatis V, Moshelion M, Raveh E, Carmi N, et al** (2015) Expression of arabidopsis hexokinase in citrus guard cells controls stomatal aperture and reduces transpiration. *Front Plant Sci* **6**: 1114
- Mansfield TA, Hetherington AM, Atkinson CJ** (1990) Some current aspects of stomatal physiology. *Annu Rev Plant Physiol Plant Mol Biol* **41**: 55–75
- Manzoni S, Vico G, Katul G, Fay PA, Polley W, Palmroth S, Porporato A** (2011) Optimizing stomatal conductance for maximum carbon gain under water stress: a meta-analysis across plant functional types and climates. *Funct Ecol* **25**: 456–467
- Martins SCV, Mcadam SAM, Deans RM, Damatta FM, Brodribb TJ** (2016) Stomatal dynamics are limited by leaf hydraulics in ferns and conifers: Results from simultaneous measurements of liquid and vapour fluxes in leaves. *Plant, Cell Environ* **39**: 694–705
- Matsubara S, Naumann M, Martin R, Nichol C, Rascher U, Morosinotto T, Bassi R, Osmond B**, (2005) Slowly reversible de-epoxidation of lutein-epoxide in deep shade leaves of a tropical tree legume may 'lock-in' lutein-based photoprotection during acclimation to strong light. *Journal of Experimental Botany* **56**(411): 461-468
- McAdam SAM, Brodribb TJ** (2012) Stomatal innovation and the rise of seed plants. *Ecol Lett* **15**: 1–8
- McAdam SAM, Brodribb TJ** (2015) The Evolution of Mechanisms Driving the Stomatal Response to Vapor Pressure Deficit. *Plant Physiol* **167**: 833–843
- McAinsh MR, Pittman JK** (2009) Shaping the calcium signature. *New Phytol* **181**: 275–294
- McAusland L, Davey PA, Kanwal N, Baker NR, Lawson T** (2013) A novel system for spatial and temporal imaging of intrinsic plant water use efficiency. *J Exp Bot* **64**: 4993–5007
- McAusland L, Violet-Chabrand S, Davey P, Baker NR, Brendel O, Lawson T** (2016) Effects of kinetics of light-induced stomatal responses on photosynthesis and water-use efficiency. *New Phytol* **211**: 1209–1220
- Meacham K, Sirault X, Quick WP, von Caemmerer S and Furbank R** (2017) Diurnal solar energy conversion and photoprotection in rice canopies. *Plant physiology*, **173**(1): 495-508
- Medlyn BE** (1998) Physiological basis of the light use efficiency model. *Tree Physiol* **18**: 167–176
- Medrano H, Tomas M, Martorell S, Flexas J, Hernandez E, Rossello J, Pou A, Escalona JM, Bota J** (2015) From leaf to whole-plant water use efficiency (WUE) in complex canopies: limitations of leaf WUE as a selection target. *The Crop J* **3**(3): 220–228
- Meinzer FC, Grantz DA** (1990) Stomatal and hydraulic conductance in growing sugarcane: stomatal adjustment to water transport capacity. *Plant, Cell Environ* **13**: 383–388
- Mencuccini M, Mambelli S, Comstock J** (2000) Stomatal responsiveness to leaf water status in common bean (*Phaseolus vulgaris* L.) is a function of time of day. *Plant, Cell Environ* **23**: 1109–1118
- Messinger SM, Buckley TN, Mott KA** (2006) Evidence for involvement of photosynthetic processes in the stomatal response to CO<sub>2</sub>. *Plant Physiol* **140**: 771–778

- Moriana A, Villalobos FJ, Fereres E** (2002) Stomatal and photosynthetic responses of olive (*Olea europaea* L.) leaves to water deficits. *Plant, Cell Environ* **25**: 395–405
- Monteith JL, Szeicz G, Waggoner PE** (1965) The measurement and control of stomatal resistance in the field. *J Appl Ecol* 345–355
- Morison JIL** (2003) Plant water use, stomatal control. *Encycl. water Sci.* Marcel Dekker, New York, pp 680–685
- Mott KA** (1988) Do Stomata Respond to CO<sub>2</sub> Concentrations Other than Intercellular? *Plant Physiol* **86**: 200–203
- Mott KA, Parkhurst DF** (1991) Stomatal responses to humidity in air and helox. *Plant, Cell Environ* **14**: 509–515
- Mott KA, Sibbersen ED, Shope JC** (2008) The role of the mesophyll in stomatal responses to light and CO<sub>2</sub>. *Plant, Cell Environ* **31**: 1299–1306
- Mott KA** (2009) Opinion: Stomatal responses to light and CO<sub>2</sub> depend on the mesophyll. *Plant, Cell Environ* **32**: 1479–1486
- Mott KA, Peak D** (2013) Testing a vapour-phase model of stomatal responses to humidity. *Plant, Cell Environ* **36**: 936–944
- Müller P, Li XP, Niyogi KK** (2001) Non-photochemical quenching. A response to excess light energy. *Plant Physiol* **125**: 1558–1566
- Muller E, Guilloy-Froget H, Barsoum N, Brocheton L** (2002) *Populus nigra* L. in the Garonne valley: legacy of the past and present constraints. *Comptes rendus biologiques* **325**(11): 1129–1141
- Mullineaux PM** (2006) Spatial dependence for hydrogen peroxide-directed signaling in light-stressed plants. *Plant Physiol* **141**: 346–350
- Murchie EH, Horton P** (1997) Acclimation of photosynthesis to irradiance and spectral quality in British plant species: chlorophyll content, photosynthetic capacity and habitat preference. *Plant, Cell Environ* **20**: 438–448
- Murchie EH** (2005) Acclimation of photosynthesis to high irradiance in rice: gene expression and interactions with leaf development. *J Exp Bot* **56**: 449–460
- Murchie EH, Lawson T** (2013) Chlorophyll fluorescence analysis: a guide to good practice and understanding some new applications. *J Exp Bot* **64**: 3983–3998
- Naumburg E, Ellsworth DS** (2000) Photosynthetic sunfleck utilization potential of understory saplings growing under elevated CO<sub>2</sub> in FACE. *Oecologia* **122**: 163–174
- Noe SM, Giersch C** (2004) A simple dynamic model of photosynthesis in oak leaves: Coupling leaf conductance and photosynthetic carbon fixation by a variable intracellular CO<sub>2</sub> pool. *Funct Plant Biol* **31**: 1195–1204

- Okegawa Y, Long TA, Iwano M, Takayama S, Kobayashi Y, Covert SF, Shikanai T** (2007) A balanced PGR5 level is required for chloroplast development and optimum operation of cyclic electron transport around photosystem I. *Plant Cell Physiol* **48**: 1462–1471
- Ooba M, Takahashi H** (2003) Effect of asymmetric stomatal response on gas-exchange dynamics. *Ecol Modell* **164**: 65–82
- Outlaw WH** (2003) Integration of cellular and physiological functions of guard cells. *CRC Crit Rev Plant Sci* **22**: 503–529
- Outlaw WH, William H J** (2003) Integration of cellular and physiological functions of guard cells. *CRC Crit Rev Plant Sci* **22**: 503–529
- Papanatsiou M, Amtmann A, Blatt MR** (2016) Stomatal spacing safeguards stomatal dynamics by facilitating guard cell ion transport independent of the epidermal solute reservoir. *Plant Physiol* **172**: 254–63
- Parsons R, Weyers JDB, Lawson T, Godber IM** (1998) Rapid and straightforward estimates of photosynthetic characteristics using a portable gas exchange system. *Photosynthetica* **34**: 265–279
- Paul MJ, Foyer CH** (2001) Sink regulation of photosynthesis. *J Exp Bot* **52**: 1383–1400
- Paul MJ, Pellny TK** (2003) Carbon metabolite feedback regulation of leaf photosynthesis and development. *J Exp Bot* **54**: 539–547
- Pearcy RW** (1990) Photosynthesis in plant life. *Annu Rev Plant Physiol Plant Mol Biol* **41**: 421–453
- Pearcy RW** (1994) Photosynthetic utilization of sunflecks: a temporally patchy resource on a time scale of seconds to minutes. *Exploit Environ Heterog by plants* 175–208
- Pearcy R** (2007) Responses of plants to heterogeneous light environments. In F Valladares, F Pugnaire, eds, *Funct. Plant Ecol.*, Second. CRC Press, pp 213–246
- Pearcy RW, Way DA** (2012) Two decades of sunfleck research: looking back to move forward. *Tree Physiol* **32**: 1059–1061
- Pfitsch WA, Pearcy RW** (1989) Daily carbon gain by *Adenocaulon bicolor* (Asteraceae), a redwood forest understory herb, in relation to its light environment. *Oecologia* **80**(4) 465-470
- Poorter H, Fiorani F, Pieruschka R, Wojciechowski T, van der Putten WH, Kleyer M, Schurr U, Postma J** (2016) Pampered inside, pestered outside? Differences and similarities between plants growing in controlled conditions and in the field. *New Phytol* **212**: 838–855
- Porcar-Castell A, Palmroth S** (2012) Modelling photosynthesis in highly dynamic environments: The case of sunflecks. *Tree Physiol* **32**: 1062–1065
- Porcar-Castell A, Garcia-Plazaola JI, Nichol CJ, Kolari P, Olascoaga B, Kuusinen N, Fernández-Marín B, Pulkkinen M, Juurola E, Nikinmaa E** (2012) Physiology of the seasonal relationship between the photochemical reflectance index and photosynthetic light use efficiency. *Oecologia* **170**: 313–323

- Qu M, Hamdani S, Li W, Wang S, Tang J, Chen Z, Song Q, Li M, Zhao H, Chang T, Chu C, Zhu X** (2016) Rapid stomatal response to fluctuating light: an under-explored mechanism to improve drought tolerance in rice. *Funct Plant Biol* **43**: 727–738
- Raschke K** (1975) Stomatal action. *Annu Rev Plant Physiol* **26**: 309–340
- Raven JA** (2014) Speedy small stomata? *J Exp Bot* **65**: 1415–1424
- Retkute R, Smith-Unna SE, Smith RW, Burgess AJ, Jensen OE, Johnson GN, Preston SP, Murchie EH** (2015) Exploiting heterogeneous environments: does photosynthetic acclimation optimize carbon gain in fluctuating light? *J Exp Bot* **66**: 2437–2447
- Roelfsema MRG, Hedrich R** (2005) In the light of stomatal opening: new insights into ‘the Watergate.’ *New Phytol* **167**: 665–691
- Ruszala EM, Beerling DJ, Franks PJ, Chater C, Casson SA, Gray JE, Hetherington AM** (2011) Land plants acquired active stomatal control early in their evolutionary history. *Curr Biol* **21**: 1030–5
- Sage RF** (1994) Acclimation of photosynthesis to increasing atmospheric CO<sub>2</sub>: the gas exchange perspective. *Photosyn Res* **39**: 351–368
- Santelia D, Lawson T** (2016) Rethinking Guard Cell Metabolism. *Plant Physiol* **172**: 1371–1392
- Schluter U, Muschak M, Berger D, Altmann T** (2003) Photosynthetic performance of an *Arabidopsis* mutant with elevated stomatal density (*sdd1-1*) under different light regimes. *J Exp Bot* **54**: 867–874
- Schymanski SJ, Or D, Zwieniecki M** (2013) Stomatal control and leaf thermal and hydraulic capacitances under rapid environmental fluctuations. *PLoS One* **8**(1): 54231
- Sharkey TD, Raschke K** (1981) Separation and measurement of direct and indirect effects of light on stomata. *Plant Physiol* **68**: 33–40
- Sharkey TD, Bernacchi CJ, Farquhar GD, Singaas EL** (2007) Fitting photosynthetic carbon dioxide response curves for C3 leaves. *Plant Cell Environ* **30**: 1035–1040
- Shimazaki K, Doi M, Assmann SM, Kinoshita T** (2007) Light regulation of stomatal movement. *Annu Rev Plant Biol* **58**: 219–247
- Sibbersen E, Mott KA** (2010) Stomatal responses to flooding of the intercellular air spaces suggest a vapor-phase signal between the mesophyll and the guard cells. *Plant Physiol* **153**: 1435–1442
- Sperry JS, Venturas MD, Anderegg WRL, Mencuccini M, Mackay DS, Wang Y, Love DM** (2016) Predicting stomatal responses to the environment from the optimization of photosynthetic gain and hydraulic cost. *Plant, Cell Environ*
- Suorsa M, Järvi S, Grieco M, Nurmi M, Pietrzykowska M, Rantala M, Kangasjärvi S, Paakkanen V, Tikkanen M, Jansson S, et al** (2012) PROTON GRADIENT REGULATION5 is essential for proper acclimation of *Arabidopsis* photosystem I to naturally and artificially fluctuating light conditions. *Plant Cell* **24**: 2934–48

- Tallman G** (2004) Are diurnal patterns of stomatal movement the result of alternating metabolism of endogenous guard cell ABA and accumulation of ABA delivered to the apoplast around guard cells by transpiration? *J Exp Bot* **55**: 1963–1976
- Tanaka Y, Sugano SS, Shimada T, Hara-Nishimura I** (2013) Enhancement of leaf photosynthetic capacity through increased stomatal density in *Arabidopsis*. *New Phytol* **198**: 757–764
- Terashima I, Hanba YT, Tazoe Y, Vyas P, Yano S** (2006) Irradiance and phenotype: comparative eco-development of sun and shade leaves in relation to photosynthetic CO<sub>2</sub> diffusion. *J Exp Bot* **57**: 343–354
- Ticha I** (1982) Photosynthetic characteristics during ontogenesis of leaves. 7. Stomata density and sizes. *Photosynthetica*
- Tikkanen M, Grieco M, Kangasjärvi S, Aro E-M** (2010) Thylakoid protein phosphorylation in higher plant chloroplasts optimizes electron transfer under fluctuating light. *Plant Physiol* **152**: 723–735
- Tinoco-Ojanguren C, Pearcy RW** (1992) Dynamic stomatal behavior and its role in carbon gain during lightflecks of a gap phase and an understory Piper species acclimated to high and low light. *Oecologia* **92**: 222–228
- Tinoco-Ojanguren C, Pearcy RW** (1993) Stomatal dynamics and its importance to carbon gain in two rainforest Piper species - II. Stomatal versus biochemical limitations during photosynthetic induction. *Oecologia* **94**: 395–402
- Tominaga M, Kinoshita T, Shimazaki K** (2001) Guard-cell chloroplasts provide ATP required for H<sup>+</sup> pumping in the plasma membrane and stomatal opening. *Plant Cell Environ* **42**: 795–802
- Tricker PJ, Trewin H, Kull O, Clarkson GJJ, Eensalu E, Tallis MJ, Colella A, Doncaster CP, Sabatti M, Taylor G** (2005) Stomatal conductance and not stomatal density determines the long-term reduction in leaf transpiration of poplar in elevated CO<sub>2</sub>. *Oecologia* **143**: 652–660
- Tuzet A, Perrier A, Leuning R** (2003) A coupled model of stomatal conductance, photosynthesis. *Plant, Cell Environ* **26**: 1097–1116
- Urban O, Sprtová M, Kosvancová M, Tomášková I, Lichtenthaler HK, Marek M V** (2008) Comparison of photosynthetic induction and transient limitations during the induction phase in young and mature leaves from three poplar clones. *Tree Physiol* **28**: 1189–97
- Vanden Broeck A** (2003) EUFORGEN Technical guidelines for genetic conservation and use for Black poplar (*Populus nigra*). Biodiversity International
- Violet-Chabrand S, Dreyer E, Brendel O** (2013) Performance of a new dynamic model for predicting diurnal time courses of stomatal conductance at the leaf level. *Plant, Cell & Environ* **36**: 1529–1546
- Violet-Chabrand S, Matthews JSA, Brendel O, Blatt MR, Wang Y, Hills A, Griffiths H, Rogers S, Lawson T** (2016) Modelling water use efficiency in a dynamic environment: An example using *Arabidopsis thaliana*. *Plant Sci* **251**: 65–74
- Vico G, Manzoni S, Palmroth S, Katul G** (2011) Effects of stomatal delays on the economics of leaf gas exchange under intermittent light regimes. *New Phytol* **192**: 640–652

- Viger M, Smith HK, Cohen D, Dewoody J, Trewin H, Steenackers M, Bastien C, Taylor G** (2016) Adaptive mechanisms and genomic plasticity for drought tolerance identified in European black poplar (*Populus nigra* L.). *Tree Phys* **36**: 909–928
- Von Caemmerer S, Lawson T, Oxborough K, Baker NR, Andrews TJ, Raines CA** (2004) Stomatal conductance does not correlate with photosynthetic capacity in transgenic tobacco with reduced amounts of Rubisco. *J Exp Bot* **55**: 1157–1166
- Walters R, Horton P** (1994) Acclimation of *Arabidopsis thaliana* to the light environment: changes in composition of the photosynthetic apparatus. *Planta* **195**: 248–256
- Wang P, Song CP** (2008) Guard-cell signalling for hydrogen peroxide and abscisic acid. *New Phytol* **178**: 703–718
- Watling J, Ball M, Woodrow I** (1997) The utilization of lightflecks for growth in four Australian rainforest species. *Funct Ecol* **11**(2): 231–239
- Way DA, Pearcy RW** (2012) Sunflecks in trees and forests: From photosynthetic physiology to global change biology. *Tree Physiol* **32**: 1066–1081
- Weraduwege SM, Chen J, Anozie FC, Morales A, Weise SE, Sharkey TD** (2015) The relationship between leaf area growth and biomass accumulation in *Arabidopsis thaliana*. *Front Plant Sci* **6**: 167
- Weston E, Thorogood K, Vinti G, López-Juez E** (2000) Light quantity controls leaf-cell and chloroplast development in *Arabidopsis thaliana* wild type and blue-light-perception mutants. *Planta* **211**: 807–815
- Weyers JDB, Lawson T, Peng ZY** (1997) Variation in stomatal characteristics at the whole-leaf level. SEB Seminar Series volume - Scaling Up. Edited by van Gardingen, P.R., Foody G.M., Curran, P.J., Cambridge University Press, Cambridge. 129-149
- Weyers JDB, Lawson T** (1997) Heterogeneity in Stomatal Characteristics. In *Advances in Botanical Research*, Academic Press **26**: 317–352
- Whitehead D, Teskey R** (1995) Dynamic response of stomata to changing irradiance in loblolly pine (*Pinus taeda* L.). *Tree Physiol* **15**: 245–251
- Willmer C, Fricker M** (1996) *Stomata*. Springer Science & Business Media
- Wolf A, Anderegg WRL, Pacala SW** (2016) Optimal stomatal behavior with competition for water and risk of hydraulic impairment. *Proc Natl Acad Sci* **113**: E7222–E7230
- Wong SC, Cowan IR, Farquhar GD** (1979) Stomatal conductance correlates with photosynthetic capacity. *Nature* **282**: 424–426
- Wong SL, Chen CW, Huang HW, Weng JH** (2012) Using combined measurements for comparison of light induction of stomatal conductance, electron transport rate and CO<sub>2</sub> fixation in woody and fern species adapted to different light regimes. *Tree Physiol* **32**: 535–544
- Yamori W** (2016) Photosynthetic response to fluctuating environments and photoprotective strategies under abiotic stress. *J Plant Res* **129**(3): 379-395

- Yan W, Zhong Y, Shangguan Z** (2016) A meta-analysis of leaf gas exchange and water status responses to drought. *Sci Rep* **6**: 20917
- Yin ZH, Johnson GN** (2000) Photosynthetic acclimation of higher plants to growth in fluctuating light environments. *Photosynth Res* **63**: 97–107
- Zapata M, Rodríguez F, Garrido JL** (2000) Separation of chlorophylls and carotenoids from marine phytoplankton, a new HPLC method using a reversed phase C8 column and phridine-containing mobile phases. *Marine Ecology Progress Series*. **195**: 29–45
- Zeiger E, Zhu J** (1998) Role of zeaxanthin in blue light photoreception and the modulation of light–CO<sub>2</sub> interactions in guard cells. *J Exp Bot* **49**: 433–442
- Zhang K, Xia X, Zhang Y, Gan S-S** (2012) An ABA-regulated and Golgi-localized protein phosphatase controls water loss during leaf senescence in *Arabidopsis*. *Plant J* **69**: 667–78
- Zhu X-G, Long SP, Ort DR** (2010) Improving photosynthetic efficiency for greater yield. *Annu Rev Plant Biol* **61**: 235–261